A DYNAMIC STRUCTURAL ANALYSIS OF TREES SUBJECT TO WIND LOADING

BY

KENNETH RONALD JAMES

Submitted in total fulfilment of the requirements
of the degree of Doctor of Philosophy
October 2010
Melbourne School of Land and Environments
The University of Melbourne

ABSTRACT

A dynamic structural analysis of trees under wind loading is described. This project examines open grown trees from a structural perspective under real wind conditions in urban areas. Open grown trees differ from forest grown plantation trees due to morphological differences, in particular the slenderness ratio of the tree and the size of branches. Branches play a dominant role in modifying the dynamic response of open grown trees under wind loading. Previous theoretical models of trees have not included branches as dynamic elements.

A range of open grown trees were studied, based on their structural shapes and branching morphology, including Palm (*Washingtonia robusta*), Italian cypress (*Cupressus sempervirens*), Hoop pine (*Araucaria cunninghamii*), Red gum (*Eucalyptus tereticornis*), NZ Kauri pine (*Agathis australis*), Spotted gum (*Corymbia maculata*), She oak (*Allocasuarina fraseriana*).

New instruments have been designed to measure dynamic wind loads on trees during storms. These instruments are attached to the trunk at the base of a tree and measure the strain of the outer fibres of the trunk as it bends in the wind. Two sensors are orthogonally oriented on a trunk, usually in a North/South and East/West direction to record the complex sway response of trees due to wind blowing from any direction. Each sensor is accurate to one micron and readings at 20Hz record the dynamic motion of the tree. The tree is calibrated using a static pull test so that strain readings can be converted into bending moment values which are used as the measure of wind load. Wind speed, wind direction, and temperature are also recorded via a data logger and computer. This method can be used on all trees and differs from most previous studies which have put instruments into the upper canopy of a tree and have therefore been limited to excurrent shaped trees with a central trunk form.

Trees have been monitored under wind storm conditions for several years and the results indicate that trees sway in a complex manner, due to the dynamic contribution of branches. In order to explain this complex motion a new theoretical model is proposed which includes branches as dynamic masses attached to the trunk. This model represents the tree as a multi-degree-of-freedom system which is different from previous studies that used a single degree-of-freedom model. The new model uses dynamic masses attached to other dynamic masses to represent the branches of a tree

and introduces the concept of mass damping. Mass damping occurs when two or more masses dynamically interact in a complex manner to cancel out the overall motion with an out-of-phase response. This is a component of the overall damping in a tree which acts to dissipate energy and minimize damage in wind storms.

The application of dynamic measurement of forces will lead to a better understanding of how trees withstand winds. Knowledge of the actual wind forces allow a better understanding of tree stability and has implications for pruning techniques, and safe work practices during tree felling and dismantling operations.

DECLARATION

This is to certify that

i. *the thesis comprises only my original work towards the PhD except where indicated in the Preface,*
ii. *due acknowledgement has been made in the text to all other material used,*
iii. *the thesis is less than 100,000 words in length, exclusive of tables, maps, bibliographies and appendices.*

Signed ____________________________

Date: _____________________

ACKNOWLEDGEMENTS

I gratefully acknowledge the assistance of Associated Professor Dr Nick Haritos for his friendly guidance on the technical and mathematical treatment of dynamics and its application to the study of trees. It has been a pleasure to work on this project with him over a number of years. Dr Brian Kane, University of Massachusetts, has been invaluable for his guidance and discussion of details regarding trees, assistance in collecting data and discussions at numerous conferences, presentations and workshops in Australia and the United States. Dr Peter Ades and Dr Greg Moore are acknowledged for their academic guidance and support in reviewing the thesis.

Phil Kenyon is thanked for his challenging ideas and understanding of real trees and was the first person to offer some different views that eventually grew into this study. Ross Payne has been invaluable for his technical assistance and many in depth discussion on the finer points of instrumentation, electronics and data collection. His constant good humour and help on field trips to pull trees and collect data is gratefully acknowledged. Martin Norris, Arborist, Shire of Wellington, Sale, Victoria has been very supportive with his time and resources during field trips to Gippsland, Victoria, to study trees on windy sites.

I have been fortunate to meet very supportive people on trips to international conferences including Nelda Matheny and Dr Jim Clark and thank them for their constant positive support over many years. I also wish to thank Dr Tom Smiley and Sharon Lilly for their discussions on trees and friendly support.

My wife Emma and daughter Stephanie have been a great support and inspirational at times when the end did not seem in sight, and I thank them for their encouragement and patience over many years which have helped to keep me going.

TABLE OF CONTENTS

TABLE OF CONTENTS (cont.)

List of Figures

List of Figures (cont.)

List of Figures (cont.)

List of Figures (cont.)

Page

List of Figures (cont.)

List of Figures (cont.)

List of Figures (cont.)

List of Tables

TABLE OF SYMBOLS

Symbol	Definition
a	Initial displacement
a_n	Fourier constant
A	Effective area of tree canopy exposed to wind
A_1	Amplitude of periodic motion (Ch2)
A_2	Curve fit parameter for spectra
A_o	Canopy area in no wind conditions
A_s	Constant used when fitting the structural magnification function
b_n	Fourier constant
BM	Bending moment
β	Constant used in equations of drag
c	Damping
c_c	Critical damping
c_d	Damping of a mass damper
C_D	Drag coefficient
d	Distance, diameter
δ	Logarithmic decrement ratio
Δ	Change of a quantity
DBH	Diameter at breast height
ε	Strain, change in length divided by original length
E	Young's modulus (also called Modulus of elasticity)
$E_{branches}$	Energy in branches
E_{eddy}	Energy in eddies
E_{ground}	Energy in ground
E_{trunk}	Energy in trunk
E_{wind}	Energy in wind
F	force
F_o	Force at natural frequency
$F(t)$	Time varying force
F_w	Force of due to wind
f	frequency
f_n	Natural frequency
G	Gust factor
g	Forced frequency ratio
g_1	Peak factor of approximately 3.5
h	Height of tree
h_m	Height from base of a tree to point of force application
Hz	Frequency, Hertz
$\lvert H(f)\rvert^2$	Base Bending Moment transfer function (Zhou and Kareem 2001)
I	2nd Moment of area (moment of inertia)
I_t	Turbulent intensity
K	a constant
k	Spring constant
k_d	Spring constant of a mass damper

TABLE OF SYMBOLS (Cont.)

Symbol	**Definition**
L	Length
m	mass
$\overline{m}$	Mass ratio
m_d	Mass of a mass damper element
M	Moment
$\overline{M}$	Mean moment
MDOF	Multi-degree of freedom system
n	Exponent of velocity, for bluff bodies equals 2.
ϕ	Phase angle
P	Period of oscillation (Mayhead 1973a)
ρ	density
SDOF	Single degree of freedom system
$S(f)$	Spectral density function
$S_x(f)$	Spectral data of displacements
$S_{\ddot{x}}(f)$	Spectral data of accelerations
$S_M(f)$	Spectral data of base bending moment
$S_M(f)$	Spectral data of base bending moment after applying aerodynamic admittance function
$S_v(f)$	Spectral data of wind speed
T	Period of oscillation
TMD	Tuned mass damper
$T^2(f)$	Transfer function
t	time
$\hat{U}$	Peak gust wind speed
$\overline{U}$	Mean wind speed
u	Displacement (same as x) (Connor 2002)
$v(x)$	Deflection shape of a uniform beam
V	velocity
$\overline{V}$	Mean velocity
x	Displacement
x_{st}	Static displacement
$\dot{x}$	Velocity
$\ddot{x}$	acceleration
$x(t)$	Time varying displacement
y	Distance, from the centre to the perimeter of a section
ψ	Phase shift
$\psi_n(x)$	Assumed set of displacement functions
$\chi_a^2(f)$	Aerodynamic admittance function
$\chi_m^2(f)$	Structural magnification factor
Z_n	Amplitude terms referred to as generalized coordinates

	TABLE OF SYMBOLS (Cont.)
Symbol	**Definition**
α	Compound parameter used in drag calculation
σ	stress
σ_n	Standard deviation
ω	Circular frequency
ω_d	Natural damped frequency
ω_n	Natural circular frequency
Ω	Forcing frequency
θ	angle
μ	mass ratio
ζ	Critical damping ratio
ζ_1	Damping from curve fitted to static range
ζ_2	Damping from curve fitted to inertial range
ζ_3	Damping from curve fitted to equal areas
ζ_4	Damping from curve fitted with -5/3 power law for wind

Chapter 1. INTRODUCTION

1.1 Trees and Structural Analysis

This project examines trees from a structural perspective since understanding the structural properties of trees is fundamental to understanding how the tree adapts and survives in its environment. Niklas (1992) states that it is a fundamental premise that plants like all other types of organisms cannot violate the laws of physics. As trees grow in size and height, the added biomass develops greater self-loading, and also exposes the upper reaches of the tree to higher wind speeds, which develop larger bending moments at its base, (Niklas and Spatz 2000). The growth of trees is largely determined by physiological constraints, particularly those affecting photosynthesis and water transport, but if these are optimal, limitations of size and shape are still imposed by biomechanical constraints, (Spatz and Bruechert 2000).

A tree must be able to withstand all the physical loads throughout its life. For nearly all trees, the greatest load is from the wind that comes as gusts of rapid, periodic, dynamic events. Wind is the most persistent of the harmful natural forces to which any individual tree or forest stand is subjected (Jacobs, 1936). There may be some exceptions. Trees that grow deep in rain forests may never experience large wind forces. Trees in arctic and sub-arctic climates may experience heavy static loading of ice and snow which may cause them to fail. However, in most situations wind constantly influences the tree from germination until death (Jacobs, 1936). Wind forces become critical as trees age and grow to large sizes because in high winds, the forces induced in the trunk, branches, and roots can approach critical limits, which, if exceeded, will result in failure. While high winds may occur only rarely in the life of a tree, its resistance to breaking or overturning is critical to its survival (Vogel 1989).

How trees react in high winds is of considerable practical importance. In forests tree failure due to wind is a significant problem because of damage resulting in economic losses and adverse changes to forest ecosystems (Grace 2003, Peltola 1996a, Peltola et al. 1999; Cucchi and Bert 2003, Zeng et al. 2007). European forests suffered severe losses with over 180 m^3 of timber levelled during storms in December 1999 (Zeng et al. 2007). In Sweden during 2004, 70 million m^3 of timber was lost in storms and in Finland during 2001, 7 million m^3 of timber was damaged. Economic impact of wind damage is particularly severe in managed forests due to yield reduction, unscheduled thinning and clear cutting, below optimal cutting schedules (Peltola 1996a). In France, winds of over 170 km h^{-1} devastated forests causing losses of 26.1 million m^3 of wood, or 19% of the standing volume (Cucchi and Bert 2003).

The affect of climate change is expected to increase the wind-throw risk of trees (Peltola 1999a) because the more humid, warmer weather patterns predicted for the future are likely to reduced tree anchorage due to a decrease in soil freezing in Finland between late autumn and early spring, which are the most windy months of the year. In the future, as many as 80% of mean winds that cause uprooting (11–15 m s^{-1}) would occur during months when the soil is unfrozen in southern Finland, whereas the corresponding proportion at present is about 55%. In northern Finland, the percentage is 40% today and is expected to be 50% in the future. Thus, as the strongest winds usually occur between late autumn and early spring, climate change could increase the loss of standing timber through wind throw, especially in southern Finland. Understanding the effect of wind on trees is likely to be even more important as these effects increase.

In urban areas, individual trees can fail in high winds and cause injury to people or damage to property. Errors or oversights in assessing trees by an arborist can result in costly litigation, especially in the United States (Mortimer and Kane, 2004). At present, tree assessment by qualified arborists is based on visual methods, one of which is VTA (Visual Tree Assessment, Mattheck and Breloer 1994). There are no current tree assessment procedures which collect data on tree strength and wind loads. The issue of liability is making tree assessment more conservative and there is a trend to recommend tree removal if even small imperfections or hazards can be seen.

Managers of open grown trees must make decisions on keeping or removing trees, by assessing the tree's structure and estimating its ability to withstand future windstorms of varying and unknown intensity. This can be very difficult because there are currently no tree assessment methods that use actual measurements or data from real wind loads on trees. Wind forces on trees have been estimated using a static tree pull test, developed in Europe in recent years (Brudi 2002) but how this relates to dynamic tree loading is still in question and the method is not widely adopted. Wind loading on open grown trees is important in order to assess the effect of how different pruning techniques change the wind loading on the canopy, while still maintaining tree amenity value. Serious liability issues can arise if there is the perception that poor or negligent tree care practices have contributed to tree failure. In the management of trees in large forest plantations, it is important to assess the effects of wind and minimise the economic losses that occur due to wind throw and trunk failure in storms (Moore and Maguire 2005). Safety of arborists and risk management of trees is another significant area where a better understanding of tree dynamics can assist in the development of new and safer techniques of pruning and tree felling.

A structural approach to tree biomechanics, using a static force analysis, and some mathematical simplifications was presented by Mattheck and Breloer (1994) who developed an axiom known as “the axiom of uniform stress”. This axiom suggested the concept that the growth of the tree is in response to the loads placed upon it, and highlighted the importance of understanding the loads that a tree endures, and the stresses that develop within the structural components of the trunk and the branches. The mechanical analysis of Mattheck was limited to a static approach to loads and no dynamic analysis was attempted. Wind loading was considered as a statically applied force, although different values were assigned to cope with varying wind forces, since it was acknowledged that the wind loads are the largest loads that a tree endures. Later work using a static approach to evaluating wind forces is presented by Brudi (2002) in which the tree is pulled with a rope to an equivalent of an estimated wind force, and the stability of the tree is evaluated. Care should be used with the static pull test under calm conditions, as Hassinen et al. (1998) report previous studies in which trees have been observed to blow down or snap at wind speeds considerably lower than predicted by the static pull test.

Various authors have presented structural and biomechanical studies of trees in winds over the last forty years. Technology and instrumentation used in the first studies (Sugden 1962, Mayhead 1973) had limited capacity to take accurate readings. In these studies, stopwatches were used to measure and record sway movement of trees. The sway was induced by pulling with ropes and was not a result of wind excitation. Because of the limits of this technology, averaging methods were used in an attempt to refine the data. When measuring the sway periods of trees, several tests were averaged so that a figure for natural frequency could be established. These early studies could only detect broad changes in dynamic behaviour and may have missed important effects, especially due to the dynamic influence of branches. Recent developments in the technology of instrumentation and electronic data loggers and computers, have provided more accurate measurement of tree motion but how they are used to measure tree response may influence the results and possibly the conclusions. The instrumentation and influence on results are discussed further in Chapter 2.

There are two main strategies for investigating dynamic response of trees. One examines the upper canopy and the other examines the basal trunk region. Instruments placed in the upper canopy can accurately record the dynamic response of the trunk section or a branch, but may miss some important information to do with dynamic interaction of other branches. Instruments placed on the trunk at the base of the tree can measure all the integrated dynamic motion of the many limbs and the sum of all forces that must pass from the canopy, through the trunk and transfer to the root plate. The second strategy has been used in this study. New instruments have been designed which provide dynamic data from the trunk region (James and Kane 2008). Because all the motions of the branches (and the resulting forces) of the canopy pass through the trunk, these data represent the total response of the tree and the results indicate the important contribution of branches to the dynamic behaviour of trees in winds.

1.2 Static and Dynamic Methods

Structural analysis examines the response of a structure to an applied load. The two main methods used are either static or dynamic, depending on the nature of the loading and the response of the structure. If the load is constant, the response of the structure will also be constant and a static analysis is sufficient to determine deflections and stresses. For trees, constant load situations would be due to self-weight, snow loads or ice loads. If the load on the structure varies with time, then the response of the structure will also vary with time and dynamic methods are needed because static methods may no longer be sufficient to give a complete solution. Time varying loads on trees are due to winds so dynamic methods of structural analysis must be used.

In discussing the storm-resisting features of the design of trees, Vogel (1996) suggests that a central theme is how nature uses flexible structures like leaves, branches, trunks, and roots. “Human technology mainly uses more rigid materials such as metals, ceramics, dry wood and so forth”. Consequently there is little experience in designing structures that change shape in high winds. Simply applying an engineering analysis of rigid structures to trees may not provide the required solutions. The flexible structures and materials of trees not only twist and bend but do other things like absorb and either store or dissipate energy (Vogel 1996). He suggests that we can learn from trees and the careful study of trees may reveal new concepts of behaviour of structures under dynamic loading.

There has been considerable study of tree structures using static analyses (Sugden 1962, Gardiner 1992, Mayhead 1973, Oliver and Mayhead 1974, Blackburn et al. 1988, Bell et al. 1991, Roodbaraky et al. 1994, Lilly and Davis Sydnor 1995, Rodgers et al. 1995, Wessolly 1995, Neild and Wood 1999, Brüchert et al. 2000, England et al. 2000, Silins et al. 2000, Moore 2000, Peltola et al. 2000, Ilic 2001, Brudi 2002, Cucchi 2003b, Vidal et al. 2003, Cucchi et al. 2004, Fraser and Gardiner 1967, Herajarvi 2004, Peltola 2006, Bergeron 2009). The history of plant biomechanics is summarised by Niklas (1992) who describe how the basic principles of structural engineering theory are applied to the study of plant forms including trees. Niklas cautions that care must be taken because applying well developed engineering beam theory to trees may not accurately describe how the tree responds under wind loading. Often assumptions are made in order to simplify the mathematical calculations. One frequently used simplification is to treat a tree as a beam or a tapered pole without considering any of the branches. This would miss any dynamic contribution from branches. Live trees and living green wood differs from normal engineering material in several important aspects. Wood is a composite material, is anisotropic and heterogeneous, and mechanical behaviour at failure is not an all or none process, (Spatz and Bruechert 2000). Structural analysis has used both static and dynamic methods but in general dynamic analysis is more complex. Care needs to be taken when applying any simplifying assumptions to make sure they are valid.

Dynamic loads can be defined simply as time-varying (Clough and Penzien 1993) and may vary with magnitude, direction and/or position with time. The response of the structure also varies with time and there are two basic approaches to evaluate structural response to dynamic loads, i.e. deterministic and non-deterministic. The choice depends on how the load is applied. If time variation of the load is fully known, called prescribed dynamic loading (Clough and Penzien 1993), the analysis of the response is defined as a deterministic analysis. If the time variation is not completely known, but can be described in a statistical sense, the loading is termed random dynamic loading and the analysis is defined as a non-deterministic analysis.

In general, structural response to any dynamic loading is expressed in terms of displacements. Thus, deterministic analysis leads to displacement/time histories corresponding to prescribed load histories. A non-deterministic analysis provides only statistical information about displacements resulting from statistically defined loading. Deterministic loading can be divided into two basic categories, periodic and non-periodic (Clough and Penzien 1993). The simplest periodic motion has sinusoidal variation, termed simple harmonic, and an example would be a rotating unbalanced mass on a machine. Periodic loading has the same time variation for a large number of cycles and by means of Fourier analysis, even complex motion can be represented by the sum of a series of simple harmonic components. Non-periodic loading, e.g. blast loading, is short duration impulsive loading and special simplified forms of analysis can be used.

Dynamic analysis differs from statics in two important ways. Firstly, because of the time variations of both load and response, a dynamic problem does not have a single solution whereas a static problem does. The dynamic analysis is therefore more complex and time consuming than a static analysis. The second difference is that dynamic systems have inertial forces opposing accelerations produced by the dynamic loads, compared to static systems which are analysed using principles of force equilibrium only. This is illustrated in Figure 1.1 which shows (a) the static load p on a beam and (b) the dynamic load $p(t)$ which generates accelerations. Inertial forces which resist accelerations of the structure and are the most important distinguishing feature of a structural dynamics problem (Clough and Penzien 1993).

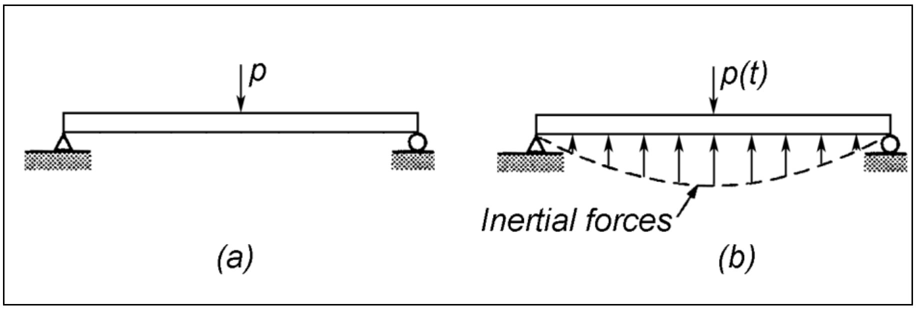

Figure 1.1. Basic difference between static and dynamic loads: (a) static loading; (b) dynamic loading (Clough and Penzien 1993).

If the motions of a structure are fast and produce large inertial forces, then dynamic methods must be used. If the motions are slow and inertial forces are negligible then static methods can be used, even if the load may be time varying. Applying this concept to trees, it is clear that under time varying wind loads, the large sway motions of the canopy will require a dynamic analysis to account for the inertial forces of the branch masses as they sway.

Three different approaches are described by Clough and Penzien (1993) to study dynamic behaviour of structures. These are (a) lumped-mass procedure, (b) generalised displacements for uniformly distributed beams, and (c) the finite element method.

The lumped mass procedure assumes the mass of a beam to be concentrated at discrete points (Figure 1.2). This greatly simplifies the analysis because inertial forces develop only at these mass points. The lumped mass procedure is used in this study to model trees and branches. This is considered appropriate, particularly for open grown trees where there is significant mass in the branches which dynamically interact with the trunk.

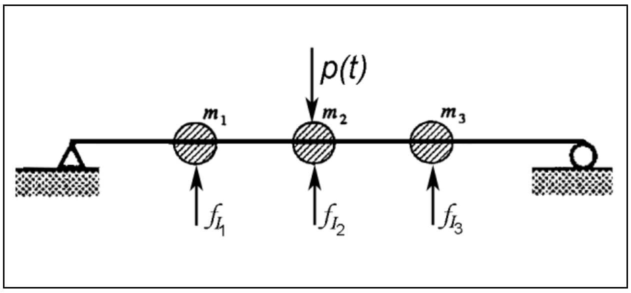

Figure 1.2. Lumped-mass idealization of a simple beam (Clough and Penzien 1993).

Dynamic analysis methods for structures using a uniformly distributed mass method, is based on an assumption that the deflected shape of the structure can be expressed as the sum of a series of displacement patterns which become the displacement coordinates of the system (Clough and Penzien 1993). The assumed shape patterns can be used to write a generalized expression for displacements which for a one dimensional structure might be written as

$$v(x) = \sum_n Z_n \psi_n(x) \tag{1.1}$$

Where $v(x)$ – deflection shape of a uniform beam
Z_n – amplitude terms referred to as generalised coordinates
$\psi_n(x)$ – assumed set of displacement functions

The generalised coordinate method (uniformly distributed mass) assumes that a tree can be approximated to a central trunk, and ignores the dynamic effect of branches. This may be valid for some limited types of slender plantation trees but is not representative of most trees that have different forms, such as tree without a central trunk, or typical open grown trees where the branches constitute significant proportion of the total mass.

These simplifications can produce results which may be true for beams but may not be true for trees. For example, the equations of motion for a uniformly distributed beam use the Bernoulli-Euler law which states that the bending moment (M) is linearly proportional to the second spatial derivative of the beam displacement (*w*), (Balachandran and Magrab 2004).

$$M = EI \frac{\partial^2 w}{\partial x^2}$$

Where *E* – Young's modulus
I – Moment of inertia
x – displacement along beam

Uniform beams have an infinite number of degrees of freedom and the dynamic solutions include eigenfrequencies and eigenvectors with possible mode shapes which can be determined as shown in Figure 1.3. The generalised displacement method has only limited application to trees because of the assumptions of uniform mass distribution, mode shapes, approximations based on small displacements and the omission of the dynamic masses of branches. This method produces complex mode shapes when applied to beams. In this study, measurements made on several trees over many months indicate that the complex mode shapes do not occur naturally in trees under wind loading.

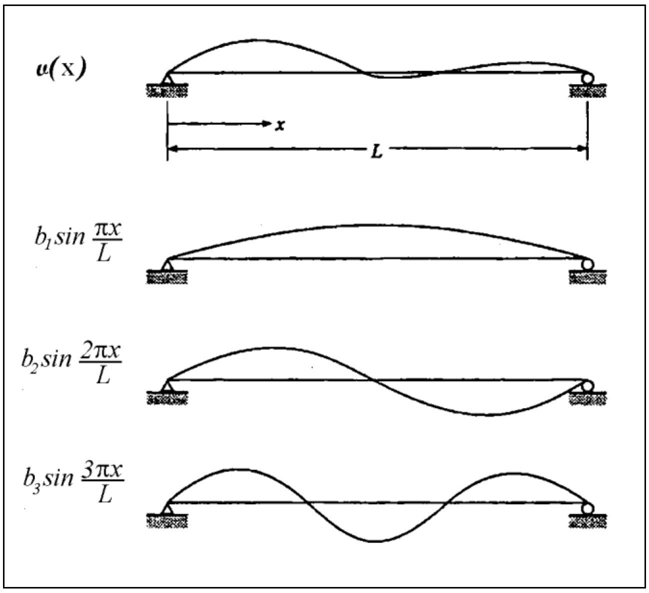

Figure 1.3. Uniformly distributed mass along a beam with deflection comprising superposition of simple mode shapes to produce a complex solution (Clough and Penzien 1993).

The method is useful for uniform beams, poles and slender forest trees, where most of the mass is located in the central trunk and there is little other branch mass. A particular application for this method to trees could be when felling operations occur and trees are stripped of branches so that they effectively become poles.

The third method of expressing displacements uses the finite element method which combines features of both the lumped mass and generalised displacement procedures. It is applicable to all structures and requires computer analysis due to the complex calculations. A structure or beam is divided into an appropriate number of elements whose size may vary, and the ends of each element (nodes) become the generalised coordinates. The deflection of the complete structure can then be expressed in terms of generalised coordinates (Equation 1.1). This method is good for one and three dimensional structures and has the advantages of being able to select the desired number of generalised coordinates by dividing the structure into the appropriate number of segments. For uniform materials, interpolation functions of each segment may be identical and computations are simplified. Applying this method to trees would require taking into account the non-homogenous qualities of material and shape, the complex three dimensional structure and require a complex mathematical solution. The method has been applied to sections of a tree is described by Mattheck (1990) and a branch section is shown in Figure 1.4. The finite element method is not used in this thesis but has potential for developing a more complete (and complex) analysis.

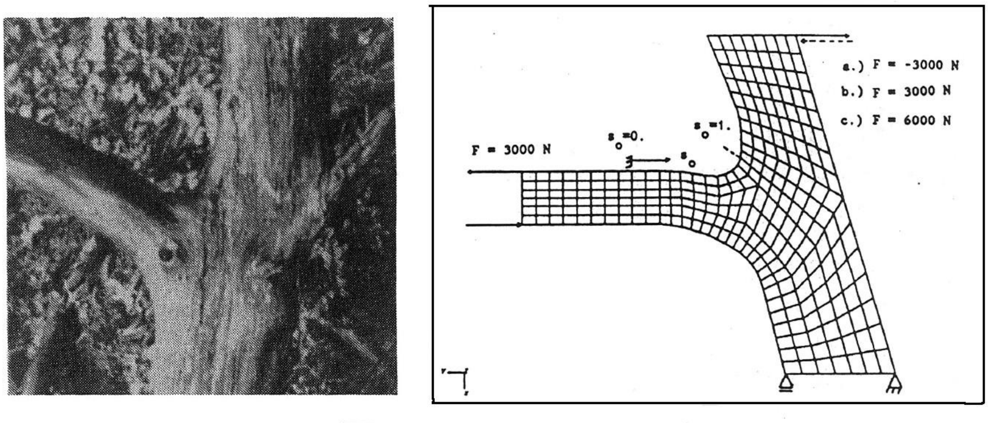

Figure 1.4. Branch joint of a tree, with finite element representation to visualize stress distribution (Mattheck 1990).

1.3 Tree Diversity and Data Sets

This study investigates the dynamic response of trees to wind so it is important to consider the diverse structures of trees, their growing conditions and wind environments, particularly when comparing forests and urban conditions. Forest trees can grow very close together, so that the wind may only impact on the very top part of the canopy. The mean profiles of wind speed along a stand edge of Scots Pine show almost constant velocity from bottom to top of the canopy (20% less at the bottom), but within the stand the wind profile is concentrated in the top 30% of the tree (Peltola 1996b, Moore and Maguire 2008). Due to strong competition for light below the crown top, forest trees (particularly plantation trees) grow with a tall, slender form and may not develop significant side branches. The significance of branches on the dynamic response of trees to wind is a fundamental issue in this thesis.

The size of a tree is also an important parameter because large trees have a different morphology to small trees and it is probably unsound to test trees less than 3-4.5m (10 to 15 ft) high (Mayhead 1973). Further discussion of variability in results arising from differences in morphology and Mayhead (1973) emphasises the need to allow for natural variation of trees within species and across species, and to be careful when attempting to extrapolate data. Gilman et al. (2008a) used 6.1m high trees with a slenderness ratio of 68 in wind tests using a high powered wind generator to study effect of wind, but also cautioned against extrapolating the results to larger trees.

The ability of a tree to withstand wind forces is greatly affected by its slenderness which is defined as the ratio between the height (h) and the trunk diameter at breast height (DBH) which is usually taken as 1.3 m in height above the base (Peltola 1996b). The ratio of height to diameter (h/DBH) gives a measure of slenderness. A stable tree that is well able to withstand high wind loading will have a lower slenderness ratio than a tall, thin tree which can become so slender that it can buckle and not be able to stand under it own weight. Depending on which type of tree is studied, particularly when focussing on wind responses, the data set of results will vary and possibly different conclusions may be drawn.

Trees have evolved over millions of years by adapting to a wide range of environments to become the species and individuals of today. Some trees have evolved in closed forest environments and some in open savannah environments (White 1986). Trees evolved along two different paths to become either conifers (gymnosperms) or flowering plants (angiosperms). The tallest conifer is the coast redwood of California, USA (*Sequoia sempervirens*) (The Gymnosperm Database 2008) and the tallest angiosperm is the mountain ash of Australia (*Eucalyptus regnans*), (Forestry Tasmania 2008). Even in a given habitat, trees are a diverse lot and almost nowhere has one design emerged as clearly superior (Vogel 1996). Trees do not grow at random but do so in predictable ways following strict principles (Harris et al. 1999). Mechanical forces have challenged plants throughout their evolutionary history (Grace 2003) and the size and form of an individual tree is the product of a basic genetic blueprint modulated by the external environment over time. Vogel (1996) suggests that part of the explanation for the diversity lies in the large number of factors involved in standing up to the wind and the number of functions to which each structural element must contribute.

The physical limitation of the height and size of a tree, due to the limits of the strength of wood, was first published by Galilei (1638) in a discussion on how large a tree can grow. "For every machine and structure, whether artificial or natural, there is set a necessary limit beyond which neither art nor nature can pass; it is here understood, of course, that the material is the same and the proportions preserved. An oak tree two hundred cubits high would not be able to sustain its own branches if they were distributed as in a tree of ordinary size." (Galilei 1638, p3, p4). Another way of expressing this idea is that as trees get bigger, they approach the limits of strength of the wood and get nearer to a failure point. The tree can increase in size but the material properties of wood cannot increase beyond certain natural limits. The effect is that tall trees are different in a structural sense from small trees. Therefore height and age of trees should be considered in any structural analysis. The allometry of tree height with respect to trunk diameter occurs throughout the life of trees as they age and grow larger (Niklas 1997a). The slenderness ratios of trees in a forest vary with age and silvicultural treatment (thinning) and a simulation by Cucchi et al. (2005) for Maritime pine (*Pinus pinaster*) showed a decrease in slenderness ratio of 70 to 54 from age 25 to 50 years as the trees grew taller.

The slenderness ratio of a tree, is expressed as a ratio of height (m) divided by diameter (m) for single trees in urban situations (Harris et al. 2004, Mattheck 1994) or as a slenderness coefficient in forest studies where the height is measured in meters and the diameter measured in centimetres (Rudnicki et al. 2001). Although both are measures of the same slenderness ratio, a slenderness ratio of 75 will be expressed as a slenderness coefficient of 0.75. This variation in quoting slenderness is usually overlooked in the literature but can have a significant effect on the dynamic response of a tree to wind loading. A very tall slender forest plantation grown tree will have a central trunk and very few branches so it will respond dynamically like a pole or chimney which is the approximation used by Kerzenmacher and Gardiner (1998) when modelling tree behaviour (Sitka spruce) with a slenderness ratio of 75. An extreme example of a tall thin forest tree with a slenderness ratio of 160 (expressed as slenderness coefficient of 1.60) was used in a dynamic study of tree sway (Rudnicki et al. 2001). These trees were lodgepole pine (*Pinus contorta*) in a forest stand in Alberta, Canada with a height range of 9.4 to 15.3 m. In a similar study, Rudnicki et al. (2008) used trees with a mean slenderness ratio ranging from 79 to 134 which was a different definition of slenderness from their previous study. This is a very high to extreme slenderness figure for a tree and the results from this data set will be very different from trees with a much lower slenderness figure.

Slenderness coefficients above 100 generally indicate low stability and a tree is likely to buckle under its own weight. For forest trees, slenderness ratios below 80 indicate excellent stability (Slodicak and Novak 2006). For trees in urban areas, lower slenderness ratios of 50 have been proposed by Mattheck et al. (2003) because the wind environment is more exposed than in forests. To put these values into perspective, the slenderness ratio for the tallest tree, a coast redwood, (*Sequoiadendron giganteum*) is in the order of 10.5 (Niklas 1992). This is based on a height of 83.9m (275 ft) and a basal girth 25.1m (82.3 ft) which may not be the extreme but is representative of a tall tree that have survived for many centuries. A list the trees and their height, diameter and h/d ratios as well as some other trees for comparison are presented in Table 1.1.

Tree No.	Common Name	Botanical Name	Location	Height *h (m)*	DBH *m*	*h/DBH*
1	Hoop pine 1	*Araucaria cunninghamii*	Burnley	22.0	.796	28
2	Hoop pine 2	*Araucaria cunninghamii*	Burnley	19.0	.939	20
3	Hoop pine 3	*Araucaria cunninghamii*	Burnley	23.5	.875	27
4	Italian Cypress	*Cupressus sempervirens*	Burnley	17.0	.232	73
5	Mountain Ash	*E. regnans*	Erica Tree	N/A	N/A	N/A
6	Flooded gum	*E. grandis*	Burnley	19.3	.522	37
7	Palm	*Washingtonia robusta*	Burnley	18.1	.436	41.5
8	Red gum1	*E. tereticornis*	Sale	14.0	.843	17
9	Red gum2	*E. tereticornis*	Sale	14.0	.886	15
10	NZ Kauri pine	*Agathis australis*	Sale	23.2	.75	31
11	Branch pluck	*Elm*	Burnley			
12	Mountain Ash	*E. regnans*	Mt Dandenong	50	2.61	19.2
13	Spotted Gum	*Corymbia maculata*	Monash University	25	0.716	34.9
14	She Oak	*Allocasuarina fraseriana*	Melbourne University	23	0.440	52.3
15	Redwood	*Sequoiadendron giganteum* (Niklas 1992)	California, USA	83.9	7.95	10.5
16	Lodgepole pine	*Pinus contorta* (Rudnicki et al. 2001))	Canada	15.4	0.103	160

Table 1.1. Height, diameter and h/d ratio for trees in this project and other selected trees for comparison. Diameter of trunk taken at breast height (DBH).

To emphasise the differences in stability, a diagrammatic representation of some trees from Table 1 may be drawn with respect to slenderness (Figure 1.5).

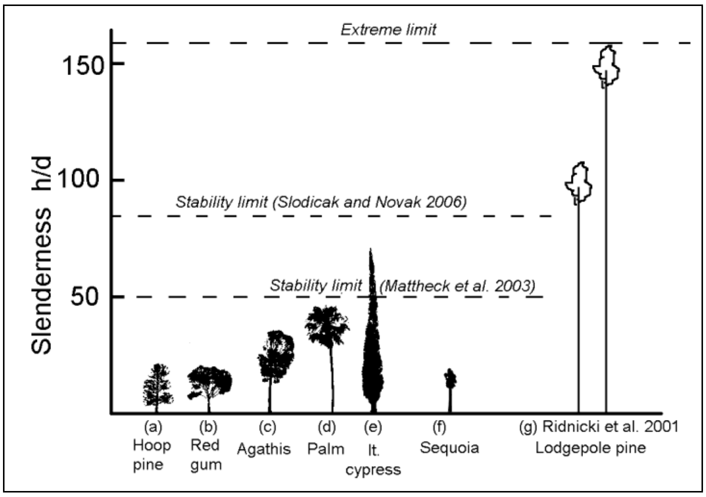

Figure 1.5. Comparison of slenderness ratios of trees, (a) Hoop pine (*Araucaria heterophylla*) (b) Red gum (*Eucalyptus tereticornis*) (c) NZ Kauri pine (*Agathis australis*) (d) Palm (*Washingtonia robusta)* (e) Italian Cypress (*Cupressus sempervirens*) and trees from selected references, (f) Sequoia (*Sequoiadendron giganteum*) (Niklas 1992) (g) lodgepole pine (*Pinus contorta*) (Rudnicki et al. 2001).

It should be noted that the tallest tree, the coast redwood, (*Sequoiadendron giganteum*) has a height of 110 m yet is in the low range for slenderness, showing it is very stable. The sequoia has a structure that has been able to stand all forces for approximately 2000 thousand years. The most extreme example of a slender tree is Lodgepole pine (*Pinus contorta)* only 15.4 m high and growing in a closed forest environment to a slenderness ratio of 160 (Rudnicki et al. 2001). This tree is in a managed forest and would not stand without the support of its neighbours (Slodicak and Novak 2006).

In urban areas, trees from a wide range of species are grown as individuals in environments that may be very different from their native habitat in which the evolutionary process occurred. The trees studied in this project were open grown trees of medium to large size (height range 14 to 50 m) with a slenderness ratio well below 50, except for the palm and the Italian cypress. The palm is technically not a tree (a monocotyledon) and has no branches and the Italian cypress is an exceptionally slender tree with a unique flexible response. Both these trees survive extreme wind speeds and are discussed separately.

An important consequence of this diversity is that trees with different height, diameter and slenderness can give different results, depending on the tree selected. For a dynamic analysis this can be important. Open grown trees grow predominantly as single trees in open spaces and can develop large branches. As they grow in size, the dynamic interaction of these branches can become significant. Hence, the trees selected for this study are large open grown trees, with a range of shapes and branch architecture, so that the effect of branches on the dynamic response to wind can be examined.

1.4 The Philosophy of Structural Assessment

Arborists often ask if a tree is safe and when will it fail? They want an immediate answer to assess the tree for the likelihood of failure and to decide whether to keep the tree or condemn it as unsafe. Trees can fail in two ways, (a) by breaking at the trunk or (b) by uprooting and overturning when the soil/root plate structure fails. If a structural analysis can provide accurate measurements on tree strength and loading under storm conditions, the information may be useful in making decisions about the future of trees which may be considered at risk. However a structural analysis of a tree may not predict failure because of the great variability in trees and their environment including the wind conditions, the above ground tree strength and below ground conditions of the roots and the soil. Because of this great variability, for any one particular tree, measuring the strength may not be enough to predict failure.

It is instructive to consider an engineering perspective on the properties of materials and man-made structures such as bridges. Engineering materials like steel are usually considered homogeneous and isotropic and structural tests are made under controlled conditions until failure occurs. Wood is neither homogeneous nor isotropic. Structural wood that is a uniform product after drying and milling behaves in a predictable manner and can be treated like an engineering material. A typical structural test of two wood samples of different species is shown in Figure 1.6 (Brudi 2002).

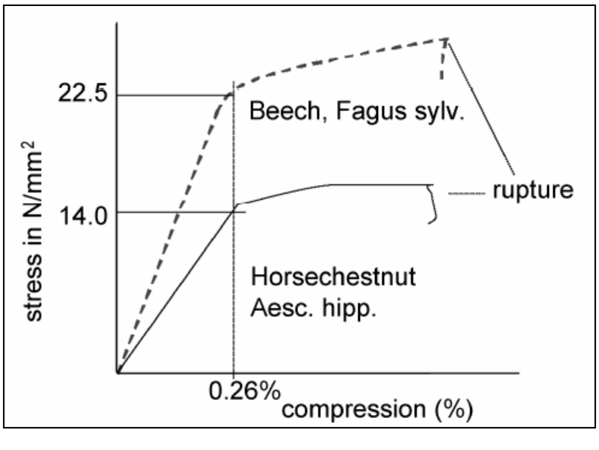

Figure 1.6. Structural compressive tests on green wood for two tree species (Brudi, 2002).

From these tests, the structural properties of wood can be determined. Perhaps the most famous and the most useful of all concepts in engineering is called Young's Modulus, which defines the stiffness or floppiness of a material (Gordon 1968). The Young's modulus can be calculated from the initial straight line response of the curve in Figure 1.6. The straight line part of the curve is known as the elastic range because the material can be loaded and unloaded over many cycles without any damage or deformation occurring. At the top of the straight curve, the material begins to deform so the curve deviates from the original straight line. This is known as the plastic range. The slope of the straight line gives the value of E. The units quoted for E values are varied and can be confusing because there is not one standard unit used in the literature. E values presented here are in units used in the original referenced paper where applicable. (For conversions 1 GPa = GN m^{-2} = 1000 MPa = 1000 N mm^{-2}).

Plastic failure begins to occur as the material starts to fail and the curve becomes flatter until finally the specimen completely fails at the point marked as rupture (Figure 1.6). Many tests are made until an average curve is developed and it is possible to predict failure based on these tests, as long as the material has the same properties as the test specimens. There are considerable data on the properties of structural wood (Brudi 2002) but not much on wood in living trees Niklas (1992). Great caution should be exercised in treating the mechanical properties of botanical materials like wood as constants since they vary with the age and relative moisture content of the sample (Niklas 2002). From the limited studies on living trees, it has been shown that wood properties vary with age on the same tree (Mencuccini et al. 1997).

Structures such as bridges are built by engineers with a certain design load set as a specific structural criterion. Once the bridge is built, the structure is tested by applying loads to values above this design load to ensure that it is strong enough to withstand all expected loads. This is known as a proof test, i.e. to prove that the structure is strong enough for the design loads. A proof test does not predict failure and may not be capable of predicting failure but does demonstrate that the structure can safely withstand expected loads. The concept of a proof test is useful to apply to trees and has been successfully used to measure the loads on trees considered at risk, and establish that they are strong enough to withstand expected wind loads (James and Haritos 2008). The methods described in Chapter 4 are therefore useful to quantify the dynamic loads on the trees and provide data that may assist to evaluate how a tree may be able to withstand future wind events. However, the methods may not be able to predict failure.

1.5 Outline and Aims of the Research Project

This project aims to investigate the wind forces on trees and measure the tree dynamic response to wind loads during storms.

This project will examine a range of trees that are commonly used in urban areas. The purpose is to compare a variety of structural shapes and configurations. A focus will be on studying how branches influence the dynamic response of a tree so the following configurations of trees will be monitored:

1. trees with no branches – palms
2. trees with a tall, slender form – Italian cypress
3. trees with a central trunk, and side branches – conifers
4. trees with no central trunk, and a spreading form with considerable side branches – Eucalyptus, Agathis.

All trees will be as large as possible and attempt to represent typical trees found in urban situations.

A literature review is presented that examines previous studies and attempts to demonstrate how they have largely ignored branches. Limitations of previous models are also discussed because they mainly consider the tree as a single tapered stem structure and branches are either ignored (Greenhill 1881) or are considered as simple masses rigidly attached to the central mass (Guitard and Castera 1995, England et al. 2000, Saunderson et al. 1999 and Wood 1995).

The complexity of the dynamic loading has usually resulted in studies which make simplifying assumptions about the shape and structure of a tree, and the wind loading upon it. These assumptions include considering trees as an inverted pendulum (Coder 2000); as single stem tapered columns (Wood 1995); and as single stem, multi-section columns with masses at different heights to simulate canopy (Guitard and Castera 1995, Saunderson et al. 1999). These studies attempt to model tree structure and movement but ignore branches, or treat them as static masses on the single central trunk. Wood (1995) states that until now, analysis of tree bending and vibration has not been sufficiently sophisticated to take account of branches as anything other than added masses at each level.

Simplifying assumptions are also applied to wind which is considered as a constant force (at some maximum value) which impacts on the tree canopy as a sail on a ship (Mattheck and Breloer 1994). Further inherent assumptions, often not stated, are made when the analysis uses fundamental mathematical equations of harmonic motion and not surprisingly, the conclusion is that a tree has a natural frequency and sways back and forth in the wind.

A new structural model of trees is presented, which incorporates the dynamic interaction of the trunk and branches. This dynamic model includes elements for the mass (m), Young's modulus (k), and damping (d - aerodynamic and viscoelastic) of the trunk and branches, both individually and collectively. A new element in this model, not previously identified in the literature on tree dynamics, accounts for the dynamic interaction of branches by introducing mass damping. Mass damping occurs when one swaying mass interacts with the main swaying mass, in an out-of-phase manner that dampens the oscillations of both masses, or 'detunes' the structure. The effect is to minimize the sway movement of the main mass and hence minimizes the forces within the structure during periods of high excitation. In trees, the effect of mass damping is considered to occur when the branches sway in an out-of-phase manner relative to the main trunk, during periods of high winds.

New instruments have been designed to measure wind loads on trees. These instruments attach to the base of the trunk of a tree and can monitor dynamic response continuously, during wind storms. Field collection of data on a range of trees has continued over four years with several trees being monitored continuously for many weeks. The results are presented and discussed to evaluate the proposed model and examine the effect of mass damping.

The specific aims of the project are to;

1. develop new methods to measure dynamic responses of the tree to wind loading. Purpose built instruments will be located at the base of a tree trunk to measure changes in the base bending moments. These instruments will measure dynamic changes and record data over periods of many weeks continuously.

2. develop a new dynamic structural model for trees which introduces the dynamic interaction of branches. The hypothesis to be tested is that the dynamic interaction of individual branches with the whole tree is critical to the dynamic response of the tree. It is further proposed that this dynamic interaction is due to a mass damping effect that has not previously been identified in the literature on trees and wind.
3. conduct field trials on a range of trees commonly used in urban areas, in order to measure the dynamic response of these trees to wind loading.
4. analyse the results from field trials, by applying dynamic principles of structural and dynamic engineering, in order to identifying basic dynamic parameters of each tree, such as,
    a. natural frequency
    b. damping characteristics
    c. drag coefficients
5. discuss the results and relate the observed response of trees under wind loading conditions to dynamic theory and the new model.

Chapter 2. LITERATURE REVIEW

The structural properties of trees must be determined in order to evaluate their strength and stability, particularly in relation to their ability to withstand wind loads under storm conditions. In urban areas it is important to assess the risks associated with tree failure so that managers can make decisions on whether to keep or remove a tree.

Wind damage to forest trees is a major problem resulting in huge economic losses (Quine et al. 1995, Peltola et al. 1999, Achim et al. 2003, Cucchi et al. 2005, Peltola 1996a, 1996b, Zeng et al. 2007, Gardiner et al. 2000, 2008, Schelhaas 2008, Wood et al. 2008). Wind speed is the most important factor contributing to wind throw but other factors including topography, soil conditions, silvicultural treatment and stand structure are also important (Quine et al. 1995, Moore 2000, Cucchi and Bert 2003, Gardiner et al. 2008). Structural information on tree stability is useful to managers of forests who need to assess the likelihood of wind damage and consequent economic loss and to managers of trees in urban areas who must assess the risk of failure that may results in death or injury to people or damage to property (Mattheck et al. 2003).

2.1. The Structural Analyses of Trees

The first quantitative structural analysis applied to a tree was an attempt to calculate its maximum size by Leonard Euler and later Greenhill in 1881 (Spatz 2000). The tree was considered as a tapered pole and only static methods were used. The analysis evaluated the gravitational loads of self weight of the tree and the maximum height before it failed under its own weight. There was no consideration of branches and there was no attempt to investigate dynamic response of the tree under wind loading. The analysis was applied to a pole made of a homogeneous material which was a simplification used to approximate a tree.

In the last twenty years there has been considerable study of tree structures using static methods. Advances in the technology of instrumentation and data logging has allowed more accurate measurements at high speeds which has resulted in dynamic methods of tree analysis being more widely used. Niklas (1992) summarises the history of plant biomechanics and describes the basic principles of structural engineering theory which are being applied to the study of plant forms. However, care must be taken in applying well developed engineering beam theory to trees, as green wood differs from normal engineering material.

A mechanical approach to tree biomechanics, using some mathematical simplifications was used by Mattheck and Breloer (1994) to develop the axiom of uniform stress which described a concept whereby growth of the tree is in response to the loads placed upon it. This work highlighted the importance of understanding the loads that a tree endures during its life and explained how the growth response of a tree can influence the stresses that develop within the structural components of the trunk and the branches. The mechanical analysis of Mattheck was limited to a static approach where loads were considered to be constant. This is valid for gravitational forces of weight, snow and ice, especially on large trees in forests where dynamic forces such as wind may not be significant. The static approach does not represent the conditions where rapidly changing loads occur, especially loads due to wind. Mattheck and Breloer (1998) considered wind as a statically applied force, and any variations were considered by changing the value of the static load.

Structural and biomechanical studies of trees in winds have been presented by Coutts and Grace (1995) in which the interaction of trees and wind was studied by various authors, using either a static analysis or some elementary dynamic studies. Previous studies of tree structures have used a range of methodologies which include, (a) field experiments of tree response to winds or mechanical pulling (Sugden 1962, Hoag et al. 1971, Mayhead 1973a, Mayhead et al. 1975, Oliver and Mayhead 1974, Holbo et al. 1980, Mayer 1987, Petty and Swain 1985, Bell et al. 1991, Milne 1991, O'Sullivan and Ritchie 1992, Gardiner 1995, Rodgers et al. 1995, Baker 1997, Hassinen et al. 1998, Peltola et al. 1993, 2000, Flesch and Wilson 1999b, Rudnicki et al. 2001, Moore 2000, 2002, 2003, Moore and Maguire 2005, Brudi 2002, Fleurant et al. 2004, Cucchi et al. 2004), (b) wind tunnel experiments of model canopies (Mayhead 1973b, Finnegan and Mulhearn 1978, Smith et al. 1987, Vogel 1989, Gardiner 1994, Gardiner et al. 1997,2005, Hedden et al. 1995, Rudnicki et al. 2004, Volsinger et al. 2005, Wood 1995), (c) field or laboratory testing to obtain the mechanical properties of trees and parts of trees (Cannell and Morgan 1987, Milne and Blackburn 1989, Rodgers et al. 1995, Peltola et al. 2000, Silins et al. 2000, Brüchert and Gardiner 2000, Spatz and Brüchert 2000, Herejavi 2004, Moore and Maguire 2008), and (d) theoretical mathematical modelling (Baker 1995, England et al. 2000, Kerzenmacher and Gardiner 1998, Spatz and Brüchert 2000, Guitard and Castera 1995, Saunderson et al. 1999a).

Forests trees and open grown trees

When reviewing the literature on structural testing of trees, differences in strategies and results are noted which depend on the structural configuration and shape of the trees under consideration. Different outcomes may occur due to the structural shape of the tree, particularly its slenderness and the number of branches and differences in the wind environment that a tree endures.

The structural shape of the tree depends on its environment. In a forest plantation, trees are nearly always of an excurrent shape because they grow close to their neighbour and become tall and thin with little side branch development and small crowns. In urban areas, trees often grow as single specimens and develop significant side branches and have greater trunk thickening which makes them more stable. Their shape may be either excurrent or decurrent (Harris et al. 1999) and if large side branches are present, they will contribute to and modify the dynamic response of the whole tree. Important differences between forest and urban grown trees also occur in the wind loading environment. Closely spaced forest and plantation trees experience wind loads only on the top of their canopy. Trees growing in urban areas will be in a wind environment where significant side loads may occur.

This chapter reviews previous studies of trees that have taken a structural perspective and have used engineering methods. The application of engineering structural theory to plant biomechanics has led to a greater understanding of loads on trees and their growth responses to these loads. There have been considerable studies using static methods but there have been only limited studies of the dynamic response in high winds of large open grown trees in the field.

2.2 Structural Properties of Trees and Wood

The structural properties of wood in trees which are of interest in this study include strength, Young's modulus (E), and the modulus of rupture (MOR) at failure. Gordon (1968) notes the difference between strength and stiffness (or Young's modulus) by stating "*Lest there be any possible, probable, shadow of doubt, strength is not, repeat not, the same thing as stiffness. Stiffness, Young's modulus or E, is concerned with how* *stiff, flexible, springy, or floppy a material is. Strength is the force or stress needed to break a thing. . . . The two properties together describe a solid about as well as you can reasonably expect two figures to do."*(Gordon 1968 p41).

The importance of the stiffness or E value of wood in trees is emphasised in dynamic studies of trees. Results from finite element analysis on Douglas fir trees showed that structural damping due to branches is an important component of the overall damping of tree oscillations, particularly when branch E values are low (Moore and Maguire 2008). Low stiffness values in the upper part of the tree and branches allow the tree to streamline in high winds (Spatz and Brüchert 2000) which reduces their exposed frontal area, consequently reducing the total wind force. Effect of wind exposure on mechanical properties of trees and wood may also contribute to variation in stiffness. Trees respond to load (Mattheck and Breloer 1994) and parts of a tree strengthen in response to wind loads. Brüchert and Gardiner (2000) showed that wood stiffness properties vary within a tree, especially in relation to orientation of wood within the stem relative to the prevailing wind direction (leeward versus windward).

The structural properties of wood in living trees are different from those of wood used for construction which has been sawn and kiln dried. This study investigates living trees and appropriate structural properties are described later, but for comparison some brief discussion of the structural properties of sawn wood products is appropriate. Timber properties and methods of testing are described in standards such as Australian Standard AS 1720.2 (2006) Timber structures and Timber properties, and the American Standard for testing wood ASTM 143 2007 and ASTM Standard D143 (2009) Standard Test Methods for Small Clear Specimens of Timber. Silins et al. (2000) reported results which support the notion that mechanical properties measured from small green-clear wood samples may not be representative of true properties for whole living trees. Results from Silins study showed significant differences in both stiffness (E) and strength (MOR) of 43 year old, 10 metre tall lodge pole pine trees between winter when sapwood is frozen and spring when sapwood is thawed. The values were 50% greater in winter than in spring. This contrasts with tests performed on a variety of species of street trees in England (Roodbaraky et al. 1994) using the pull and release tests and also measuring tree response under wind loading. These tests concluded that for the eight street trees tested there was no variation of stiffness with season.

Wood samples are taken from trees or sawn logs, kiln dried then tested in a number of ways to determine their mechanical properties. The most common mechanical tests use wood samples free of defects to test for tensile strength, compression strength and flexural strength. Wood is a composite material, is anisotropic and heterogeneous, and mechanical behaviour at failure is not an all or none process (Spatz and Brüchert 2000). The strength of wood is three to four times as strong in tension as in compression (Gordon 1968) because the cell walls fold up in compression. Wood is difficult to test in tension so it is more common to quote figures for compressive strength. It is also important to note that strength properties of living wood in trees (in situ) is quite different from the strength properties of kiln dried structural grade wood or timber. There is less information on strength values of wood in living trees.

In addition to the variations in tensile and compressive strength, Niklas (1992) identifies the difference in wood strength in three orthogonal directions, longitudinal, radial and circumferential (Figure 2.1). When dealing with plants, the material is not isotropic but rather orthotropic, and will have different properties in each direction. It is therefore be important to identify the E value in each direction. These directions can be designated longitudinal E_L, transverse E_T and radial E_R. Unfortunately, the literature on plant materials rarely provides all of the elastic moduli (Niklas 2002).

The elastic modulus of wood, under uniaxial compression along the grain, E_L, can differ by one or two orders of magnitude from the elastic moduli measured in the tangential and radial directions to the grain, E_T and E_R. Values for Balsa of E_L = 3.12 GN m^{-2}, E_R = 0.144 GN m$^{-2,}$ and E_T = 0.0468 GN m^{-2} illustrate this difference Niklas (2002). Niklas points out that the literature on plant materials rarely provides all of the elastic moduli and it is normal to quote only one value.

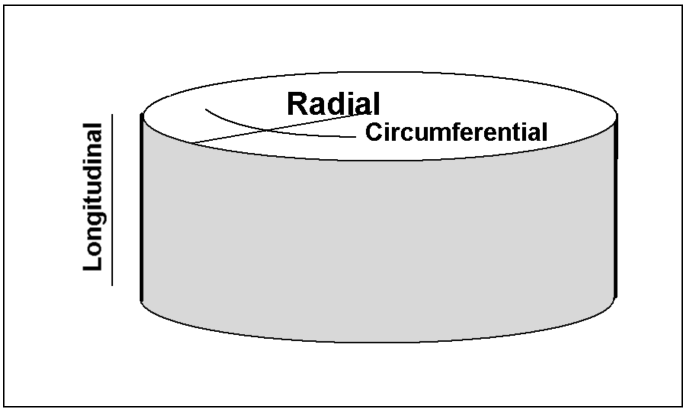

Figure 2.1. Young's modulus (E) of wood (balsa) in three directions. Longitudinal (in compression) E_L = 3.12 GNm^{-2}, radial E_R = 0.144 GNm^{-2} and tangential E_T= 0.0468 GNm^{-2} (Niklas 1992).

The units used to describe Young's modulus vary. Units used by different authors include N mm^{-2} (Brudi 2002), MPa (Silins et al. 2000), GPa (Milne and Blackburn 1989, Rodgers et al. 1995), GN m^{-2} (Niklas 1992) and some unusual units of kgf cm^{-2} (Vidal et al. 2003). For comparison, some values from previous published literature are presented in Table 2.1 with the values converted from the original publication to MPa where necessary.

Tree Common Name	**Tree Botanical Name**	**Young's Modulus MPa**	**Comment**	**Reference**
Balsa		3120	Longitudinal value	Niklas 1992
Pine Wood		8510		Niklas 1992
	Betula pendula	14500	Bending tests on wood samples	Herajavi 2004
	Betula pubescens	13200		Herajavi 2004
Lodge pole pine		6621	Living trees winched in Spring	Silins et al. 2000
	Terminalia ivorensis	9443	Wood samples in bending test	Okai et al. 2002
Horse chestnut	*Aesculus hippocatarium*	5250	From wood samples	Brudi 2002
Beech	*Fagus sylvatica*	8500	Wood sample	Brudi 2002
Scots pine	*Pinus sylvestris*	*11350*	Tree pull tests, Finland	Peltola et al. 2000
Norway spruce	*Picea abies*	*7730*	Tree pull tests, Finland	Peltola et al. 2000
Birch	*Betula spp.*	*11060*	Tree pull tests, Finland	Peltola et al. 2000
Sitka spruce	*Picea sitchensis*	2400 to 7500	Green timber sections from trunk	Cannell and Morgan 1987
Sitka spruce	*Picea sitchensis*	2000 to 6400	Pull test on living trees, Scotland	Milne and Blackburn 1989
Sitka spruce	*Picea sitchensis*	*5700*	Tree pull tests, Ireland	Rodgers et al. 1995
Sitka spruce	*Picea sitchensis*	*5120*		Saunderson et al. 1999
Sitka spruce	*Picea sitchensis*	*3600-9600*	Sections of living trunks and branches	Cannell and Morgan 1987
Sitka spruce	*Picea sitchensis*	*5000 to 8000* *12000 max*	60 standing trees, Scotland	Brüchert and Gardiner 2000

Table 2.1. Values of Young's modulus of trees from previous studies. Note: Values expressed on MPa in this table for comparison, have been converted from previous studies where necessary.

The Young's modulus value or stiffness varies with tree species, the method of testing and also with the position and maturity of the wood in the tree. Tests from wood samples that are removed from a live tree and tested in a laboratory will differ from values obtained from a live tree due to absence of growth stresses (Kubler 1987) and the testing method used (Niklas 1992).

As wood ages it stiffens and the Young's modulus value for new wood is different to older wood (Mencuccini et al. 1997). In their study of the structural characteristics of Scots pine (*Pinus sylvestris L.),* tests from wood samples showed that as wood aged and matured, it changed its elastic properties and gradually became stiffer. Young's modulus increases with tree age from about 1700 MPa at 7 years to about 7900 MPa at 25 years and then remained substantially constant. This compares with E values assumed to be 7000 MPa (Peltola and Kellomaki 1993) which is considered typical for green coniferous wood such as Scots pine.

The flexural stiffness of a tree stem, given by multiplying Young's modulus (E) by the second moment of area (I) was determined in a study of 56 Norway spruce subject to pulling tests (Brüchert et al. 2000). Within a single stem, the flexural stiffness of the axis was found to decrease with increasing height (Figure 2.2). Examples of obtaining structural properties of wood are given by Illic (2001), Vidal et al. (2003), and Herajarvi (2004).

Vidal et al. (2003) tested 27 Pinus radiata trees from a Chile plantation with a planting density 625 trees/ha, that had been thinned to 171-192 trees/ha. Wood samples were taken from these trees and dried to 12%.

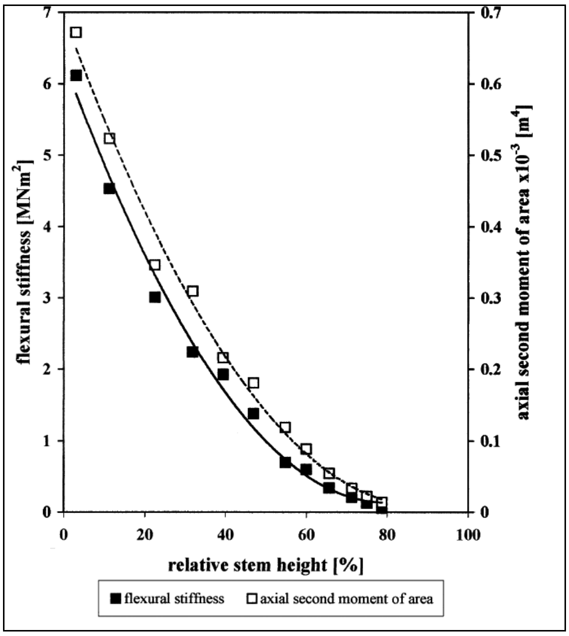

Figure 2.2. Variation of flexural stiffness (EI) along a stem of Norway spruce (*Picea abies*) (Brüchert et al. 2000).

Each sample was cut to a standard size of 25 x 25 x 410 mm, then tested under static bending in a Universal testing machine according to ASTM D 143 (1994). Young's Modulus values (MOE) of 69.7 x 10^3 kgf cm^{-2} were found. Illic (2001), who tested dry specimens of *Eucalyptus delegatensis* in Australia and obtained values in the longitudinal, radial and tangential directions. Herajarvi (2004) obtained Young's modulus (MOE) values of Finnish birch (*Betula pendula Roth* and *B. pubescens Ehrh*). For *B. pendula* MOE 14.5 GPa, MOR 114 MPa; *B. pubescens* 13.2 GPa, 104 MPa. Norway spruce (*Picea abies* (L.) Karst) trees were subject to winching tests and young's modulus values ranging from 5350 MPa to 22700 MPa were found by Jonsonn et al. (2006). The method used to estimate E was to iteratively change its value until measured and calculated stem rotations corresponded.

Niklas (1992) notes the importance of torsional forces in plant structures which develop when a shaft is twisted. It is recognized that torsion is a contributing force to the total forces developed in a tree during wind loading but the methods and equipment to measure torsion in trees in the field have not yet been developed. Modeling of Maritime pine tree (*Pinus pinaster*) and particularly the transverse displacements significantly underestimated the actual displacements measured in the field and it is suggested that torsional forces contribute significantly to the discrepancy (Sellier et al. 2008). Modelling was used to predict failure of Scots pines due to bending or torsional loads during critical wind exposure (Skatter and Kucera 2000). There was no difference between the stands when it came to predicting failure modes which suggest that torsion may be as critical as bending as a failure mode in trees. The fact that torsion may be as critical as bending was a new finding however no field measurements were made or critical failure values for torsion given. It is recognized that the analysis used in this study is limited to longitudinal forces due to bending only.

Recent studies use a more complex analysis of tree dynamic response under wind loading using sophisticated methods such as finite element analysis (Sellier and Fourcaud 2009). In their investigation of how wind can alter plant growth and hence mechanical properties such as Young's modulus, a study of a 35 year old Maritime pine (*Pinus pinaster*) was made and the influence of branches and tree morphology was evaluated. It was concluded that the material properties play only a limited role in tree dynamics and that other factors such as branches and tree morphology may be more important. Sellier argued that small morphological variations can produce extreme behaviours such as very little or nearly critical dissipation on stem oscillations. The effects of branch geometry on dynamic amplification are substantial yet not linear. This concept may be important to consider and modify the emphasis placed on structural properties of trees in influencing tree dynamic response to wind loading.

2.3 Static Analysis of Trees

This section describes the methods of static structural analysis which are used to assess trees. The static approach considers the forces as constants which results in a constant response, usually measured as deflection. This is valid when considering gravitational forces such as weight or dead loads such as snow and ice. The static method of testing trees is highly developed in Germany and is used as a method to evaluate tree stability under wind loads (Brudi 2002). This test has not been widely adopted in other countries as a static approach may have only limited application because the wind induced forces and the tree response are not constant but vary rapidly with time. The dynamic methods of analysis are treated in later sections.

2.3.1 Static pull tests

A static method of assessing the structural properties of trees, called the static pull test, has been used in several studies which are reviewed in this section. This static test uses a rope attached to the upper part of a tree and a controlled pulling force is applied to the rope which causes the tree to deflect in the direction of the pull. The pulling force on the rope is gradually increased until some maximum value is reached. The static pull test may be used to test for a range of tree properties which include (i) to determine mechanical resistance to overturning (Moore 2000, Cucchi et al. 2004); (ii) to estimate strength parameters of a tree which include the strength of the trunk and the anchorage strength of the root plate and soil combination (Silins et al. 2000); (iii) to approximate the wind force acting on a tree and use the results for modelling tree response in winds (Moore and Maguire 2004) and (iv) to estimate the Young's modulus of the trunk or branches (Milne and Blackburn 1989).

Many studies have used the static pull test to assess tree strength and stability (Brüchert et al. 2000, Peltola et al. 2000, Rodgers et al. 1995, Gardiner 1995, Nield and Wood 1999, Papesch et al. 1997, Stokes 1999, Moore 2000, Meunier et al. 2002, Wessoly 1995, Oliver and Mayhead 1974, Brudi 2002, Blackburn et al. 1988, Roodbaraky et al. 1994, Smith et al. 1987, Flesch and Wilson 1999, Silins et al. 2000, Cucchi et al. 2003, 2004, Achim et al. 2003, 2005, Lundstrom et al. 2007, Hedden et al. 1995 and Bergeron et al. 2009). During the static pull test a controlled load is applied to the tree by the rope attached at some height above the base. This results in an overturing moment about the base. Tree failure may occur by either the trunk breaking or by overturning. Measurements are taken during the test, of applied force (kN) and the angle of the root plate. If the root plate rotation exceeds a certain limit, taken as 0.25 degrees by Brudi (2002), the test may be stopped due to concerns about failure of the roots or soil.

Cucchi et al. (2004) describe the static pull method (Figure 2.3) and applied it to 100 Maritime pine trees (*Pinus pinaster* Ait.) in France. The trees were pulled with a force (F) until failure occurred so that the maximum or critical loads could be determined. The nominal height of cable attachment (H_{cable}) was 10-50% up the tree which was lower than one-third to a half used by Moore (2000) and Peltola et al. (2000), and 70% of tree height used by Milne and Blackburn (1989). The bending moment at the base is calculated by multiplying the horizontal component of pull (F_x) and the height of cable attachment (H_{cable}). A winch was used to apply a pulling load to the attached rope and the load was recorded with a load cell. In these tests, the inclinometer at the stem base was used to evaluate soil-root plate rotation and the measurements were recorded every second. The compass direction of pull was also noted so that some correlation with wind direction was possible in later monitoring.

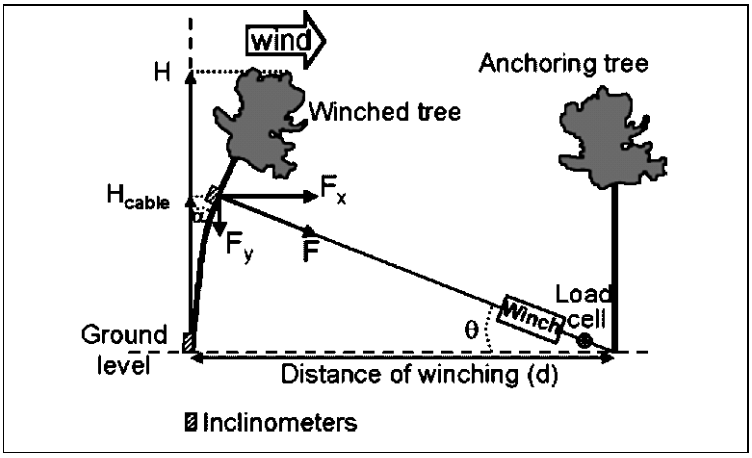

Figure 2.3. Static tree pull configuration to measure overturning load on a tree. Horizontal component of applied force (F_x) is multiplied by cable height (H_{cable}) to calculate bending moment at the base (Cucchi et al. 2004).

The bending moment at the tree base ($BM_{crit,applied}$) that is applied by the pulling rope or needed to cause tree failure was determined from the load cell data according to Equation 2.1

$$BM_{crit,applied} = F_x \cos\alpha H_{cable} + F_y \sin\alpha H_{cable} \qquad (2.1)$$

Where F_x is the horizontal component and F_y is the vertical component of the maximum applied force F(N), H_{cable} is height of cable from the ground and α is the deflection angle of the trunk when the force is maximal. The maximum overturning moment or critical turning moment was calculated for the 100 trees. No tables of critical turning moment were listed in the paper but values can be deduced graphs (Figure 2.4) with a maximum at approximately 350000 Nm (or 350 kNm).

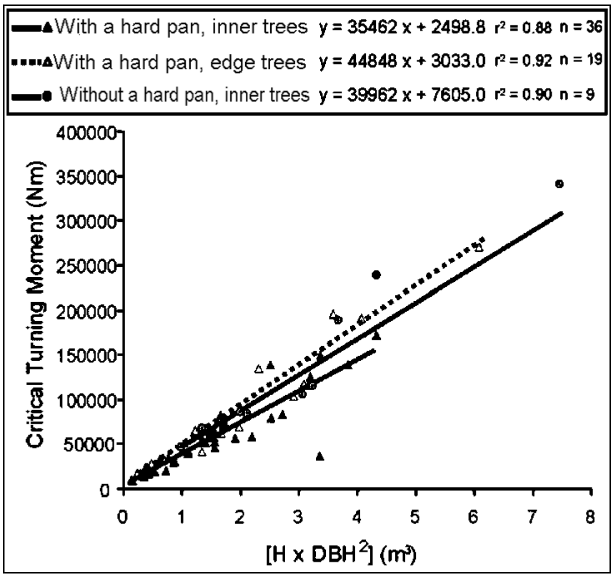

Figure 2.4. Static tree pull results. Maximum overturning moment is 350 kN.m. Pull related to formula (H x DBH^2) to predict stability and failure (Cucchi et al. 2004).

In order to predict tree failure, the critical turning moment was correlated to tree size and particularly to stem weight or volume for Maritime pine. The best predictive variable used the expression ($H \times DBH^2$) which was also used by Moore (2000). This variable was used as the x axis in Figure 2.4 but could not completely explain the variability in the critical turning moment. The slenderness ratio of the forest trees ranged from 54 to 82.

Ten Sitka spruce trees (*Picea sitchensis*) from a 22 year-old plantation in Scotland were winched to failure to determine critical bending moments and compare values to maximum wind speeds (Blackburn et al. 1988). Windthrow was considered as a static process and the maximum values measured ranged from 3.24 to 14.14 kNm for trees with a slenderness ratio varying from 51 to 101. The critical wind speeds to cause uprooting were calculated using measured wind profiles and assuming the wind acted as a statically applied load. The results from these tests found that the static pull test over-estimated the bending moments needed to cause failure and estimated critical wind speeds greatly exceeded real wind speeds recorded during a gale which caused tree damage.

The static pull method was used on a similar 22 year-old Scottish plantation of *Picea sitchensis* to determine elasticity and the vertical distribution of stress. A static analysis using simple beam theory found Young's modulus values to vary from 2 to 6.4 GPa (Milne and Blackburn 1989).

Living lodge pole pines were tested with the static pull method to examine how changing temperature due to seasonal variation affected the strength of trees (Silins et al. 2000). Randomly selected trees with an average height of 9.9 m were winched near or past the point of breakage over a range of temperatures (-16 to +17 °C). Static flexure theory for cantilever beams was used to estimate, stress, strain, Young's modulus (E) and modulus of rupture (MOR). Trees were stiffer and stronger in Winter when the wood was frozen by nearly 50% than when wood was thawed in Spring. Results also suggested that sway behaviour is temperature dependent and should be considered in wind sway models used on trees in the Canadian regions.

Tree pulling tests in Finland on Scots pine, Norway spruce and birches in frozen and unfrozen soil were conducted by Peltola et al. (2000) to evaluate mechanical stability. The maximum resistive bending moment before failure was most significantly and positively correlated with diameter at breast height (DBH) and tree height (H). The best predictor of BM_{max} for uprooting was the relationship H x DBH^2, and the best predictor of BM_{max} for stem breaking was the relationship H x DBH^3.

Highly tapered trees were more likely to break at the stem than to uproot. Maximum bending moment values of 5.9 to (19.2 kNm were recorded for trees of height 12 to 17 m and H/DBH of 96 to 115. These are tall slender plantation trees, near the limit of stability according to Slodicak and Novak (2006).

Tree pull tests were conducted on 164 radiata pine tree (*Pinus radiata* D.Don) in NZ on six different soil types (Moore 2000). Trees were pulled with a hand winch and maximum resistive bending moments were recorded when the trees failed. Three failure modes were observed, stem failure, root failure and uprooting with a maximum bending moment value of 300 kN m being recorded (Figure 2.5). Trees with a high taper (low slenderness ratio) had higher maximum resistive bending moment than trees with low taper. There was a positive correlation for bending moment with tree height, diameter at breast height and stem volume.

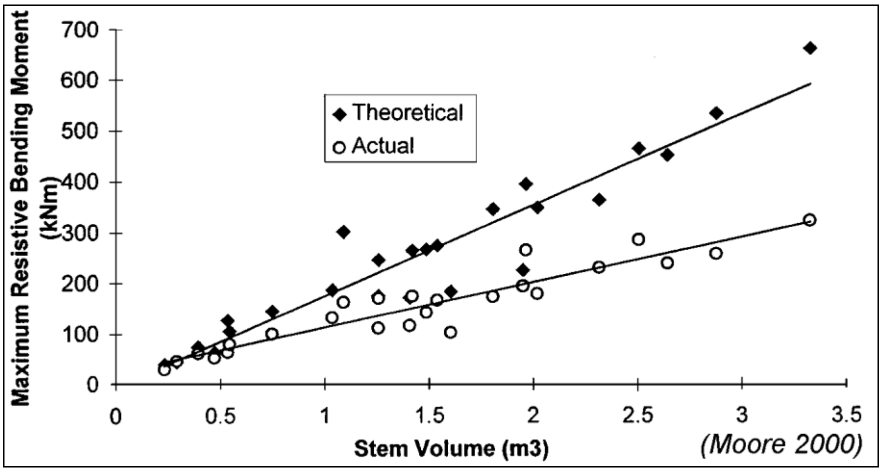

Figure 2.5. Maximum resistive bending moment (kNm) from 164 radiata pine tree (*Pinus radiata* D.Don) in NZ, compared to theoretical values calculated using stem volume (Moore 2000).

Soil type also had an effect on maximum bending moment at failure but could not be successfully modelled using elementary beam theory because of the breakdown of the assumptions of uniform stress and defects in the tree. Pull tests to failure were performed to investigate root-soil rotation stiffness of 5 Norway spruce (*Picea abies* (L.) Karst) growing on sub alpine forested slopes (Jonsonn et al. 2006). Root plate rotation limit to 0.1 degree was used which was lower than the 0.25 degree used by Brudi (2002). Results were evaluated using finite element analysis and evaluation of rotation and Young's modulus of the stem. No definite conclusions regarding soil-root plate rotation were made but they recommended further research and that the tree should be pulled in all four directions to establish soil-root plate stiffness values.

Static pull tests were performed on 66 Norway spruce (*Picea albies* L. Karst) until failure occurred (Lundstrom et al. 2007). Trees aged 45 to 170 year old were used with heights ranging from 9 to 42 m and DBH ranging from 14 to 69 cm. These trees were in a forest stand and were relatively tall, thin trees with slenderness ratios varying from 59 to 119. The maximum overturning moment developed during the winching tests was 880 kNm for the largest spruce tree (H=39 m, DBH = 69 cm) and the minimum value was 11 kNm for the smallest tree (H= 16 m and DBH = 16 cm). During overturning the self weight contribution of the tipping force varied between 10 and 25 % but the value increased greatly with trees of DBH<30 cm but also varied widely. For one tree the self weight contribution to tipping was 68% (DBH = 16 cm) but the lowest value was 6%

(DBH = 64 cm). This compared to previously published values of 60% for self weight contribution to tipping (Coutts (1986).

Tree winching tests were conducted on 107 black spruce (*Picea mariana* (Mill.) B.S.P.) trees in Canada (Bergeron et al. 2009) to determine the critical bending moment at failure. These trees were in forest stands and ranged in height from 12 to 20 m with a slenderness ratio varying from 59 to 129. The maximum bending moment value was 54 kNm for overturning and 25 kNm for snapping (Figure 2.6). There was a strong relationship between stem mass and overturning moment. It was concluded that in windy environments the slenderness ratio should be kept low to increase stability. Silvicultural practices of thinning should not occur too rapidly as trees take time to adapt to wind loading. It was also recommended to examine individual trees as well as trees in groups to assess potential to wind damage.

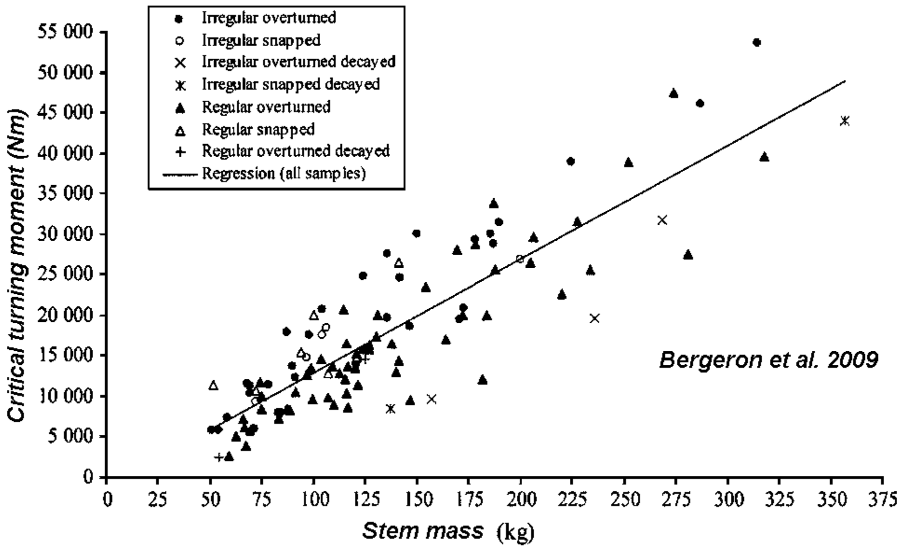

Figure 2.6. Critical turning moments (Nm) versus stem mass (kg) of 107 black spruce (*Picea mariana* (Mill.) B.S.P.) trees in Canada (Bergeron et al. 2009).

Achim et al. (2003) pulled 36 Sitka spruce in Scotland to failure and maximum loads of 80 kNm were found. Tree height was between 25 and 30 m and mean diameter at breast height was 23.4 cm giving a slenderness ratio of 106 to 128 which is considered to be towards the upper limit for a self supporting tree.

The application of the static pull test to estimating the wind loads on trees needs to be more critically examined to evaluate claims that the values obtained represent actual wind loads in the field. The manner in which the tree is loaded is different and may be important in understanding how the trees respond to and survive windy conditions. The rope applies a constant pulling force at one point on a tree, which is very different to the wind which applies a dynamic pushing force that is distributed over the tree canopy. However, the static methods are useful for evaluating structural properties of the trunk and root plate but care needs to be taken when trying to apply results that predict critical wind speeds and failure (Blackburn et al. 1988).

The static test is unlikely to predict failure but is useful for confirming strength. Failure cannot be predicted because the static test stops before the failure zone is reached and with variable biological materials of soil and trees which include imperfections, it is not possible to be definitive about future load bearing capacity and failure. The static test does not give any information about the dynamic response of the tree under wind loading so has some limits in its application to assessing how a tree will perform under future wind events.

2.3.2 Static loads and tree failure

Static tests may be useful to assess the structural properties of a tree but how closely do they represent the actual forces in the field, especially wind forces that come from many directions and are not constant? Can the static test be used to predict the future response of the tree to wind loading or is there a need to use more sophisticated methods that allow for dynamic responses? There is a need for a more comprehensive structural assessment of trees so managers can use the information to assist in making decisions about tree care or removal, especially in urban areas where the consequences of tree failure can be very serious.

The static pull test does not really simulate wind loading because there is no allowance for dynamic sway (Oliver and Mayhead 1974, Gardiner et al. 1997) and the direction of pull is usually in one direction only which may or may not represent the direction from which the wind blows and loads the tree. Results from a static pull test may overestimate the critical wind speed that is predicted to cause tree failure (Hassinen et al. 1998). The conditions of the test may also be different from the conditions at failure, especially if soil moisture has changed due to rain. A test performed under dry soil conditions may be very different from a test when the soil in the tree root plate is wet. The structural properties of wet soil may reduce the stability of a tree which may fail during a storm at loads less than those predicted by the previous test carried out under dry soil conditions.

Because trees are biological structures and the material properties are both variable and subject to degradation if attacked by disease or fungus, their structural performance cannot be guaranteed. Therefore not all tree failures are predictable and therefore not all tree accidents cause liability. Liability may come into account if the failure has been predictable (Mattheck et al. 2003). The issue of tree failure, risk and liability in urban areas is becoming critical for managers of trees who must assess trees for stability and risk of failure (Mortimer and Kane 2004). There is a need to develop a method to evaluate tree stability based on quantifiable measurements to augment the visual assessment methods used at present to assist managers when making decisions to keep or remove trees in urban environments.

In urban areas, most tree assessment is done by qualified arborists on a purely visual basis using a method called "Visual Tree Assessment" (VTA) which is a widely used method based on the "Axiom of uniform stress" (Mattheck et al. 2003). This axiom is described as a major design rule for load carry biological systems and says "that load-adaptive growth in living structures attaches more material at overloaded spots and less or even no material at under loaded parts of the structure" (Mattheck et al. 2003, p219). The VTA method is based on knowledge of the axiom of uniform stress and an understanding of how tree growth develops over the life of a tree. VTA attempts to evaluate the shape and form of a tree as well as identify hazards and areas of potential weakness. It is a purely visual method and no measurements of strength are taken. Many different failure modes occur in trees (Mattheck et al. 2003) often due to invisible factors such as disease or fungi that cause hollows. Mattheck suggest that the probability of failure increases in hollow trees, trees with a high slenderness ratio, trees with cracks and trees that experience a loss of growth stress, particularly angiosperms. Tree trunks can be up to 70% hollow before the probability of failure suddenly increases.

Different species have different failure patterns. In a study of 186 failure reports for Monterey pine (*Pinus radiata*) in California, approximately 60% of failures were due to limb failure rather than trunk or root failure. The majority were considered to be heavy lateral limbs with structural defects suggesting a wood strength problem rather than decay which was not frequently associated with failure for this species (Edgberg et al. 1994). The height of trees in relation to their breast height diameter, their slenderness ratio, seems to be one of the single most important factors determining stem deflection and strength of the tree to resist wind (Peltola and Kellomaki 1993)

Failure of tall thin trees with a high slenderness ratio is a serious problem when the ratio of height (H) to diameter at breast height (DBH) reaches a threshold. Trees with a higher slenderness ratio are at risk of firstly being bent sideways by wind then being pulled down by the weight of their crown. Mattheck et al. (2003) quote a field study of 2500 trees in which standing trees and failed trees were correlated with the slenderness ratio to support the threshold figure of H/DBH ≅ 50 (Figure 2.7).

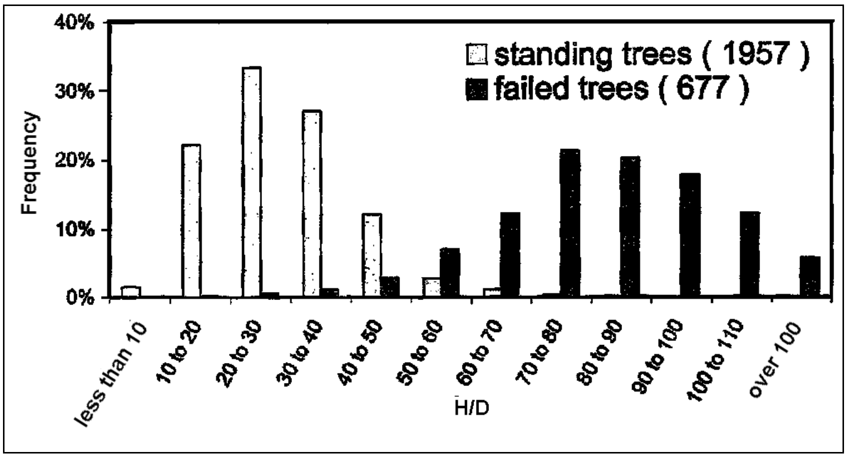

Figure 2.7. Failure of trees depends on slenderness ration (H/D). Values of H/D>50 are considered dangerous for trees standing without support from neighbours (Mattheck et al. 2003).

Petty and Swain (1985) found that slenderness ratio (taper) is probably the most important factor affecting susceptibility to wind breakage. with trees of low taper (high slenderness ratio) being much more susceptible to damage. Slenderness values of less than 60 generally produced stability while values of approximately 100 produce instability.

A summary of static test results expressed in base bending moments (kNm) from previous studies is presented in Table 2.2. The values go from low to high figures and it is apparent that the largest moment values apply to the largest trees. For actual field measurements the largest bending moment published is 800 kNm for a Norway spruce of height 39 m, DBH of 69 cm giving a slenderness ratio of 56 (Lundstrom et al. 2007). The maximum published value of 1219 kNm (Mattheck & Bethge 2000) was determined from calculations based on a theoretical consideration of outer fibre strength of a tree, but no actual measurements were made.

Tree	kN.m	Comment
Sitka spruce (*Picea sitchensis)* (calculated)	0.374	Wind speed 14 $ms^{-1.}$ Kerzenmacher and Gardiner (1988)
Eucalypt -200mm dia. With root rot, Erica, Victoria	6	Data from James, K (unpublished) Winch test in forest, Aust. - failed
Eucalypt - 500 mm dia. Burnley	60	Data from James, K (unpublished) tree stable though with noticeable movement
Sitka spruce (*Picea sitchensis)*, 20 m high	10-52	(Bell et al. 1991)
Norway spruce, 15 m high	13.5 17.5	Uprooting snapping (Peltola et al. 2000)
160 Balsam fir stands, Canada, height 14 to 17m, approx 50 years old.	54	146 trees overturned, 14 snapped. Achim et al. (2005)
Black spruce (*Picea mariana*) 107 trees in Canada.	54 25	for overturning, (Bergeron et al. 2009), for snapping, height from 12 to 20 m, slenderness from 59 to 129.
Spruce 20m high	15-80	Petty and Swain (1985)
36 Sitka spruce (*Picea sitchensis)*, Scotland,	80	Maximum value, Achim et al. (2003) height 25-30m, slenderness 106-128.
NZ trees, 7 sites x 13 trees, 9-39 years old, 28-35 m high	300	Max from winch tree pulls, Moore (2000) PhD.
100 Maritime pine trees (*Pinus pinaster* Ait.) in France.	300	Static pull method ,Cucchi et al. (2004)
Computer generated tree, 25 m height	505	(Brudi 2002)
Plane trees 18m high Parkville	600	Australian Wind Code (AS 1170.2) - Calculated James, K. (2007) unpublished
Static pull tests to failure of 66 Norway spruce (*Picea albies* L. Karst). Age 45 to 170 year old. slenderness ratio from 59 to 119	880	largest spruce tree (H=39 m, DBH = 69 cm) Slenderness ratio 56 (Lundstrom et al. 2007)
	11	for smallest tree (H= 16 m and DBH = 16 cm) Slenderness ratio 100 (Lundstrom et al. 2007)
Calculated from max wood fibre stress. Wind load of 127 kN acts on tree at height of 9.6 m.	1219	(Mattheck & Bethge, 2000) Figure 5. Resultant bending moment is 1219 kNm though this figure not actually quoted.

Table 2.2. Summary from previous studies of overturning moments from static tree pull tests on trees.

Factors influencing tree breakage of conifers in high winds using static beam theory (Petty and Swain 1985) were related to wind speeds. Critical wind speeds were obtained for trees of various heights, tapers and crown to stem weight ratios and it was found that trees with low taper were most likely to break. Tree failure predictions may be based on critical winds speeds but it is difficult to link wind speed to the wind loads on an individual tree and make a valid prediction of failure. It would seem appropriate to use a common unit for wind load and tree strength so the two can be directly compared. The structural properties of a tree are assessed from the static pull test which produces an overturning moment at the base measured in kNm. Wind acting at some speed produces dynamic forces acting on a tree canopy to produce an overturning moment at the tree base which is also in kNm. If both wind load and tree strength can be measured in the same units of kNm then it may be possible to make more accurate predictions of tree failure. This idea is explored more fully in the next section.

2.4 Wind and Trees

A static analysis of how a tree responds in the wind is not a realistic assessment and is an over-simplification which may result in incorrect analysis (Mayhead 1973b). The static analysis hypothesizes that dynamic sway is not directly responsible for wind throw and assumes trees deflect to a point of failure under constant wind speed.

Tree failure has been reported at wind speeds less than those predicted by static pull tests (Hassinen et al. 1998, Fraser and Gardiner 1967, Gardiner 1995, Oliver and Mayhead 1974), presumably because the dynamic forces during storms are so different from the statically applied forces of the test.

A dynamic analysis is complex, even for one tree in isolation (Sellier and Fourcaud 2009). Fluctuating wind forces induce a dynamic response in a tree, including its branches, so more complex methods than simple statics need to be used. The tree is a flexible structure that under wind loading will change the exposed canopy area by realignment and streamlining as the wind speed increases. Drag forces are difficult to assess accurately and may not vary as the square of the wind speed as in engineering structures but at some lesser rate, and even in a linear manner as suggested by Mayhead (1973b).

In the studies of wind and tree dynamic response, various methods have been used and experimental data collected on a variety of trees including models, small saplings and large trees in the field. The results from small trees of one species may not be applicable to other species of the same size or even to larger trees of the same species. This is emphasized by Mayhead (1973b, p124) who stated that it is important "*to use as large a size of fresh tree as possible in order to approximate to true life. It is impossible to model the trees, and it is probably unsound to test trees less than 3 to 4.5m high, for larger trees have a different morphology*". This concept is reinforced in recent studies (Sellier and Fourcaud 2009) who have used complex finite element analysis and conclude that small morphological variations may be very significant in the dynamic response of trees.

A static analysis treats wind from a steady state perspective. A dynamic analysis needs to consider the changes in the wind due to gusts as well as the quasi- steady state component or the average over some time period. It is possible to measure wind speed at some point but it is not possible to directly measure the wind force that is distributed over the canopy of a tree. When the wind acts on a tree, the aerodynamic forces generate a tipping moment at the base which is resisted by the root base (England et al. 2000). It is this base bending moment that gives a measure of the wind loading on a tree and is a product of the wind force (kN) multiplied by the height at which the force acts (m). The two useful measures are therefore wind speed (ms^{-1}) and wind load (kNm). The wind speeds at which tree failure begins to occur are known as critical wind speeds and some previous studies are reported in the next section.

The wind loads measured in base bending moments are not easily measured and have required purpose built instruments to be made for tree studies. Only a few studies have taken this approach (Rodgers et al. 1995, Guitard and Castera 1995, Gardiner et al. 1997, Peltola et al. 2000, Moore et al. 2005, James et al. 2006, James and Kane 2008). Most previous studies of tree dynamics have used more readily available instruments, usually located in the upper part of the tree to measure tree response parameters such as displacement, tilt, accelerations which were used as estimates of wind loading. Discussion on instrumentation in tree dynamics is included later in this chapter.

The resisting moments of the tree have been measured for Sitka spruce (*Picea sitchensis*) (Coutts 1986) and found to depend on the resistance of the hinge at the base of the trunk, the soil tension, the soil shear, the strength of the windward roots, and the weight of the root-soil plate. The combined resisting moment as a function of angle of inclination to the vertical is shown in Figure 2.8 and the curve is considered to be typical of many found in tree pulling experiments (England et al. 2000).

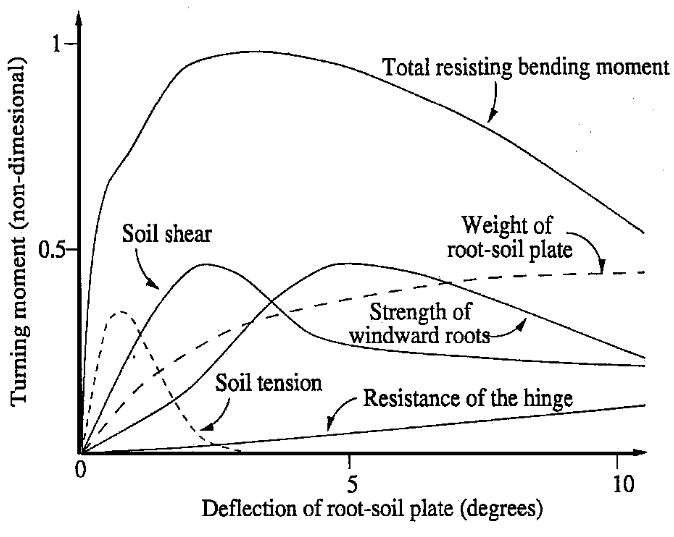

Figure 2.8. The combined resisting moment as a function of angle of inclination to the vertical for a tree which is considered typical of many found in tree pulling experiments (England et al. 2000).

2.4.1 Critical wind speeds and wind loads on trees

In this section previous studies of trees and wind are reviewed together with some wind engineering studies which use methods that may be useful and relevant to tree research. Wind forces are dynamic and notoriously variable, both spatially and temporally (Ennos 1999). Trees are flexible structures, with dynamically swaying trunks and branches, so that the interaction between trees and wind requires a dynamic system of measurement and analysis.

The wind speed at which tree failure begins to occur is called the critical wind speed and has been studied by (Oliver and Mayhead 1974, Petty and Swain 1985, Coutts 1986, Blackburn et al. 1988, Peltola and Kellomaki 1993, Hedden et al. 1995, Peltola 1996b, England et al. 2000, Zhu et al. 2000, Gardiner et al. 2000, 2008, Cullen 2002, Zeng et al. 2007, Schelhaas 2008, Wood et al. 2008).

This contrasts with an engineering approach which considers wind forces on inflexible buildings known as bluff bodies and the dynamic effects of gusts and eddies due to vortex shedding (Davenport 1960). Buildings are rigid and built without flexibility so that occupants do not feel uncomfortable on moving floors, so there is a difference in design concept between buildings and trees. Wind engineering theory applied to very large buildings uses an aerodynamic admittance function (Holmes 2007) to allow for gusts impacting on the windward face and this may have application to large trees. Currently in the engineering wind standards in Australia (AS/NZS 1170.2:2002) trees are not considered. Usually wind excitation on buildings is of interest to evaluate the response as measured by deflection at some height up the building or by using accelerometers but there is an interesting paper advocating the measurement of base bending moment (Zhou and Kareem 2001) which has relevance to trees and is discussed in this section.

Wind speed and gust factors

Most engineering design codes for wind loading use peak gusts for design purposes (Holmes 2007). The nature of wind is random but it is possible to define an expected, or average value within a certain period, which Holmes suggests as 10 min. Assuming longitudinal wind velocity (U) has Gaussian probability density, the expected peak gust ($\hat{U}$) is given by approximately,

$$\hat{U} = \overline{U} + g_1 \sigma_n \quad (2.2)$$

Where - g_1 is a peak factor of approximately 3.5, and

σ_n is the standard deviation

Meteorological instruments do not have perfect response and peak wind speed depends on their response characteristics. Response of small cup anemometers usually requires a 2-3 s averaging time to be quoted. Gust factor is the ratio of maximum gust speed to mean gust speed within the defined period.

$$G = \frac{\hat{U}}{\overline{U}} \quad (2.3)$$

Values of 1.45 for open country and 1.96 for suburban terrain are quoted (Holmes 2007).

A more complex definition of gust factor was suggested by Peltola et al. (1993) who considered several dimensionless factors including a peak factor, an exposure factor, a background turbulence factor and a gust resonant factor. This is probably too complex for this study, so the simpler definition of Holmes (2007) will be used.

Gustiness of wind is an important factor in tree studies that consider failure under wind loading (England et al. 2000, Gardiner et al. 2008). Critical wind speeds have been estimated by England et al. (2000) who used a steady wind speed value which was modified by a gust which acted over a short period of time. The gustiness was incorporated into the wind model and estimates of critical wind speed to cause failure were made. The analysis treated the tree as a cylindrical rigid body and was essentially a quasi-static approach. Dynamic factors including a phase relationship between the tree and gust were not considered which could change the impulse loads significantly.

Design guides

The Australian Standard AS/NZS 1170.2 (2002) provides design guidelines of structures subject to wind actions and is used for buildings less than 200m high, structures with roof spans less than 100 m and structures other than offshore structures, bridges and transmission towers. The Standard is useful to investigate the factors that influence critical wind speeds in different locations but it does not specifically mention trees. The site wind speeds are based on the regional 3 second gust wind speed which is modified with an annual probability estimate. Other factors such as wind direction, terrain or height, shielding and topography are considered using a multiplier based on site conditions. For ultimate limits the design wind speed is not to be less than 30 ms^{-1} which is very high when compared to studies involving trees. Dynamic wind effects on structures are considered using a dynamic response factor which is calculated using many elements of a building such as height, orientation, and the structural damping characteristics. This code applies to buildings but does not allow for flexible structures such as trees without considerable simplifications being made. The high value for design wind speed reflects the very conservative design criteria of this code.

Topography was found to have a marked effect on wind speed in a study by Sagar and Jull (2001). Wind speeds in forest areas in British Columbia were measured over a five year period, 1995 to 2000 in ten locations. Ten towers, each of height 9.1m were erected and one second wind records were taken using an anemometer and wind vane (Young Model 05130). Extreme wind events were defined as 1 second wind speed exceeding 20 m s^{-1} (72 km/h). Such extreme wind events occurred at 3 sites with the maximum value of 28 m s^{-1} (100 km/h). Spatial and temporal distribution of extreme wind events was very dependent on local topography and the wind was very gusty in nature. Critical wind speeds causing tree failure were determined from data obtained during a gale in southern Britain on Monday, 2 April 1973 (Oliver and Mayhead 1974). Gusts of wind were estimated to be 15 m across and of 5 s duration based on observations of the swaying tree patterns.

Terrain roughness effects over forests contributed to a reduction in average wind speed compared to wind speeds over flat surfaces of a RAF base which were 170% higher. The gust speeds were not so affected by roughness as they were only 130% higher over the smoother RAF base surface. For an aerodynamically rough surface the maximum gust can be estimated as approximately twice the calculated maximum hourly mean wind speed. Critical wind speeds were estimated at 17 m s^{-1} at tree top when some trees failed in the forest. Comparison of this figure was made with critical wind speed estimates based on static pull tests which predicted that wind speeds of 40-45 m s^{-1} were necessary for overturning. This implies that the static pull tests considerably over estimate the critical wind speeds needed to cause tree failure.

Wind loads are the largest loads on trees (Petty and Swain 1985, Mattheck and Bethge 1998). Bending moments about the base of trees were calculated (Petty and Swain 1985) by dividing the stem into segments of one metre lengths and determining the moment contribution due to stem weight, crown weight and wind force exerted on the crown. Typical results (Figure 2.9) show that wind contributes the largest component of bending moment which was 15 kNm for a 16 m high pine tree at a wind speed of 17 ms^{-1}. The authors noted that if a common assumption that the wind acted on the centre of pressure of the canopy was used, the bending moment value changed to 23 kNm. This is a marked difference that would be even greater for trees with less localized crowns.

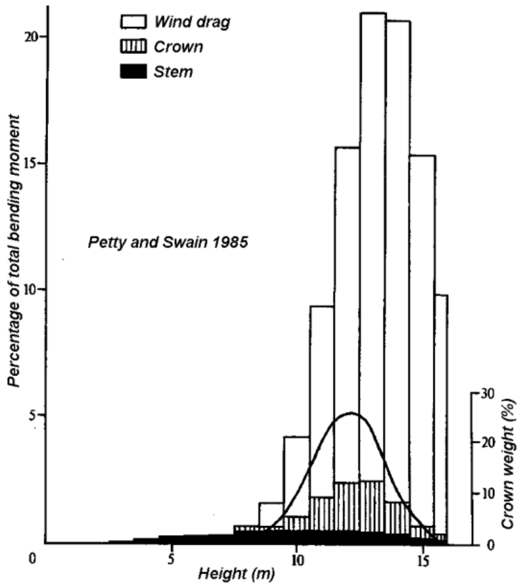

Figure 2.9. A histogram showing the contribution to the total bending moment made by one meter height increments of a pine tree of height 16m, DBH 22.5 cm at a wind speed of 17 m s^{-1} (Petty and Swain 1985).

Peltola and Kellomaki (1993) modeled Scots pines on the edge of a forest stand to determine critical wind speeds and critical overturning moments. Crown streamlining was taken as a function of wind speed with a reduction of 20% area for wind speeds less than 10 ms^{-1}, and a 60% reduction for wind speeds more than 20 ms^{-1}. Constant wind speeds were used to evaluate bending moment. Total turning moments needed to uproot trees of various sizes were calculated with a critical turning moment of 76 kNm determined for a 20 m tree with a slenderness ratio of 70. (Figure 2.10).

Critical wind speeds were estimated for a range of tree heights and slenderness ratios with the maximum critical wind speed of 25 ms^{-1} for short trees (12m) and a slenderness ratio of 70, and minimum critical wind speed of 8 ms^{-1} for tall trees (20m) and high slenderness ratio of 100.(Figure 2.10). Wind speeds in forest areas in British Columbia were measured over a five year period, 1995 to 2000 in ten locations. Ten towers, each of height 9.1m were erected and one second wind records were taken using an anemometer and. Wind vane (Young Model 05130). Extreme wind events occurred at 3 sites with the maximum value of 28 m s^{-1} (100 km/h).

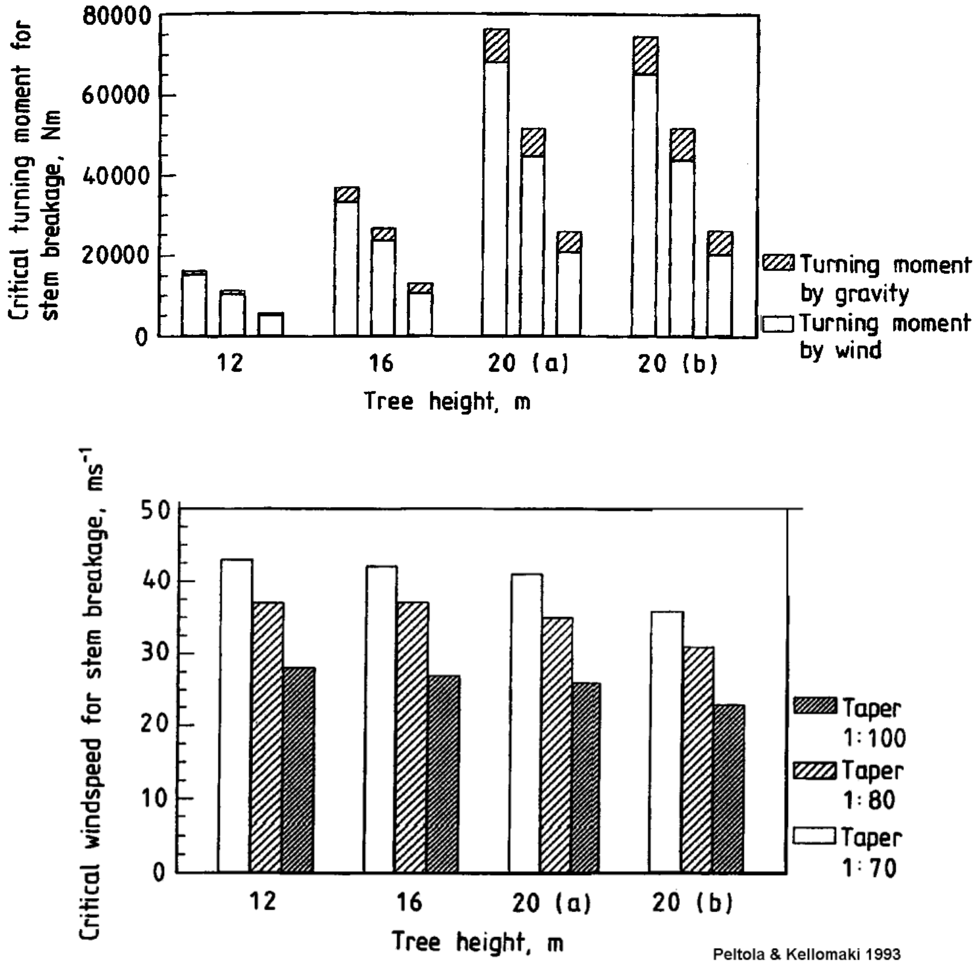

Figure 2.10. Critical tree height and critical wind speed for Scots pine (Pinus sylvestris) calculated from a mechanistic modeling approach (Peltola and Kellomaki 1993).

The effect of crown shedding and streamlining on the survival of mature loblolly pine (*Pinus taeda* L.) trees exposed to acute wind were studied using a theoretical model to compare forces from tree winching experiments in South Carolina (Hedden et al. 1995). Hurricane wind speeds (165 km/h) and peak speeds (249 km/h) were used to compare modes of failure. At the highest wind velocities, stem bending afforded greater protection against wind-generated mortality than 25% crown loss or branch streamlining. The trees most susceptible to wind throw were tall with a high center of gravity, large crown weight, and small stem taper.

Zhu et al. (2000) measured wind speeds and crown thickness within a normal crown of a single Japanese black pine (*Pinus thunbergii* Parl.). Results suggest crown features make a large influence on the wind profiles within the crown. Vertical wind profiles within the crown were measured (Figure 2.11) using a three cup anemometer (Kona, Sapporo, Japan). Where the distribution of leaves and branches within the crown is essentially uniform with height, and the tree is of a similar form to the Japanese black pine, the vertical profile can be derived from a single wind speed measurement outside the crown.

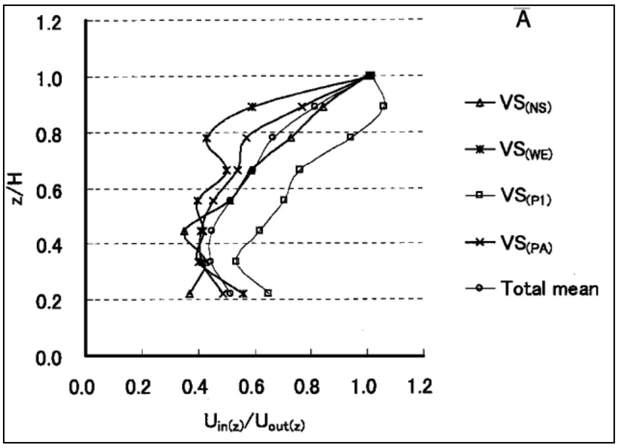

Figure 2.11. Vertical wind profile within a single crown of Japanese black pine (*Pinus thunbergii* Parl.) (Zhou 2000).

The wind speeds necessary to cause failure were estimated for pine trees and spruce trees (Petty and Swain 1985) using calculations based on critical bending moments and an assumed breaking stress for wood. It was evident that taper or slenderness ratio (H/DBH) was the most important factor affecting susceptibility to wind breakage. The variation in wind speed calculated to cause breakage for trees of different taper is shown in Figure 2.12.

Predicted critical wind speeds for tree breaking and overturning were presented by Cucchi et al. (2005) who used a similar method to Petty and Swain (1985) but related slenderness ratio to age of simulated stands of maritime pine species then plotted critical wind speed and age of tree. This modeling approach predicted critical wind speeds of 35 ms^{-1} for trees aged 20 years with a slenderness ratio of 70. Overall, their values for critical wind speed were lower than Petty and Swain (1985).

Wind models for forests

Mechanistic models are used to predict wind damage in forest plantation trees (Peltola et al. 1999, Zeng et al. 2007, Gardiner et al. 2000, 2008, Schelhaas 2008, Wood et al. 2008) by first calculating the critical wind speed required to break or overturn trees, and then to calculate the probability of damage at the geographic location of the trees, based on some assessment of local wind climatology.

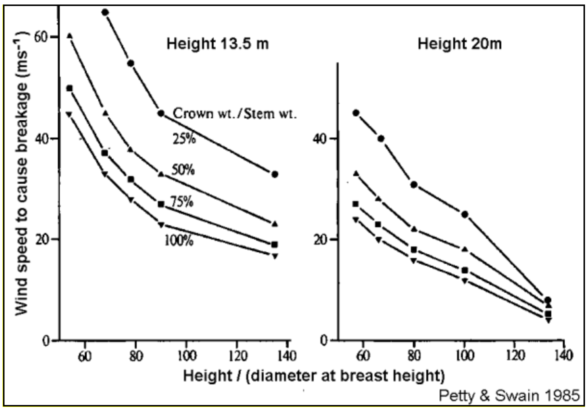

Figure 2.12. Wind speeds calculated to cause breakage versus height/DBH for spruce trees at two heights and four crown weights (Petty and Swain (1985).

Mechanistic models calculate the critical wind speed based on applied forces on individual trees and the resistive forces of the roots and stem. The applied forces depend on factors such as local wind speed, upwind conditions, and tree characteristics such as size, shape, and mass. The tree resistive forces depend on factors such as stem characteristics, wood strength, root plate strength and soil characteristics. The resistance to overturning and breakage is based on empirical relationships developed form tree pulling tests and timber strength tests. The best predictor of uprooting is stem volume (e.g. height x $(DBH)^2$) and the best predictor of stem breakage is $(DBH)^3$. Two current models called GALES and HWIND are reviewed. HWIND calculates wind loading using a wind profile method and GALES calculates wind loading using a roughness method. The mechanistic models provide useful predictions for relatively uniform stands of trees without defects. However the deterministic nature of these models is sometimes at odds with field observations of wind throw, particularly in more complex stands and landscapes. By definition the models are restricted to excurrent trees in plantations and are not yet applicable to decurrent trees in urban areas.

Critical wind speeds and turning moments needed to uproot and break the stems of coniferous forest trees have been calculated using computer models. Gardiner et al. (2000) compared two models (GALES and HWIND) and the results were tested against field data. Almost 2000 trees were uprooted during pulling experiments to compare with data from the models. Individual Scots pine (*Pinus sylvestris* L.) and Norway spruce (*Picea abies* L.) with varying tree height and stem taper (dbh/height) were evaluated.

There was good agreement for the critical wind speeds at the forest edge required to break and the best agreement was for trees with a taper of 100. At higher taper the GALES model generally predicted higher critical wind speeds than the HWIND model whereas at lower taper the reverse applied.

The critical wind speeds to cause failure depend on tree species, growth pattern and location, and estimates vary as shown in the previous studies. However, ultimately no tree species can survive violent storms with mean wind speeds over a period of 10 min exceeding 30 ms^{-1} near the top of the canopy without damage (Peltola 1996b). A summary of critical wind speeds from previous studies is presented in Table 2.3.

Reference	**Wind throw or break** (m s^{-1})	**Comment**
Oliver and Mayhead (1974	17	Tree top wind speeds, data from gale in Britain, 1973.
Cullen (2002)	25-28	Wind scales and critical wind speed comparison from previous studies
Hedden, R.L. (1995)	46	Winch tests, Sth Carolina, hurricane 165 (max 249) km/h
Spatz (2000)	20-30	Norway spruce, 56 y. 27 m high
Saunderson et al. (1999b)	28	Mathematical model, values seem high (his comment)
Coutts (1986)	3-17	Ref from Saunderson et al. 1999
AS1170.2. (2000)		48-60 m s^{-1}. Code values for return period of 100 years
Petty and Swain (1985)	45-60	Critical speed depends on slenderness ratio.
Peltola and Kellomaki (1993)	25	Short trees (12m), slenderness ratio 70
Cucchi et al. (2005)	35	20 year old Maritime pine, slenderness ratio 70.
Achim et al. (2005)	20	Balsam pine.

Table 2.3. Critical wind speed at which tree failure is predicted.

Critical wind speeds for balsam fir (*Abies balsamea*) stands were determined from modeling based on pulling tests in Canada (Achim et al. 2005). Values were based on critical turning moments that caused failure of 160 trees ranging in height from 14 to 17m. The critical wind speeds were higher for stem breakage than for overturning at approximately 20 m s^{-1} before declining due to the senescence of the trees (Figure 2.13). Thinning treatments that removed 30% of basal area in the plantation reduce critical wind speed by approximately 4 m s^{-1}.

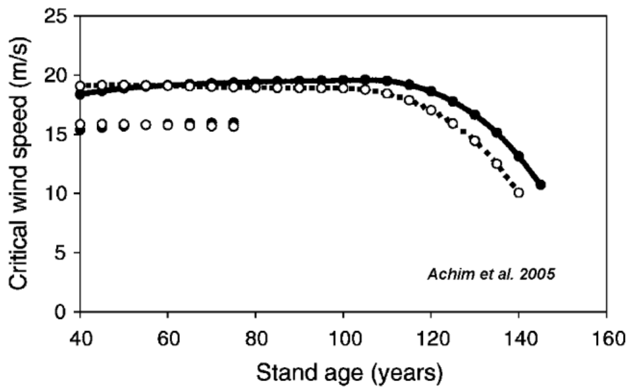

Figure 2.13. Critical wind speeds for balsam fir (*Abies balsamea*) from modeling computations (Achim et al. 2005).

2.4.2 Drag estimation and wind tunnel tests

A crucial factor in determining the forces on a tree in high wind is the drag (Vogel 1989). Drag is the link between the wind speed and the force on a tree (Wood 1995) and its value is determined by defining a drag coefficient C_D. A major determinant of drag is the exposed surface area which in broad leaved trees is presented by its leaves. Typically leaves are borne in the canopy far above the base and are exposed to the highest winds. It is therefore the upper part of the canopy which greatly contributes to the turning moment about the base. Deciduous broad leaved trees seem to more commonly suffer wind-throw when leaved than when bare (Vogel 1989).

Solid objects, known as bluff bodies have been used by engineers to study drag forces, often under controlled conditions such as in wind tunnels (Holmes 2007). The objects are not flexible and can be scaled down to give indicative results that can then be applied to full sized objects. Bluff bodies have a fixed frontal area exposed to the wind and a fixed shape which has a set value of streamlining. When scaling up wind effects on large objects such as tall buildings, additional factors such as the aerodynamic admittance function may need to be considered (Holmes 2007). These methods may not be suitable for flexible objects such as trees because the response of small scale models under constant wind speed conditions may not represent the response of large trees under actual wind conditions (Mayhead 1973b).

Trees and their canopies of leaves are flexible and the surfaces realign themselves in high winds. This occurs in two ways. First the exposed area decreases as the wind increases, due to the leaves turning and reconfiguring their shape as well as the total canopy area reducing (Vogel 1989). The second flexible change is that the whole canopy bends and changes shape and becomes more streamlined which reduces drag (Rudnicki et al. 2004). The streamlining depends on the mechanical and aerodynamic properties of stems, branches and foliage (Niklas 1992). The effect of flexibility on drag is usually detrimental and may be far higher than for a flat rigid object. Vogel (1989) compares a rigid flat plate such as a weather vane to a flexible flag which flutters in the wind and states that the drag forces on a flag are much higher due to its flexibility. The effect of flexibility on the value of the drag is far from self-evident (Vogel 1988).

Several studies assumed a constant frontal area (Mayhead 1973b, Smith et al. 1987, Peltola and Kellomaki 1993, Hedden et al. 1995) which leads to an under-estimate of drag. Attempts have been made to allow for the change in frontal area (Wood 1995, Spatz and Brüchert 2000) by estimating branch deflection under load. Estimates of crown streamlining were provided by Hedden et al. (1995) but there have been few studies where crown drag and streamlining have been measured simultaneously (Rudnicki et al. 2004).

The drag coefficient reflects the combined effects of the skin friction as the air moves over the surface of the drag element and the pressure differential between the windward and leeward sides of the element (Vollsinger et al. 2005). Canopies are porous so that the total drag coefficient is the sum of the pressure and skin-friction components of leaves and branches (Niklas 1992). In tree studies the drag has been studied for individual leaves (Vogel 1989) and of whole trees (Mayhead 1973b, Gardiner et al. 1997, Rudnicki et al. 2004, Vollsinger et al. 2005).

In the mathematical treatment of drag, the classical equation used is for a bluff body placed in a steady air stream (Vollsinger et al. 2005). The drag force is the along-wind force F(t) acting on the tree. It is considered to be drag dependent and thus velocity dependent as described by,

$$F(t) = \tfrac{1}{2}\, \rho\, C_D .\, A\, V^2 \qquad (2.4)$$

Where *ρ is the air density (~ 1.22 kg/m^3)*

C_D is the total effective drag coefficient of the tree (dimensionless)

A is the orthogonal area of the canopy exposed to the wind, and

V is the velocity of the air passing the tree.

Wind tunnels have been used to study the effect of wind on trees by a number of authors, (Mayhead 1973b; Vogel 1989; Gardiner et al. 1997, 2005; Novak et al. 2001, Tevar Sanz et al. 2003, Rudnicki et al. 2004, Vollsinger et al. 2005 and Gromke and Ruck 2008). Several wind tunnel studies have investigated forest trees in order to assess wind damage, by finding the wind speed at which structural damage begins to occur. These values are then used in predictive formulae or models to calculate the point at which failure occurs by estimating a critical tree height (Mayhead 1973b) or a critical wind speed (Rudnicki et al. 2004). Several wind tunnel studies have established drag coefficients of trees but of necessity they use models (Tevar Sanz et al. 2003) or small juvenile trees (Rudnicki et al. 2004, Vollsinger et al. 2005) and the drag coefficient values need to be verified for mature standing trees.

Mayhead (1973b) used data from previous wind tunnel tests on trees to determine the drag coefficient (C_D) by using the measured horizontal force ($F(t)$) on a tree in a wind tunnel and rewriting Equation 2.4 as

$$C_D = \frac{F(t)}{\frac{1}{2}\rho A V^2} \tag{2.5}$$

The trees in these tests were a selection of small conifers commonly used in British forestry. Trees of height 5.8 to 8.5 m high were tested in a wind tunnel with a height of 7.3 m at Farnborough in two runs made in 1962 and 1967. The unpublished results are summarised by Mayhead (1973b) for wind speeds varying from 9 to 26 ms^{-1}. Trees were fixed in an upright position with their butts fixed to metal pipe and bolted to a platform balance which read the horizontal drag force directly. The equipment did not permit the measurement of the couple produced (base bending moments) so no centre of pressure data could be determined. The drag coefficients differed between and within species and there was a sharp reduction in drag with increasing wind speed. This work is frequently cited without comment on the large variation in data and the limitations of the study which included variations arising from poor experimental technique which are well described. For example some trees were taller than the 7.3 m diameter of the wind tunnel and were tested with their leading shoots out of the airflow. Despite these limitations it was considered that the large variations in the data were likely to be due to the differences in tree morphology. Mayhead found that drag varied linearly with wind speed and not as the square, but for simplicity, fixed drag coefficients were developed for the species tested and ranged form 0.14 for Western hemlock to 0.36 for Grand fir.

Small trees, 2.5 to 5 m high, were tested in a wind tunnel with wind speeds ranging from 4 to 20 m s^{-1} (Rudnicki et al. 2004). Crowns were cut to a height of 1.9m, the lower branches were trimmed, and trees were mounted inside a wind tunnel that had a maximum height of 1.65 m. Trees were subject to progressive wind speeds and instruments at the base of the tree recorded wind loads. The results were converted to drag values using the standard drag equation and the results for red cedar are presented in Figure 2.14.

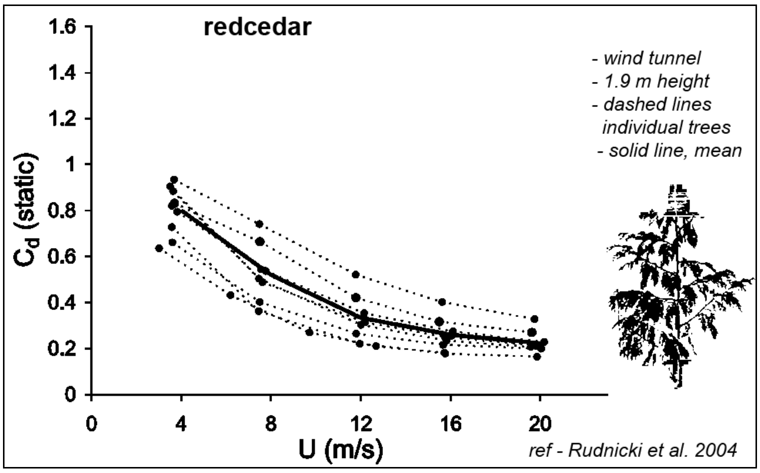

Figure 2.14. Drag values for a red cedar (height 1.6m) in wind tunnel tests (Rudnicki et al. 2004).

Drag coefficients at 20 m s^{-1} were 0.22, 0.47 and 0.47 for western red cedar (*Thuja plicata*), Western hemlock (*Tsuga heterophylla*), and lodgepole pine (*Pinus cordata*) respectively.

Rudnicki et al.(2004) examined the effect of streamlining and the change in frontal area as wind speed increased. An interesting result was noted in that the frontal area increased slightly as the wind speed changed from 0 to 4 m s^{-1}. This was explained by the way branches realigned themselves, especially those branches facing the wind or perpendicular to the wind. These branches bent a small amount in light winds and actually increased the frontal surface area, but as wind speeds increased the branches bent more severely and aligned themselves with the wind stream so that the area then decreased. At wind speeds above 4 m s^{-1} streamlining reduced frontal area by 54% for red cedar, 39% for hemlock and 36% for lodgepole pine. Streamlining results in variable drag coefficients and a near linear relationship between drag and the product of branch mass and wind speed was found. Between-species differences in drag relationships reflect differences in streamlining, within-crown sheltering, and foliage shape. The study concluded that given the small sample size, further work was needed to investigate the variability of drag relationship within species of trees of different age classes and provenances.

Ten freshly cut crowns of juvenile specimens of three hardwood species common to north western North America, black cottonwood (*Populus trichocarpa*), red alder (*Alnus rubra*) and paper birch (*Betula papyrifera*) were tested in a wind tunnel in wind speeds ranging from 4 to 20 m s^{-1} (Vollsinger et al. 2005). The samples were small so that they could fit into the wind tunnel which was 1.65 m high and 2.44 m wide. At 20 m s^{-1} streamlining reduced frontal area to 28% of initial area for black cottonwood, 37% for red alder and 20% for paper birch. Drag coefficients using frontal area in still air decreased with wind speed. At 20 m s^{-1} drag varied from 0.15 to 0.22. There was a complex relationship between species and components of the stem, branch and leaf would require further study. These tests were on small samples of the crowns of sapling and the leaf component was not dense. This may limit the application of results to larger trees but there was an interesting linear relationship between drag and the product of mass and wind speed.

Drag coefficients for stem sections have been quoted at 0.7 (Sinn 2003) and for parts of crowns a lower drag factor of between 0.12 and 0.35 is recommended for high wind speeds. The aerodynamic drag on crown sections that expose a large sail area to the air is much greater than for small trees (Detter et al. 2008) but no experimental results or values for drag were presented.

Wind tunnel tests on models of forests and individual trees (Novak et al. 2001) were described from tests using a wind tunnel 1.5m high and 2.4 m wide. Model forests were positioned in the wind tunnels and an individual model tree was mounted was mounted on a strain gauge balance to measure base bending moments and drag. Values of drag values for C_D were found between 1.04 and 0.88. The strain gauge balance was found to properly measure mean drag. It was concluded that the standard aerodynamic drag formula was in good agreement with balance method and the wind tunnel realistically described wind and turbulence with what occurs at the full scale in the real world.

Wood (1995) used a wind tunnel to test a scale model of forest trees for wind loading and inserted a single model tree which was instrumented to measure forces and to compute drag coefficients. Wood (1995) suggests that drag does not follow the usual formula for a bluff body and is proportional to $V^{1.8}$ rather than V^2 due to streamlining of the canopy at wind speeds between 0 and 27 ms^{-1}.

Forests.

Wind tunnel tests of 1:75 scale model trees designed to model a forest were conducted to examine the influence of canopy structure on the formation of turbulent gusts above the forest (Gardiner et al. 2005). The hypothesis was that an irregular canopy structure produces less intense gusts because change in wind speed with height at the canopy top is less severe. Results showed that mean wind and turbulence above the forest were similar when heights are normalized by the height of the tallest tree but differences do exist within the canopy. Gardiner cautioned that these wind tunnel tests are a simplification of a real forest and in some instances can only provide a rough approximation to reality. However a key conclusion was that there is no simple solution which optimises stand stability and change in forest structure due to clear felling, thinning, or group selection, but when making changes, it is better to make ‘little and often’ rather than ‘a lot and frequently’ (Gardiner et al. 2005)

Bell et al. (1991) suggest that streamlining of tree canopy reduces the cross-sectional area of the tree so that drag becomes more linearly proportional to velocity and the drag coefficient decreases as velocity increases. No values for drag coefficients were quoted.

Peltola and Kellomaki (1993) investigated the wind forces for a single Scots pine (*Pinus sylvestris*) and assumed the crown area changed due to streamlining as the wind velocity increased. They assumed a crown area reduction of 20% for wind speeds less than 10 m s^{-1} and 60% for wind speeds more than 20 m s^{-1}, and interpolated between these two values where necessary. Measurements of tree deflection in the wind (for a semi-mature plane tree) enabled drag coefficient values to be measured. It was shown that these coefficients are substantially greater when the tree is leaf, than when it is not in leaf. These experiments did not lend support to the hypothesis that tree drag is proportional to velocity, rather than velocity squared as has been previously suggested (Roodbaraky et al. 1994).

Black spruce (*Picea mariana*) was modelled assuming drag was approximated using the drag formula for cylindrical bodies (Smith et al. 1987). The tree was transformed, first into a stack of cylinders and then into a stack of solid impermeable cylinders. The drag was taken to act on the centre of pressure of each cylinder that for a uniform wind is located at the midpoint. The drag values were used to estimate bending moments at the base of the tree at different wind speeds up to 150 km/h. The maximum bending moments are 25 kNm which is a low value compared to large trees. This is an interesting method but is only applicable to specific plantation trees of this shape. Assumptions of constant wind speed result in a quasi-static approach and no account of branches or dynamic analysis was used.

Sellier et al. (2008) assumed a constant drag coefficient value of 0.26 for two slender Maritime pine trees (*Pinus pinaster*) with heights of 21.6 and 19.8 m and slenderness ratios of 84 and 89. This value was evaluated at 0.84 of the height of the tree using a previously published value based on wind tunnel tests on waving wheat.

Individual leaves, leaflets and clusters of leaves were studies in wind tunnel tests subject to turbulent winds of 10 and 20 m s^{-1} (Vogel 1989). Drag coefficients decreased with increasing wind speed for all species except leaves of white oak due to change in orientation and reconfiguration, especially of broadleaves. Results were not directly comparable to Mayhead (1973b) because he based values on projected areas of whole crowns. Some interesting data were presented on threshold wind speeds at which physical damage to leaves began to occur. and are useful to compare with values of critical wind speed for whole trees (Table 2.4).

Species	**Wind Speed (ms^{-1})**	**Std. dev.**
Black locust leaflet	20.0	2.74
Black locust compound leaf	26.71	2.04
Red maple leaf	23.3	2.58
White oak leaf	16.7	1.29
Willow oak leaf	29.6	1.88
White poplar leaf	>31.0	-

Table 2.4. Threshold wind speed for physical damage to leaves from wind tunnel tests (Vogel 1989).

Cullen (2002b) gives a review of wind data, scales and drag coefficients and describes the drag relationship as being proportional to wind speed (v) or the square of wind speed (v^2). He concludes after reviewing the literature that drag values are probably less than predicted using the velocity squared relationship but there is still no definitive answer.

Speck (2003) describes field measurements of wind speed and suggests drag values change with wind velocity due to streamlining effects. Speck suggests that drag is proportional to the square of wind speed (v^2) for wind velocities of 0 to 1 ms^{-1}, but as leaves realign themselves and the canopy shape streamlines to reduce the cross sectional area, the relationship reduces and drag is linearly proportional to velocity for wind speed values of 1.5 to 10 ms^{-1}.

Estimates of the drag coefficient for trees have been obtained from wind tunnel tests on models (Tevar Sanz et al. 2003). A scale model reduced to 1:35 was produced for a tree (*Populus sp).* and the shape was based on a standard silhouette which was defined from the average of several real tree silhouettes. Holes were drilled into the model to simulate porosity and it was assumed that the tree behaved under wind as a flat porous plate. A load cell was used to record horizontal force on the model in wind tunnel tests. The dynamic pressure was assumed to be uniform over the model and therefore the resultant aerodynamic centre of pressure was applied at the centre of gravity of the silhouette. Values of the drag coefficient were recorded against wind speed and are presented in Figure 2.15. There were no data to compare the performance of the model to real trees and a brief conclusion stated that the method offered a simple and quick way to determine the wind force in a tree and so to know its resistance to breaking and uprooting.

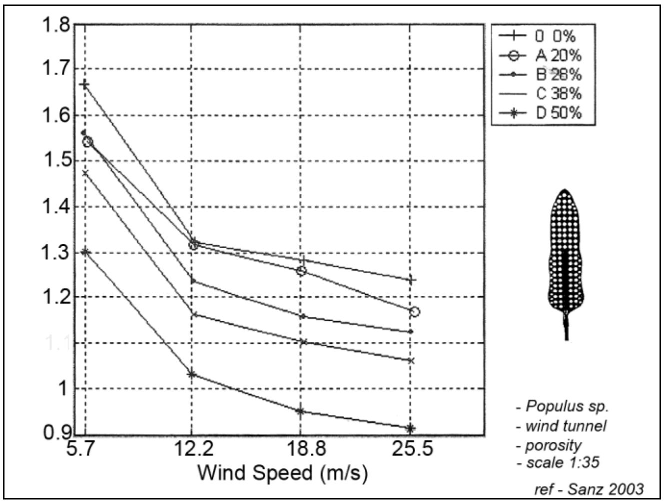

Figure 2.15. Drag values on 1:35 scale model of a tree (Populus sp.) from wind tunnel tests (Tevar Sanz et al. 2003).

This is a claim that needs to be tested as the obvious limitations of using a small, two-dimensional model, without any dynamically interacting branches does not account for the complex dynamic response of large trees. The bluff body in a constant wind stream may not represent the dynamic behaviour of real large trees to any great extent.

Spatz and Brüchert (2000) discussed drag and the changes with wind speed in relation to a Norway spruce, 52 y old and 27m high. A two step procedure was suggested to estimate drag, which was initially taken as 1 (equal to a flat plate) then finally taken as a function of wind speed and height of the tree as the branches flex and the canopy streamlines. The effective drag coefficient reduction was found to be up to 2.5 fold for wind speeds between 1 and 30 m s^{-1}, based on the assumption of a logarithmic wind profile. Evaluation of horizontal branches on a Norway spruce indicated that up to 20 m s^{-1} the branches seemed stable but at 30 m s^{-1} they experienced over-critical drag. Speck (2003) used a similar two step approach to drag in the study of the giant reed (*Arundo donax*) where drag was taken as proportional to velocity squared for wind speeds up to 1 ms^{-1}, then linearly proportional for wind speeds between 1.5 and 10 m s^{-1}.

Gromke and Ruck (2008) used a wind tunnel to investigate drag and airflow around 12 scale models of trees made with different materials to simulate changes in crown porosity. Drag coefficients in the range of 0.8 to 1.2 were found which were considered to agree with values for natural trees for wind velocities < 10 ms^{-1}. This study was interesting in that the airflow before and after the tree was studied. They observed a change in energy of the wake airflow from lower to higher frequencies in some trees, indicating a breakdown of large eddy structures to smaller eddies. It was also noted that there has been very little work in this specific area.

2.5 Dynamic Analysis of Tree Structures and Tree Models

2.5.1 Introduction

The static analysis of trees is useful to obtain some fundamental structural information but the static approach is a simplification which misses important information. Under wind loading conditions the dynamic effects are different from the static loads and are likely to increase the bending of the stem and the load on the root system (Milne 1991). Trees growing in plantations experience storm damage that may not be predicted using static methods. For example trees growing on the edge of plantations are subject to a different wind environment to those growing in the centre, and are stronger and less likely to fail. This becomes important during silvicultural practices such as thinning and pruning where tree failure may increase after the operation due to changes in the dynamics of the wind and the trees (Cucchi et al, 2005, Peltola 1996a). Trees are dynamic structures with elements of trunk and branches that sway with a time varying response to wind excitation. A dynamic analysis is needed to investigate the dynamic response of a tree to wind loading and determine parameters such as natural frequency and damping characteristics which are important parameters when modeling the wind and tree interaction (Jonsson et al. 2007).

The natural frequency of a tree is relatively easy to measure (Wood 1995) but measuring the damping is not trivial. As the wind pushes on a tree canopy there is complex transfer of energy from the wind to the tree. The tree "absorbs" this energy at all its natural frequencies, with most energy absorbed at the tree's first natural frequency (Holbo et al. 1980, Mayer 1987, Peltola 1996a). Damping is the dynamic parameter which estimates how this energy is absorbed or transferred and is the key to understanding how the tree responds in storm conditions. The term absorb may not be the most accurate to use because energy from the wind may not be transferred to the tree but returned back to the wind via small vortices at the scale of leaves (de Langre 2007). This idea is explored later in the discussion.

An important method to evaluate the energy transfer process is spectral analysis where the time domain data are transferred to the frequency domain using Fourier transformations to obtain the spectrum, also known as the power spectrum (Jenkins and Watts 1968). The spectral analysis has been used to study trees (Peltola 1996a, Flesch and Wilson 1999b, Moore 2002, James et al. 2006, Rudnicki et al. 2008) and is reviewed in this section with a mathematical treatment described in the next chapter.

Two approaches to quantifying the response of a tree to a given fluctuating wind force are described by Moore (2002);

(i) measuring the wind force and the tree response spectra and determining the mechanical transfer function that relates the two measured spectra, and

(ii) using a mechanical modeling approach to characterize a tree's response to any known applied force. This method relies on knowing the tree's dynamic properties of natural frequency and damping.

However Moore (2002) points out that information on tree natural frequencies and damping ratios is sparse and often unpublished. This lack of information and data is reported by other authors including Vogel (1996) who notes that it is especially striking that there is a very limited amount of experimentally based information in the primary scientific literature that addresses the question of tree structures and flexibility (dynamics). There is still one area of work that has not been considered to any great detail to date, which is the mathematical modelling of tree behaviour in high winds (England et al. 2000).

2.5.2 Estimation of natural frequency

The frequency of a vibrating system (f) can be measured as the number of cycles per sec (Hz) or as the circular frequency (ω) with units of (radians per sec) in which $\omega = 2\pi f$. The natural frequency (f_o) or (ω_n) is the frequency of oscillation that a single degree-of-freedom system will oscillate under free vibration (no external force applied during vibration). For multi degree-of-freedom systems the natural frequency is the frequency of the first mode of vibration.

In tree studies using slender plantation trees that consist mainly of the central trunk, estimating the natural frequency is relatively straight forward as after a little trial and error the resonant sway vibration can be easily established by hand pressure and the cycles counted against time (Wood 1995). This is not always the case, especially for decurrent trees in urban areas where there is no central trunk and significant mass in the side branches.

A significant limitation and consequence of the central column model is that if a tree is considered only as a single central column, and the static and dynamic effects of branches are ignored, any dynamic analysis will inevitably find that this structure has a natural frequency. A single column is not a tree. If a tree is approximated as a column and is analysed as a dynamic structure, the simplifying assumptions inevitably represent the column as an oscillating structure with a natural frequency. A tree without branches is not a tree (Shigo 1991) and the central column model for a tree has severe limitations, especially for dynamic analyses. The central column model of a tree has dominated the studies of dynamic tree behaviour and ignores the dynamic contribution of branches, which in open grown trees is shown to be important (James 2006a).

The natural frequency is an important parameter to be used in modeling of tree response to wind in an attempt to predict behaviour (Moore and Maguire 2004). The response of a tree is frequency dependent with the tree responding most to the wind gusts at frequencies close to its resonant frequency and its harmonics (Gardiner 1992). Information on natural frequencies and damping ratios of trees is sparse and is often contained in unpublished reports and a review of previous studies and a summary of natural frequencies is presented by Moore and Maguire (2004, Table 1, p197).

Studies which collect data on the natural frequencies of trees usually attempt to model these frequencies as a function of tree size (Moore and Maguire 2004). The equations used by these authors come from considering the tree as either (a) a beam with negligible mass and a top load or (b) as a beam with distributed mass but without a top load. Both these options make an inherent assumption that the tree is a central column shape but this is rarely stated in the literature.

Moore and Maguire (2004) present a summary of raw data from previous studies to determine natural frequency in tabular form and cite various formulae used by authors used to predict sway periods. The relationships relate tree height (H) and diameter at breast height squared (DBH^2). The natural frequency of a tree is the frequency it will inherently oscillate under free vibration (Moore 2002) and at which resonance will occur if it is excited at one or more of these frequencies. For dynamic vibrating systems the natural frequency is defined as (Balachandran and Magreb 2004);

$$\omega_n = 2\pi f_n = \sqrt{\frac{k}{m}} \text{ rad/s} \qquad (2.6)$$

Where

- k is the stiffness of the system
- m is the system mass.
- f_n is the natural frequency with the units of Hz and
- ω_n is the natural frequency with the units of radians per second

The period of oscillation (T) is also of interest and is defined as the time required to complete one cycle. Period is the inverse of the frequency and for an unforced and undamped system, is given by;

$$T = 1/f \qquad (2.7)$$

The amplitude (A_1) of the periodic motion is defined as the displacement from the rest position and is important because damping ratio is often found to be amplitude dependent (Clough and Penzien 1993). Vibrating systems may oscillate at their natural frequency or at other higher frequencies which are associated with different modes of vibration (Balachandran and Magreb 2004). The mode of vibration for a structure such as a pole is determined by the number of half sine waves that occur in the vibrating structure. The lowest frequency is termed the first natural frequency which is normally the most important in determining the response of a structure and the forces that are generated by the dynamic motion.

Degrees of freedom

In many studies of tree dynamics there is an unstated assumption that the tree is a single degree-of-freedom (SDOF) system and only oscillating mass is the trunk. The dynamic effect of branches is ignored. This may be a good first approximation for a slender plantation tree with very little mass in the branches but as the proportion of branch mass increases with respect to the trunk mass, the natural frequencies of the trunk become less dominant. In a few studies of tree natural frequencies and the effect of branch removal, it has been found that the oscillating frequencies of trees were greater after their branches were removed (Milne 1991, Gardiner 1992, Moore and Maguire 2004). This can be attributed mainly to the mass removal and still does not account for any dynamic contribution of the branches.

In this study the tree is considered as a multi degree-of-freedom system (MDOF) and the response to wind induced vibrations is greatly influenced by the dynamic effect of the branches (James et al. 2006). Studies of dynamic response of olive trees under forced vibrations (Castro-Garcia et al. 2008) treat the tree as a MDOF and identify complex multi-modal responses that show the dynamic influence of branches on tree response to forced vibration. For trees, it is the first natural frequency that most studies have focused on when determining dynamic properties (Moore and Maguire 2004).

Previous studies.

The natural frequencies of trees has been found from either (a) inducing sway in still air conditions, usually with an attached rope (Sugden 1962, Mayhead 1973a, Mayhead et al. 19075, Milne 1991, Gardiner 1992, Roodbaraky et al. 1994, Baker 1997, Flesch and Wilson 1999b, Hassinen et al. 1998, Moore and Maguire 2004, Jonsson et al. 2007) or (b) by measuring the tree response in wind conditions and using a power spectrum approach (Holbo et al. 1980, Peltola et al. 1993, Hassinen et al. 19098, Gardiner 1995).

Early studies of the natural frequency of trees used single stemmed forest trees and forced a sway motion by pulling with an attached rope (Sugden (1962). In this study of 826 red (*Pinus resinosa* Ait.) and white pines (*Pinus strobe*s L.) were swayed and their sway periods measured with a stopwatch. This methodology has many limitations since artificially inducing sway by pulling is not how the tree sways in the wind and results in only a few sway motions (3 to 7) before the tree comes to rest. Averaging readings with a stopwatch is insufficiently accurate to detect small changes in sway periods and averaging the reading will inevitably result in an average estimate of a natural frequency for a tree. During the 1960's, the same method was used to measure the sway of 143 plantation-grown trees from five different species: Sitka spruce (*Picea sitchensis* Bong Carr), Douglas-fir (*Pseudotsuga menziesii* Mirb. Franco), Norway spruce (*Picea abie*s L.), Lodgepole pine (*Pinus contorta* Dougl. ex Loud.) and Corsican pine (*Picea nigra* Arnold). These data were analysed by Mayhead (1973a) who used average values from all trees to develop an equation for the natural frequency of a tree.

Mayhead (1973a) considered the tree to be "no different from any other tall structure" and viewed the tree from an engineering viewpoint. Mayhead (1973a) assumes an analogue to a tree to be that of a uniform metal rod of length (L) firmly attached at one end, of mass (M), diameter (D) and vibrating at its natural frequency. This will have a period of (P) where

$$P = \frac{KL\sqrt{ML}}{D^2} \tag{2.8}$$

This is quoted as a "common engineering formula" with K being a constant.

This equation is used to evaluate the data from the 143 trees grown in a forest environment. Each tree was forced to sway with an attached rope, then released. The sway period was determined using a stop watch and taking an average of 3-4 sets of 3, 4 or 5 complete oscillations. Even with repeated tests and averaging, this is a small number of cycles and may not be adequate to determine the dynamic properties of sway and damping. Mayhead discusses the results and notes poor distribution of data and the poor relationship of tree mass with period, although mass occurs in the theoretical equation. The range of tree species studied had height variations between 9-19 m, but no quoted values were given of tree sway period. Average values were taken and regression analysis applied to each variable.

The assumption that the tree is like a single, uniform metal rod makes no allowance for branches and Mayhead notes that the sway periods increase with age and mass is probably a compounding factor in that branches probably contribute considerably to the damping system of trees. The limitations of using a stop watch and the method of averaging results may not be sensitive enough to find small variations in natural frequency so although Mayhead quotes a formula for the natural frequency of trees, there is no real supporting data or values to support the equation.

Moore and Maguire (2004) present a summary of raw data from previous studies to determine natural frequency in tabular form and cite various formulae used by authors used to predict sway periods. The relationships relate tree height (H) and diameter at breast height squared (DBH^2).

Milne (1991) manually swayed six 26-year-old Sitka spruce trees in a Scottish plantation. The structure of these trees was a single central stem, and they were located in a forest environment so the density of the side branches is low. The trees are described as having a mean height of 14.2 m and mean stem diameters of 14.5 cm (at a height of 1.3 m). In calm conditions, the trees were set to sway by pulling on an attached rope. The resulting motion was recorded with displacement transducers at 10 Hz. The average natural frequency of the trees from these tests is quoted as 0.35 Hz. The trees were caused to sway by manually pulling, and there were no measurements taken under wind excitation. The sway was developed over several repeated pulls before sufficient movement was developed. After the rope was released, the number of oscillations of the tree is quite small, before coming to rest. Although the tests were repeated four times, the amount of sway data gathered is quite low. The number of cycles used in the calculations were very small, being two cycles for the case where the trees contacted neighbours, 4-5 cycles when the neighbouring trees were held away from the swaying tree, and 6-10 cycles when the branches were removed and only the trunk was left to sway. The mass of the stem and foliage was assumed to be located along the centre line of the trunk. This assumption ignored any dynamic effect from branches which were only considered as a point mass. The mathematical analysis used the basic formulae for a vibrating structure.

The simplifying assumptions of Milne (1991) that the branch mass of a tree is located along the centre line and the tree architecture consisted of a central stem reduces the tree to a single degree of freedom system and ignores any dynamic contribution from branches. The analysis of using simple mathematical equations of a vibrating structure inevitably leads to the conclusion that these trees have a natural frequency. Milne does add the comment that near the end of the swaying, the pattern of movement became more variable because of the interference with neighbours or asymmetry in tree form. Pull and release tests were performed on 24 Norway spruce tree (*Picea abies* (L.) Karst) growing on forested slopes to investigate natural frequencies and damping ratios (Jonsson et al. 2007) For trees ranging in height from 20.7 to 34.5 m the natural frequencies varied from 0.14 to 0.29 Hz. The first natural frequencies correlated best with the diameter at breast height and the squared total tree height (DBH/H^2).

2.5.3 Spectral analysis

Tree response to wind excitation can be examined using a spectral analysis which investigates the coupling between the wind input and the tree dynamic response in the frequency domain. The method uses Fourier transformations and power spectra to analyse the frequency of the wind gusts and the frequency response of the tree. The spectral method is described in mathematical texts such as Jenkins and Watts (1968), Clough and Penzien (1993) and is useful to investigate which frequency components of the wind are important in contributing to the tree response. Spectral analysis has been used in tree sway studies by several authors (Mayer 1987, Holbo et al. 1980, Baker 1995, Baker and Bell 1992, Gardiner 1994, 1995, Roodbaraky et al. 1994, Wood 1995, Guitard and Castera 1995, Saunderson et al. 1999, Ilic 2001, Peltola 1996, Flesch and Wilson 1999b, Moore 2002, James et al. 2006, Rudnicki et al. 2008, Gromke and Ruck 2008). This section covers a review of these studies. The method of spectral analysis is treated mathematically in Chapter 4.

Holbo et al. (1980) measured tree sway under medium wind conditions (2.5-6.75 m s^{-1}) on three Douglas fir trees in a forest environment. Fourier analysis was used to determine wind spectra using data from a propeller anemometer at a data acquisition speed of 10 Hz. and corresponding tree deflection spectra. Three wind periods of one hour each were studied and discrete Fourier transformations were obtained using data sets of 100s i.e. 1000 data points per set, which allowed limited wind spectra to be determined showing wind gusts with 10-20 s periods. Tree sway spectra showed peaks indicating the natural frequency at 4-5s and spectral response was constant under varying wind conditions. Holbo et al. (1980) used a simplified analysis that related the output variable (deflection) to the input variable (force) to obtain a compliance transfer function. This assumes that the spectra of wind speed are the same as for wind force. Results indicated a complex relationship between wind force and tree response and that there was a marked tendency for vibrations to build up as turbulent energy in the wind increased. The stated aim of the study by Holbo et al. (1980) was to develop predictive equations to relate wind speed to tree wind throw, not to measure the natural frequency of trees. Trees selected were of single stem architecture, and no details were given of branch or crown masses. These trees were forest trees planted at a density of 287 trees per hectare so their structural shape is tending towards a single central column, with few branches. This shape of tree would approach that of a single columnar structure and one would expect a dominant natural frequency to be exhibited in the spectral analysis.

Roodbaraky et al. (1994), measured displacement of several open grown trees under pull and release tests and also wind loading. Displacement spectra of trees in leaf and no leaf conditions were obtained with data sample rates of 4 Hz. This is a relatively slow sample rate which results in a very noisy spectral graph and the authors comment that large errors are to be expected. This limits the results from the study and particularly the damping ratio values need to be more fully investigated as the curve fitting procedure would be difficult to achieve with any great accuracy.

Gardiner (1995) used spectral analysis to examine the response of four trees to wind loading in a dense spruce plantation. Spectra were calculated over half-hour periods by averaging five transforms calculated from 4096 points of 10 Hz data and normalized by dividing by the variance. The shape of the wind speed spectra at the canopy top decreased with a slope of -2/3 within the inertial sub-range as expected and the transfer function was calculated for one tree. The spectra were used to interpret the energy transfer from the wind to the tree and it was found that the trees did not resonate with turbulent wind components close to their natural frequency but behaved like damped harmonic oscillators. Tree movement correlated to wind gusts, but not very closely and there was no evidence of increased amplitude with successive gusts.

Rudnicki et al. (2008) studied lodgepole pine with a mean slenderness coefficient of 134 and used spectral analysis to determine the frequency of periodic motion as affected by collisions with neighbours. The spectral analysis indicated a decrease in the sway frequency with wind speed for one stand but no corresponding result for another stand. These very slender trees experienced intense collisions with neighbours which was a major contributor to damping. There was a linear relationship between sway frequency and amplitude at high wind speeds due to the collision of crowns that suggest these trees act as an organised system.

Most of these studies were on excurrent trees with a dominant central main stem such as spruce, pine and Douglas fir. A table summarizing the raw data from these studies is presented by Moore (2002). There have been few applications of spectral analysis to the study of open grown trees with many branches. Baker (1997) measured sway of 62 open grown trees around Nottingham University and found that there were three distinct types of spectra, indicating that shape or tree morphology is a factor in the spectral response of trees. Baker and Bell created three categories or types with Type 1 (the most common) showing low frequency peak in summer (0.3 to 0.6 Hz) and (0.5 to 1.5 Hz) in winter, Type 11 showed no significant peaks in summer or winter and Type 111 which was similar to type 1 but with significantly lower natural frequencies. The three different types categorized on spectra, corresponded to three different geometries of tree with type 1 having normal canopy shape with branches at 20-30 degrees to the vertical, type 11 having a "bushy" canopy , many branches and generally younger trees and type 111 being trees in an avenue and branches at 10 degrees.

The dynamic resonant response of structures subject to wind loading introduces the complication of a time-history effect (Holmes 2007). The response at any time depends not just on the instantaneous wind gust velocities acting on a structure but also on the previous time history of the wind gusts. The approach to the wind induced vibration of structures is based on random vibration theory (Davenport 1960) and uses the concept of the stationary random process to describe wind velocities, pressures and forces (Holmes 2007). This assumes that wind speeds always vary and can never be exactly predicted (i.e., wind speed is non-deterministic) but can be described by a spectral approach where calculations are performed in the frequency domain. The elements of the spectral approach are shown in Figure 2.16 with the upper graphs representing time domain data and the lower graphs showing the corresponding frequency domain spectra. The upper time domain graphs illustrate the relationship between the wind velocity, the resulting wind force and the induced response of the structure such as a tall building or a tree. The wind velocity is not constant over the surface of the structure and produces a time varying force on the structure. This force results in a time varying response which has been measured in buildings as displacement (Holmes 2007) or as base bending moment (Zhou and Kareem 2001).

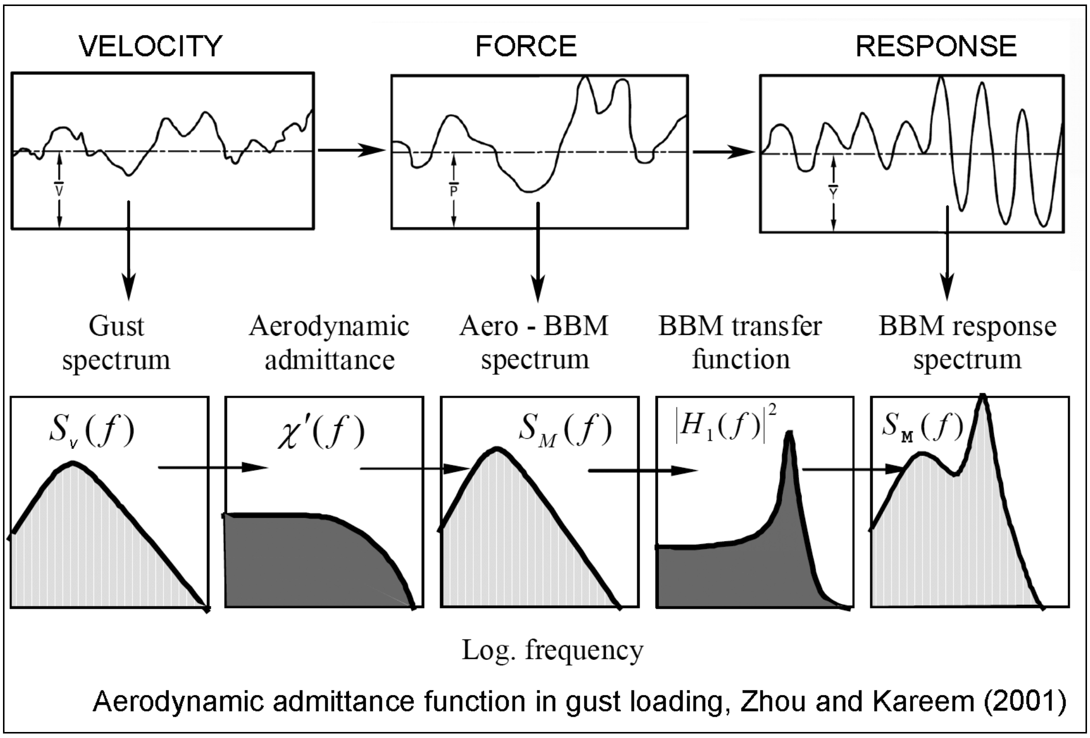

Figure 2.16. Relationship between wind velocity, gust loading using aerodynamic admittance function, wind load and tree response measured using base bending moment (based on Zhou and Kareem, 2001).

The spectral approach is shown in the lower sequence of diagrams in Figure 2.16 which represents calculations in the frequency domain. By using a spectral approach, the spectrum of wind velocity $S_v(f)$ produces a spectrum of aerodynamic force $S_M(f)$. The two spectra are related by the aerodynamic admittance function $\chi'(f)$ which is the transfer function that describes how the wind velocity impacts on the structure and is converted to wind force over the surface area of the structure. Similarly the aerodynamic force spectrum $S_M(f)$, produces the response spectrum of the structure which in this case is shown as the base bending moment spectrum $S_m(f)$.

The transfer function $H_1(f)^2$ describes the relationship between the force and response spectra. A mathematical model using a similar relationship to link the wind spectra to wind force using the aerodynamic admittance function was outlined for trees (Baker ad Bell 1992) who extended the concept to include extreme moment values of tree stems and hence criteria for failure.

It is normal practice to measure vibration response in the upper part of buildings where accelerations and displacements are large. It is also possible to measure moments at the base of a structure and, if sampling rates are high enough, to obtain the same spectral information. Zhou and Kareem (2001) present a method of wind load analysis for tall buildings based on the equivalent static wind load and a “gust loading factor” approach proposed by Davenport (1967). They discuss the traditional displacement gust loading factor (DGLF) approach and suggest that a more accurate concept which uses the base bending moment gust loading factor (MGLF). The MGLF is suggested to have two advantages over the displacement method due to (a) a more concise description of the relationship between aerodynamic loads and the induced wind effects which facilitate conventional evaluation of equivalent safe wind loads, and (b) the difficulty of ascertaining the traditional formulation of the aerodynamic admittance function.

For large structures, the wind velocity is not uniform over the entire windward face of the structure and velocity fluctuates and hence the force variations on the exposed surface area must be considered. This effect is allowed for with the introduction of an aerodynamic admittance function, $\chi^2(n)$, which has been described with an empirical equation by Holmes (2007).

$$\chi(n) = \frac{1}{1+\left[2n\sqrt{A}/\overline{U}\right]^{\frac{4}{3}}} \tag{2.9}$$

The aerodynamic admittance function, $\chi(n)$ tends to unity at low frequencies and for small structures (Figure 2.17) where low frequency gusts are nearly fully correlated and fully envelope the face of a structure. For large buildings and at higher frequencies, the gusts are ineffective in producing total forces on the structure, due to their lack of correlation, and the aerodynamic admittance tends towards zero.

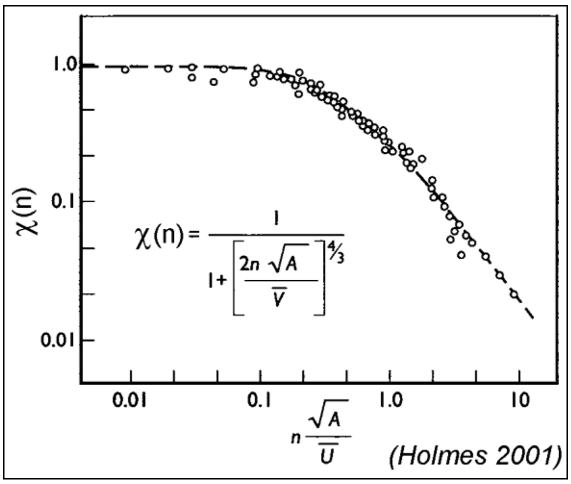

Figure 2.17. Aerodynamic admittance – experimental data and fitted function (Holmes 2007).

The spectral density of the structural response to wind will have two components consisting of the ‘background’ wind force spectrum (W) and the structural response spectrum (R), (Figure 2.18).

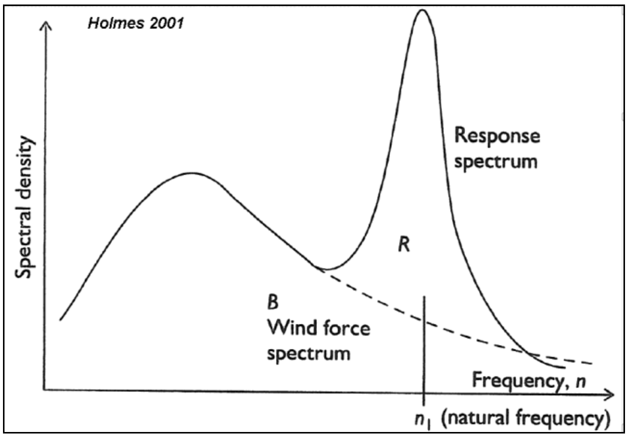

Figure 2.18. Structural response spectra showing components of background wind force spectra (B) and structure resonant response (R). (Holmes 2007).

The background factor (B) represents the quasi-static response caused by gusts below the natural frequency of the structure (Holmes 2007) and it is suggested that for many structures under wind loading the background response of the wind is dominant in comparison with the resonant response of the structure.

The influence of gusts on fluctuating wind forces on trees and the aerodynamic admittance function was discussed by Wood (1995) who suggested that it is important to take measurements of these effects in order to determine the tree response. Moore and Maguire (2008a) discuss the aerodynamic admittance function in a study of Douglas-fir trees *(Pseudotsuga menziesii)* under applied loads using a finite element method. The aerodynamic admittance is usually assumed to be unity but it is suggested that the model would be improved if the aerodynamic admittance function was considered, especially at higher frequencies. Spectral analysis was used to compare a mathematical model of a 13 m tree divided into 13 segments each 1 m long, to a real spruce tree (Kerzenmacher and Gardiner 1998) The transfer function is quoted as being similar to other modeled trees, and for the tree modeled on the parameters of Gardiner (1994), gave a natural frequency of 0.48 Hz for the fundamental mode, and a second mode at 3.1 Hz, both with high gains in excess of 30. At higher frequencies, the gain was less than one, showing high damping. The transfer function is reproduced in Figure 2.19.

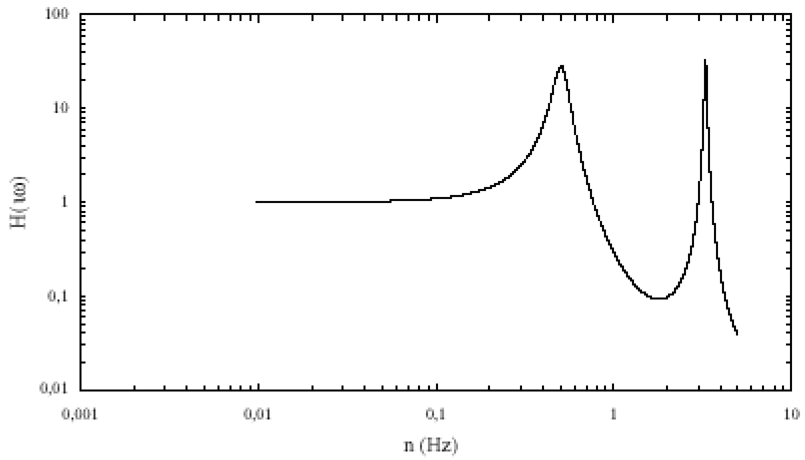

Figure 2.19. The transfer function at 8m on the model tree as a function of frequency (Kerzenmacher and Gardiner 1998).

When the power spectrum of displacement from the model is compared to that of the tree, both spectra showed a peak at the tree natural frequency of 0.48 Hz, with a rapid decrease in the power at higher frequencies (Figure 2.20). The second resonance at 3.1 Hz, predicted by the model is not evident in the measured spectra. The absence of higher mode resonance in the measured spectra indicates that the tree is absorbing energy only at and below the natural frequency and that the tree acts like a low pass filter to the wind.

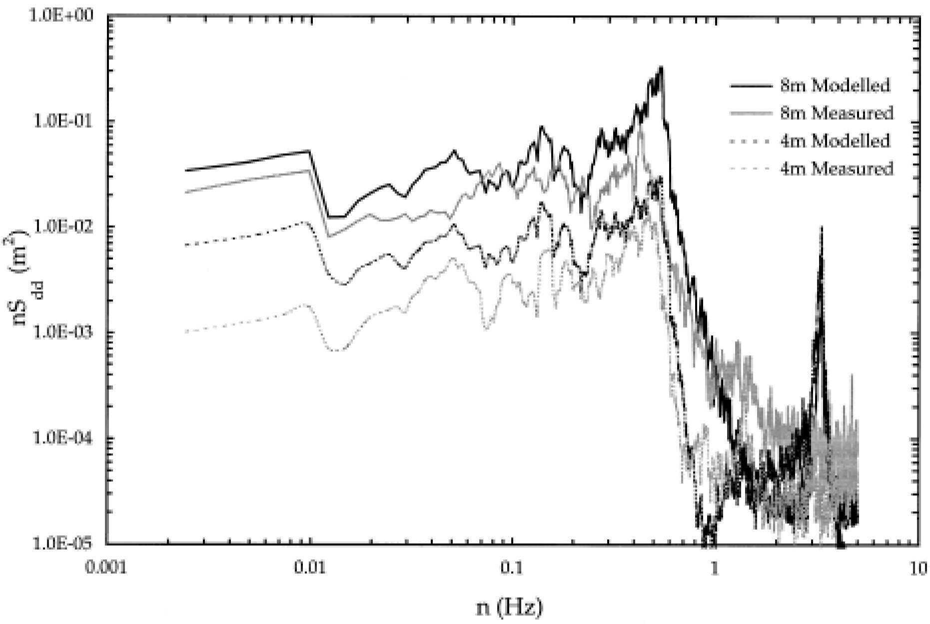

Figure 2.20. Power spectrum of the measured and modeled deflection at 8m and 4m height over a 6.83 min period (Kerzenmacher and Gardiner 1998).

Peltola (1996b) used a spectral analysis of tree sway measurements made from video measurements of displacement used together with accelerometers. The wind spectra near the top of the canopy were used with the accelerometer spectra to determine the transfer function of Scots pine in a Finnish plantation. The displacement spectra were obtained from video and the mechanical transfer function was found for thinned and unthinned stands. The spectra were used to determine natural frequencies but little information on damping was presented. This was probably due to high noise at frequencies above 1.5 Hz. There was almost no difference in the spectra between two treatments of Scots pine and the lack of variation was due to heavy damping of closely packed trees in dense stands and the crown contacts between neighbouring trees.

Gromke and Ruck (2008) built small scale physical models of trees and used small scale modelling methods in a wind tunnel to investigate air flow around twelve different model trees made of different materials to simulate different crown porosities. Spectral analysis was used to investigate the energy of the approaching airflow and in the wakes of the tree models. The spectra of the approaching airflow was in agreement with the -5/3 slope in the inertial sub-range but the spectra of the wake for some trees (e.g. sisal fibre model) did not follow this pattern, indicating a shift in the energy from lower to higher frequencies which was attributed to a breakdown of larger eddy structures into smaller eddies in the crown region. It was noted that information is very limited on the comparison of spectra in the wakes of single trees and entire forest stands.

2.5.4 Damping

Damping in an oscillating system dissipates energy and attenuates dynamic motion. In this section, previous studies of the effect damping in trees are reviewed. Damping is treated more formally in Chapter 4, with a mathematical approach in which damping elements are introduced into equations of vibrations for dynamic systems. This section introduces a damping element of a tuned mass damper which is new to the literature in tree studies (James 2003, James et al. 2006) and helps to describe the dynamic effect of branches and the main stem of trees. The concept of a tuned mass damper is incorporated into a new model for trees and described in Chapter 3, and introduced in a mathematical treatment in Chapter 4.

The swaying motion of a tree under wind excitation is one example of an oscillating system in which inertial elements (masses) undergo oscillating motion due to energy transfer in stiffness elements (springs). The dynamic response of the masses under forced vibration is attenuated by damping elements (dampers) which dissipate energy.

Under free vibration (without external input of force) the oscillating motion decreases with time as the energy in the system decreases due to energy dissipating elements (dampers) until the system comes to rest. Damping elements are assumed to have neither inertia nor the means to store or release potential energy. In classical vibrations analyses, four common types of damping mechanisms are used to model vibratory systems (Balachandran and Magrab 2004). They are;

(i) viscous damping
(ii) Coulomb or dry friction damping
(iii) material or solid or hysteretic damping, and
(iv) fluid damping

In all these cases, the damping force is usually expressed as a function of velocity and may be grouped together to give one value for overall damping which in tree studies is usually assumed to be viscous damping (Moore and Maguire 2004).

Up until this point in the discussion on tree dynamics, the concepts presented have dealt with simplifications which usually assume that a tree has a monopodial architecture (Rodriguez et al. 2008) with a central trunk and acts as a single degree of freedom (SDOF) system. The tree has been treated as a single oscillating mass (Nield and Wood 1999, Brüchert et al. 2003) or a stem with a rigidly attached canopy mass (Saunderson et al. 1999) or as a stem with several rigid masses fixed at different heights to represent the canopy distributed up a stem (Guitard and Castera 1995). These tree models represent a stem or a stem and canopy as rigidly attached masses and model the tree as SDOF systems. The analysis of tree bending and vibration has not been sufficiently sophisticated to take account of branches as anything other than added masses at each level (Wood 1995). Few studies have attempted to model damping due to the lack of understanding of the energy loss mechanism in trees (Moore and Maguire 2004). If trees are considered only as SDOF systems, this is a simplification that ignores any dynamic contribution of branch masses. The lack of branch dynamics was identified by Kerzenmacher and Gardiner (1998) as a weakness in their model of a tree approximated to a tall free-standing chimney and they suggested treating branches as cantilevers attached to the main cantilever. When investigating tree dynamic response under wind excitation it may be more appropriate to consider trees as multi degree of freedom systems. This concept is developed further in Chapter 3.

Simple damping in a SDOF system is used to explain resonance phenomena in many machines, to obtain natural frequencies of structures and to describe or model vibrating systems (Den Hartog 1956) but may not completely explain the motion of more complex systems. It is only by considering more complex vibrating systems, which include many vibrating masses that another damping concept termed “Tuned mass dampers” becomes apparent. This form of damping is not present in a SDOF system. In order to explain the dynamic response of complex systems with several vibrating masses it is necessary to extend the theory to multi-degree of freedom systems (MDOF). This can be done by first considering two vibrating masses (a two degree of freedom system or 2DOF) in which the solution to vibration analysis becomes more complex, and then further extending the concept to include many vibrating masses which make a MDOF.

By extending the discussion on damping to include two masses (a 2DOF), it is possible to identify another damping element called a mass damper. This damping element is not present in a SDOF. This concept has application in tree studies where the main mass is the trunk and the second mass is a branch. Both masses are vibrating elements so the concept can be used to account for the dynamic contribution of branches (James 2003, James et al. 2006). In previous tree studies, the dynamic coupling of branches has been observed to dissipate energy (i.e., contribute to damping) and has been referred to as structural damping (Niklas 1992) and multiple resonant damping (Spatz et al. 2007) but has not been specifically linked to the mass models of a 2DOF or MDOF systems. In this study the term mass damping is taken from the engineering literature (Abe and Fujino 1994, Connor 2002).

This damper acts to attenuate motion and is described by Den Hartog (1956) as a dynamic vibration absorber or as a mass damper (Abe and Fujino 1994, Connor 2002). The dynamic vibration absorber is a device which consists of two oscillating masses, one coupled to the other via a system of springs (Figure 2.21). This concept was first applied by Frahm in 1909 to reduce the rolling motion of ships and ship hull vibrations (Den Hartog 1956). The same concept is described as a tuned mass damper (TMD), (Abe and Fujino 1994) and may be incorporated into a structure as a device which will transfer some of the structural vibrational energy from the primary structure to the tuned mass damper (Soong and Dargush 1997).

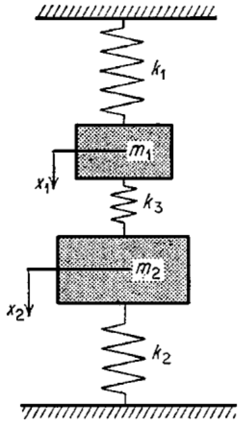

Figure 2.21. A two degree of freedom (2DOF) vibrating system representing a vibration damper (Den Hartog (1956) or a mass damper (Connor 2002).

The concept of a tuned mass damper has been extended to multiple tuned mass dampers (Figure 2.22) which have been shown to be more stable (robust) than a conventional single tuned mass damper while maintaining the same efficiency (Abe and Fujino 1994).

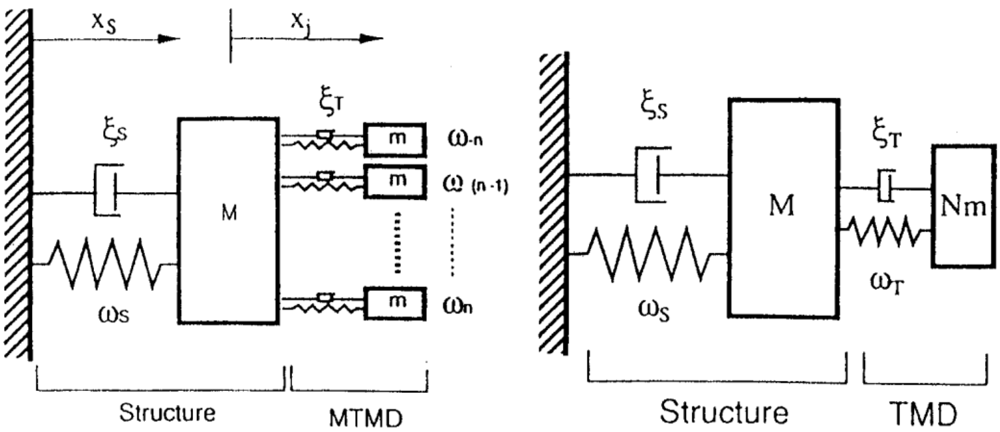

Figure 2.22.Tuned mass dampers, (a) multiple systems and (b) a single tuned mass damper (Abe and Fujino 1994).

Tuned mass dampers or vibration absorbers have become popular methods of mitigating vibrations due to wind in tall buildings. These systems have been successfully installed in the Sydney Tower in Australia, the Citycorp Centre, New York, the John Hancock Building, Boston, U.S.A. and in the Chiba Port Tower in Japan (Holmes 2007).

In tree studies, damping is usually treated as a single quantity of a single degree of freedom system though this is usually assumed and unstated. Damping in trees is complex and consists of many components which can be grouped into internal and external components (Moore and Maguire 2004). Internal damping may be due to root-soil interaction (Mayhead et al. 1975), internal friction of the wood (Milne 1991, Wood 1995) and structural damping (Niklas 1992) which is associated with branch movement.

The external damping components are due to aerodynamic drag of the leaves and crown of the tree and in close forest or plantation situations, collision between crowns of neighboring trees (Rudnicki et al. 2001). Foliage also affects the sway characteristics as the natural frequency of a tree in leaf was lower and the damping higher than when not in leaf in tests by Roodbaraky et al. (1994) on eight English street trees.

The energy loss mechanisms associated with damping in trees are not fully understood so it is usually not possible to determine the amount of damping using physical considerations (Moore and Maguire 2004). It is common to assume that damping is proportional to velocity and can be approximated by considering it as viscous damping.

A number of methods are used to determine the damping in a tree. Most commonly used on trees is the free vibration decay method (Moore and Maguire 2004) in which the tree is subject to a pull and release test in still air conditions. Once the tree is pulled then released it sways backwards and forwards until it comes to rest. By carefully measuring the amplitude of oscillations and the rate of decay in the motion, a measure of damping or energy dissipation can be made. The viscous damping ratio (ζ) is commonly used to describe the total damping of a tree (Moore and Maguire 2004) and can be determined from experimental results (Clough and Penzien 1993).

The results from a pull and release test of a tree are considered as free vibrations (no excitation force) and the rate of decay of the sway oscillations give a value for damping. Several methods are used to determine the value of damping and these include

(1) the logarithmic decrement method (Milne 1991, Moore and Maguire 2004, Wood 1995),
(2) the half power band width method (Moore and Maguire 2004),
(3) theoretical equations of motion, the Hilbert transformation and power spectra (Jonsson et al. 2007,
(4) an equivalent area method applied to the structural magnification factor for a single degree of freedom system (Haritos 1993).

The logarithmic decrement method uses the change in amplitude in the time domain of two adjacent peaks to determine the damping ratio (Milne 1991, Moore and Maguire 2004). Using the ratio of two peaks has limitations of accuracy when applied to tree sway because the decay amplitudes may not be regular and so the ratios will change depending on which two adjacent peaks ore chosen. As the tree is released it sways back towards its rest position, directly away from the release point. But this usually does not continue and a circular or looping motion develops as the tree comes to rest. This means that energy is transferred from the along pull direction to the across pull direction and back again. This looping motion is clearly seen when data from a pull and release test are plotted using two sensors which record both along pull and across pull directions of motion (James 2009). If the data from only one sensor are plotted the amplitude decay may show an initial decay period then a strengthening period or beats (Figure 2.23a). In this case the damping value calculated using the logarithmic decrement method will vary depending on which two adjacent peaks of the data are selected.

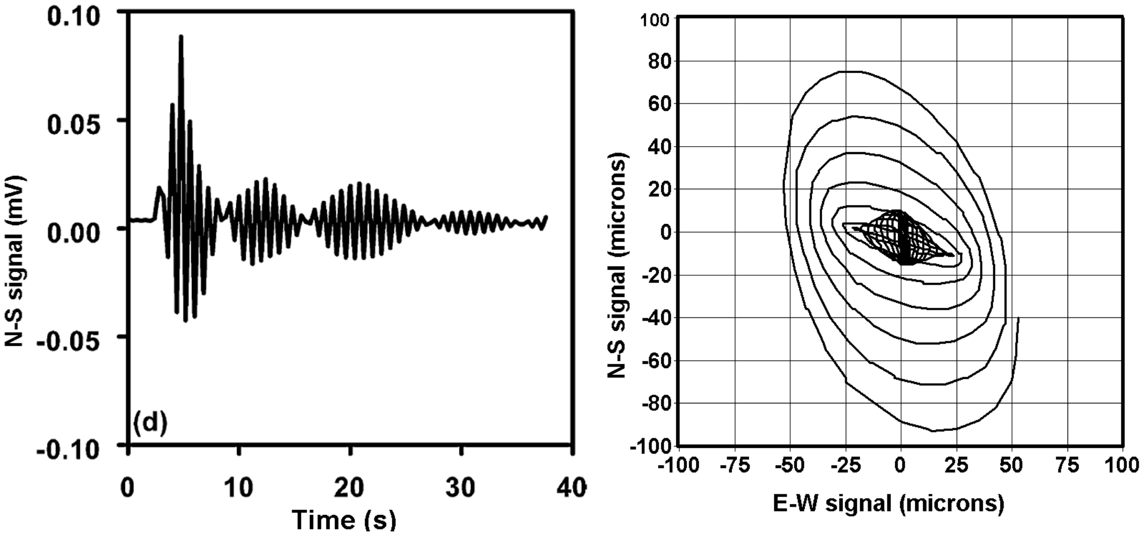

(a) Beats of in-plane signal during pull release test (Moore and Maguire 2005b)

(b) In-plane and across plane data of tree response during pull/release test

Figure 2.23. Data from pull and release test. (a) beats using in-plane data (Moore and Maguire 2005b) and (b) in-plane and across plane data plotted together showing transfer of energy as tree undergoes a looping response (James 2009).

For many structures the damping ratio is often found to be amplitude dependent with the damping ratio decreasing with decreasing amplitude of free vibration response (Clough and Penzien 1993).

The half power bandwidth method is described by Moore and Maguire (2004) and Jonsson et al. (2007). This method uses the response data from a structure under free or forced vibration and analysis in the frequency domain is used to establish the peak of the response amplitude which is reduced by a value of $1/\sqrt{2}$ (Clough and Penzien 1993). Trees subject to this forced loading eventually begin to oscillate in an elliptical pattern (Rodgers et al. 1995) which is also evident in Figure 2.23b. Haritos (1993) evaluated this method and suggested that it may not be accurate because of the noisiness inherent in the experimentally determined data. The noise in the frequency domain makes it difficult to clearly identify the peak amplitude which is always overestimated and hence results in an under-estimate of the damping ratio.

Damping can be found using the equations of motion for a single degree of freedom system to represent the sway oscillations of a tree undergoing the pull and release test. Jonsson et al. (2007) used a simplified equation

$$x(t) = ae^{-\varpi\xi . t}\left(\sin\left(\varpi\, t + \psi\right)\right) \tag{2.10}$$

In which $\varpi = 2\pi f$ the angular frequency

ζ is the damping ratio

a is the initial displacement

ψ is the phase shift.

This equation is limited to small amplitudes of oscillation. At larger amplitudes which are likely to occur when trees sway, this equation needs further refinement due to errors which can be introduced. A more accurate equation is used where large amplitudes of vibration are present (Chopra 1995) which can be written as;

$$x(t) = ae^{-\varpi_n \zeta . t}\left(\cos\left(\omega_d t\right) + \left(\frac{\varpi_n \zeta}{\varpi_d}\right)\sin\left(\varpi_d t\right)\right) \tag{2.11}$$

Noting that $\varpi_d = \varpi_n \sqrt{\left(1-\zeta^2\right)}$ or $\varpi_d = \dfrac{\zeta}{\sqrt{\left(1-\zeta^2\right)}}$

a is the initial displacement

This equation is used in Chapter 4 to analyse the data from free vibration tests on trees.

Jonsson et al. (2007) continued the analysis using the Hilbert transformation and power spectra to analyse accelerometer data of tree sway to determine the damping ratio from the slope of the power spectra. Haritos (1993) suggests an equal area method to optimally curve-fit the theoretical natural frequency and damping to an experimentally obtained spectral curve. This was found to increase the accuracy of values for damping for noisy systems and is based on fitting equal areas under the curves which represent equal energies over a defined frequency range. This has been applied to trees (Haritos and James 2008a) and is used later in this study to obtain estimates of damping.

Damping – previous studies.

Oscillations of plant stems and their damping were studied by Brüchert et al. (2003) and a discussion of damping in biological structures includes friction with other plants, structural damping, aerodynamic damping and viscoelastic damping. Comparison between oscillations of slender grass like plants (*Arundo donax* and *Cyperus alternifolius*) and spruce trees (*Picea sitchensis*) showed that trees were more complex structures and not all trees conformed to a variation of their properties in the analysis. Of thirty three spruce trees tested, only 25 were closely correlated with frequency and no damping ratio data were presented for the trees.

The dynamics of swaying trees was discussed by Milne (1988) who treated damping as a single coefficient in an equation of motion for a SDOF system. Damping had several components caused by air resistance, structural damping of the stem, and in forests branches rubbing together. No data were presented but further research to examine tree sway and damping using wind tunnel tests was suggested. Milne (1991) found that damping of sway consisted of three components, (1) interference of branches with those of neighbours, (2) aerodynamic drag on foliage, and (3) damping in the stem. For the six 26 year old Sitka spruce tested, the importance of these components to overall damping was 5/4/1 for the median tree size. Damping was found using the log decrement method. Damping values vary widely for unpruned trees (Moore and Maguire 2005b). In a study of nine plantation grown Douglas fir trees (*Pseudotsuga menziesii*), in Oregon, three trees were almost critically damped (ζ=100%) and returned to their rest position in a pull and release test within one or two cycles. Three other trees were relatively lightly damped (ζ=4 to 9%). When the crowns were removed, damping for all trees was less than 10%.

Damping ratio values ranging from 1.2% on Sitka spruce to15.4% on Douglas fir are reported by Moore and Maguire (2004) i n a review of several studies. Values varied considerably between individual trees and between species and no clear relationship was presented. Results suggested that internal damping ratios were typically less than 0.05 (i.e., 5%) and were not related to tree diameter. External damping was mainly due to aerodynamic drag on the foliage and contact between crowns of adjacent trees in plantations. Analysis from previous authors suggests that damping due to aerodynamic drag is a non-linear function of velocity. Wood (1995) suggests that the damping ratio increases with wind speed and may approach or even exceed the critical value above which resonance cannot occur. He also suggests that a change in focus to more careful examination of direct wind loading could be useful.

Jonsson et al. (2007) investigated natural frequencies and damping ratios of 24 Norway spruce tree (*Picea abies* (L.) Karst) growing on forested slopes. Pull and release tests were performed and damping ratio was evaluated using a new method of the Hilbert transformation. This allowed damping ratio to be investigated for all excited modes of vibration in the tree structure and to study if velocity proportional damping (Viscous damping) is a reasonable assumption when predicting tree response to different external actions. It was found that the damping ratio at 75% of H (tree height) was slightly higher than at 53% of H. For damping ratio, no significant correlation with different tree characteristics could be found Non-linear velocity proportional damping was observed in two out of 24 Norway spruce trees and this was considered a low number so that using a velocity proportional damping (viscous damping) assumption is an appropriate assumption for trees. A second mode of oscillation was also observed and the damping ratio of both modes was of the same order of magnitude.

Moore and Maguire (2008) simulated the dynamic behaviour of Douglas fir (*Pseudotsuga menziesii*) trees under applied loads using the finite element method and used spectral analysis to determine transfer functions for three 20 year old trees. Power spectra were calculated for the wind force input from 4096 points of 5 Hz data. Power spectra of stem displacement at 10m height were calculated for each tree enabling the transfer function to be determined. The spectra provided evidence of energy transfer from the wind to the tree and indicated the importance of branches in contributing and modifying the total tree response.

Sellier et al. (2008) measured wind induced movement of two slender Maritime pine trees (*Pinus pinaster*) with heights of 21.6 and 19.8 m and slenderness ratios of 84 and 89 in France. Data were generated from tilt sensors attached at heights up the stem and collected at 10 Hz. Spectra using 30 minutes of data were calculated for stem angular displacement and the spectral slopes were steeper than the reference -4/3 value in the sub-inertial range. Additionally there were three main peaks with the first representing the natural frequency of the tree. The other peaks at higher frequency may indicate higher modes of vibration but could also reflect energy transfer to torsional forces, or oscillations of clusters of branches. It was noted that these subsequent peaks could not be evaluated solely using the spectra from tilt data.

Previous studies of tree dynamic response to free vibration (pull and release test) or to forced excitation (wind loading) has been reviewed but another forced excitation study involving a mechanical forcing with a machine shaker gives an interesting insight into the multi-degree of freedom response of trees and the associated damping. Castro-Garcia et al. (2008) investigated dynamic response of olive trees in Spain under forced vibration from a mechanical tree shaker commonly used for mechanical harvesting of fruit. Dynamic analysis was performed on 17 olive trees (*Olea europaea* L.) under forced vibration over a range of excitation frequencies. The mechanical excitation was applied with a perpendicular force to the trunk at an approximate height of 0.6 m from the ground. Tri-axial accelerometers located in different measurement points on the tree recorded vibrations. Results generated a geometrical model with 27 to 54 degrees of freedom. Under forced excitation the first mode of vibration was at 20.2 Hz with a second mode established at 37.7 Hz and the third mode at 72.7%. The damping ratios were 26.9, 17.1 and 9.8%, respectively. The large number of local modes in the branches had natural frequencies close to that of the identified modes of vibration. The independent movement of different branches with respect to the trunk is of great importance in the dynamic behaviour of the tree making it complicated to find resonance phenomena in the main tree structure. Olive trees behaved as a damped harmonic oscillator. The damping ratio for the first two modes under forced vibration was higher than values in the literature such as 4 to 15% (Moore and Maguire 2004). Damping was markedly non-linear and was inversely proportional to frequency. Damping showed little correlation to stiffness but was significantly related to inertia in the first two modes of vibration. The elevated values of damping can be attributed to the inertial masses of the vibrating branches and the vibrating mass of the soil in the root zone which absorbs significant amount of energy.

2.6 Field Measurements of Tree Sway

Field measurements of trees swaying have been studied by a number of authors including Sugden (1962), Mayhead (1973a), Milne (1991), Papesch (1974), Baker (1997), Mayer (1987), Peltola et al. (1993), Peltola (1996b), Flesch and Wilson (1999b), Moore (2002), Gardiner (1995), Holbo et al. (1980), Kerzenmacher and Gardiner (1998), Rudnicki et al. (2001, 2008), James (2006a, 2008), Spatz and Brüchert (2000), Gilman et al. (2008a, 2008b), Schornborn et al. (2009). There have been two main approaches used to measure tree sway in the field. The first approach examines motion in the upper part of the tree or canopy and the second investigates trunk response at the base of the tree by measuring bending or strains in the trunk. This study uses the second approach by measuring strains on the trunk near the base of the tree.

Studies which examine motion in the upper part of a tree are usually limited to excurrent trees, i.e., trees with a central trunk configuration. , and the methodology and results cannot be applied to trees of other configurations such as trees with co-dominant stems or decurrent trees with many large side branches and no central trunk. This limitation is usually not emphasised in the literature. In studies of trees growing in forest and plantation stands, where the tress are tall and slender with few side branches the approach is valid. But for open grown trees of different configuration, it does raise questions about the relevance of the conclusions from some studies. Can the results from trees in forests, with a central trunk configuration and often very few side branches, be applied to trees with significantly different shapes, especially when there is considerable mass in side branches?

Field measurements of wind and swaying of two Scots pines (*Pinus sylvestris*) were made in a forest in Finland, to assess the potential of stem breakage or uprooting during wind storms by Peltola et al. (1993). In the introduction Peltola states that "the danger of stem breakage or uprooting is much increased when the frequency of gusts is in resonance with the oscillations of tree stems." This is a tacit assumption that firstly a tree sways with a natural frequency and secondly that the wind can gust and apply varying loads on the tree at frequencies at or near the natural frequency of the tree. The aim of the study by Peltola et al. (1993) was to analyse wind at the forest edge, and the subsequent swaying of two Scots pines. Wind measurements were made about 10 meters from the forest edge. The forest stand consisted of trees with a mean height of 18 –20 meters and a density of 350-400 stems ha^{-1}. The two Scots pones were 13.5 m and 9.5 m in height. The wind was measured using cup anemometers and the sway of the trees was measured using accelerometers with 90Hz sampling, and then averaged to 9 Hz to remove noise from the signal. The analysis of the wind is comprehensive and data was recorded over the wind speed range of 2 –10 m s^{-1}. The gusts of wind were variable and the gusting wind speed was defined as the mean wind speed for the gusting period which was selected as twenty seconds for calculation purposes.

Tree dynamic response to wind was measured with accelerometers located in the upper canopy. A limitation of the tree sway analysis by Peltola et al. (1993) is that the natural frequency of each tree was not measured, but was calculated using the method of Mayhead (1973a) whose analysis assumed that a tree response to wind was like a uniform metal rod. Mayhead's formula was developed using coarse data which was based on manual tree pull sways that were recorded with a stop watch and averaged over several repeated tests. The quoted calculated natural frequency of each tree was 1.89 s for the 9.5 m high tree and 2.2s for the 13.5 m tree. In the conclusion, Peltola states that the swaying of trees is more or less irregular, and the measured results do not support the sway patterns reported by the previous studies of Mayer (1987). A comment is made from observing the tree sway that "the stems never seemed to come back to the upward position, i.e. the stems were bending constantly more or less in the direction of the prevailing wind" (Peltola et al. 1993, p 121).

The study of Peltola et al. (1993) is significant in that the measured tree sway and the observed tree motions do not support the introductory statement that the danger of stem breakage or uprooting is much increased when the frequency of gusts is in resonance with the oscillations of tree stems, cannot be supported by these observations. The wind gust period of 20s does not match the quoted tree frequency periods of 1.89s or 2.2s. The tree natural frequency was never measured, and in fact tree sway at the natural frequency was observed not to occur.

Gardiner (1995), measured tree movement of four Sitka spruce trees (*Picea sitchensis*) in Scotland in a closely planted plantation forest (planting density 3584 stems ha^{-1}). These were small slender trees, with a height of approximately 15 m and diameter at breast height of 12.9 cm giving a height to diameter ratio of 116 which is above the limit of stability quoted by Slodicak and Novak (2006). There were four windy days and the tree response to wind resulted in an elliptical orbit, with the major axis in the direction of the wind. The dynamic behaviour in response to the wind loading was compared to a forced damped harmonic oscillator. Two trees were studied closely and their resonant frequencies were found to be virtually identical.

From the extreme data, the maximum average wind force was 94 N, acting on the tree at the mean canopy height of 9.3m. Gardiner does not calculate the overturning moment at the base of the tree, which would be 874.2 N m. This figure would be useful in wind throw analysis. The correlation between the wind gusts and tree movement was good for tree 2, which was nearest the tower where the wind was measured, but was quite low for the other trees.

Gardiner (1995) uses a spectral analysis to examine the frequency information in the wind data and the tree movement data. The wind spectral data showed that the wind at the top of the tree had an expected frequency range, but the wind within the canopy had a steeper decay slope which indicated that the tree was dissipating energy. This is an interesting observation and is explained as either (a) the tree absorbs energy from the wind at low frequencies and subsequently emits it at higher frequencies, or (b) energy is lost by work against drag of plant-elements.

Gardiner quotes previous work on the influence of branches by Scannell (1984) who found that branches have a resonant frequency corresponding to a harmonic of the whole tree frequency, and sub-branches resonance is a harmonic of the branch, and so on down to the smallest scales on a tree. Gardiner therefore proposes that energy is absorbed by the whole tree and is efficiently transferred through the branches and sub-branches to needles and re-emitted as wake turbulence at much higher frequencies.

The tree displacement spectra show a range of frequencies with a weak peak at 0.48 Hz, indicating the fundamental natural frequency mode of the tree. The peak was not as clearly defined as stated by Holbo et al. (1980) and Mayer (1987), so Gardiner proposes that the trees in this study were more heavily damped, so did not sway as much. Gardiner concluded that the tree behaved as a forced damped harmonic oscillator. A further analysis using coherence to test for the presence of resonance found however, that there was no indication of strong resonance in any of the trees studied. Also of interest was the statement that gusts of wind may occur near the natural frequency of a tree and cause greater movement than in normal winds. There was no evidence that the tree amplitude increased with successive gusts of wind. The wind gusts are important in providing the energy to cause tree sway but the tree acts like an energy absorber and does not appear to resonate.

The natural frequencies of 62 trees around Nottingham University were measured by Baker (1997) using a laser interferometer to measure sway motion. The trees included 27 healthy limes (*Tilia x europea*), 13 with signs of disease, 10 healthy other species and 12 diseased trees. Measurements were made in July 1995 in summer and full leaf conditions, and in November 1995 in winter with no leaves present. A range of responses was noted and three different sway spectra types were identified, Type I, II and III. Type I spectra had a low frequency peak at between 0.3-0.6 Hz in summer and in winter 0.5-1.5 Hz. This is a range (or average) and is not specific to any one tree. It was noted that for any one tree size, there was a wide spread of values and this limits the usefulness of this information. It seems that it would be important to quote a value of natural frequency for a specific tree, not just quote a range. Type II had no identifiable peak spectrum, so no preferred natural frequency occurs. Type III spectra was similar to type I but with a natural frequency range significantly lower than type I. Type III spectra corresponded to trees within avenues with steeply inclined branches less than 10 degree to the vertical. The size of the trees ranged from a DBH of 80 cm down to 10 cm which may be too small to use in this type of analysis. The study of Baker (1997) did not really establish the natural frequency of any one tree and gives a range of values for a range of tree sizes. It was noted that higher frequency harmonics were absent and this may imply that all harmonics are absent. An explanation of the variation refers to the aerodynamic effect of the leaves and root system, but there is no discussion of the effect of branches and the possible influence on the dynamic sway characteristics of the tree.

Flesch and Wilson (1999b) made field measurements of trees in plantation forests in Canada, to investigate the effect of cutting strips in the across wind and along wind directions. A simple mass spring damper model was used to evaluate and predict critical wind speeds. It was found that in designing cut blocks to reduce wind throw, the cut blocks should not exceed three times the tree heights in width.

Spatz and Brüchert (2000) applied basic biomechanics principles to the study on wind loads and gravitational loads on a single Norway spruce tree (*Picea abies*) which was uprooted in a storm on 5 March 1988, in Attglashütten, Germany. This tree was 56 years old, 27.6 m high with a diameter at breast height (dbh) of 65 cm resulting in a slenderness ratio of 42, though this was not stated. Branch whorls carried an average of 5.6 branches with an average distance of 63 cm apart, starting at a height of 5 m above the ground. The tree structure consisted of a central trunk with a conical canopy and was regarded as a solitary tree. This study gives an excellent perspective of tree growth and biomechanics and outlines an excellent strategy for the application of biomechanical considerations. “Growth of trees is determined largely by physiological constraints, in particular those affecting photosynthesis and water transport. If these are optimal, limitations to size and shape are still imposed by biomechanical constraints." (Spatz and Brüchert 2000, p33). Spatz and Brüchert (2000) apply a static analysis to determine the stresses applied to this tree and the Euler buckling analysis is used to calculate the critical height for buckling of 84 m or 45 m allowing for additional crown weight and snow load. Both these critical height values are above the tree height of 27.6m so it is concluded that the tree is within safe limits from failure due to buckling. The authors then analyse the wind loads using a steady or quasi-steady approach which is justified by assuming the solitary tree, with its large sail area as having large enough aerodynamic damping to give steady state conditions. This treats the wind as a steady force and as a distributed load acting on the canopy. This quasi-steady state approach does not allow for the effects of gusts nor take any dynamic effects of the trunk or branches into account. The authors state that the assumption of constant wind speed within the crown certainly neglects the influence of other branches from the same whorl, giving wind shelter to the branch under consideration. The bending stresses along the stem due to the steady state wind are calculated and it is shown that only under wind loading do critical stresses develop in the tree.

The dynamic response of a tree to overturning, due to the dynamic effect of a gust of wind superimposed on a steady wind has been studied by England et al. (2000). Resistance of root systems to rotational motion is known from tree pulling experiments. A gust of wind generates an impulsive load on the system and hence the dynamics of the tree may be modeled. An empirical formula which relates the speed of a gust of wind and its duration to the mean wind speed is used to determine the mean wind speed necessary to overturn a tree, and critical wind speeds are quoted for trees such as Sitka spruce (*Picea sitchensis*).

Field tests to measure the natural frequency of trees have been performed by pulling on trees with rope, and pulsing the pull to get the tree swaying, and then recording the subsequent movement and the period of vibration (Moore 2002). In the tests of Moore (2002), nine Douglas fir trees of about 20m height were pulled five times to develop a sway, then released. The movement was recorded using strain gauge instruments attached to the trunk of the tree. A limitation of this method is that the damping of the trees was so great that only 5 to 7 sway periods were recorded before the motion was completely damped and the tree came to rest. Frequencies were determined from this small amount of data and the quoted values were in the range of 0.37 Hz up to 0.63 Hz.

Interestingly, this study examined the effect of the removal of the branches on the natural frequency of the structure, and as the branches were removed and the structure approached a slender column, so the natural frequency became more defined. Results of branch removal showed that up to 80% of the crown mass needed to be removed before there were noticeable changes in the measured natural frequency.

Moore (2002) cites previous studies of tree natural frequencies, where the trees are forced to sway using an attached rope. Early studies used rudimentary methods of timing the sway period, such as with a stop watch and visual estimates (Sugden 1962). Other similar studies by the British Forestry Commission in the 1970's used displacement instruments and chart recorders. Recent studies in the 1990's have used modern electronic instrumentation and portable data loggers (Milne 1991, Gardiner 1992, Roodbaraky et al. 1994).

2.7 Instrumentation

This section reviews the instrumentation used in previous studies on tree response to dynamic excitation. It is instructive to review these studies to show how the approach of the researcher and the choice of instruments have influenced the results and conclusions from these tests. The instruments used depend on the strategy chosen by the researcher. For this discussion two strategies can be considered. One strategy studies dynamic response in the upper part of the tree, and the other studies dynamic response in the lower trunk near the base. If it is decided to examine motion in the upper part of the tree or canopy, then certain instruments will be chosen, such as, accelerometers or displacement transducers, that measure response in the upper tree area. If the other strategy of investigating tree response at the base of the trunk is chosen another range of instruments needs to be used to measure the dynamic response in a different way.

Instruments used to study dynamic response in the upper canopy of a tree

Previous studies of the upper part of the tree have used a range of methods which include stopwatches (Sugden 1962, Mayhead 1973b), accelerometers (Blackburn et al. 1988; Peltola 1996b), displacement transducers, (Gardiner 1995, Kerzenmacher and Gardiner 1998, Milne 1991, Roodbaraky et al. 1994), prism based systems (Hassinen et al. 1998), lasers (Baker 1997), tilt sensors (Flesch and Wilson 1999b, Sellier et al. 2003, 2008, Sellier et al. 2006, Gilman et al. 2008, Rudnicki et al. 2001) and video based techniques (Peltola 1996). Instruments which record motion in the upper part of a tree may record the motion accurately at that specific location but may not be capable of recording the total dynamic response of the tree. For example the dynamic effects from branches in the lower parts of the tree may not be recorded by an instrument in the upper part of the tree. In studies that record motion in the upper part of a tree, there is usually an unstated assumption about the tree shape being an excurrent tree with a central stem. Most forest plantation trees are of this shape so studies which look only at these trees collect dynamic data which may be suitable for that specific tree shape, but may not be applicable to trees of other configurations, particularly decurrent open grown trees with large side branches and no central trunk.

The instruments and technology used by researchers to study trees and the response to winds has developed over many years. One of the earliest studies used a stopwatch to record tree sway in test that induced sway by pulling with a rope then releasing the tree (Sugden (1962). Measurements from 862 red pine (*Pinus resinosa* Ait.) and white pine (*Pinus strobus* L.) growing in plantations were taken and averaged to find the natural frequency. The same method was used by the British Forestry Commission to collect data during the 1960s that was later used by Mayhead (1973a) to determine natural frequencies. This technology had limited accuracy and the method of averaging several observations restricted the precision of any one test. Modern technology has much greater accuracy and resolution and has the ability to record data at fast rates which means that dynamic responses can be measured more precisely to give much more detailed data than these simple methods.

More recent technology and electronic instruments such as strain gauges, displacement sensors and portable data loggers have been used to obtain more accurate information on tree response under static and dynamic loading (Brüchert et al. 2000, Milne 1991, Baker and Bell 1992, Gardiner 1995, Roodbaraky et al. 1994, Flesch and Wilson 1999b, Hassinen et al. 1998, Holbo et al. 1980, Sellier and Fourcaud 2005).

Thin wires and potentiometers

Tree displacement during sway tests has been measured at several heights up the tree by attaching wires from the trunk, back to displacement transducers on the ground (Holbo et al. 1980, Milne 1991, Baker and Bell 1992, Roodbaraky et al. 1994 and Gardiner 1995). Milne (1991) used thin nylon wires connected to the tree stem 6 m above the ground to measure the displacement of Sitka spruce trees (*Picea sitchensis*), (Figure 2.24). Displacement sensors were attached to posts in the ground at distances of 4 and 6 m from the stem in two directions at right angles. Displacement data from the sensors were recorded at 10 Hz on a data logger. In calm conditions, the trees were set to sway by pulling on an attached rope. This system was suitable for manual excitation tests in calm conditions but the wires are subject to wind and cause errors so no measurements under wind conditions were taken in this study.

Baker and Bell (1992) measured displacements at several heights on a number of trees at Nottingham University by attaching thin nylon wires to displacement transducers at ground level. Wires were oriented orthogonally to the trunk to record sway in all directions at a sampling rate of 4 Hz with length of record usually limited to 10 to 15 minutes. This gave some useful frequency data but the slow sampling rate of 4 Hz limited the resolution of the displacement spectral information which had significant noise in the curve that masked any peaks and made natural frequency identification difficult.

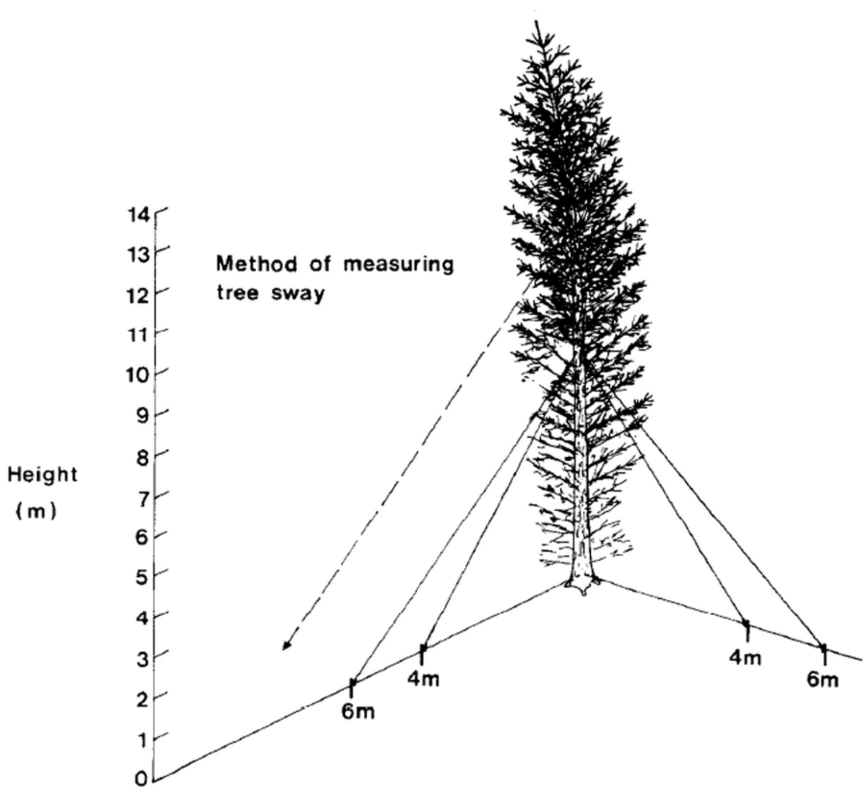

Figure 2.24. Example of displacement sensors used to measure tree sway in the upper part of the canopy (Milne 1991).

The displacement response of four Sitka spruce trees (*Picea sitchensis*) in a Scottish plantation was measured(Gardiner 1995) using displacement transducers secured to pegs in the ground, and attaching fine steel wires at 45° to the tree. Wind speeds were measured on a 30 m tower, located several metres from the trees. During a 10 month period, there were four windy days used for data collection. Wind speeds ranged from 3.54 to 8.26 m s^{-1}. The fine steel wires vibrated in the winds which limited their accuracy

Roodbaraky et al. (1994) used thin fishing wires fixed between the ground and several points up the trunk to connect linear displacement transducers that recorded displacement at 4 Hz. These lines were fixed along one direction only so deflections measured were not necessarily in the same direction as the wind. The mechanical properties that were measured (stiffness, natural frequency, and damping) were obtained from tree winching and quick release experiments. Only one tree was used for collecting wind data and some of the results presented show significant across wind components in the time domain. Using only one direction of measurement limited the conclusions regarding the relationship between wind speed and drag coefficients.

Holbo et al. (1980) measured tree sway under medium wind conditions (2.5-6.75 m s^{-1}). Three Douglas fir trees (*Pseudotsuga menziesii*), aged 40 years old and 26-30 m high were studied in forest conditions. Fine steel wires were attached to the trees at 16m height, and displacements were measured using displacement transducers. Wind speed was measured using a propeller anemometer at height of 35m. Data acquisition was at 10 Hz. Nield and Wood (1999) presented and analysis of data collected by Gardiner on four trees pulled under calm wind conditions with horizontal deflection measured using plumb lines attached to the stem at four heights. This method has very limited accuracy due to movement of the long plumb line. The tests were limited to calm conditions and small deflections.

Strain gauges

Brüchert et al. (2000) used strain gauges attached at 0.5-2.0 m intervals along the stem of Norway spruce (*Picea abies*) at 4 sites in Germany. These gauges were attached to the peripheral fibres of the stem during static pull tests in order to measure flexural stiffness and material properties on the tree. No specific details of the instruments were given. Orthogonally oriented strain gauges attached to branches of pine saplings were used to measure bending strains in both vertical and horizontal planes (Sellier et al. 2003, Sellier and Fourcaud 2005). Kyowa strain gauges were glued to the wood after the bark was removed. The strain gauges on branches were used in conjunction with inclinometers (Sensorex) on the stem and motion of the pine saplings under pull and release free vibrations were studied.

Tilt sensors

Tilt sensors or inclinometers have been used by a number of authors (Flesch and Wilson 1999b, Gilman et al. 2008, Rudnicki et al. 2001, Sellier and Fourcaud 1995, Sellier et al. 2008, Schornborn et al. 2009) to measure the tilt of the stem during wind excitation. These sensors give the maximum readings in the upper part of the canopy and have minimum response resolution near the base of the stem where deflections are small. Their output gives a measure of the angle of tilt which needs to be related to stem deflection, often with assumptions about stem deflection shapes which may be specific to each tree. If the sample rate is fast enough these sensors act like accelerometers and give excellent data for frequency analysis and spectral analysis. A limitation of these sensors is that it is difficult to relate the tilt angle to other parameters of wind loading such as base bending moments.

Flesch and Wilson (1999) measured tree sway with bi-axial tilt sensors (Mountain Watch, Calgary, AB) mounted on stems at approximately 3 m height gave angular displacements in the x and y directions. Data collected at 5 Hz for duration of 15 or 30 minutes. Six forest trees were monitored, each selected because they were near 5m high, were isolated from other trees and were near to an anemometer. The data were related to a model tree and were sufficient to obtain the frequency and spectral analysis for each tree.

Tilt sensors were used to measure tilt angle or pitch of the central trunk of 6 m high *Quercus virginiana* (Gilman et al. 2008b) and on branches of a 12.5 m high Norway maple (*Acer platanoides)* (Schornborn et al. 2009). Gilman used a high powered fan to simulate wind and the results from different pruning trials were expressed as pitch angle plotted against wind speed. The data provided useful information on tree response for different pruning methods but the results could not be used to determine base bending moment and hence wind loads. Similar tilt information and spectral analysis were presented by Schornborn et al.(2009) on branch deflection response in winds which showed an interesting upward response in winds but could not be expressed in base bending moments of the branches. It is suggested that using tilt sensors is useful for tilt and spectral information but is limited because the results cannot be translated into base bending moments which can be used as a measure of wind loading.

Sellier et al. (2003, 2008) used bi-axial tilt sensors on two slender Maritime pine (*Pinus pinaster*) to measure natural frequencies and damping ratios. These instruments were excellent for evaluating the frequency, damping and modes of vibration but it was noted that the saplings were small and the mass of the inclinometers most likely affected the swaying response of the trees (Sellier et al. 2003). These inclinometers were not useful to estimate wind loads or base bending moments.

Prism based system

A prism-based system for accurate measurement of the stem movement and frequency response of trees under dynamic wind loading is described by Hassinen et al. (1998). Tree movement was measured along with wind speed at the edge of a stand of Scots pine (*Pinus sylvestris* L.) close to 11 m in height. A 16 m mast was erected just upwind of the edge and instrumented to measure wind profile and wind direction. One tree located close to the upwind mast was instrumented with a target prism and accelerometers at the mid-canopy level in order to study tree swaying and frequency response. The suitability of this system for measuring the frequency response of trees under field conditions was tested by comparing the mechanical transfer functions for the tree obtained in this way with those from the accelerometers. Good agreement was found at frequencies close to and above the tree's natural frequency but differences emerged at low frequencies, suggesting that the accelerometers overestimate the low frequency response. The accuracy and repeatability of stem displacement measurements made using the prism-based system were found in laboratory tests to be very high. The new system can be adjusted quickly to make measurements at different heights on the same tree or on other trees by simply adding additional target prisms.

Accelerometers

Accelerometers are small electronic instruments which respond to movement and have been used in tree studies to investigate dynamic response under wind loading (Peltola et al. 1993, 1996b, Hassinen et al. 1998 and Blackburn et al. 1988). Modern electronics have developed very small sensors which can act as both accelerometers and tilt sensors. Both of these instruments must be used in the upper part of the canopy where significant movement occurs, and will not be suitable for use near the trunk base.

Accelerometers offer a convenient method for measuring dynamic motion and the frequency response of a structure but are less suitable for measuring displacements in the time domain due to problems of drift (Peltola et al. 1993, Blackburn et al. 1988). Accelerometers can only start to record after some initial movement and so miss the first component of displacement. A double integration of the acceleration is required before displacements are determined. The initial position of the tree must be estimated, and any error is then compounded during the two stages of integration required to obtain displacement (Moore and Maguire 2004). This leads to an accumulation of errors and makes it difficult to assess the magnitudes of very low frequency components in the motion with reasonable confidence (Peltola 1996b, Gardiner 1992, 1995). Wind loads can be estimated by integration of accelerometer data and quoting values of displacement (Peltola et al. 1993). However it is not possible to use this to convert to base bending moment values without assumptions on the trunk material properties and shape so it is difficult to compare wind load values from one study to another.

Video

Video was used to record tree motion (Peltola 1996b) which was converted to displacement values. A lamp sensor system was placed on the stem of Scots pines in a plantation in Finland. A video camera monitored the movements of the stem and was used to obtain displacement data. This method was used in conjunction with accelerometers which were not able to accurately measure displacement. The video camera took images at 50 times per second and was suitable for obtaining spectral information and transfer functions for the tree. This method was used on an excurrent tree with a single central stem and could be useful for other shaped trees and branches although the complexity of measurements would be very high.

Laser Doppler interferometer

Baker (1997) measured tree sway using a tripod mounted Laser Doppler Interferometer since the method had been used successfully to measure natural frequency of building structures. Small movements in the target structure produce interference of reflected light from a helium neon laser in a pair of photo-detectors and the voltage signal is proportional to tree velocity in the direction of the incident beam. This gives a measure of velocity in one direction only and was used to determine velocity spectra over the range of 0-1o Hz with intervals of 0.04 Hz. The authors consider this instrument to be suitable for measuring the natural frequency of the open grown trees that were monitored around Nottingham University.

Summary of instruments used in upper canopy

All the instruments in the above review are used to measure dynamic tree response of the upper part of the tree. Each of these instruments has a particular application in monitoring the sway motion of trees, especially in measuring oscillation frequencies and gathering frequency data which are useful for spectral analysis. They usually measure only one or two parameters very well with the most common methods measuring the deflection of the trunk, or tilt at different heights up the trunk, or acceleration as the trunk sways. The data are useful for finding fundamental dynamic parameters such as frequency and damping ratio and which can be used for modelling applications. However, a limitation of all these instruments is that they cannot be directly used as a measure of wind load on the tree.

Most of the instruments reviewed have limitations in their application and accuracy so that their suitability for measuring oscillation behaviour of branches is questionable (Moore et al., 2005). Accelerometers are useful to obtain frequency data but errors accumulate during double integration which makes position and displacement data difficult to accurately record (Peltola 1996b). Tilt sensors record variation in tilt angle very accurately, but assumptions must be made about bending shapes of trunks to determine deflections. Tilt values are also non-linear, with the least sensitivity near the vertical axis of an upright tree trunk. Prism based sensors are very accurate but the system described by Hassinen et al. (1998) had limited range due to the beam moving off target so could not record the large deflections of trunks in wind storms. There are several systems using displacement sensors, such as the system described by Gardiner (1995) in which long wires were used from the ground to the tree trunk to connect a sensor at approximately half the tree height. This worked well but had limited accuracy, with the wires being subject to wind deflections. Modern laser systems offer extreme accuracy and the method described by Baker (1997) worked well and could be developed further.

The wind load is best evaluated by measuring the bending moment induced at the trunk base and quoted in kNm. The methods that try to measure response in the upper canopy can estimate this but must make assumptions such as bending shapes of the trunk, or indeed that the tree has a central trunk. These methods are limited because they are used on excurrent trees and are not suited to other trees with different configurations such as decurrent trees. The displacement systems that use wires attached form the ground to the trees will be subject to considerable wind excitation which will mask any tree displacement data so are unlikely to be useful in strong wind situations. One significant limitation is that instruments in the upper part of a tree cannot record all the dynamic branch responses of a tree and so miss important information. Instruments that record movement in the upper part of a tree may not be successful at recording the dynamic contribution of branches in the lower regions of a tree. This is significant for decurrent and urban tree where there is considerable contribution to the total tree response due to branches which act as dynamic masses oscillating in the wind with their own individual characteristics.

In order to develop more robust methods that can be applied to all trees in wind and storm situations, it is suggested that the strategy of measuring tree response in the lower part of the tree is preferred. Some reviews of these methods are included below.

Measurements in the lower part of the tree

The second strategy of measuring tree response is to place instruments on the lower part of the trunk, near the base and record the bending response during wind loading. This approach has been used by Rodgers et al. (1995), Guitard and Castera (1995), Peltola et al. (2000), Gardiner et al. (1997), Moore et al. (2005), Moore and Maguire (2005) and Spatz et al. (2007). Rodgers et al. (1995) used an instrument called a “strain measuring device” mounted on the side of trunk at the base of Sitka spruce trees (*Picea sitchensis*) during a pulling experiment in Ireland but no specific details of the instrument were given. The instrument was calibrated using a static pull test so that the instrument output could be converted from microstrain to moment with units of kNm. Maximum bending moment of 10 kNm was recorded during a rocking test and failure occurred at 12 kNm. These values are low due to the wet soils and the limited holding capacity of the root plate. Some basic monitoring of wind induced response of the trees was made but this was very limited by the technology available at the time. Scanning rate was 5 Hz and data for only 8 seconds was used over five time periods.

Guitard and Castera (1995) measured sway frequency in a tree scale model using an extensometer plugged under the bark at the tree stem base. Problems with measurements made in only one plane were observed as the tree oscillated in out of plane modes and it was recognized that torsion may also contribute and should be included in the spectra. Gardiner et al. (1997) measured base bending moments at the base of experimental trees using Linear variable differential transformers (LVDT) mounted on the stem at right angles to each other. Each LVDT had a span of ±1 mm with a resolution of 0.6 μm and were attached to the tree at 0.5m above the ground. They were calibrated on the tree by applying a known static pull so that the LVDT voltage output could be converted to base bending moments. Data were collected on magnetic tape for one hour periods. No data rate was quoted but was sufficient to determine the natural frequency for each tree. Eleven experimental trees, Sitka spruce (*Picea sitchensis*), ranging in height from 14.3 to 21.8 m and slenderness ratio of 54 to 89 were monitored from a stand in Cumbria, UK.

A device termed a “Young’s modulus sensor was used during static pull tests on Scots pine (*Pinus sylvestris*) and Norway spruce (*Picea abies*) in Finland (Peltola et al. 2000). This device consisted of a displacement transducer mounted at the base of the trunk with a design similar to Rodgers et al. (1995). No technical details were given and the instrument successfully recorded bending moments though the values were in the lower range of 5.9 to 19.2 kNm. These instruments were not used to measure the dynamic response of the tree under wind loading.

Moore et al. (2005) describe a relatively inexpensive calliper type strain gauge transducer which was capable of measuring the oscillations of both the stem and branches of a tree subject to wind loading. This instrument used two stiff lever arms to concentrate the bending into a metal hinge and the strain gauges were mounted in the hinge where the bending was at a maximum and therefore the sensitivity was greatest (Figure 2.25). Two strain gauge transducers were mounted on the trunk of a tree near the base in orthogonal directions such as N/S and E/W to record tree response under wind loading. These instruments were also suitable for mounting on branches. Data were recorded at 10 Hz to successfully record bending response of trunk and branches. These instruments were used by Moore (2002) in a PhD study and later by Moore and Maguire (2005) to measure the natural frequencies and damping ratios of Douglas fir trees.

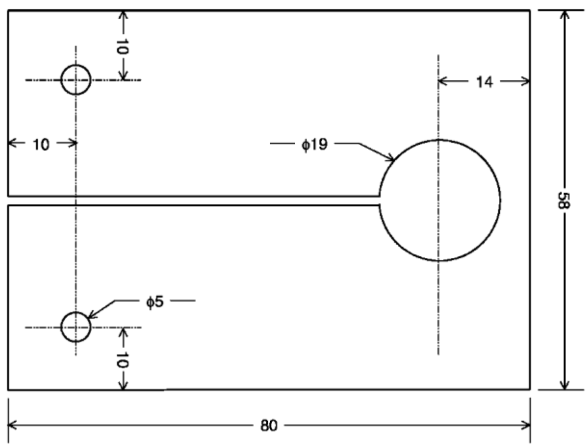

Figure 2.25. Lever arm type strain gauge transducer used to measure base bending moment of trees and branches (Moore et al. 2005).

The data sampling rate was 2.5 Hz which was sufficient for spectral analysis but resulted in aliasing in the time domain representation of pull and release tests causing a star pattern rather than the smooth looping pattern found at higher sampling rates of 10 to 20 Hz which would have improved the resolution of this instrument.

In German forest, a 12 year old Douglas fir, 5.03 m high, DBH of 7cm (slenderness ratio of 72) was physically measured, including all 90 primary branches and 28 primary sprigs of length greater than 0.2m (Spatz et al. 2007). Oscillations were recorded with an extensometer (manufactured by Wessolly, Stuttgart, Germany) but no details were given of the instrumentation. Two extensometer attached in two orientations at height 2.26m above the ground and data recorded at 10 Hz. Rope attached to the tree 2.63 m above the ground and used to oscillate the tree. The extensometer data was used to determine frequency and damping response of the trunk and branches but no base bending moment values were given.

Summary of instruments used in the lower part of the tree

Measurements made in the lower part of the tree, near the base of the trunk, will record all the collective response of the trunk and branches above the point of measurement. The wind pushing on the canopy creates a force in each branch and all the branch forces must pass down through the trunk to the ground. These forces create a bending moment at the base and as the tree bends, the outer fibres of the trunk will stretch on the windward side and contract on the leeward side. If instruments can detect this bending or fibre elongation, then they have the potential to measure all the forces from the all the branches. An advantage of this method is that it works for all structural forms of trees and is not restricted to excurrent tree shapes. The total tree response can be detected and the wind load can be measured in bending moment units. This is difficult to achieve with instruments located in the upper part of the tree, because if tilt or displacement values from high in the tree are to be converted to bending moments, the conversion depends on the trunk bending properties which are unique to each tree. Because trunk bending depends on material properties and the shape of the trunk, it is difficult to relate tilt values from one tree to another. Instruments in the upper part of the tree may also not be able to detect some of the tree response from branches located below the point of attachment and therefore not record the total response.

Chapter 3. STRUCTURAL MODELS OF TREES

In this chapter, previous studies of tree structural behaviour using models are reviewed. The simple models of trees that are based conceptually on a single central trunk with no branches are reviewed in first section. Models of this type are considered to be single degree of freedom (SDOF) systems which make dynamic analysis reasonably simple. Models of trees are used in order to understand the response of trees to dynamic structural loading, especially in winds. Often the aim is to assess how trees will be affected by wind and to predict the risk of damage (Moore and Maguire 2004). Studies in recent years have shown that tree response is complex and more sophisticated models are needed (England et al. 2000) particularly to take account of branches and their contribution to the dynamic response of the whole tree (Sellier and Fourcaud 2009).

There are few models that include branches as dynamic masses (Fleurant et al. 2004) and consider the tree as a multi-degree-of freedom (MDOF) system. Recent more sophisticated methods using finite element analysis (FEM) are showing that still more complexity needs to be developed to fully describe how a tree responds to wind loading (Moore 2002, Moore and Maguire 2008, Sellier et al. 2006, 2008, Sellier and Fourcaud 2009). The below ground response of the roots and soil also influence the response of trees by dissipating energy and contributing to damping. Some models of roots have been developed (Blackwell et al. 1990, Nield and Wood 1999, Bergeron et al. 2009, Fourcaud et al. 2008) but only the above ground components of trees are considered in this study.

This chapter concludes by describing a new conceptual model for trees (James 2003, James et al. 2006) that includes branches as oscillating masses which act to dissipate energy as a dynamic damper. This dynamic damping is termed mass damping which has not been previously described for trees.

3.1 Previous Models of Trees

Models of trees are used in an attempt to describe their response under different loads and to predict how trees will respond under dynamic conditions such as wind loading (England et al. 2000, Coutts and Grace 1995, Kerzenmacher and Gardiner 1998, Baker and Bell 1992, Baker 1995, Guitard and Castera 1995, Saunderson et al. 1999, Peltola and Kellomaki 1993, James et al. 2006), snow or ice loading (Fridman and Valinger 1998, Peltola et al. 1999, Gaffrey and Kniemeyer 2002), in forests after silvicultural treatments such as thinning (Gardiner et al. 2000, 2005, Cucchi et al. 2005, Novak et al. 2001, Flesch and Wilson 1999b and Peltola 1996a), and in changing climatic and environmental conditions (Peltola 1999). Models are useful to predict the likelihood of tree failure and the risks of damage in urban areas of economic loss in forests. Some simple cantilever models used for grasses and crops (Finnegan and Mulhearn 1978, Spatz and Speck 2002, Spatz and Zebrowski 2001) have been used to discuss behaviour of single stem plants such as grasses and tall thin trees though the simplifying assumptions limit their application to open grown trees with multiple branches.

All models must make some assumptions in order to simplify the analysis but some assumptions such as ignoring branches or treating them as rigid lumped masses may not adequately represent the complex dynamic response of trees (Moore and Maguire 2004). Simple models that consider the tree as a central column and use equations that assume a SDOF system must inevitably conclude that trees will resonate at a natural frequency. Field measurements of dynamic response indicate that resonance does not occur (James and Kane 2008) and more complex models are needed to take account of different tree shapes and species and in particular to account for the dynamic influence of branches (England et al. 2000).

The first structural model of a tree, used by Greenhill in 1881 (Spatz 2000) considered the tree as a pole (Figure 3.1) in order to apply simple static mathematics and calculate how high a tree could be before it buckled under its own weight. There was no consideration of dynamic loads such as wind or other factors such as branches. This central column model is a first approximation, and applies to some trees such as forest trees in dense stands, or conifers but does not consider branches at all and does not begin to approximate single multi-stemmed tree species which are most common in urban areas.

Greenhill's simple pole model for trees has been the conceptual basis for both static and dynamic analyses, and has been the basis of the approach used in many tree research projects including, Guitard and Castera (1995), Peltola and Kellomaki (1997), Gardiner (1992), Baker (1995), Saunderson et al. (1999), Brüchert et al. (2003), Spatz (2002) and Nield and Wood (1999).

Greenhill's model has some application to excurrent trees with a central trunk structure when considering purely static loads such as gravity and the potential for buckling. However, the central pole model has major limitations in dynamic analyses of a tree because the dynamic response of a pole to excitation will be very different to that of a tree. The dynamic response of a pole to excitation will be to behave as a SDOF structure.

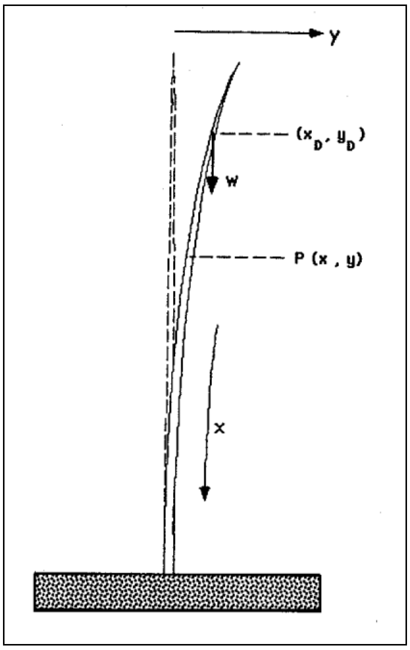

Figure 3.1 A simple tree model, considered as a tapered pole, from Greenhill's 1881 formulation of the Euler buckling problem (Spatz 2000).

The consequence of this approach is that a SDOF model will resonate at a defined natural frequency and will oscillate backwards and forwards with regular cyclic motion. This is an inevitable outcome of a SDOF model such as a single column which is not a tree. The simple pole model of trees has been further developed to study dynamic effects such as natural frequency and damping. Studies which collect data on the natural frequencies of trees usually attempt to model these frequencies as a function of tree size (Moore and Maguire 2004). The equations used come from considering the tree as either (a) a beam with negligible mass with a top load or (b) as a beam with distributed mass but without a top load. Both these approaches make an inherent assumption that the tree is a central column shape but this is rarely stated.

Pole or column models have been used to analyse trees growing in closely spaced plantations or forests (Gardiner et al. 2000, 2005, Cucchi et al. 2005, Novak et al. 2001, Flesch and Wilson 1999, Peltola 1996b, Jonsson et al. 2007, Moore and Maguire 2008, Rudnicki et al. 2008, Schindler 2008) because these trees are tall and slender with little or no branch mass and the simple model is a good approximation of the actual tree. However, the model is limited to trees of this shape.

A useful measure for assessing how closely the simple model approximates a tree is the slenderness ratio defined as the height to diameter ratio. For slender plantation trees a slenderness ratio above 55 to 60 is common, with limits on stability at approximately 80 (Slodicak and Novak 2006). The range of quoted slenderness ratio values in even aged spruce stands is narrow with values higher than 100 implying low stability of stands (Milne 1995). Critical slenderness values of 90 are quoted for trees with snow damage in young stands and lower values were recommended, with an optimal slenderness ratio of 79 and an acceptable maximum of 83 (Slodicak and Novak 2006). The significance of the slenderness ratio is that trees with a value in excess of 80 will have a dynamic response similar to the central pole model so the assumption of a SDOF system could be used as a first approximation. An extreme value of slenderness ratio of 162 (Rudnicki et al. 2001) is quoted for a 15.4 m high lodgepole pine (*Pinus contorta*) in a Canadian plantation. This tree would not be stable if it grew alone in an urban environment.

Trees with slenderness ratios below 80 may not be approximated by the central pole model which is an oversimplification that does not adequately describe the dynamic response of these trees to wind forces. Open grown trees grow in a very different environment to plantation trees and develop side branches that are a significant proportion of the total mass of the tree. Because they grow as single trees and endure a varying wind environment throughout their life, urban tree develop a lower slenderness ratio and values in the current study ranged from 14 to 25. The lower slenderness is due to an increase in trunk diameter compared to height and is an adaptation to increase their stability (Peltola 2006b, James 2006).

Mayhead (1973b) studied tree sway in tests induced by hand pulling. A model was developed by assuming that a tree was like a uniform metal rod but this model was not a good approximation as demonstrated by the observed differences between the model and the data from the trees. There were significant differences in the sway response between trees of the same species and between trees of different species. Mayhead discussed the influence of branches on the dynamic behaviour of trees and suggested that differences between species might be due to differences in factors such as branch form, branch flexibility, length of canopy and a form factor. Their observations were supported by later studies of oscillation frequencies which found an increase in frequency after branches were removed (Milne 1991, Gardiner 1992).

In a dynamic analysis of a tree and its branches, properties such as frequency and damping need to be evaluated. A comparison of natural frequency between stem only and whole tree (stem plus crown) for 16 Sitka spruce, 6 red pine and 9 Douglas-fir trees showed a linear relationship between DBH/H^2(Moore and Maguire 2004). Differences in crown mass and crown length were also significant factors. The influence of branches on structural damping was also discussed by Niklas (1992) and estimated in tree pull release experiments summarized by Moore and Maguire (2004).

A simple model of a single central trunk without branches was used by Milne (1988) in the dynamic analysis of tree sway in winds which used several assumptions although they were not stated, i.e.,

1. that a structure of this configuration had a natural frequency,
2. the sway motion would be backwards and forwards, and
3. the mass and dynamic effects of branches could be ignored.

Milne discussed the tree as a structure which stores energy from the wind as it bends, then releases this energy on the back swing. The conifer of about 15 metres tall swayed back and forth at a “natural frequency” every 2 to 3 seconds. The mathematical analysis used by Milne, was a simple second order equation of motion (Equation 1) which had the inevitable outcome of finding a natural frequency. Milne correctly identified that the wind did not act as a steady force on a tree but was turbulent and always came in gusts. He stated that if the wind gust is in time with the tree’s natural frequency (2 to 3 s for conifer 15m high), the repeated gusts would displace the tree three or more times as much as constant wind because the tree gathers momentum. This build up of momentum was modified by damping, which Milne briefly described and attributed to three factors, air resistance, structural damping of the stem, and branches rubbing together in forest trees. No data were presented to support this discussion and the unstated assumptions of a pole and a SDOF system limited the conclusions of his study.

A dynamic analysis of tree sway frequency and damping by Wood (1995, p133) begins with the statement “Measuring the natural frequency of a tree is easy”. The justification is that after a little trial and error, a resonant sway vibration can be established by periodic hand pressure, and the cycles counted against time. Wood used a static bending analysis model but no data supported the mathematical analysis which used the second order equations of motion to calculate the tree's natural frequency. The limitations of this analysis of tree bending and vibration were discussed and he stated that it was not sufficiently sophisticated to take account of branches as anything other than added masses at each level. He also identified the possibility of needing more elaborate theories which would require more detailed information about the spatial distributions of mass and stiffness of the branches themselves.

A model of trees in forest plantation systems, developed by Flesch and Wilson (1999b) described the tree as a simple mass-spring-damper that rotated about the base. The tree stem was considered as a rigid rod with uniformly distributed mass that responded to wind excitation by rotating about a rotary spring at the base. This is a very simple SDOF model which does not include any elements for the branches. The accuracy of the tree model was considered to be in reasonable agreement with actual tree displacements and considered as tolerable agreement based on angular displacement but had poor agreement above 0.6 Hz. One of the reasons suggested for this poor agreement at higher frequencies was that the model was too simple and may not have accounted for the shaking of branches.

Guitard and Castera (1995) developed a mechanical model of a tree to interpret experimental frequency spectra. The model considered the tree as a single central column (Figure 3.2) divided into n logs, with branch whorls being considered as masses along the trunk.

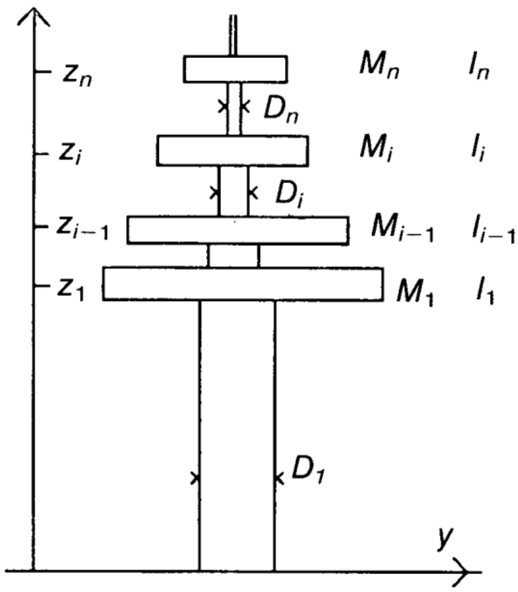

Figure 3.2. Model of a tree with central trunk and solid masses approximating the canopy. (Guitard and Castera 1995).

This model is more complex than the simple central column model and makes some allowance for the distribution of branch mass along the tree trunk. It is noted by the authors however, that the model will not account for the stiffness of the branches nor does not take into consideration any dynamic effect of the branches. Mathematical equations of motion for this model are developed using an energy analysis for a harmonic system with the objective being to estimate the fundamental first harmonic sways. The tree scale model dynamics were measured using an instrument described as an extensometer which was attached to the tree under the bark of the stem. The frequency spectrum was obtained using a FFT (Fast Fourier Transformation) program.

The experimental data from the mechanical tree model in Figure 3.2 were compared to the mathematically calculated frequencies and the authors considered that the agreement between the experimental data and the mathematical calculations was good enough to allow the use of the model. It was noted that the results were useful in identifying the resonance maxima in the spectra of the model, but this was not so simple in the case of a real tree. The spectra for the tree identified a fundamental natural frequency, which changed from 0.75 Hz in the winter conditions with no leaves, to 0.66 Hz in spring when there were leaves. This method could not identify the second mode natural frequency in data obtained from a real tree and the conclusion was not strongly in support of using this mechanical model to represent a tree. It was noted that twisting modes also occurred but were not considered in this model. Guitard and Castera (1995) built a resonant structure to represent a tree and used simplifying assumptions to produce data which when analyzed gave a natural frequency. It is interesting to note that the model results did not match the preliminary results from a 6.2 m tall young red oak and this indicates that the tree does not behave in the same way as their model.

A mechanistic model for calculating the wind throw and stem breakage of Scots pine growing on the edge of a forest stand was investigated by Peltola and Kellomaki (1993). This tree model consisted of a single beam in the ground with a crown shape assumed to be formed by two triangles having a common base equal to twice the length of the longest branch in the crown. This SDOF model has application for tall plantation trees with a slenderness ratio greater than 70 and is useful in evaluating tree stability for plantation trees but has limited value for evaluating more stable open grown trees with a slenderness ratio less than 50.

Gardiner (1992) used a model of a tapered cantilever beam to model plantation conifers. The canopy was approximated as a lumped mass at 70% of tree height. Dynamic analysis of the model obtained natural frequencies and the mean and fluctuating components of displacement.

A simple wind throw model was presented by Mattheck and Bethge (2000) in a discussion on wind forces and soil mechanics. Their model considered the tree as a central trunk with lumped mass canopy and it was noted that it was an approximation to tree. A descriptive approach was taken to investigate the overturning forces and the resistance of the soil with different modes of soil failure. Baker (1995) used a model that assumed a weightless elastic stem with a lumped mass on top to represent trees and crops. A spectral approach was used to calculate critical wind speeds that could induce crop and tree failure for different ground and meteorological conditions.

A mathematical model to represent the dynamic behaviour of Sitka Spruce (*Picea sitchensis*) in high winds was presented by Saunderson et al. (1999) in which the tree is represented as a central tapered column with a cylindrical mass at the top of this column to represent the canopy (Figure 3.3). This is a SDOF model that treats the trunk as a simple harmonic oscillator with a static canopy mass at the top of the column, having a sail area which interacts with the wind.

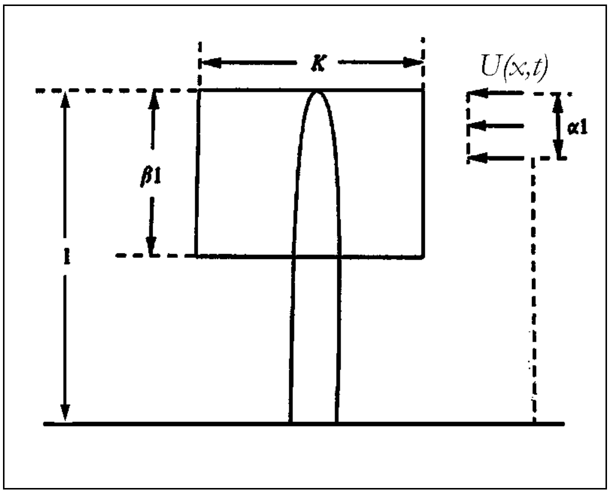

Figure 3.3. Dynamic model of a tree with rigid cylindrical canopy mass (Saunderson et al. 1999).

The basic equation used by Saunderson to analyse this model was a general equation of motion for a vertical tapered cantilever, with a time varying load to represent the wind. This equation was applied to the trunk only as the canopy is considered as a static mass attached to the trunk, with no dynamic characteristics to influence the trunk motion. The solution results in an estimate of the tree displacement spectrum, a transfer function and the wind power spectrum. A comparison is made of the mathematical solutions with experimental data of tree displacements to obtain the transfer function and compare it to the theoretical transfer function (Figure 3.4).

Saunderson concludes from this comparison that the model gives a good prediction of the first natural frequency and matches the experimental data well up to 0.7 Hz. For higher frequencies the results of the model are not so good. For example a second natural frequency is predicted around 1.5 Hz which is not observed in the experimental data. In conclusion, Saunderson notes that "overall, however, the agreement is encouraging and gives some confidence in the model."

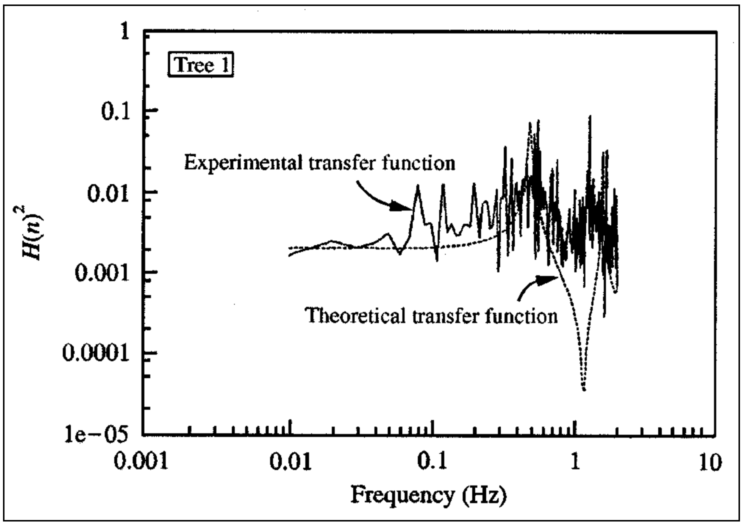

Figure 3.4. Comparison of experimental and measured transfer functions, for tree sway (Saunderson et al. 1999).

Another interpretation of the data in Figure 3.4 is possible. It could be argued that the experimental transfer function shows a broad range of natural frequencies over the range 0.1 to 3 Hz and that this is due to the many branches on the tree, exhibiting their own dynamic behaviour which combines with that of the central trunk. The central trunk has a natural frequency, and combined with the many branches and sub-branches, each with their own different natural frequency, gives a dynamic response of the overall structure that shows a broad range of natural frequencies, as seen in the Figure 3.4.

The central column model was modified by dividing a tree into segments (Kerzenmacher and Gardiner 1998). A 13 m tall spruce tree was modelled by 13 rigid, mass less beams hinged together, each section representing a 1 m length of the 13 m tall tree. The mathematical model was based on a free-standing chimney model of Newland

(1989) to describe the dynamic response and the results were compared to the field measurements of the spruce tree described by (Gardiner 1995). The analysis developed differential equations of motion and used a 13 x 13 matrix for defining the tree's mass, damping and stiffness. This developed a 13-degree-of-freedom linear system whose calculated natural frequency was different from previously measured values of Gardiner (1989) and in order to get good agreement, the upper part of the stem had to be made stiffer than measured values would suggest. The transfer function was determined by assuming the system was passive, meaning that steady-state harmonic oscillations could be established and were checked against chimney movement calculated by Newland (1989) to verify the formulations.

The ability of the mathematical model to emulate the behaviour of a real tree was evaluated by calculating the coherence, or the correlation between the data from the model and the tree. The coherence of the model is quoted as very good at 8m and 6m up to a frequency of 0.1 Hz, but at higher frequencies and lower heights the model is poor. This meant that there was good agreement at the top of the tree, but the model was less than satisfactory lower down and close to the base. The comparison showed the complexity of tree response to the wind and the inadequacies in the basic model. In particular, the branches need to be considered, as dynamic coupled cantilevers and not simply as lumped masses (Kerzenmacher and Gardiner 1998). Essentially this means that the mathematical model was not good at approximating the dynamic movement of the tree in the wind. The authors note that "the lack of coupling of the branches and stem is a major weakness of the current model." The initial assumptions limit the application of this model to trees. It is clear that a tree does not dynamically sway like a chimney, and that the branches must be considered in a dynamic analysis of a tree in the wind.

Recent studies in tree dynamics have developed models that indicate the importance of tree morphology (Sellier and Fourcaud 2009) and the importance of treating branches as dynamic masses (James 2003, Fleurant et al. 2004, James et al. 2006). A general mathematical model for the morphometric description of trees based on fractal theory (Fleurant et al. 2004) has the advantage that the tree can be considered as MDOF system which allows the component of damping, termed mass damping to be identified.

The finite element method (FEM) is another method of analyzing the dynamic response of trees and branches and recent studies have used this method to model tree dynamic responses (Moore 2002, Moore and Maguire 2008, Sellier et al. 2006, 2008, Sellier and Fourcaud 2009).

A dynamic model based on the FEM analysis was developed by Moore (2002) where the branches were connected to the stem and described as flexible oscillating elements. This allowed the branch dynamic properties to be considered as part of the tree and the changes in the dynamic response of the whole structure could be evaluated.

Three year old Maritime pine (*Pinus pinaster*) saplings were modeled using FEM by Sellier et al. (2006). The tallest tree was only 2.57 m high and the branches were modeled as either beam elements, pint masses or as cylindrical bodies. The model was satisfactory in estimating the fundamental modes of vibration but was limited in evaluating the damping response of the stem movement.

Further development of the finite element model was applied to two mature *Pinus pinaster* trees of height 21.6 m and 19.8 m (Sellier et al. 2008). This dynamic model aimed to simulate tree response to turbulent wind excitation and no evidence of resonant response was found. The mechanical transfer function of the modeled trees and the measured trees was in close agreement at the peak frequency but at higher frequencies the damping was over estimated by the model.

The effect of crown structure and wood properties on tree sway in high winds was evaluated on a 35 year old *Pinus pinaster* (Sellier and Fourcaud 2009) using FEM and results showed that material properties play only a limited role in tree dynamics. Small morphological changes produced extreme behaviour such as very little or nearly critical dissipation of stem oscillations. Dynamic loading resulted in 20% higher forces near the base of the tree than those calibrated for static loading.

The finite element method of structural analysis was used to model three 20 year old Douglas fir (*Pseudotsuga menziesii*) trees (Moore and Maguire 2008). These trees had heights of 30, 19 and 38 m with slenderness ratios of 59, 82 and 52 respectively. so were representative of tall slender plantation conifers with a central trunk configuration. The FEM model included the trunk and branches which allowed the dynamic response of the tree and the branch interaction to be studied. The branch configuration was taken from detailed measurements of each tree so that the model could closely represent the actual trees. Finite element models were constructed using finite element software package (ANSYS) and the stem and branch elements were represented as a series of beams of circular cross section. Values of density, viscous damping ratio and modulus of elasticity were estimated for each element, with the damping ratio constrained not to exceed 0.073 because of maximum values found in field tests. Values of stem E were estimated from sway tests as 5.8, 6.2 and 5.1 GPa for the three trees.

The fundamental frequency of each tree was found from modal analysis and values were compared to those obtained from discrete mass models and actual tree swaying.

Dynamic response of each tree was investigated using an arbitrary force as a ramped load applied as a distributed force among the branches or as a single point load at the centre of force. These forces were scaled to produce arbitrary base bending moments of 10 to 20 kNm which are low compared to values from previous studies (Moore 2000, Brudi 2002, Achim et al. 2003, Cucchi et al. 2004, James and Kane 2008, Lundstrom et al. 2007).

Response to fluctuating forces was examined by Moore and Maguire (2008) with an artificial 15 minute time series of wind force created by measuring wind speed with a cup anemometer on a 16m tower collecting data at 5 Hz. Wind force (F_w) was taken as proportional to $\boldsymbol{V}^{1.5}$. Spectral analysis was used to analyse the tree responses and transfer functions were evaluated against the theoretical transfer function for a damped harmonic oscillator. It was concluded that structural models of trees using FEM offer additional insight in to tree mechanics under wind loading because they can represent branches as individual cantilever beams rather than a series of masses attached to the stem. These models are better able to predict natural frequency however, there was a 20% overestimation for one of the three trees. Energy transfer was discussed as a process involving structural damping in which the transfer is “from the main axis of the tree to the primary branches and then to higher order branches” (Moore and Maguire 2008, p82). Wind energy is probably transferred in the reverse direction but the principle is valid and requires that the structural elements (the branches) have natural frequencies that are similar and their frequency bands overlap such that the range of frequencies of the second order branches overlap the primary branches which in turn overlap that for the whole tree. This structural damping is an important component of the whole tree damping, particularly for low values of stiffness (E) of branches. The low value of stiffness allows a flexible response so that the tree can streamline in high winds (Spatz and Brüchert 2000) which reduces the frontal area and therefore the wind forces that the tree endures. They concluded that the model could be improved with introduction of aerodynamic admittance in calculating wind force which was assumed to be unity in their calculations.

The models discussed have considered the above ground components of the tree but the below ground components of the roots and soil are also significant. Blackwell et al. (1990) developed one of the few of these models for a root system of *Picea sitchensis*. The mathematical model was developed by regarding the tree and soil as a simple mechanical system. This model treated the root-soil plate as a single rigid body and it was acknowledged that the non-rigid behaviour of the tree, stem and soil alters the calculated turning moment. The model is useful to predict changes in tree stability but should be regarded as a research tool that needs further development.

In these previous studies the central column model has been used as a first approximation to a tree, but it has significant limitations for trees whose structure departs from a central pole, particularly if there are large branches in the canopy.

Closely spaced trees in forests or plantations, which are tall and thin, with a slenderness ratio above 50, may be approximated by the central column model but trees growing as individuals in an urban environment are not usually as slender and will have a height to diameter ratio, around 20 or less, and much more mass distributed in branches and the canopy. It is the dynamic interaction of these branches that will greatly modify the dynamic response of the tree to wind loading. This raises questions about the significance of mass distribution and corresponding dynamic behaviour and the differences between slender forest trees and stouter open grown trees. Decurrent trees and open grown trees that have considerable side branch masses are structurally different from a central pole and their dynamic response to wind loading may be significantly affected by these differences.

The central column model is a SDOF system which does not consider branch dynamic interaction with the trunk and is not a good approximation to multi-stemmed trees, growing individually and apart from any neighbouring tree as is common in urban areas. It would appear that more sophisticated methods of dynamic analysis, and more complex MDOF models of trees must be developed if the dynamic behaviour of both the trunk and the branches are to be taken into account. Mass damping does not occur in SDOF systems so without a MDOF model it is not possible to incorporate the mass damping contribution of branches.

3.2 Proposed New Model

The structural models of trees reviewed in the previous section, have used simplifications which largely ignored the effect of branches. The central column model of Greenhill was originally used for a static analysis to examine buckling in an attempt to identify the limits of height of a tree. It was not meant to be a model for dynamic analysis because a simple SDOF model is an over-simplification and the model needs to be more complex if it is to represent a MDOF system such as a tree. Trees are more complex that a single pole because branches contribute to the total dynamic response of the structure due to their mass and dynamic interaction. Trees growing in urban areas develop substantial side branches which have considerable mass. The central trunk may still be the dominant mass but there will be significant proportion of the total mass residing in the branches. These act as dynamic masses attached to the main trunk and interact dynamically with the trunk to produce the overall response of the tree to dynamic forces from wind.

A limitation of the central column model is that there is no consideration given to branches. As Shigo (1985, p208) states, “A tree without branches is not a tree. A tree is a collection of branches. In a sense, each branch “repeats” itself or reiterates the tree”. A logical development of the central column model is to include inertial elements that represent branches. The number of degrees of freedom will clearly increase to a very large number and make the analysis extremely complex.

In order to develop a MDOF model for a tree the basic components of mass, spring and dampers need to be arranged so that they may more closely represent a tree. The numbers of degrees-of-freedom are determined by the inertial elements (masses) present in a system (Balachandran and Magrab 2004). A SDOF system will have one inertial element and be constrained to move in one direction (Figure 3.5a). A two degree of freedom system can be either one inertial element whose motion is described by two independent coordinate systems, or two inertial elements whose motion is described by two independent coordinate systems (Figure 3.5b). In general the number of degrees of freedom is not only determined by the inertial elements present in a system but also by the constraints imposed on the system (Balachandran and Magrab 2004). The SDOF model can be extended to a 2DOF model (Figure 3.5) where two masses oscillate, one attached to the other and is described by Den Hartog (1956) as a vibration damper and by Connor (2002) as a mass damper.

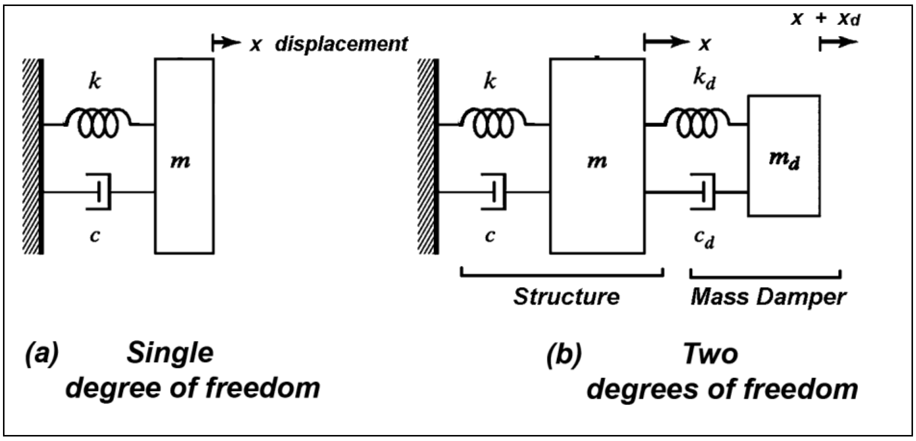

Figure 3.5. A single degree of freedom (SDOF) system (a) with a mass (m), spring (k) and damper (c) and a two degree of freedom (2DOF) system (b). The second mass (m_d), spring (k_d) and damper (c_d) collectively constitute a mass damper attached to the main mass (m).

The addition of the second oscillating mass dramatically alters the dynamic response of the system. When the two masses have a similar magnitude, their dynamic interaction creates an effective damping system. The second mass (m_d), spring (k_d) and damper (c_d) collectively constitute a mass damper attached to the main mass (m).

The number of degrees of freedom for an excurrent tree can be determined by considering a coordinate system in space and describing the possible displacement directions of the tree under dynamic excitation (Figure 3.6).

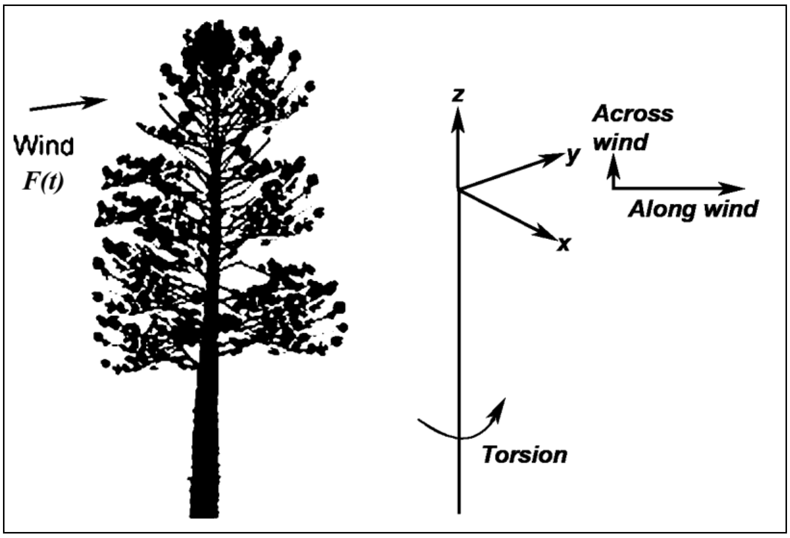

Figure 3.6. Fundamental coordinate system for a tree used to define a multi-degree-of-freedom dynamic system.

As a first approximation, if the branches are ignored so that the tree is simplified and based on Greenhill's model of a central column, the response of the tree to external time varying force such as wind can be determined. The tree stem could sway about the base in two possible directions (x and y) and also rotate about the z axis under torsional forces to give a three degree of freedom system. Torsion has largely been ignored in the literature as there is yet to be a satisfactory method developed to accurately measure torsional forces of trees under wind loading. In this study, torsion is not considered beyond this discussion.

A new dynamic structural model is proposed (Figure 3.7) which considers the dynamic interaction of the branches with the main tree trunk and provides an explanation for the measured tree sway spectra in windy conditions. This dynamic model accounts for each structural member of the whole tree including a trunk, all the branches and, at the limit, could be extended to include all the leaves. The model is an extension of the 2DOF system and continues to add dynamic mass elements to produce a MDOF model that is conceptually based on a model of multiple tuned mass dampers described by Abe and Fujino (1994) and previously shown in Figure 2.22.

The model in Figure 3.7 considers each structural element as an oscillating mass (m) attached via a spring (k) and a damper (c) to another mass/spring/damper element. The main mass of the trunk is supported on the ground and in turn supports the masses of the branches.

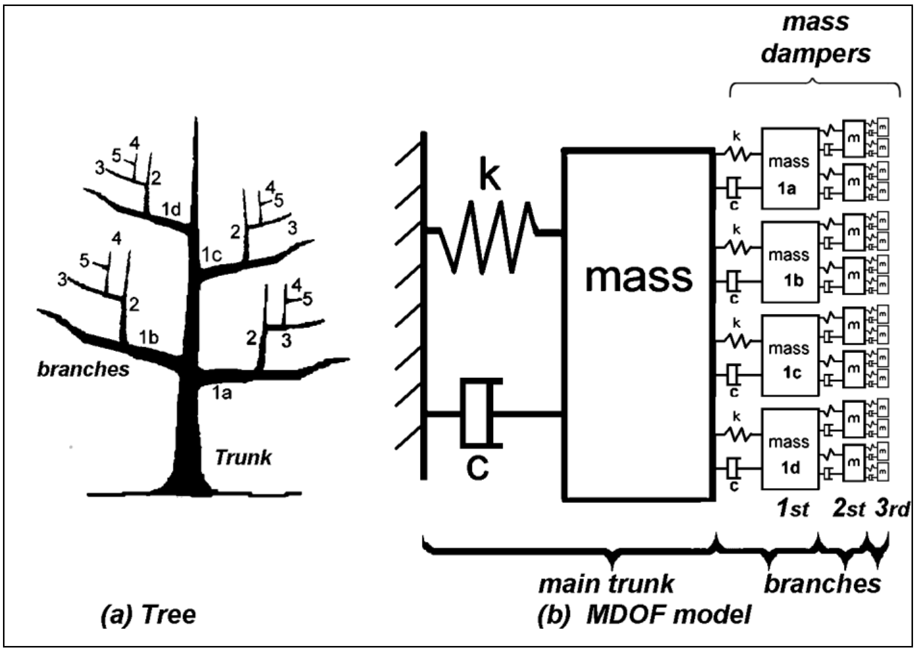

Figure 3.7. Dynamic structural model of a tree, introducing the concept of mass damping (James et al. 2006).

The spring acts to store and release energy during the oscillations and the damper acts to dissipate energy so the oscillating motion eventually ceases without external input of force. Each branch mass can be modelled so that the branches attached to the trunk are considered as 1st order branches, and they support 2nd order branches which in turn support 3rd order branches and so on until every branch may be represented. The model reiterates itself in the same manner that the branches of a tree reiterate themselves. The value of each mass could be adjusted to model a specific tree so that the largest mass represents the trunk and smaller masses represent the main branches if the tree were a conifer or excurrent tree. If the trunk was not the greatest mass, as in a decurrent tree with massive limbs, the main mass representing the trunk may be less than the collection of first order masses representing the branches.

The spring constants of each element could be adjusted to represent the spring constant or Young's Modulus of each branch which vary throughout the tree (Mencuccini et al. 1997). The value of each damper could also be adjusted to represent the damping or energy dissipation of each element. For the main mass (the trunk) the damping would be relatively low. At the outer end of the model, the smallest elements could represent the leaves whose mass and damping are small but collectively would contribute to a large overall value of both mass and damping.

The discussion of the model begins by considering the first structural element. The mass of the main trunk is represented in the model (Figure 3.8) as a mass (*m*) that oscillates on a spring (*k*) and has some damping (*c*). The spring represents the stiffness or Young's Modulus of the wood in the trunk.

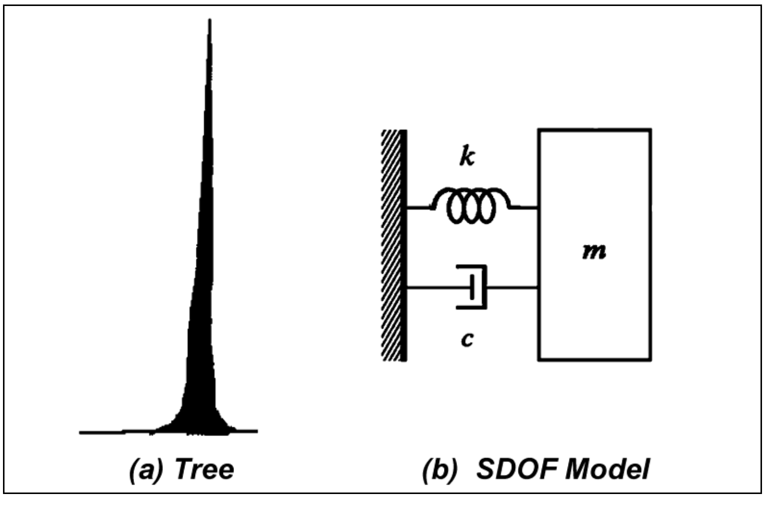

Figure 3.8. Dynamic SDOF model of a tree trunk represented as a mass (m) oscillating on a spring (k), with damper (c).

The damping acts to dissipate energy and consists of (a) visco-elastic damping of the internal wood and the root and soil mass, and (b) a minor aerodynamic damping component because the trunk in this case has no foliage. The damping would not include mass damping in this case. For simplicity, a two dimensional view is presented, but in actual trees, movement would be in three dimensions. The dynamic model shown in Figure 3.8 is a SDOF system and is a representation of a simple oscillating mechanism. The dynamic response of the mass to some applied dynamic force Would be to oscillate about some mean point, with a regular sway cycle at a defined natural frequency. An example of such a SDOF system would be a pole or a pendulum that is allowed to oscillate freely after being excited by some external force.

The spectrum of the dynamic response of a SDOF would show a sharply defined peak at a specific frequency (Figure 3.9). This is the natural frequency of the system and if the input force is the same frequency, resonance occurs resulting in large and possibly dangerous amplitudes of sway motion. The area under the spectral curve represents the energy in the dynamic response, so the larger the amplitude the greater the energy in the oscillations.

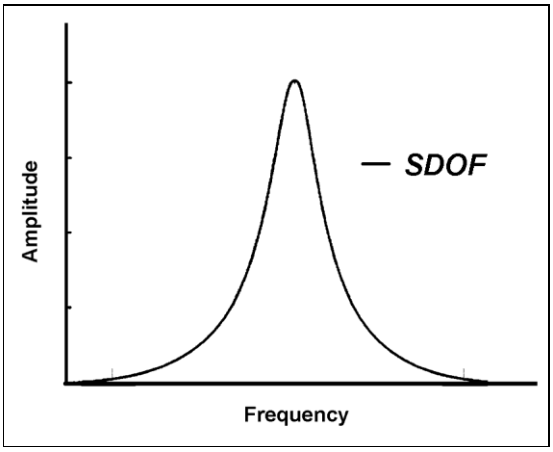

Figure 3.9. SDOF response spectrum showing a well defined peak amplitude at a specific frequency.

The SDOF model for a tree (Figure 3.8) needs to be modified to include branches attached to the trunk if it is to be able to model the complex dynamic response of the whole structure. As a first step, the trunk and one branch can be represented as a 2DOF system (Figure 3.10) in which a smaller mass (m_d) representing the branch is attached to the main mass (m) that represents the trunk. This smaller mass oscillates on its own spring (k_d) and damper (c_d) and greatly influences the amplitude of oscillation of the trunk. The ratio of the two masses in a 2DOF system is important. If the branch has a mass within 20% of the trunk mass, the effect is to cause a strong dynamic interaction between the structure (m) and the mass (m_d), (Balachandran and Magrab 2004).

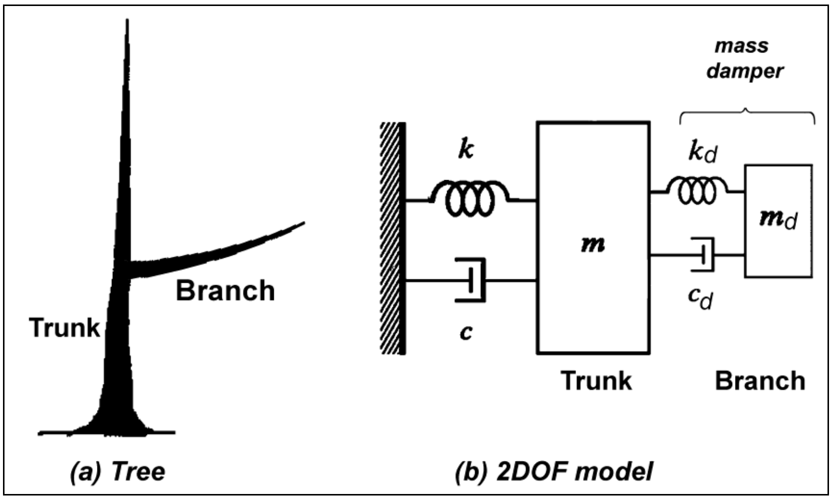

Figure 3.10. (a) A tree trunk with oscillating branch and (b) a 2DOF model including a mass (m) of the trunk and mass (m_1) of the branch. The mass (m_d), spring (k_d) and damper (c_d) together constitute a mass damper and represent a branch.

The frequency and large oscillation amplitude apparent in a single trunk (a SDOF system) is significantly reduced by one branch (a 2DOF system) and replaced by two smaller peaks, one sightly below and one slightly above the original frequency (Figure 3.11). The oscillating energy of the structure partly transfers into the mass damper, which dissipates the energy through the damper c_d. The contribution of the mass damper is to reduce the amplitude of vibration and also to reduce the energy within the vibrating system. The reduction in energy is shown by the area under the curve which is significantly less for the 2DOF system than for a SDOF system (Figure 3.11).

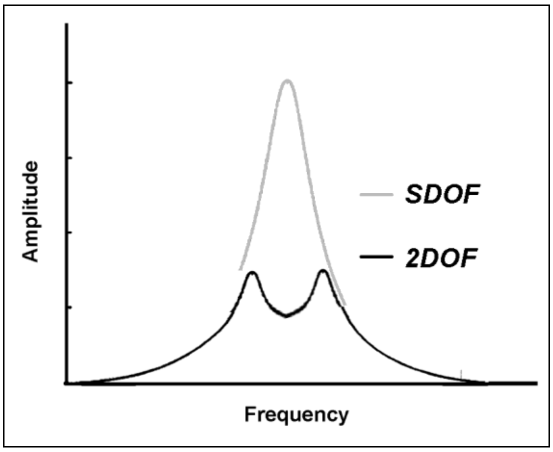

Figure 3.11. Dynamic effect of a 2DOF system reduces amplitude of a SDOF (grey line) and produces two “split modes” (black line) where each mass oscillates at a frequency close to the original natural frequency.

There are usually several main branches (or 1st order branches) attached to the trunk of a tree and each will act as a mass damper. Collectively this creates a structure with multiple mass dampers which is a concept reported in earthquake engineering literature (Abe and Fujino 1994) and requires sophisticated mathematical techniques for analysis. More mass dampers may be added to the model to represent the 1st order branches of a tree. The model may therefore be modified to include many masses, each attached to the main mass to produce a MDOF system with multiple tuned mass dampers. Figure 3.12 illustrates a tree trunk with four 1st order branches and the equivalent model with four masses attached to the main mass.

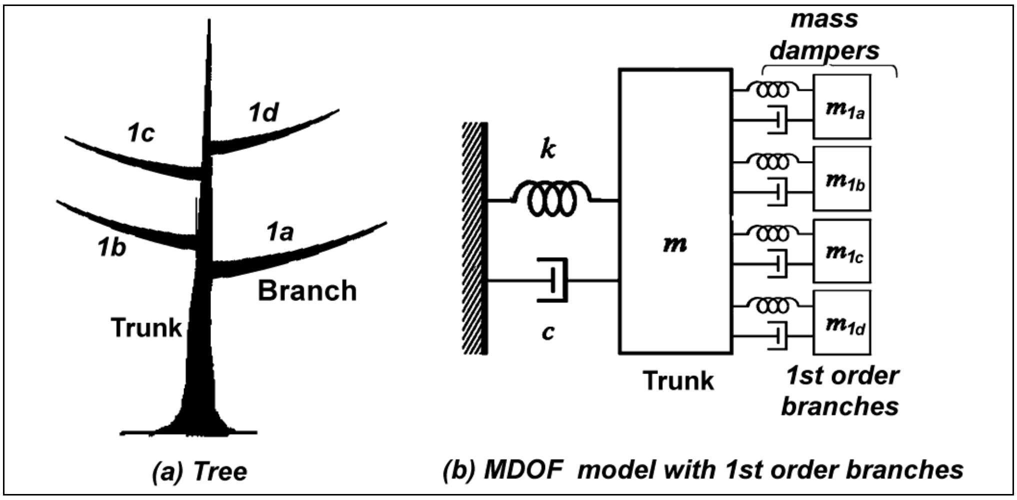

Figure 3.12. (a) A tree trunk with several 1st order branches and (b) a MDOF model with several mass dampers attached to the main mass.

For a complete model of a tree, all the branches including the 1st order branches, 2nd order branches etc., need to be considered. The first order branches are themselves mass damped with second order branches. This is equivalent to adding a mass damper to the first mass damper. The second order branch is also affected by smaller 3rd order branches and these smaller branches are in turn branched until a network of branches is created. These branches are represented in Figure 3.7 as 1st, 2nd, and 3rd order branches which act as mass dampers attached to other mass dampers in a cascading pattern. At the limit of this model, the final element would represent a leaf with a very small mass and spring constant, but with a significant damping component. Collectively, the damping of all the leaf elements would aggregate and become the aerodynamic damping of the whole tree.

The overall effect of these mass dampers on the dynamic response of the tree is complex. The interaction of the swaying branches creates a range of oscillating modes with peak amplitudes that are spread over a broad range of frequencies. This can be modelled as a MDOF system where the peak amplitude of the trunk only (SDOF system) is significantly reduced with a corresponding reduction in the energy as indicated by the reduced area under the curve (Figure 3.13). This arrangement of branches acting as mass dampers prevents the main structure of the tree trunk from developing large and potentially dangerous sway motion in response to wind loading.

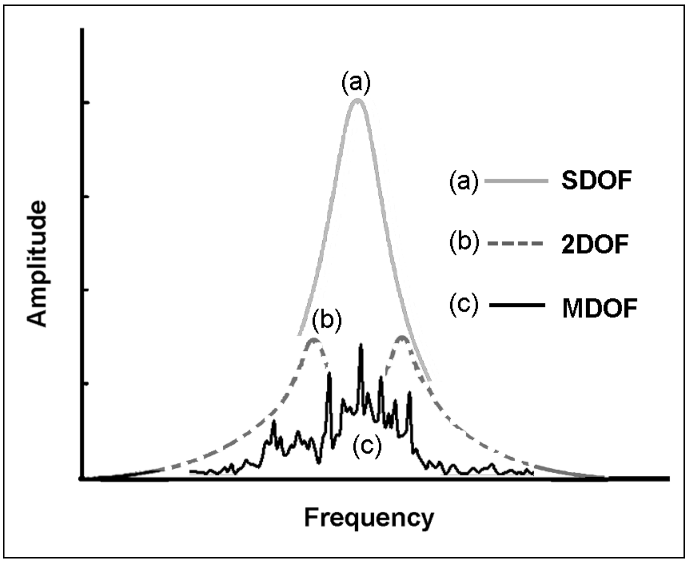

Figure 3.13. The effect of mass damping on dynamic response with (a) no mass damping in a SDOF system and a large peak amplitude, (b) one mass damper in a 2DOF system and two smaller peaks, and (c) many mass dampers with several small peaks spread over a range of frequencies in a MDOF system.

The effect of mass damping may be illustrated by looking at situations in which it is removed. An interesting study by Moore (2002), investigated the effect of removing branches from the canopies of Douglas-fir (*Pseudotsuga menziesii* Mirb. Franco) and studying the effects on natural frequency. It was concluded that at least 80% of the crown mass needed to be removed before any increase was noticeable. This indicates the important influence of side limbs and that it needs only a few branches have a significant influence on the dynamic sway of trees.

3.3 Mass Dampers and Structures

The concept of mass damping has been described in engineering texts for mechanical systems and building structures (Connor 2002). Two translational tuned mass dampers weighing 2700 kN each were used on the 60 storey John Hancock Tower in Boston in 1975, to reduce the sway by 40 to 50%. The Citicorp Centre in Manhattan (1977) is a 279 m high building with a sway period of around 6.5 s. A tuned mass damper with a mass of 366 tonnes was located on the sixty-third floor and reduced the sway amplitude by about 50%. The mass damper of 366 tonnes saved an estimated 2800 tonnes of steel that would have been required to satisfy deflection constraints (Connor 2002). Fluid filled tuned mass dampers were used on the Centrepoint Tower in Sydney to reduce sway periods (Soong, 1997). Taipei 101 is one of the world's tallest buildings and uses a tuned mass damper consisting of a 730 tonnes pendulum to reduce sway movement under wind loading by 40%. Early tuned mass dampers used complex mechanisms, relatively large masses and were quite expensive. Connor (2002) describes recent developments which minimise these limitations and use multi-level elastomeric rubber bearings, in a compact assembly that provides multi-directional damping with unsophisticated controls (Figure 3.14).

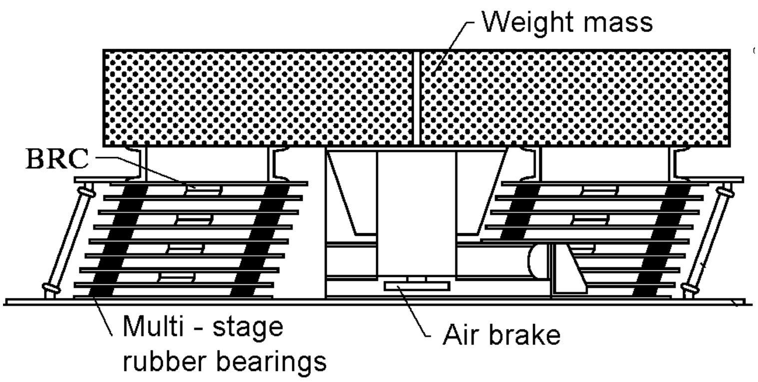

Figure 3.14. Tuned mass damper with spring and damper assemblage for buildings (Connor 2002).

The use of mass dampers has become conventional in the design of tall buildings and demonstrates how they can minimise the sway response of the building in high winds. The principle of mass damping may also apply in other structures, including trees.

Chapter 4. METHOD AND MATERIALS

4.1 Introduction

This study of trees and wind, takes an engineering and structural perspective to investigate the dynamic response of trees to wind excitation. The method uses standard engineering principles that have been developed for dynamic oscillating structures and applies them to a biological structure, the tree. The distribution of branches and their mass through the tree can influence the total dynamic response and because trees have different forms and structural configurations, it is important that a structural analysis considers the different morphologies of trees. In essence, the differences in tree structures are defined by the branches and the branching pattern. Each branch acts as an individual oscillating mass with its own dynamic response and collectively, all the branches contribute the total tree response. To study this complex system, new instruments have been built to monitor the tree response under wind loading. This chapter describes the instruments and methods used to collect field data and analyse the results using dynamic methods.

When applying engineering principles of dynamic structural analysis to trees, it is useful to identify the terms that are used so that comparison can be made between conventional engineering structures and trees. A dynamic system can be described in terms of its inertial properties (mass, m), its energy storing properties (spring constant, k) and its energy absorbing properties (damping, c). The overall dynamic parameters which are of interest when studying trees are natural frequency, and damping. The three basic elements (Figure 4.1) of a dynamic oscillating system are;

- Mass (m) – the inertial elements
- Spring (k) – the energy storage elements, and
- Dampers (c) – the energy dissipation elements.

The mass of an oscillating structure could be the concrete and steel of a building, a bridge or a simple pole. The mass of the tree is considered as the above ground mass, consisting of trunks, branches and leaves. Any below ground mass of the tree is assumed to be rigid so that it does not dynamically interact with the above ground components. There will be some energy loss into the root system, but for trees firmly rooted in the ground, it is assumed that this effect is negligible and does not change the above ground dynamic response of the tree in winds.

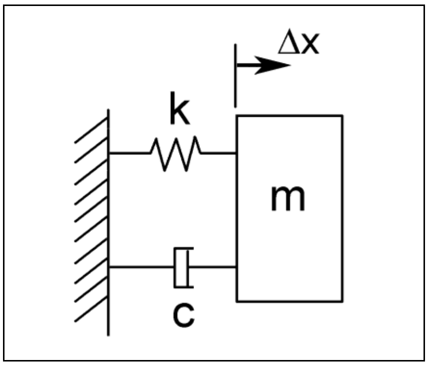

Figure 4.1. Three basic elements of a single-degree-of-freedom oscillating system.
Mass (*m*), Spring (*k*) and Damping (*c*). Displacement (Δx) is back and forth about a mean.

The spring elements represent the trunk and branch sections because the elastic properties of both act in a similar manner. The elastic element stores and releases energy and helps to maintain dynamic oscillations. Energy storage and release is important in the pull and release test of trees described in this chapter. When the tree is pulled sideways by a rope and held in position, potential energy is stored in the spring elements of the trunk. When the rope is released, the stored potential energy is released and the tree oscillations begin. This approach is useful for describing the differences between the energy transfer in a pull and release test and the energy transfer from wind induced oscillations.

The dampers are the energy absorbers or energy dissipating elements. In trees the damping is complex as it consists of several components including, aerodynamic damping of the leaves, visco-elastic damping of the trunk and branches (and root mass in the ground), and mass damping in which the dynamic masses of the branches interact to lessen the sway of the tree. In the mathematical equations the complexity in damping is simplified which is conventional approach in texts such as Clough and Penzien (1993) or Balachandran and Magrab (2004).

4.2 Measuring Tree Structural Properties and Dynamic Wind Loads

In order to measure the dynamic response of trees in wind storms, two main strategies have been used by different authors. One strategy investigates movement or deflection in the upper part of the tree and the other examines the trunk flexure near the base. Each strategy requires different instruments which have been reviewed in Chapter 2.

Usually not stated, but implicit in these studies using instruments placed in the upper tree, is that the tree has a shape with a central trunk, described in Harris et al. (2004) as an excurrent form. They state that the most significant aspect of crown form is the presence of a central leader or the main trunk (Figure 4.2a) and examples given by Harris et al. include angiosperms (tulip tree, *Lirodendron tulipofera*, sweet gum, *Liquidamber styraciflua,* and most conifers). This basic shape can be further modified if trees are grown in a plantation and are very close to each other (Figure 4.2b) and grow like poles with very small canopies. The other tree form has a spreading canopy with many side branches and no central trunk (Figure 4.2c). These trees are described as decurrent trees (Harris et al. 2004) and examples would include most angiosperm trees (Oaks, elms, Sydney Blue Gum (*Eucalyptus saligna*), Spotted Gum (*Corymbia maculata*) and She Oak (*Allocasuarina fraseriana*).

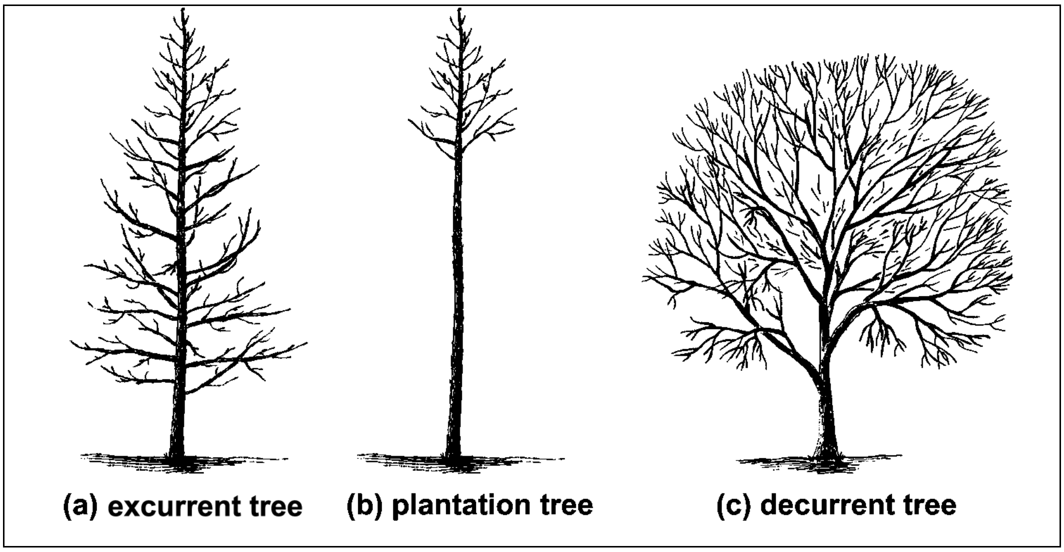

Figure 4.2. Different tree forms including (a) excurrent tree with a central trunk, (b) special case of a excurrent tree grown in a plantation and (c) a decurrent tree with spreading form and no central trunk (Harris et al. 2004).

The point at which the instruments are attached for studying tree sway response to wind loading is an important consideration because of the variations in dynamic behaviour of the different tree forms, and particularly the dynamic effect of branches. Branches are often assumed to be a negligible part of the tree, or if they are considered, they are taken as lumped masses, rigidly attached to the trunk (Nield & Wood 1998, Saunderson et al. 1999, Guitard and Castera 1995).

Instruments placed in the upper canopy of an excurrent tree can measure the displacement, tilt or acceleration of one particular point on the trunk but the response of the instrument at this point may not represent the total dynamic response of the tree and all its branches. A tree which has most of its mass in the central trunk, and relatively little mass in side branches will have a dynamic response that is close to the response of the instruments in the upper canopy. Any dynamic contribution from small branches lower down will not greatly influence the response of the tree. This would be true for plantation trees which grow closely together and have few branches in the lower regions. However, for trees with significant mass in the branches low down on the trunk, instruments placed in the upper tree may not record any contributing dynamic response from to the lower branches. This would be a major limitation for some tree shapes where major branching occurs. Decurrent trees with no central trunk would not be suited to placement of instruments in the upper crown as one instrument may not record the total dynamic response of the tree. Since this study has focused on open grown trees which have many different forms, often with no central trunk and a significant proportion of dynamic mass in large branches to form the canopy, a different approach was needed.

In order to overcome the above problems, and to ensure that the total dynamic response of trees, including all the branch dynamic response were recorded, this study used an alternative approach in which the trunk flexural response near the base was measured. Strain instruments were attached to the tree trunk near the base and below the lowest branch. These instruments measured the outer fibre elongation (or contraction) of a trunk, along the axis, as it bends in the wind. New instruments were been built to measure the movement (δl) between two points axially aligned along the trunk. Measurements were recorded to an accuracy of one micron using digital instruments which had the advantage of not being subject to environmental signal noise which could distort readings. Measurements were made at a rate of 20 Hz which was considered suitable for registering the dynamic response and the oscillations frequencies of large trees. The instrument output (Δl) in microns, could be simply converted to strain (ε) using Equation 4.1, since the length of the instrument (l) is set to 500 mm.

$$\varepsilon = \Delta l / l \tag{4.1}$$

The advantage of measuring strain was that strain had no units and the value could be entered directly into equations of mechanics in order to calculate the stress, and material properties of the tree or Young's modulus (E). Within the elastic range of a material, Hooke's Law (Equation 4.2) may be used to calculate stress;

$$\sigma = E\varepsilon \tag{4.2}$$

where stress (σ) is expressed in N m^{-2}, and Young's modulus (E) is in N m^{-2}. Young's modulus can be determined from Hooke's Law by calculating the stress from a static pull test and using the strain measurement from the instrument attached to the trunk;

$$E = {}^{\sigma}\!/_{\varepsilon} \tag{4.3}$$

Stress from the static pull test can be calculated using Equation 4.4, (Timoshenko, 1955);

$$\sigma = {}^{My}\!/_{I} \tag{4.4}$$

Where, M is the applied bending moment (kNm), y is the distance from the neutral axis to the outer wood fibres and *I* is the moment of inertia (m^4).

Care must be taken when measuring the diameter of a tree trunk (or branch) as the cross-sectional dimensions are usually not circular. Non-circular cross sections will affect the bending response and stress distributions, so a tree section is treated as an ellipse with radii *a* and *b* in the directions of the principal axes y and z (Figure 4.3). This method accounts for circular cross-sections when a equals b.

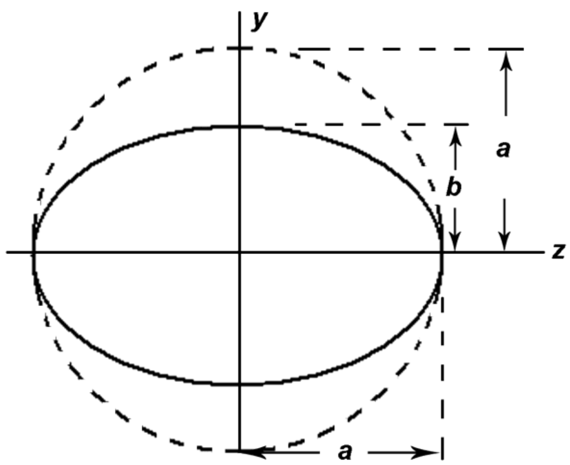

Figure 4.3. Trunk cross-section represented by an ellipse, with maximum width (a) and minimum width (b) with respect to principal axes y and z (Timoshenko 1955). Note when a = b the cross-section is circular.

The moment of inertia with respect to the principle axis z is

$$I_z = \pi a b^3 / 4 \tag{4.5}$$

In the same manner, for the vertical axis y,

$$I_y = \pi b a^3 / 4 \tag{4.6}$$

The direction of bending in a non-circular trunk needs to be determined with respect to the principle axes in order to calculate the stresses. The orientation of the principal axes is important as it indicates the effect of wind direction on tree growth. The trunk adapts to cope with the wind loads by stiffening in the direction of the wind and this can result in a non-circular cross section. This also applies to branches and root cross-sections which may be non-circular (Mattheck and Breloer 1994). The direction of the wind force varies and will not usually be in alignment with either principle axis. This results in a dynamic interaction with bending and contributes to a looping sway motion instead of a linear back and forth sway. Strain data are collected at 20 Hz which is fast enough to measure the dynamic properties of frequency, damping ratio, and spectral analysis of the tree.

4.3 Instrumentation

4.3.1 Strain meter design

The wind loads on trees cause the trunk to bend and creates an overturning moment at the base. As the trunk bends the outer fibres elongate on the windward side and shorten on the leeward side. Instruments that measure this fibre elongation were attached to the trunk, near the base of the tree and recorded the trunk bending response to wind loading. By calibrating the instruments on the tree, using the static pull test, the instrument output could be related to base bending moments which was used as a measure of wind loading. This is similar to the methods used by Moore and Maguire (2005), Peltola et al. (2000) and Rogers et al. (1995).

New instruments were designed to measure the outer fibre elongation (strain) near the base of a tree trunk, which occurs during bending caused by wind excitation (James and Kane 2008). The instruments were designed to operate under field conditions and to be accurate enough to record small changes in trunk elongation. In order to measure the dynamic response of the tree the data rate needs to be fast enough and after some initial testing this was chosen to be 20 Hz. This data speed resulted in smooth curves in the time domain and was faster than the 2.5 Hz sampling rate of Moore and Maguire (2005). They used a similar principle of measuring outer fibre strain to detect tree movement, but with an instrument of a different design and a sampling rate of 2.5 Hz. This was adequate for frequency analysis, but had limitations with time domain representation due to an alias effect which produced a star shaped plot rather than a smooth curve when a sampling rate of 20 Hz as used in this study (Figure 4.4).

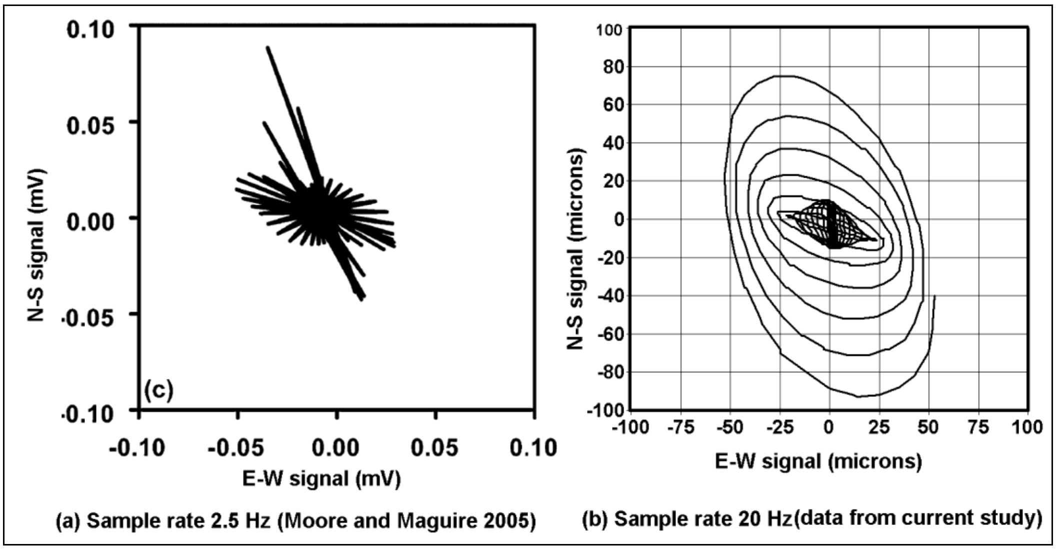

Figure 4.4. Tree response after a pull and release test plotted using different sampling rates.

In order to get a high strain resolution, the length of each strain meter was set at 500 mm. Stainless steel was used for the outer body to ensure that they were weatherproof. Located inside the body of each instrument is a digital probe sensor which has a displacement stroke of 10mm and a resolution of 1 micron, giving a strain resolution of 2 x 10^{-6}, or 2 micro strain ($\mu\varepsilon$). The digital probe (manufactured by Solatron Metrology, West Sussex, UK.), is supplied with calibration certificate that quotes an accuracy of 1 micron. The digital output has the advantage that no signal noise or other disturbance will affect readings. The probe model used is a liner probe DP/10/S with an approximate cost of US$600. The output is recorded at 20 Hz which is found to be the minimum sampling rate needed to give a smooth time domain signal for most large trees and branches. Data are logged via an interface box attached to the tree and transferred to a computer via a digital cable for recording. The strain meter instrument and interface are made by Versatile Technology, Melbourne, Australia. Purpose built software allows continuous recording so that trees can be monitored for many months until wind storm occur.

The strain instrument attaches to the side of trunk near the base and must be aligned with the vertical axis to accurately measure both tensile and compressive elongation induced during bending (Figure 4.5a). Each end of the strain instrument has purpose posts with holes through which either screws or nails may be driven to secure the instrument to the tree. It is important that the nail or screw goes through the bark and into the solid wood of the trunk, to ensure that measurements of forces in the trunk are measured. An adjustment in the instrument allows the initial position to be set at the midpoint of the sensor range, so both elongation and contraction may be recorded up to the limit of the sensor movement.

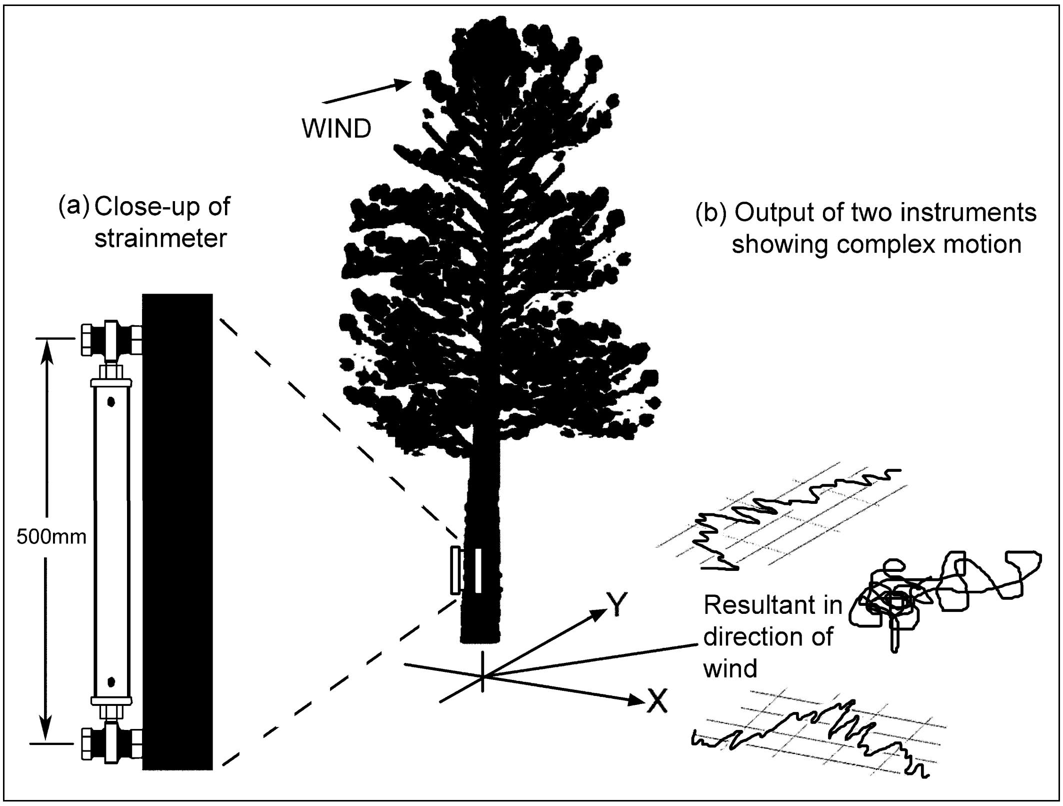

Figure 4.5. (a) Strain meters attached to tree trunk. (b) Sensor outputs in X and Y directions shown individually and combined to show resultant complex sway motion of the tree. (James and Kane 2008).

Two strain instruments are attached to the trunk of a tree near the base (Figure 4.5b), each oriented orthogonally to the other. The standard method used was to orient one sensor to measure the north/south response and the other to measure the east west response. This configuration allowed measurement of the tree bending response in all directions. The exact height and position of the instruments on the tree is not critical because they are calibrated on the tree using the static pull test but they must be aligned with the central axis of the tree trunk. The instruments were placed below the lowest branch to ensure that all the dynamic forces from the individual swaying branches above the instruments were recorded. The instruments measure the total integrated resultant bending moment passing down via the trunk to the ground at 20 Hz. In effect, the instruments are measuring the dynamic forces on the 500 mm length of trunk. A calibration procedure, described later in this chapter, allows the strain data to be converted to bending moment values for each tree and instrument position. The strain data from each instrument can be graphed to give a time varying curve, and also graphed against each other in an XY plot so that the instantaneous resultant can be represented. This gives a plot of the complex dynamic forces and is also representative of the complex looping motion on the tree (Figure 4.5b).

4.3.2 Wind instrumentation

Wind speed and wind direction were measured using a Davis anemometer Model 7911 (maximum wind speed range to 78 m s^{-1}). The anemometer is a three cup anemometer mounted on a 600 mm plastic arm and capable of reading at 1 second intervals. The anemometer was calibrated at University of Melbourne, on 21 September, 2005, in a wind tunnel with wind speeds up to 30 m s^{-1}. The calibration test indicated a linear relationship between anemometer reading and wind speed, (Figure 4.6) and the calibration information was used in all field measurements. Angle of wind direction is accurate to 1 degree.

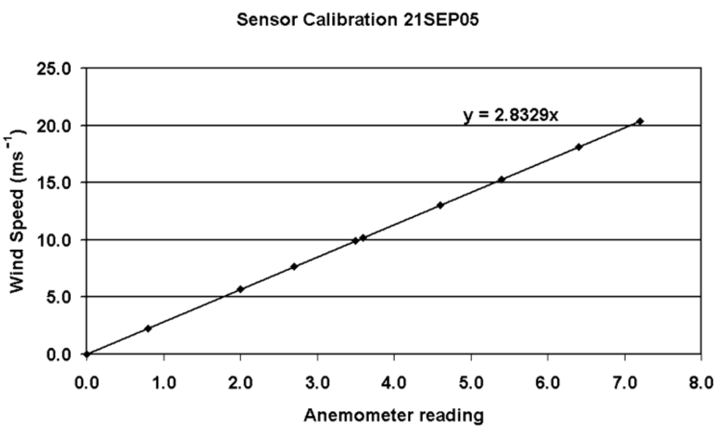

Figure 4.6. Calibration of the anemometer from wind tunnel tests, 21SEP05. (Anemometer reading verses wind speed).

The wind tunnel provides a uniform wind environment and constant wind speed which is not identical to wind patterns in the field. In order to examine the dynamic response of the anemometer, spectral analysis of the anemometer output was performed. The data file used *cal21sep0520050921122007.vtd* and excel file *calib21sep05.xls.*

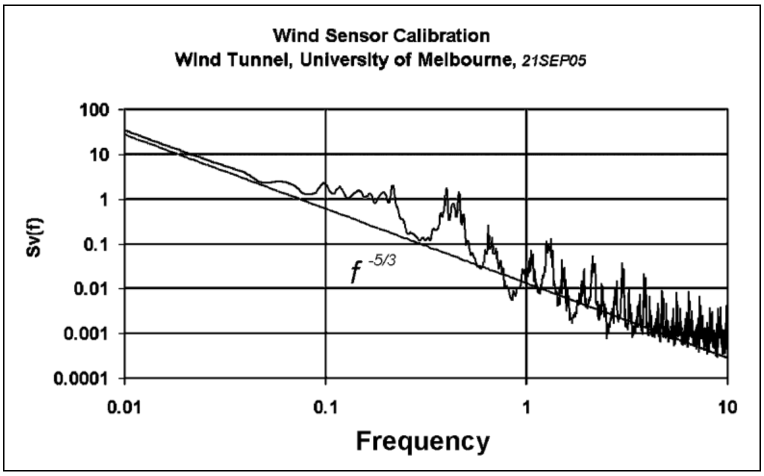

Figure 4.7. Spectrum of anemometer response *Sv(f)* in wind tunnel testing. Curve follows expected -5/3 power law. Peaks at higher frequencies due to anemometer vibrations of cups and supporting arm.

The spectral plot of the anemometer wind tunnel results (Figure 4.7) shows a smooth response curve until approximately 0.5 Hz, then a series of peaks up to 10 Hz. Since the wind speed is constant in the wind tunnel, the peaks are due to the dynamic response of the wind sensor. These dynamics responses are partly caused by the rotation of the three cups and partly by vibration of the plastic support arm. The peaks from 1 to 10 Hz are low energy and are not apparent on linear plots but do show up when a logarithmic scale is used. These peaks need to be taken into consideration when determining wind spectra and transfer functions of trees but they are of low energy and occur above 1 Hz which is outside the frequency response range where most of the tree response energy occurs. This means the overall tree response curve is only slightly affected by these small energy peaks and overall the calibration curve follows the $f^{(-5/3)}$ power law of wind spectra as would be expected.

The selection of the averaging interval for wind depends on a number of factors including the instrumentation and the object being studied. Wind velocity data are measured using a cup anemometer and need to be treated statistically in terms of mean values and deviation from the mean (Davenport 1960). The interval of time (or distance) chosen for averaging values depends on the purpose of the study with the fundamental considerations being that the interval should:

1. coincide with the periodicity of the wind

2. be “long” compared to both the natural frequency of the structure and the response of the instrument, so that there is no dynamic interaction between the structure and the mean wind value,
3. be “short” enough to record peaks
4. should correspond to the body of air that is sufficient in size to completely envelop the structure and its vortex region.

Davenport discusses the options for Canadian conditions and states that hourly mileages do not satisfy 1 and 3, and the three second average speeds do not satisfy 1,2 and 4. Arguments can be made to use either hourly averages or 3 sec averages. Because anemometers have moving parts with inertia, the response time is not instantaneous and 3 second averages are probably the shortest that are reasonable. The Davis anemometer (Model 7911) used in this project collected wind speed data every second, so the three second average results were the most appropriate. Other average periods are examined and some results are presented in the next chapter to compare the effect of changing the averaging period.

Moore and Maguire (2008) calculated wind force using an exponent of 1.5 for velocity. This was based on Mayhead (1973) and Mayhead et al. (1975) whose experimental work on trees in wind tunnel tests showed that aerodynamic drag force on a tree was proportional to wind speed to the 1.5 power, due to canopy streamlining effects. The wind profile in a stand of Douglas-fir trees was measured by Moore and Maguire (2008) and shows considerable variation below 10 m height (Figure 4.8). The profile increase is linear up to 20 m.

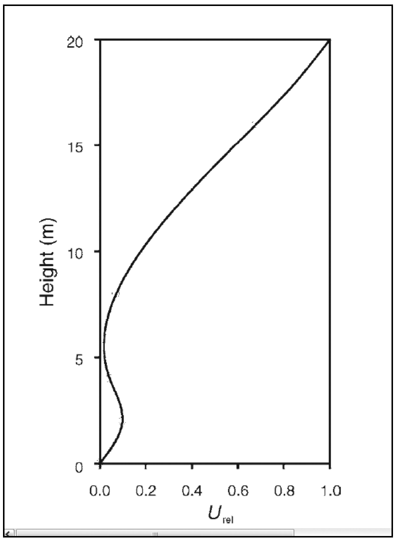

Figure 4.8. Wind profile in a forest stand of Douglas-fir trees (Moore and Maguire 2008).

The wind anemometer was positioned between 5 and 10 m height and depended on the tree location. Because wind comes from any direction, the anemometer location was sometimes on the windward side and sometimes on the leeward side. This contributes to variation in the wind data, especially when considering the time lag and delay from when the wind impacts the tree canopy and when the wind sensor records the gust.

4.3.3 Software and analysis programs

Two main software packages were used for this project. A specially written software program termed RP114 was developed in the programming language C, to drive the instrumentation in the field and record data. Another software program called Labview (National Instruments) was used for data analysis. This is a widely used commercially available program that interfaces instrumentation, data files and mathematical analyses.

The software designated RP114 was specifically written by Versatile Technology Pty Ltd to control the strain meter instrumentation and data logging capability. This software ran on a laptop computer and controlled communications and data logging options of the strain meter instrumentation, via a 100 m cable interface. The cable was used to send power to the instruments and to return digital data from the strain meters on the tree, back to the computer. Data were saved as text files and marked with *.vtd suffix to uniquely identify them. The software functions included triggering on wind events so that hours of data were not stored unnecessarily in no-wind situations.

Data files

Each file was standardized to record data at 20 Hz, and file size was limited to 30 minutes. This resulted in 36,000 lines of data per file in simple text format. At the end of each 30 minute period, the file was closed and the next file as opened. The closed file was saved with an automatically written filename which used the format *prefixYYYYMMDDHHMMSS.vtd*. This allowed the user to set a prefix to identify the tree, and the rest of the name identified the year, month, day, hour, minute, second. An example of the filename and the embedded data is shown in Table 4.1. The file had the filename “M20080329093210.vtd” which is interpreted as M (code for Monash University, tree #13), year 2008, month 3, day 29, hour 09, minute 32, second 10. (29 March 2008, 9:32:10 start of file).

A range of programs were written in Labview which could read the *.vtd data files and process the data with operations such as, replay, convert to engineering units, plot wind loads and wind speeds, perform FFT and power spectra analysis, and calculate stress and moments about the base.

20080329093210						
9321093.000	5.067	5.200	0.700	6.000	14.000	57.000
9321103.000	5.063	5.198	0.700	6.000	14.000	57.000
9321103.000	5.063	5.198	0.700	6.000	14.000	57.000
9321113.000	5.059	5.197	0.700	6.000	14.000	57.000
9321113.000	5.059	5.197	0.700	6.000	14.000	57.000
9321122.000	5.054	5.197	0.700	6.000	14.000	57.000
9321123.000	5.054	5.197	0.700	6.000	14.000	57.000
9321132.000	5.049	5.198	0.700	0.000	14.000	57.000
9321133.000	5.049	5.198	0.700	6.000	14.000	57.000
9321143.000	5.045	5.200	0.700	0.000	14.000	57.000

Table 4.1. Example of the first ten lines of data in a *.vtd file. Line 1 - Date stamp, Line 2 - Time, sensor#1, sensor#2, wind speed, wind direction, temperature, humidity. Line 3 until the end - data (as for Line 2) until line 36000, which equates to 30 minutes of data.

4.4 Laboratory Testing

Laboratory tests using slip gauges to calibrate the linear accuracy of the digital probe, confirmed the manufacturer’s calibration certificate to an accuracy of one micron.

Dynamic tests on vibrating beams in the laboratory were conducted to measure the frequency response of the strain meter. The maximum frequency was 11 cycles per second before errors occurred due to aliasing and signal distortion caused by the mass of the strain meter and the spring loading of the digital probe which was pre-set at 70 g. These tests showed that the strain meter could be used to measure dynamic motion of structures with sway frequencies up to 11 cycles per second. Above this frequency, the response time of the mass of the moving parts of the instrument began to show non-linear response in the time domain data. This showed as flat spots on a time domain curve which meant that peak readings were not necessarily recorded. The instrument response was considered to be suitable for it to be used on medium to large trees as it was approximately ten times the expected oscillation frequency of a tree. Preliminary field tests on medium sized trees confirmed this estimate, with measured sway frequencies of 0.5 to 1 Hz. The frequency response of the instrument was satisfactory for frequency and spectral analysis of medium to large trees and branches.

4.5 Static Analysis

4.5.1 Tree pull test

The static pull test has been used for several years as a method of evaluating tree stability. In this test a rope is attached to a tree and a static pulling load is applied. The method is well described by Brudi (2002) and the test is used to assess how a tree may perform under future wind loading conditions. The method has not been widely adopted because there are reports that trees blow down in wind speeds considerably lower than those predicted from static pulling tests under calm conditions (Gardiner 1995; Fraser and Gardiner 1967; Oliver and Mayhead 1974 and Blackburn et al. 1988). This may be partly due to the way in which the load is applied to the tree. The static test uses a rope to apply a concentrated, static pulling force on the tree and the wind applies a distributed, dynamic pushing force on the broad canopy of the tree. These differences between how the loads are applied to a tree may be important. For these reasons, gathering data on dynamic loads from trees in winds under field conditions is a focus of this study.

The tree pull test is used here to calibrate the instruments on the tree and find the relationship between strain readings (microns) and bending moments (kNm) at the base of the trunk. Each tree must be calibrated because of individual differences in size, shape and material properties of the trunk. The calibration results in a factor, termed the "moment factor" which is used to convert the strain readings (microns) obtained when the trunk sways in a wind storm, into base bending moment values (kN.m) which is used as the measure for wind loading on the tree.

The calibration of the strain meters using the pull test begins by attaching two strain meters, usually at breast height (1.3m), in an orthogonal orientation as previously described. A rope is attached approximately mid-way up the trunk of a tree at a convenient point (Figure 4.9). The load is applied via the rope, as far away as is practical from the tree so as to keep the rope as nearly horizontal as possible. This is done to minimize the vertical component of the load and ensure that the strain readings measure only the bending moment at the base.

A series of known loads (kN) are applied using the rope and recorded. The corresponding strain readings are recorded for each pull. The horizontal component of pull is calculated by multiplying by the cosine of the angle of pull (θ). The bending moments are calculated using Equation 4.7.

$$\text{Moment at base (kN.m)} = \text{Pull (kN)} \times \text{distance (m)} \times \cos\theta \qquad (4.7)$$

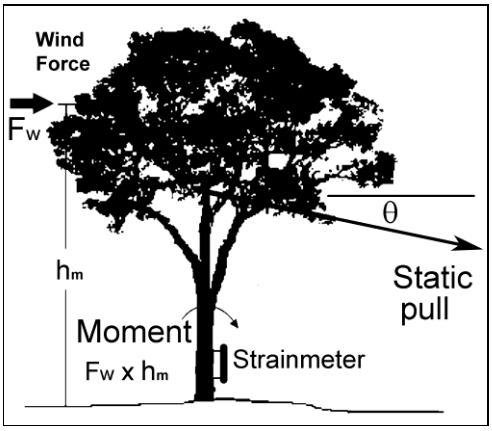

Figure 4.9. Static pull (kN) on a tree using a rope attached at distance (h_m) above the base, applies an overturning moment (kN.m) about the base. Outer fibre elongation (or contraction) on the trunk is measured using the strain meter.

The results of the static pull test are graphed by plotting strain reading (microns) versus base bending moment (kNm), (Figure 4.10). The curve is checked for linearity to ensure that loads remain within the elastic range. Non-linearity would indicate that some plastic failure or irreversible movement had occurred during the test and so make the calibration invalid. In order to compare the calibration curve with published results, an example of a static pull test on Sitka spruce (*Picea sitchensis*) trees in moist soils in Ireland (Rodgers et al.1995) is reproduce (Figure 4.10). The data were obtained using a similar configuration of strain gauges attached to the trunk near the base and the trees were pulled to destruction with a maximum recorded moment of 12 kNm.

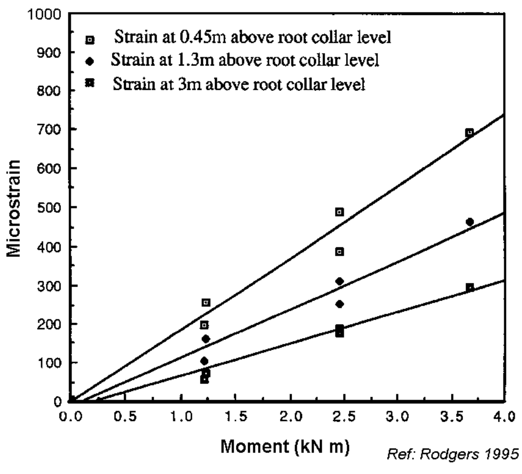

Figure 4.10. Results of pulling tests on Sitka spruce (*Picea sitchensis*), showing linear relationship between base bending moment and strain gauges on the trunk (Rodgers et al.1995).

The pull test calibrates the instruments on a specific tree and the relationship between strain and base bending moments is found from the gradient of the line of best fit, indicated by the constant in the equation. This constant is used as the calibration factor for the instruments, and is referred to as “the moment factor”. Each individual tree must be calibrated because of differences in trunk size, shape and material properties and differences in the location of the instruments, particularly the height above the trunk base. The exact height and location of the instruments is not critical but the calibration process must be repeated if the instruments are moved and located in another position on the tree.

If a tree is not vertical and there is a lean to one side, a self loading component of base bending moment would be present. If the wind blew in the direction of lean it would add to the base bending moment. For large trees on a severe lean the issue of self loading needs to be considered. If the lean is small (approximately less than 3 degrees) the moment due to self weight will be negligible compared to the wind loads and is assumed to have no effect on the wind induced loads. The tilt due to the wind is also negligible for the large trees in this study as the maximum trunk fibre elongation is always less than 1 mm and the effect of self loading on the measured wind loads is also considered to be negligible.

The moment factor determined from the pull test is used as a calibration factor to calculate wind loads when the trees are being monitored in wind storms. As the wind causes the tree to bend and the instruments on the trunk record strain data, the base bending moment is taken as the wind load and can be calculated by using Equation 4.8.

$$\text{Wind Load (kNm)} = \text{Instrument reading } (\mu) \text{ x calibration factor (kNm/ } \mu) \tag{4.8}$$

During the pull test there is a small vertical component of force acting in a downward direction which may affect the strain reading. The instrument oriented at right angles to the pull would record this vertical component (as $\Delta 2$) on graph as shown in Figure 4.11. Calculations for this test indicate that the vertical component is not significant and contributes less the 2% to the strain readings. Small wind gusts influence the data to a far greater magnitude than the vertical component which is considered to be negligible.

When small wind gusts occur during the test, the pull is keep constant for a short period so an average strain value can be determined. In high winds the readings cannot be accurately determined so the test is not performed. For large trees where the trunk cross section is greater than 500 mm, the vertical components of force generated by the pull test are less than 2% to the strain reading and is taken into account by modifying the moment factor determined from this calibration.

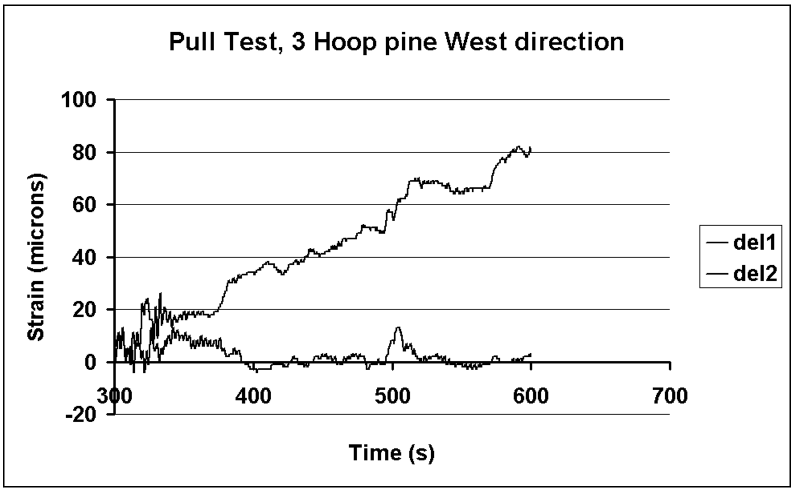

Figure 4.11. Pull test showing instrument response in the direction of pull and the orthogonally oriented sensor which registers the vertical component generated by a rope at 20° to the horizontal. Some small wind gusts are also present during this test.

Another important outcome of the static test is to verify that the tree is firmly secured in the ground and no movement or rotation of the root plate occurs. This supports the assumption that there is negligible dynamic interaction between the above ground and below ground tree parts. During the static pull test, an angle sensor is attached to the very base of the tree, at ground level. This ensures the sensor measures root plate rotation and not trunk bending. If the tree is firmly anchored in the ground, there will be only a small or even zero reading on the angle sensor which has an accuracy of 0.01 degrees. The method described by Brudi (2002) uses a critical angle of 0.25 degrees which is considered excessive and is where the test is stopped. The rotation of the root plate is used as a check during the pull test, to verify that the tree does not move and is securely fixed in the ground. In this present study, no root rotation was observed during the static pull test.

The results from the static pull test can be used to calculate the Young's Modulus values of tree trunks and branches of live trees in situ. Each instrument attached to the tree measures the change in length of the outer fibres as the trunk bends during the pull test. The length of each instrument is 500 mm so with an accuracy of one micron (1μ), the strain can be calculated using Equation 4.1. Since the moment is known from Equation 4.7, the outer fibre stress can be calculated using Equation 4.4 if the moment of inertia of the cross section can be measured. If the trunk or branch is not circular, this may need to be calculated for each of the principal axes using Equation 4.5 or 4.6. With values for stress and strain, the Young's modulus value can be calculated using Equation 4.3.

4.5.2 Relationship between strain readings and tree deflection

The strain data from the instruments at the base of the tree may be used to calculate the deflection of the trunk at any point above the instruments. This would be useful when modeling the dynamic response of the tree as deflection is a commonly used variable in dynamic analyses but determining deflection is not simple for trees. For example not all trees have a central trunk and a tree with co-dominant stems will not have one point where deflection can be determined. Trees with many side branches and no central trunk provide a similar difficulty in determining deflection at any one point. Displacement measurements are useful to use on trees with a central trunk structure and when single degree of freedom modeling is used as a first approximation. If this approach is used, a tree may be approximated to a cantilever as in Figure 4.12.

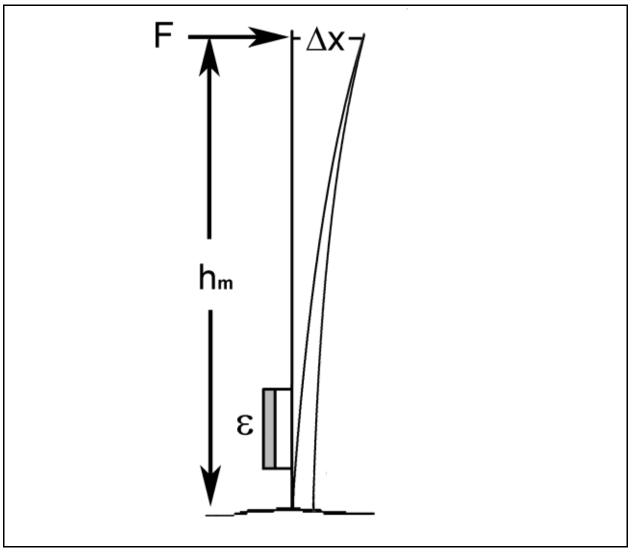

Figure 4.12. Relationship between the force (F) and the deflection (Δx) of a tree trunk at distance h_m above the ground to the strain (ε) at the trunk base which is measured by the instruments.

The relationship between the deflection at the top of a cantilever and the strain readings can be found using simple engineering formulae. The deflection (Δx) is determined using Equation 4.9, (Gere and Timoshenko 1990, p633).

$$\Delta x = Fh_m^3 / 3EI \qquad (4.9)$$

Where

F is the force pushing on the cantilever

h_m is the distance from the tree base to the point of force application

Recalling Equation 4.1 and 4.3 and substituting into Equation 4.9, the strain can be expressed as;

$$\varepsilon = {3\Delta xd}/{2h_m^2} \tag{4.10}$$

This equation shows the relationship between the strain measured at the side of the trunk and the deflection of the tree at a point where the force is acting. Since the strain is recorded at 20 Hz, the time series of strain values $\varepsilon(t)$ can be related to the time series of deflection values x(*t*). The dynamic properties of strain can be used to determine the dynamic properties of the tree using spectral analysis which is described later. This method assumes constant values of Young's modulus. For this study, the E value for the tree is calculated for the trunk section at which the instruments are located and is assumed to be constant.

4.5.3 Relationship between strain readings and spring constant (k)

Continuing the approximation of a tree to a cantilever, the relationship between the strain readings at the base and the spring constant of a cantilever can be determined. This is useful when modeling the tree so that the spring constant values in the model can be related to the Young's modulus of the tree trunk. As force F pushes on the tree at height h_m above the ground, the resulting deflection may be plotted against the force to determine the gradient which gives the value of the spring constant (k), Figure 4.13.

$$k = {F}/{\Delta x} \tag{4.11}$$

Substituting this into Equation 4.10 and rearranging for *k* gives;

$$k = {3Fd}/{2\varepsilon h_m^2} \tag{4.12}$$

This equation is useful to put into the theoretical model as the strain readings (ε) can be used to determine the spring constant value (k) of the model for a particular tree.

The two quantities of wind force (F) and the height (h_m) at which the force acts, are coupled so that their product is the bending moment about the base. Although the product of (F) and (h_m) can be measured, the two quantities cannot be uncoupled and remain unknown. In later analyses, estimates can be made of (F) and (h_m) in order to calculate dynamic properties of the tree and drag coefficients.

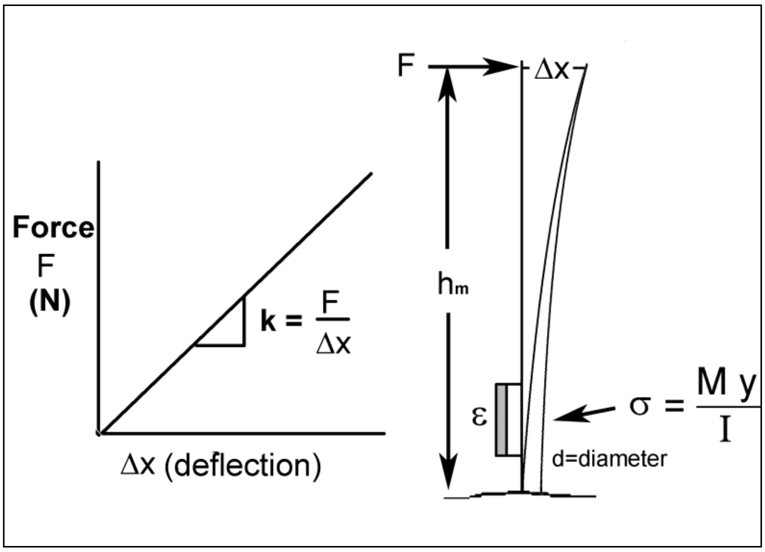

Figure 4.13. The force (F), at height (h_m) causes a deflection (Δx) of the cantilever. The strain measured at the base can be used to determine the spring constant (k) of a cantilever.

In field conditions, the moment can be determined from the strain readings after the tree has been calibrated using the pull test.

4.5.4 Relationship between Young's Modulus of tree and spring constant (k)

Using the previous analysis, it is useful to determine the relationship between the values of E, Young's modulus and k, the spring constant so that the tree can be represented by a dynamic model. This permits tree parameters to be used in a modeling analysis using fundamental dynamic equations.

Combining Equations 4.10 and 4.12 and rearranging for strain (ε), gives;

$$\varepsilon = \frac{Fh_m d}{2EI}$$

Therefore

$$\frac{3Fd}{2kh_m^2} = \frac{Fh_m d}{2EI}$$

Simplifying and solving for k

$$k = \frac{3EI}{h_m^3} \tag{4.13}$$

4.6 Analysis of Field Data

The strain meter instruments have been used over a four year period to monitor wind loads on a range of open grown trees (James et al. 2006). Data of the following parameters were recorded at a sampling rate of 20 Hz:

- the strain of instrument #1 (North/South) and instrument #2 (East/West),
- wind velocity and direction, and
- temperature and humidity.

Data files were limited to 36000 readings (30 minutes) for convenience and ease of manipulation. Recording was to the hard disc of the controlling computer in the format described under software in this chapter. These data files were used to analyse the response of the tree to wind excitation in the time and frequency domains using a sequence shown in the flow chart in Figure 4.14.

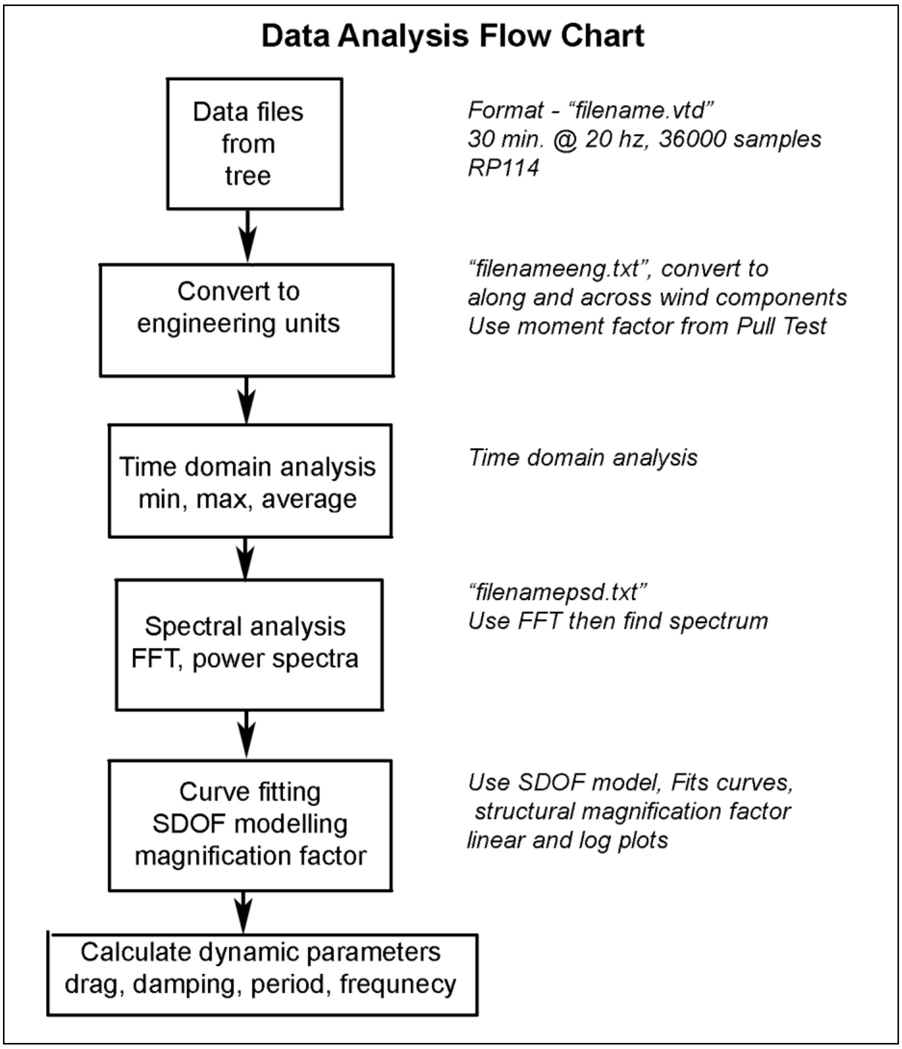

Figure 4.14. Flow chart showing data analysis method

The raw data files were converted from strain readings to engineering units using the Labview software program. The engineering files were further converted into along wind and across wind components of base bending moments using the moment factor obtained during the tree pull test. The tree response to wind loading, in the along-wind and across-wind directions was determined from these files. The time domain information was plotted and both instantaneous and long term mean values (30 minutes) were calculated. Spectral analysis was used to obtain the transfer function of the tree which was used for comparison with the theoretical SODF models. This allowed the dynamic parameters for the tree to be determined, which include natural frequency, damping and drag. The flow chart shows the process of analysis which is described in the following sections.

4.7 Dynamic Analysis

In this section the methods of analyzing vibrating systems are applied to trees. A dynamic analysis is required because of the oscillating sway response of a tree under varying wind excitation. The principles of dynamic analysis are well known for engineering and man-made structures such as machines with unbalanced rotating parts, rotary fans, turbines, bridges and buildings. Natural phenomena of earthquakes and winds may cause bridges to oscillate and buildings to vibrate, with catastrophic results in extreme cases. The elements of a vibrating system are (i) inertia elements or mass, (ii) stiffness elements or springs, and (iii) dissipation elements of dampers (Figure 4.1). In a vibrating system the inertial elements store and release kinetic energy, the stiffness elements store and release potential energy and the damper elements dissipate energy and cause the vibrations to gradually decay and finally cease when all the energy is dissipated. As a first step in applying these principles to a tree, some simplifying assumptions are made in order to develop some basic equations. Later these simplifications are modified so that the analysis more closely represents the dynamic response of the tree under wind excitation.

4.7.1 Tree motion and structural magnification

As a first approximation, a tree may be considered as a vertical cantilever (Figure 4.15a) which is excited by a time varying force F(*t*) at height (h_m) to give displacement response x(*t*). The displacement can be modeled with an equivalent single-degree-of-freedom (SDOF) system consisting of a vibrating mass (m) with a spring (k) and a damper (c) that is excited by a time varying force F(*t*) to produce a similar displacement response x(t), (Figure 4.15b).

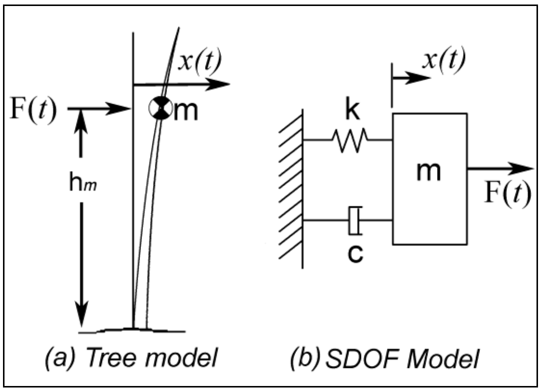

Figure 4.15. A single degree of freedom (SDOF) representation of (a) a tree and (b) an equivalent vibrating model. A time varying force *F(t)* excites a mass *(m)* that creates a displacement response *x(t).*

The tree parameters and corresponding model parameters, including units are summarized in Table 4.2. The mass and damping units are the same, but the Young's modulus of the tree and the spring constant of the model need to be considered individually.

	Tree parameters	**Model parameters**
1	Mass (m) kg	Mass (m) kg
2	Young's modulus (E) kN/m^2	Spring constant (k) kN/m
3	Damping (c) (kN.s/m)	Damping (c) (kN.s/m)

Table 4.2. Equivalence of tree parameters and model parameters.

The dynamic motion of a SDOF oscillator undergoing damped forced vibration can be described by Equation 4.14.

$$m\ddot{x} + c\dot{x} + kx = F(t) \qquad (4.14)$$

Equation 4.14 is the governing equation of motion for a single degree-of-freedom system for oscillations about a stationary equilibrium position (Balachandran and Magrab 2004). For this reason, models of vibrating systems find displacement *x(t)* from the static equilibrium position to be a convenient choice. This approach is used in the current study and is developed to include base bending moments *M(t)*, which is proposed as a more appropriate method for trees.

By taking $\omega_n = 2\pi f_n = \sqrt{k/m}$ as the natural circular frequency, and

$$\zeta = \frac{c}{2\sqrt{km}} = \frac{c}{c_c} \tag{4.15}$$

as the critical damping ratio, Equation 4.14 may be re-written as:

$$\ddot{x} + 2\omega_n \zeta . \dot{x} + \omega_n^2 x = \frac{\omega_n^2 F(t)}{k} \tag{4.16}$$

Equation 4.16 has the solution for amplitude

$$X = \frac{(F_0 / k)}{\left\{\left[1 - \left(\omega/\omega_n\right)^2\right]^2 + \left[2\zeta \,\omega/\omega_n\right]^2\right\}^{\frac{1}{2}}} \tag{4.17}$$

And a corresponding solution for phase angle

$$\phi = tan^{-1}\left[\frac{2\zeta \,\omega/\omega_n}{1 - \left(\omega/\omega_n\right)^2}\right] \tag{4.18}$$

Equation 4.17 can be divided by the static deflection (*F$_o$/k*) to give the structural magnification factor, Equation 4.19.

$$\chi_m = \frac{X}{\left(F_0/k\right)}$$

$$\chi_m = \frac{1}{\left\{\left[1 - \left(\omega/\omega_n\right)^2\right]^2 + \left[2\zeta \,\omega/\omega_n\right]^2\right\}^{\frac{1}{2}}} \tag{4.19}$$

The equations that describe the structural magnification factor (Equation 4.19) and phase angle (Equation 4.18) are described by Den Hartog (1956) as the most important in his book on vibrations. Equation 4.19 can be plotted as dimensionless quantities x/x_{stat} and ϖ/ϖ_n to create a family of curves for different values of damping ratio (Figure 4.16).

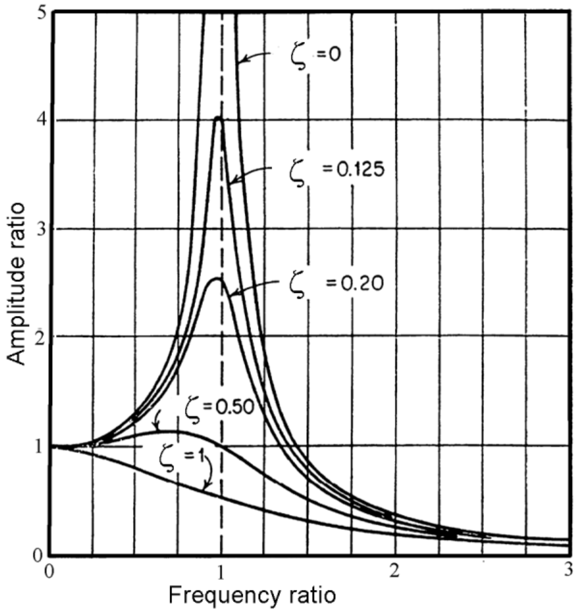

Figure 4.16. Amplitudes of forced vibration for various degrees of damping (Den Hartog 1956). (Note: Original terminology modified for consistency in this thesis).

The structural magnification function described in Equation 4.19 and plotted in Figure 4.16, has several regions in which the response of the structure is dependent on the frequency of the applied load. It is redrawn in Figure 4.17 to clearly show three different regions where response is dominated by either mass (inertia), spring (stiffness) or damper (damping).

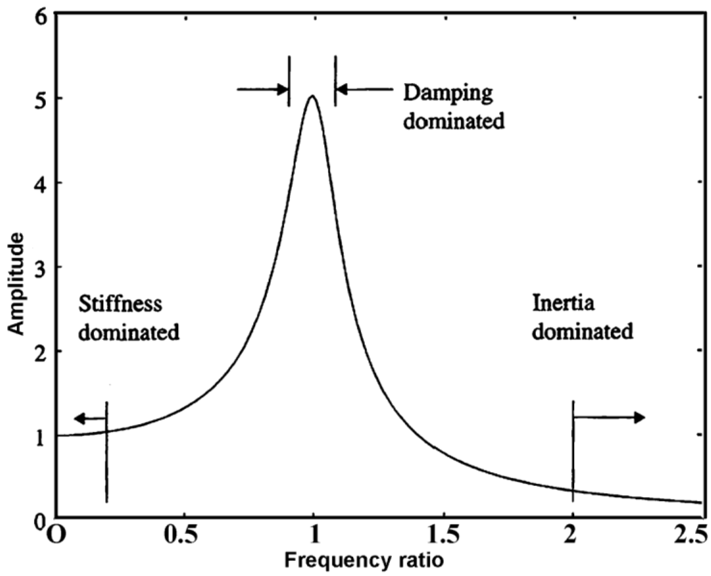

Figure 4.17. Structural magnification function for a single-degree-of-freedom system (Balachandran and Magrab 2004). (Note: Original terminology modified for consistency in this thesis)

When the load is applied very slowly (low frequency range), the system behaves in a static or quasi-static manner so that the response of the structure is almost directly proportional to the load. This is the "stiffness dominated region" in which the ratio of structural magnification of amplitude approaches 1 at a frequency of "zero". This point on the graph would represent a static pull test on a tree.

As the frequency of the applied load increases, the dynamic response of the structure increases until a maximum is reached, shown as a peak in Figure 4.17. At this point the frequency of the applied load is at or close to the natural frequency of the structure. The magnitude of the peak depends on the dynamic characteristic of the structure, in particular the amount of damping that is present. If damping is zero, the curve can asymptote to infinity and the structure will resonate. The height of the peak response (the magnification factor) depends on the damping so this region is the "damping dominated region".

At frequencies above the damping dominated region, the applied load is out of phase with the structure response and the amplitude of oscillations decreases. At even higher frequencies, the load impacts on the structure so quickly that each cycle cannot overcome the inertia of the structure. When this occurs there is little response of the structural mass to the rapidly impacting load and this is known as the inertial region of the curve or "the inertial sub-range".

4.8 Vibration Analysis; Estimating Dynamic Characteristics of Trees

4.8.1 Introduction

The main purpose of a dynamic analysis is to find the dynamic characteristics of a tree, which include, natural frequency (ω_n *or* f_n), and damping (C) or damping ratio (ζ). The damping may consist of several components which include (a) aerodynamic damping, (b) internal or visco-elastic damping, and (c) mass damping. This investigation starts by looking at the total system and then attempts to identify individual components of damping.

This section describes several structural dynamic analysis methods including;

(a) free vibration analysis called the pull and release test or "the pluck test",
(b) a spectral based modeling approach using measured field data, and
(c) a mean moment response of the tree to wind, which is a quasi-steady state method using averages of measured dynamic data.

Each method is applied to trees and used in the next chapter to analyse the results from field trials.

4.8.2 Free response oscillations (the pull and release test)

Free vibrations occur when a structure is deflected from its static equilibrium position, then released and allowed to vibrate without any external excitation. Such free vibrations are induced in a tree by pulling it sideways with a rope then suddenly releasing it, in the absence of wind. The resulting vibrating motion decays because energy is lost due to damping. Damping is often complex and usually cannot be determined analytically so this elusive property should be determined experimentally (Chopra 1995). Although the damping has several components, each acting simultaneously to dissipate energy, a mathematically convenient approach is to idealize them by equivalent viscous damping (Chopra 1995, Moore and Maguire 2004). The free vibration test, also called a pull and release test or a pluck test is useful for determine the natural frequency and the damping ratio of a vibrating structure. These values can be used later to compare with values obtained under wind excitation.

This test is conducted under wind free conditions with instruments attached to the tree, either strain meters at the base or accelerometers at a selected height up the trunk. A rope is attached to the tree and a sideways pull is applied and held. The pull is static and causes a deflection of the trunk in which strain energy is stored. The rope is suddenly released and stored strain energy in the tree causes the tree to oscillate freely, backwards and forwards, with no external driving force. The instruments record the dynamic motion during this event. The sway gradually decreases due to damping effects of the tree until the whole tree comes to rest.

The pluck test is performed to determine the dynamic properties of the structure, namely

1. amplitude (A)
2. natural frequency (ω_n)
3. critical damping ratio (ζ)

Using the governing equation of motion for a single degree of freedom system (Equation 4.14) and taking the input force *f(t)* = 0, Equation 4.16 reduces to;

$$\ddot{x} + 2\omega_n \zeta . \dot{x} + \omega_n^2 x = 0 \qquad (4.20)$$

The oscillations of the tree are recorded from the instrumentation and the resulting time domain curve is used to fit the solution to Equation. 4.20 (Chopra 1995) which can be written as;

$$x(t) = ae^{-\omega_n \xi . t}\left(cos(\omega_d t) + \left(\frac{\omega_n \xi}{\omega_d}\right) sin(\omega_d t)\right) \tag{4.21}$$

Noting that - $\omega_d = \omega_n \sqrt{(1-\zeta^2)}$ or $\omega_d = \frac{\zeta}{\sqrt{(1-\zeta^2)}}$ and

- a is the initial displacement

The solution for natural frequency and damping ratio can be found by fitting Equation 4.21 to the data. Time domain amplitude curves (*x(t)*) for (a) over-damped, (b) under-damped and (c) critically damped oscillations are shown in Figure 4.18 (Chopra 1995).

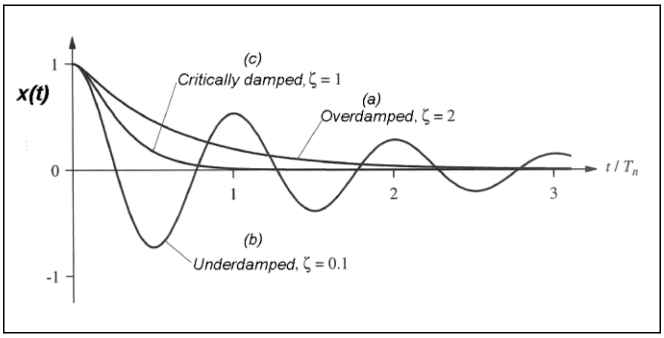

Figure 4.18. Time domain amplitude curves *x(t)* for (a) over-damped, (b) under-damped and (c) critically damped oscillations (Chopra 1995).

A simplified version of Equation 4.21 has been used by some authors (Jonsonn et al. 2007) and is valid for small amplitudes of oscillation but may not be accurate if large oscillations occur. Another method of determining damping from free vibration tests is the logarithmic decrement method (Moore and Maguire 2004) which uses two successive peaks of amplitude (Figure 4.19) to compute the critical damping and the natural frequency.

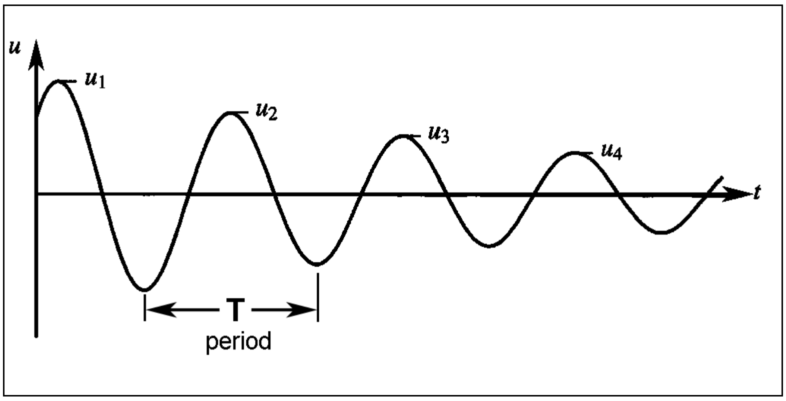

Figure 4.19. Free vibration of a structure showing successive peaks used in the logarithmic decrement method. Period (T) separates each cycle. (Chopra 1995).

The ratio of successive peaks separated by period T is;

$$\frac{u_i}{u_{i+1}} = \exp\left(\frac{2\pi\zeta}{\sqrt{1-\zeta^2}}\right)$$

The natural logarithm of this ratio, called the logarithmic decrement (δ) is:

$$\delta = \ln\frac{u_i}{u_{i+1}} = \frac{2\pi\zeta}{\sqrt{1-\zeta^2}}$$

The logarithmic decrement works well for regular cyclic vibrations, but has limitations if there are variations between each cycle because there is not a consistent decay in amplitude. When used for trees with large canopies and thus heavy damping, this method may not give consistent values of damping due to uneven or irregular sway cycles in the oscillations of the tree.

4.8.3 Spectral analysis of tree dynamic response

Spectral analysis is applied to the time varying data of wind speed and tree response to examine the data for cyclic patterns. The method is useful for analysing the frequency of wind gusts and the frequency response of a dynamic structure. Spectral analysis, as described by Jenkins and Watts (1968) has been applied to trees by several authors (Gardiner 1995, Jonsson 2007, Moore 2004, De Langre 2007). In this study a spectral based model for investigating the dynamic response of trees to wind loading is presented. The approach follows that of Davenport (1967) and the "gust load factor" (GLF) method found in wind codes such as AS/NZS 1170 part 2 (2002). The GLF method is used on man-made structures to determine an equivalent static wind loading, which is equal to the mean wind force multiplied by a GLF. The GLF accounts for the dynamics of wind fluctuations and any load amplification introduced by the building dynamics.

The data are analyzed with the assumption that the time series is;

- stochastic or non-deterministic, and
- stationary, in that the basic statistics are time invariant

The data are taken from the 30 minute files obtained from the field monitoring of trees and are 'pre-conditioned' by subtracting the mean and trend from the data series. The analysis is effectively investigating the fluctuations of the time series which gives a measure of the dynamic response of the tree.

The method uses Fourier analysis which transforms the time series into the frequency domain. The specific application used discrete Fast Fourier Transformations (dFFT). The Labview software was used to write programs to read the data files generated from this project. The dFFT used 32768 points of 20 Hz data which represents a 27.3 minute period of information in a file. The power spectral density (PSD) function *S(f)* was then calculated and is interpreted as the power density of the data series.

$$S(f) = 2T\left[\frac{a_n^2}{4} + \frac{b_n^2}{4}\right]$$

Where a_n and b_n are the Fourier Coefficients.

In order to smooth the PSD output, ensemble averaging was used by taking the 32768 data points and dividing them into 16 sets of 2048 data (Jenkins and Watts 1968). Comparisons between different trees and different wind loading are possible by normalizing the PSD, which is achieved by dividing by the signal variance. The method is applied to the wind data to find the PSD for the along wind speed, designated $S_v(f)$. The PSD is then found for the bending moment response data designated $S_M(f)$. The relationship between the along wind speed spectrum and the bending moment response spectrum is given by Equation 4.22.

$$S_M(f) = T^2(f)S_v(f) \tag{4.22}$$

where $T^2(f)$ represents the transfer function for the tree base bending moment due to wind excitation. The transfer function is unique to each tree and describes how the energy from the wind is transferred to the tree.

Consider the single–degree-of-freedom (SDOF) model of the response to wind excitation of an urban tree, where the in-line displacement at a suitable reference point, such as the centroid of the exposed area of the tree canopy is given by x(t).

The along-wind force *F(t)* acting on the tree is considered to be drag dependent and thus velocity dependent as described by,

$$F(t) = ½\, \rho\, C_D.\, A\, V^2 \tag{4.23}$$

Where ρ is the air density *(~ 1.2 kg/m^3)*

C_D is the total effective drag coefficient of the tree

A is the orthogonal area of the canopy exposed to the wind, and

V is the velocity of the air passing the tree.

The relative along-wind speed is given by,

$$V = \left(V(t) - \dot{x}(t)\right) \qquad (4.24)$$

where $V(t)$ is the wind velocity, and

$\dot{x}(t)$ is the tree velocity when the tree sways.

This gives the in-line wind force,

$$F(t) = \alpha\left(V(t) - \dot{x}(t)\right)^2 \qquad (4.25)$$

Where $\alpha = ½\, \rho\, C_D.\, A$

The α value includes two parameters C_D and A which are both dependent on wind speed. As the wind speed increases, the canopy of a tree will change by becoming (a) more "streamlined" so that C_D will vary and (b) more compact as the canopy is blown by the wind and its cross-sectional area A becomes smaller.

The α value is therefore assumed to be wind dependent so that

$$\alpha = \alpha_0\left(\frac{\overline{V}^{\,n}}{\overline{V}^{\,2}}\right) = \alpha_0 \overline{V}^{\,n-2} \qquad (4.26)$$

Where n is less than 2

$\alpha_o = ½\, \rho\, C_{Do}.\, A_o$,

C_{Do} is the drag coefficient under still wind conditions, and

A_o is the orthogonal area of canopy under still air conditions.

The wind force $F(t)$ at varying speeds can then be evaluated using,

$$F(t) = \alpha_o \overline{V}^{\,n-2}\left(V(t) - \dot{x}(t)\right)^2 \qquad (4.27)$$

The moment acting at the base of the tree is equal to the force $F(t)$ acting at an effective height h_m so that,

$$M(t) = h_m F(t) = \beta V^2(t) \qquad (\beta = h_m \alpha) \qquad (4.28)$$

$$= \beta\left(V(t) - \dot{x}(t)\right)^2$$

Wind is considered to have a mean component and a fluctuating component. For along wind speed *V(t)* consisting of a mean ($\bar{V}$) and a turbulent component *v(t)* then,

$$V(t) = \bar{V} + v(t) = \bar{V}\left(1 + \frac{v(t)}{\bar{V}}\right) \tag{4.29}$$

Expanding Equ (4.28) and substituting terms of Equ (29), the base moment is given by,

$$M(t) = \beta\left[\bar{V}^2\left(1 + \frac{v^2(t)}{\bar{V}^2}\right) + 2\bar{V}v(t) - 2\bar{V}\dot{x}(t) - 2v(t)\dot{x}(t) - \dot{x}^2(t)\right] \tag{4.30}$$

If it is assumed that both the tree response $\dot{x}(t)$ and the wind fluctuations *v(t)* are small compared to the mean wind speed $\bar{V}$, Equ (4.30) reduces to

$$M(t) \approx \beta\bar{V}^2\left(1 + \frac{v^2(t)}{\bar{V}^2}\right) + 2\beta\bar{V}v(t) - 2\beta\bar{V}\dot{x}(t)$$

or
$$M(t) = \bar{M} + m(t) - h_m c_a \dot{x}(t) \tag{4.31}$$

in which

$\bar{M} = \beta\bar{V}^2\left(1 + \frac{v^2(t)}{\bar{V}^2}\right) = \beta\bar{V}^2\left(1 + I^2\right)$ - I is the turbulence intensity $\left(\frac{v_{RMS}}{\bar{V}}\right)$

$m(t) = 2\beta\bar{V}v(t)$ - the fluctuating moment, and

$c_a = 2\alpha\bar{V}$ - considered as an "aerodynamic damping" contribution term

By combining Equ (4.28) and Equ (4.31) the base bending moment can be expressed as

$$h_m\left(m\ddot{x} + c\dot{x} + kx\right) = \bar{M} + m(t) - h_m c_a \dot{x}(t)$$

Collecting damping terms on the left hand side,

$$h_m\left[m\ddot{x}(t) + (c + c_a)\dot{x}(t) + kx(t)\right] = \bar{M} + 2\beta\bar{V}.v(t) \tag{4.32}$$

Considering the above modeling approach, the spectral description of the tree response (base bending moment) to wind excitation can therefore be obtained from fluctuation terms *m(t)* and *v(t)*. Therefore the spectra of base banding moments $S_M(f)$ is given by;

$$S_M(f) = \left(2\beta\bar{V}\right)^2 \chi_m^2(f)\chi_a^2(f)S_v(f) \tag{4.33}$$

In which - $\chi_m^2(f)$ is the structural magnification factor

$$\chi_m^2(f)=\frac{1}{\left\{\left[1-\left(f/f_n\right)^2\right]^2+\left[2\zeta f/f_n\right]^2\right\}}$$

- ζ the effective damping ratio (inclusive of all damping),
- f_n the primary mode frequency of the tree,
- $\chi_a^2(f)$ the "aerodynamic admittance" function, and
- $S_v(f)$ is the along wind speed spectrum.

This can be further simplified to:

$$S_M(f)=T^2(f)S_v(f) \tag{4.34}$$

where $T^2(f)$ represents the transfer function for the tree base bending moment due to wind excitation, such that;

$$T^2(f)=\left(2\beta\bar{V}\right)^2\chi_m^2(f)\chi_a^2(f) \tag{4.35}$$

The aerodynamic admittance function, $\chi_a^2(f)$, represents the relationship in the frequency domain between wind velocity and the resulting wind pressure or force on a building surface (Zhou and Kareem 2001) and is often assumed to be constant, $\chi_a^2(f)=1$ but does vary with frequency. Aerodynamic admittance describes the effect of wind on a large structure. The wind speed is not constant or uniform over the surface area of a large structure as it impacts first in one area and then on another part of the surface. Based on experiments, the aerodynamic admittance function is described by Equation 4.36. (Holmes 2007)

$$\chi^2(n)=\frac{1}{1+\left[\frac{2n\sqrt{A}}{\bar{U}}\right]^{\frac{4}{3}}} \tag{4.36}$$

in which A is the frontal area exposed to wind and $\bar{U}$ is the mean wind speed.

The concept of the aerodynamic admittance function has not yet been applied to trees. In order to investigate the influence of the aerodynamic admission function, Equation 4.35 is modified and divided by $\chi_a^2(f)$.

$$\left(2\beta\bar{V}^2\right)\chi_m^2(f)=T^2(f)/\chi_a^2(f) \tag{4.37}$$

This allows the theoretical structural magnification function to be plotted against the spectral data of the trees. Results using this method are presented in Chapter 5.

4.8.4 Mean moment response to estimate drag coefficients

It is possible to estimate the aerodynamic parameters of drag coefficient (C_D) and canopy area (A) by using values for the mean moment response ($\overline{M}$) of the tree to wind speed ($\overline{V}$) obtained during field monitoring. The mean moment expressed in Equation 4.31 can be written as;

$$\overline{M} = \beta \overline{V}^2 \left(1 + \frac{v^2(t)}{\overline{V}^2}\right) = h_m \alpha_0 \overline{V}^n \left(1 + I^2\right) \qquad (4.38)$$

Where $\alpha_o = \frac{1}{2} \rho C_{Do}. A_o,$

The mean moment response from the strain meters is averaged over a time period (30 min. to match file size). And the values for ($\overline{M}$), ($\overline{V}$) and I are determined from experimental data.

An example from tree#13, spotted gum *(C. maculata)* uses the following values,

h_m = 19 m, $\rho = 1.2\ kg\ m^{-3}$, and $\boldsymbol{I}$ found to be in range 03 to 04 (say 0.35), ($\boldsymbol{I}^2$ = 0.123).

Substituting these values into Equation 4.37 gives an expression for mean moment as;

$$\overline{M} = 12.8 C_D A_o \overline{V}^n$$

This process is repeated for a range of wind speed values and the results are plotted to obtain a characteristic curve of wind speed versus moment at the base of the tree, over 30 min. averages.

The line of best fit is then used to find the equation to the relationship for wind speed and moment, then calculated back to find C_D.A values. The theoretical relationship will give values of the velocity exponent n between 1 and 2. Results from experimental data are presented in the next section.

4.9 Multi-degree of Freedom Systems and Tuned Mass Dampers

The dynamic analysis of trees needs to be extended from a single-degree-of-freedom system (SDOF) to take account of the dynamic interaction of branches. In open grown trees, where the branch mass is large compared to the trunk mass, the dynamic effect of branches is significant so the approximations of a SDOF system may not account for all of the observed dynamic response. The SDOF analysis provides a first approximation and is useful for developing the dynamic analysis methodology that is used to determine fundamental parameters such as natural frequency and estimates of damping. The next step is to consider more complex dynamic systems, starting with a two-degree-of-freedom (2DOF) system then extending the analysis to a more general multi-degree-of-freedom system (MDOF).

Consider a two degree of freedom system consisting of the primary vibrating mass *m* with a supporting spring *k* and damper *c*, and another mass m_d, which is suspended from the primary mass with spring k_d and damper c_d (Figure 4.20).

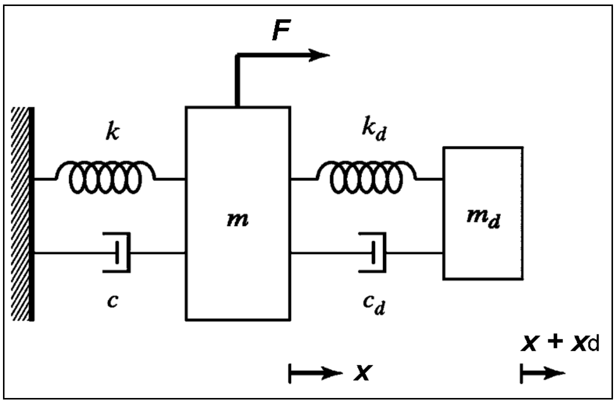

Figure 4.20. A simple tuned mass damper (TMD). The subscript d refers to the TMD (Connor 2002).

The components m_d, k_d, and c_d represent a tuned mass damper (TMD) in which the mass m_d reduces the dynamic response of the structure when its frequency is tuned to be near that of mass *m*. If the system has no damping (i.e. $c=c_d=0$), the device is termed a dynamic vibration absorber which is discussed in detail in Den Hartog (1956).

In order to be effective the TMD must vibrate at or near the same natural frequency of the main mass. Damping is achieved because energy is dissipated by the inertia force of the TMD acting on the structure, and out of phase with the motion of mass *m* (Connor 2002). Applications of TMD in buildings to reduce sway motion in wind are reported from 1975 with many examples (Connor 2002).

To illustrate the concept of a TMD, a number of equations can be developed. Here, the subscript *d* refers to the TMD and the method is after Connor (2002) who uses the following notation;

$$\omega^2 = k/m \tag{4.39}$$

$$c = 2\zeta\omega m \tag{4.40}$$

$$\omega_d^2 = k_d \big/ m_d \tag{4.41}$$

$$c_d = 2\zeta_d \omega_d m_d \tag{4.42}$$

And defining $\overline{m}$ as the mass ratio $\overline{m} = m_d \big/ m$ (4.43)

The governing equations of motion are;

Primary mass $(1+\overline{m})\ddot{u} + 2\zeta\omega\dot{u} + \omega^2 u = \frac{F}{m} - \overline{m}\ddot{u}_d$ (4.44)

Tuned mass $\ddot{u}_d + 2\zeta_d \omega_d \dot{u}_d + \omega_d^2 u_d = -\ddot{u}$ (4.45)

For engineering applications, the design of a mass damper involves specifying the mass m_d , stiffness k_d and damping coefficient c_d , so that the dynamic response of the structure is reduced and excessive dynamics loads are not generated by winds. In trees, the branches provide damping and one of their functions is to act as tuned mass dampers and minimize wind induced loads.

As an example of a tuned mass damper and its effect on a structure, the following approximations are used. For near optimal effect, the frequency of the TMD will equal the frequency of the parent structure, so that,

$$\omega_d = \omega \tag{4.46}$$

The stiffness relationship for this frequency combination is such that;

$$k_d = \overline{m}k \tag{4.47}$$

For a periodic excitation $F = \hat{F}\, sin(\Omega.t)$ (4.48)

where Ω is the forcing frequency. The displacement solution for the critical loading case (when $\Omega = \omega$) is,

$$\hat{u} = \frac{F}{k\overline{m}} \sqrt{\frac{1}{1+\left(\frac{2\zeta}{\overline{m}} + \frac{1}{2\zeta_d}\right)^2}} \tag{4.49}$$

$$\hat{u}_d = \frac{1}{2\zeta_d}\hat{u} \tag{4.50}$$

The response for no damper is $$\hat{u}_d = \frac{\hat{F}}{k}\left(\frac{1}{2\zeta}\right) \tag{4.51}$$

In order to compare the two cases, it is possible to express Equation 4.51 in terms of an equivalent damping ratio(ζ_e), such that:

$$\hat{u} = \frac{F}{k}\left(\frac{1}{2\zeta_e}\right) \tag{4.52}$$

Where $$\zeta_e = \frac{\overline{m}}{2}\sqrt{1+\left(\frac{2\zeta}{\overline{m}}+\frac{1}{2\zeta_d}\right)^2} \tag{4.53}$$

This shows the relative contribution of the damper parameters to the total damping.
It is interesting to note that:

- increasing the mass ratio ($\overline{m}$) magnifies the damping, but there is a practical limit as the total mass also increases, and
- decreasing the damping coefficient for the damper (ζ_d) also increases the damping.

There is also a practical limit on the relative motion of the TMD to the structure because excessive displacements may be physically impractical and failure may occur. These practical limitations result in a compromise between added mass and excessive displacement in designing a TMD.

Example of a preliminary design of a 2DOF TMD system

An example from Connor (2002) is presented below to illustrate how the addition of a relatively small mass (2%) can contribute significantly to the damping of a 2DOF system. Assume the main structure has no damping ($\zeta = 0$) and a tuned mass damper is added such that the overall damping is 10% ($\zeta_e = 0$).

The relationship between $\overline{m}$ and ζ_d is

$$\frac{\overline{m}}{2}\sqrt{1+\left(\frac{2\zeta}{\overline{m}}+\frac{1}{2\zeta_d}\right)^2} = 0.1 \tag{4.54}$$

And the relative displacement constraint is

$$\hat{u}_d = \left(\frac{1}{2\zeta_d}\right)\hat{u} \tag{4.55}$$

Combining Equation 4.48 and Equation 4.49 and setting $\zeta = 0$, then

$$\frac{\overline{m}}{2}\sqrt{1+\left(\frac{\hat{u}_d}{u}\right)^2} = 0.1 \tag{4.56}$$

$\hat{u}_d$ is usually taken as an order of magnitude greater than $\hat{u}$, so Equation 4.50 becomes;

$$\frac{\overline{m}}{2}\left(\frac{\hat{u}_d}{u}\right) \approx 0.1 \tag{4.57}$$

The generalized form of Equation 4.51 is;

$$\frac{\overline{m}}{2} = 2\zeta_e\left(\frac{1}{\hat{u}_d/\hat{u}}\right) \tag{4.58}$$

Finally taking $\hat{u}_d = 10\hat{u}$, gives an estimate for $\overline{m}$:

$$\overline{m} = \frac{2(0.1)}{10} = 0.02 \tag{4.59}$$

This value is typical for $\overline{m}$. The other parameters are

$$\zeta_d = \frac{1}{2}\left(\frac{\hat{u}}{\hat{u}_d}\right) = 0.05 \tag{4.60}$$

$$k_d = \overline{m}k = 0.02k \tag{4.61}$$

This illustrates the contribution of the TMD. For only an additional 2% of the primary mass, the effective damping ratio goes from 0 to 10%. The example is useful for determining the ratio of the two masses that constitute a TMD, and demonstrates the influence of a small mass to the damping of a much larger mass.

For a 2DOF system with no damping on the main mass and damping on the second (smaller) vibrating mass, the solution is written in a form using dimensionless displacement to give Equation 4.62 (Den Hartog 1956);

$$\frac{x}{x_{st}} = \sqrt{\frac{\left(2\frac{c}{c_c}g\right)^2 + \left(g^2 - f^2\right)^2}{\left(2\frac{c}{c_c}g\right)^2\left(g^2 - 1 + \mu g^2\right)^2 + \left[\mu . f^2 g^2 - \left(g^2 - 1\right)\left(g^2 - f^2\right)\right]^2}} \tag{4.62}$$

Equation 4.62 is plotted in Figure 4.21 and shows the effect of changes in damping ratio for a mass ratio of 20 (μ = 1/20), where;

- $g = \Omega/\omega_n$ the forced frequency ratio
- $f = \omega_a/\omega_n$ the frequency ratio (natural frequencies)

- μ = m/M mass ratio
- x = displacement, x_{st} = static displacement
- c = damping, c_c = critical damping

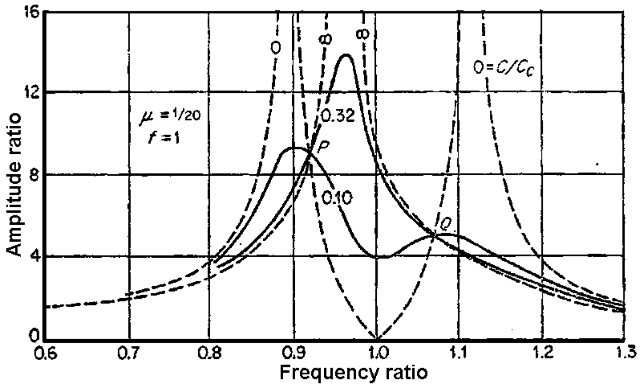

Figure 4.21. A 2DOF or a tuned mass damper, no damping on main mass (Den Hartog 1956).

Equation 4.62 describes a two degree-of-freedom (2DOF) system and demonstrates the effect of mass damping where a small dynamic mass attached to a main oscillating mass can have a significant effect on the overall damping. When more dynamically attached masses are considered the equations become even more complex and the concept can be extended to develop a model with many dynamic masses that constitute very complex MDOF systems (Abe and Fujino 1994). When applying such a MDOF model to trees, the main oscillating mass represents the trunk and the smaller attached oscillating models represent the branches whose damped oscillations produce a complex mass damping effect.

Chapter 5. RESULTS

The results from a range of open grown trees selected in this study are presented in this chapter. The trees are considered from a structural perspective and were selected according to the amount of branching within the structure. Tree structures vary from the simplest with no branches (palm, *Washingtonia robusta*), to more complex trees that have a central trunk and many side branches (Hoop pine, *Araucaria cunninghamii*), to the most complex tree structures where the tree mass is predominately in the branches and there is little or no central trunk (Red gum, *Eucalyptus tereticornis*).

This range of structural configurations is chosen in order to examine the differences in the dynamic response of the tree to wind excitation and in particular to investigate the dynamic effect of branches. Details of the trees and monitoring periods are shown in Table 5.1 and images of tree structural shapes are illustrated in Figure 5.1.

Tree No.	**Common Name**	**Botanical Name**	**Location**	**Height *h (m)***	**DBH *m***	***h/dbh Taper***	**Dates**
0	Sydney Blue Gum	*Eucalyptus saligna*	Burnley	4.8 m *(length)*	.290	16.6	15SEP-18OCT04
1	Hoop pine 1	*Araucaria cunninghamii*	Burnley	22.0	.796	28	7FEB-13FEB05
2	Hoop pine 2	*Araucaria cunninghamii*	Burnley	19.0	.939	20	8DEC-15DEC04 11JAN-7FEB05
3	Hoop pine 3	*Araucaria cunninghamii*	Burnley	23.5	.875	27	16DEC-23DEC04 2-3MAR09
4	Italian Cypress	*Cupressus sempervirens*	Burnley	17.0	.232	73	13FEB-18FEB05
5	Mountain Ash	*E. regnans*	Erica Tree pull/release				1APR05
6	Flooded gum	*E. grandis*	Burnley	19.3	.522	37	28APR05
7	Palm	*Washingtonia robusta*	Burnley	18.1	.436	41.5	25-26NOV05
8	Red gum1	*E. tereticornis*	Sale	14.0	.843	17	28NOV-3DEC05 12DEC05-7JAN06
9	Red gum2	*E. tereticornis*	Sale	14.0	.886	15	3DEC-12DEC05
10	NZ Kauri pine	*Agathis australis*	Sale	23.2	.75	31	17JAN-14MAR06
11	Elm Branch pluck	*Ulmus procera*	Burnley				18APR2007
12	Mountain Ash	*E. regnans*	Mt Dandenong	50	2.61	19.2	JUL07
13	Spotted Gum	*Corymbia maculata*	Monash University	25	0.716	34.9	14FEB08-3APR08
14	She Oak	*Allocasuarina fraseriana*	Melbourne University	23	0.440	52.3	24, 30APR08

Table 5.1. Details of trees in this study, including location, physical details and monitoring periods.

The simplest structure is the palm (*Washingtonia robusta),* designated tree #7 which has no branches and approximates a pole (Figure 5.1a). Under wind excitation its dynamic response is expected to be beam-like with distinct modes separated in frequency but dominated by the first mode.

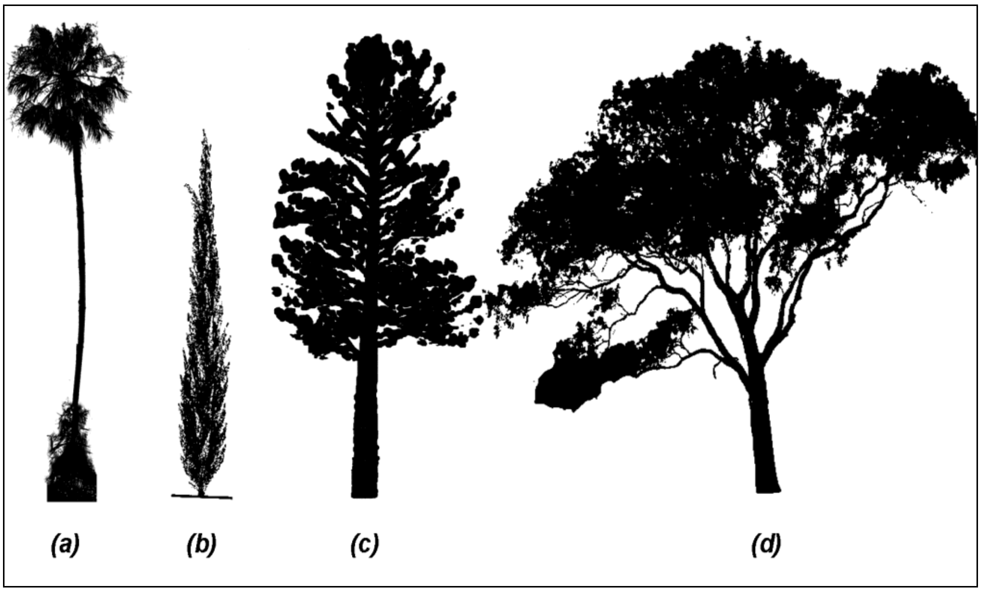

Figure 5.1. Tree selected for this study seen from a structural perspective, based on complexity of branching; (a) a tree structure with no branches, palm (*Washingtonia robusta*) (b) upright slender tree, with branches close to the trunk, Italian cypress, *(Cupressus sempervirens*) (c) a tree with a main central trunk and side branches, hoop pine (*Araucaria cunninghamii*) and (d) a tree with a complex branching structure and relatively small trunk mass, Red gum (*Eucalyptus tereticornis*).

The next level of structural complexity is represented by tree #4, Italian Cypress (*Cupressus sempervirens*) which is a tall slender tree, whose branches are closely aligned to the trunk (Figure 5.1b).

Several trees represent the next level of complexity in which the tree structure consists of a central trunk with many side branches attached to it (Figure 5.1c). Trees of this structural shape are typically conifers and pines (gymnosperms) and the selected trees were tree#1, #2, #3, hoop pine *(Araucaria cunninghamii)* and tree#10, NZ Kauri pine *(Agathis australis).*

The most complex structural configuration in trees occurs when most of the mass is located in the branches and there is a relatively small amount of mass in the trunk (Figure 5.1d). These are typically flowering trees (angiosperms) and are represented in this study by tree #5, #12, mountain ash, (*Eucalyptus regnans)* , tree #6, Flooded gum, (*E. grandis)* , tree#8, #9, Forest Red gum, *(E. tereticornis*), tree #13, Spotted Gum (*Corymbia maculata*), tree #14, She oak *(Allocasuarina fraseriana).*

5.1 Static Tests

The static pull test described in Chapter 4 was performed on trees in order to calibrate the strain meters that were installed on the trunk. Some trees were located near buildings or in positions that were unsuitable for attaching a rope so not all trees were statically tested.

The static pull test was conducted by applying a controlled force on the attached rope and monitoring the tree bending response. To ensure the integrity of the tree was not compromised, at the first sign of any distress in the tree, the root plate or the testing equipment, the test was stopped. Structural weakness may be present in the trunk due to decay or insect attack, or in the root plate due to damage below ground and because this damage may not be visible, it is important to monitor the loads and observe when unusual changes occur which may indicate weakness and potential failure.

The pull was applied with a rope and winch system, and the pulling force was monitored with a digital load cell. An angle sensor was attached to the base of the tree to check that there was no root plate rotation or movement below ground during the test. The strain meter output data were recorded at 20 Hz to a computer and the base bending moment was calculated by measuring the pull (kN), the angle of the rope (θ) and the height of attachment of the rope.

The strain data were plotted against base bending moment and several graphs from different tree pull tests are presented in Figure 5.2. A linear relationship between the moment and the strain reading indicates linear elastic behaviour. If the curve begins to deviate from the linear gradient, some structural yielding or failure is likely to have occurred so the test was stopped. In all static pull tests conducted in this study, the forces remained within the linear elastic range which was used as a guide to verify that the test remained within some limits of safety.

An example of the results from a static pull test on Tree#3 (*Araucaria cunninghamii)* is shown in Figure 5.2a. The pull data are plotted and the line of best fit gives a calibration factor of 0.5722. This can be interpreted as one micron movement of the strain meter equates to 0.5722 kN m of bending moment at the base of the tree. Using this calibration factor, strain data from this tree, gained during wind storms can be converted to wind loads which are then expressed as base bending moments with units of kilonewton meters (kN m).

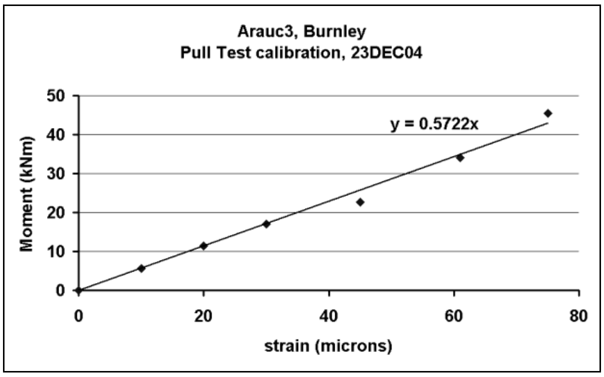

(a)Tree#3, Hoop pine (Araucaria cunninghamii)

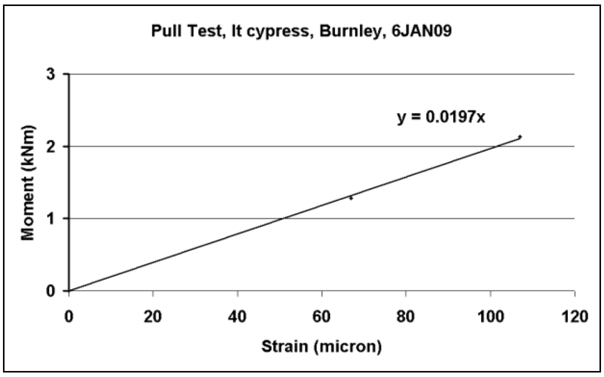

(b) Tree#4, Italian cypress (Cupressus sempervirens)

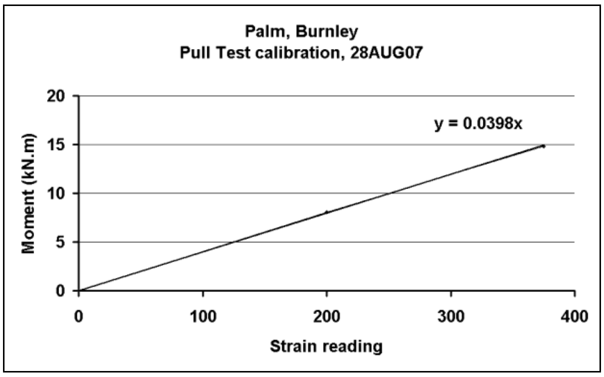

(c) Tree#7, palm (Washingtonia robusta)

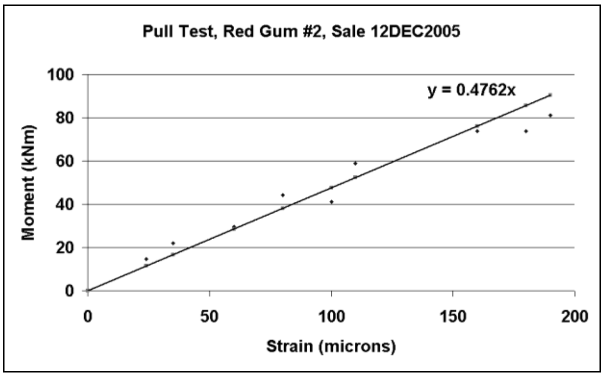

(d) Tree#9, Forest red gum (Eucalyptus tereticornis)

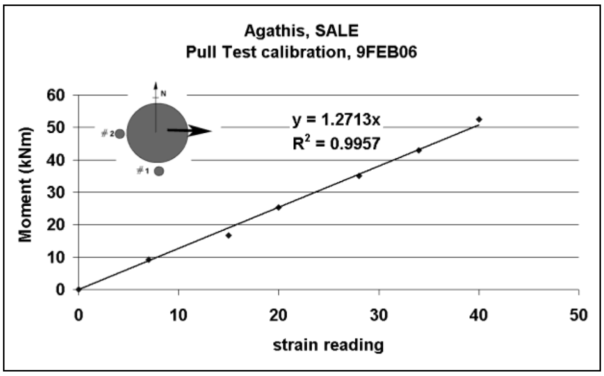

(e) Tree#10, NZ Kauri pine (Agathis australis)

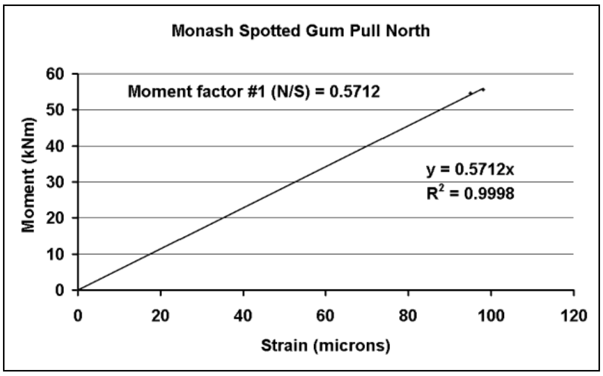

(f)Tree#13, Spotted gum (Corymbia maculata) pull North

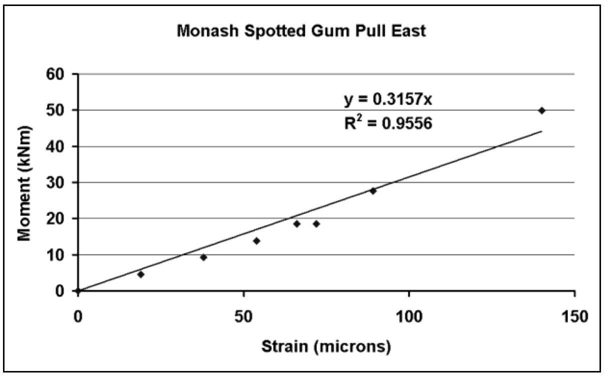

(g) Tree#13, Spotted gum (Corymbia maculata) pull East

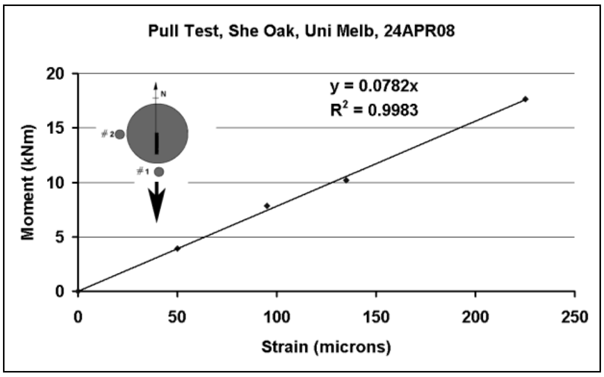

(h) Tree#14, She Oak(Allocasuarina fraseriana)

Figure 5.2 Results from static pull test for selected trees. Not all trees could be tested. Grey circle indicates tree and instrument orientation and direction of pull.

The static pull test results can be used to estimate the Young's modulus for the trunk section at the point where the instruments were attached. An example of estimating Young's modulus from a static tree pull test is described for Tree#3, Hoop Pine (*Araucaria cunninghamii*). The trunk diameter at the section where the instruments were located was near uniform at 780 mm. The rope was attached at 12.34 m above ground and a series of pulls up to 400 kg were applied with the rope which was at an angle of 20° to the horizontal.

A sample calculation is presented for a pull of 400 kg and the corresponding strain reading of 75 microns (Zero reading 6.295 – reading at 400 kg pull 6.220 = 0.075). Since the strain meter is 500 mm long, the strain can be calculated as;

Strain (ε) = 75 x 2 x 10^{-6} = 150 x 10^{-6} or 150 $\mu\varepsilon$.

Pull = F x cos 20° = 400 x 9.8 x 0.9396 = 3684 N

Moment = Pull x height = 3684 x 12.34 = 45460 Nm = 45.46 kN m

Moment of Inertia of cross section (I) = π x $(0.39)^4/4$ = 0.018169 m^4

Stress (σ) = My/I = 45460 x 0.39 / (0.018169) = 976288 N m^{-2}
= 0.98 N mm^{-2}

Young's modulus (E) = σ/ε = 0.98/(150 x 10^{-6}) = 6504 N mm^{-2}

Final E value = 6504 N mm^{-2} or (6504 MPa)

Note: The vertical component of pull (F.sin 20° = 1340 N) contributes a stress of 2800 N m^{-2} which is 0.3% of the bending stress. This results in less than 1 micron of strain which is less than the resolution of the instrument so the vertical component is ignored in this case. The above calculations were repeated for each strain meter output at different values of pull and recorded to a file as shown in Table 5.2.

Tree Pull test data 23DEC04						
Strain instrument Zero (mm)	**Tree**	**Distance (m)**	**Pull Angle**	**Depth (mm)**	**Width (mm)**	**Mom Inertia mm^4**
6.295	3	12.34	20	780	780	18169723125
Strain Reading (mm)	**Pull (kg)**	**Moment (kN m)**	**Stress (N mm-^{2})**	**Strain**	**YMod (E) (N . mm^{-2})**	**MomFactor**
6.295	0	0	0	0	-	-
6.285	50	5.682	0.12	0.000020	6098	0.5682
6.275	100	11.364	0.24	0.000040	6098	0.5682
6.265	150	17.046	0.37	0.000060	6098	0.5682
6.250	200	22.728	0.49	0.000090	5420	0.5051
6.234	300	34.092	0.73	0.000122	5998	0.5589
6.220	400	45.456	0.98	0.000150	6504	0.6061

Table 5.2. Results from a tree pull test 23/12/2004, for Tree#3, Hoop Pine (*Araucaria cunninghamii*) and calculated Young's modulus value.

When a static pull test could be performed on a tree, the value for Young's modulus was calculated using the above method and results are presented in Table 5.3

				Pull Test		
Tree No.	**Common Name**	**Botanical Name**	**Location**	**Dates**	**Moment Factor**	**Young's Modulus Nmm^{-2} (MPa)**
0	Sydney Blue Gum	*E. saligna*	Burnley	17AUG04	11.338 Nm	2350
3	Hoop pine 3	*Araucaria cunninghamii*	Burnley	23DEC04	0.5722 kNm	6040
4	Italian Cypress	*Cupressus sempervirens*	Burnley With wind data	6JAN09	0.0197 kNm	8100
7	Palm	*Washingtonia robusta*	Burnley	28AUG07	0.0398 kNm	2450
8	Red gum1	*E. tereticornis*	Sale Pruned 22/12/2005	*15MAR06*	0.6242 kNm	5330
9	Red gum2	*E. tereticornis*	Sale	*12DEC05*	0.4762 kNm	3560
10	NZ Kauri pine	*Agathis australis*	Sale	*9FEB06*	1.1270 kNm	9160
13	Spotted Gum	*Corymbia maculata*	Monash Uni	24FEB08 N/S E/W	0.5712 kNm 0.3157 kNm	8100
14	SheOak	*Allocasuarina fraseriana*	Melb Uni	24APR08	0.0782 kNm	4680

Table 5.3 Results from static pull test for selected trees including calibration factor (moment factor) and Young's modulus values.

The value for Young's modulus found from these tests is similar to previously published data such as (Niklas 1992, Brudi 2002, ASTM D2555, USDA 2001).

5.2 Field Measurements of Wind Loads on Trees

5.2.1 Time series results

Data from strain instruments of base bending moments and wind speeds were collected on a range of open grown trees. Monitoring of each tree usually continued over several months so that periods of high wind speeds could be captured. An example of data from the strain instruments for tree#3 Hoop Pine (*Araucaria cunninghamii)* during a wind event is presented in Figure 5.3 which shows a time series plot of the strain output (microns) over a 1500 s interval with the corresponding wind data (m s^{-1}). This is considered to be representative of time series data from all trees in this study. The data were recorded at 20 Hz which was sufficient to capture a smooth time series record of the dynamic variations of tree response. Wind data were recorded at 1 Hz as this was the minimum response time of the anemometer. It is evident that the variation of the wind velocity due to gusting caused a tree response that was not constant and varied from one gust to another. The wind over this period had an average velocity of 4.8 m s^{-1} and a maximum gust of 14 m s^{-1}. The tree response as measured by the strain instruments, to wind excitation is correspondingly variable with an average value of 128 microns and a peak of 420 microns.

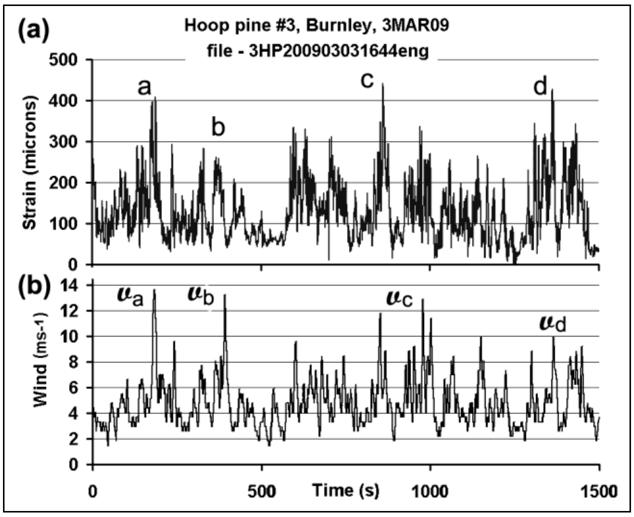

Figure 5.3. Time series plot of data from Hoop pine (*Araucaria cunninghamii* – tree#3) over 1500 s period, on 3 March 2009, showing (a) instrument strain data (tree response) and (b) wind velocity (input excitation).

The relationship between input wind velocity and resulting tree response is complex. This is shown by observing that several similar wind gusts indicated as $\boldsymbol{\upsilon}_a$,$\boldsymbol{\upsilon}_b$,and $\boldsymbol{\upsilon}_c$ (Figure 5.3b) do not consistently create the same tree response shown in Figure 5.3a as *a*, *b* and *c*. There is also a peak tree response shown as *d*, which occurs at a low value of wind velocity, $\boldsymbol{\upsilon}_d$. There appears to be no direct temporal relationship between wind velocity and a tree's response. The complex interaction between the wind and the tree is due to (a) the dynamic nature of the tree response and (b) a lag or phase difference between the input excitation and the dynamic oscillations of the tree and (c) the complex dynamic interaction of the individual branches which collectively act to produce the overall tree response to wind excitation.

In order to examine this relationship more closely, the data of wind speed and strain response shown in Figure 5.3 are plotted against each other for a full 30 minute period (Figure 5.4). The resulting graph of instantaneous data is not linear and the maximum value of strain does not occur at the highest wind speed as may be expected. The peak strain occurs at wind velocity below the maximum value and the data appear to flatten out rather than follow the linear or squared relationship that is expected. This indicates that the instantaneous data needs to be considered more closely and that there is not a direct linear relationship between the two parameters of wind velocity and bending strain response. This may be due to a short time delay which occurs between the wind speed measurement of the anemometer and the strain meter measurement on the tree. The instantaneous data were recorded in 1 second intervals for wind speed and at 0.05s intervals (20 Hz) for the tree response. This effect is discussed more closely later in this chapter and different time averaging intervals are used to refine this analysis.

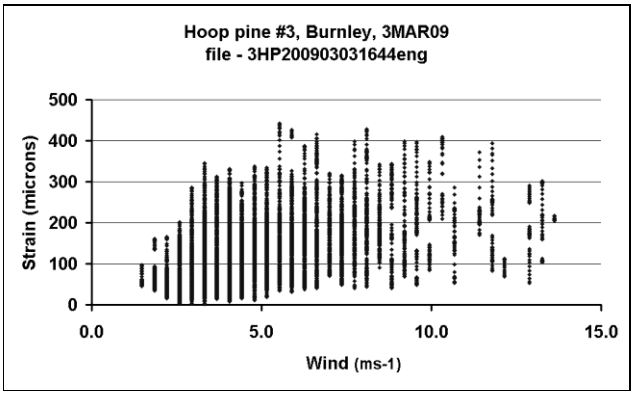

Figure 5.4 Relationship between wind velocity and strain (tree response).

The variation in tree response may be explained in part by considering the dynamic interaction of the branches that collectively make up the overall response. Some branches may be in phase with the wind gust which results in a large sway response. Some branches may be out of phase with the wind gust which would result in a reduced sway response. The inertial forces of a branch swaying back in the opposite direction to the wind would absorb some energy. In this case, some of the energy from the wind would stop the branch and some would cause it to sway, albeit with a reduced amplitude.

5.2.2 Along wind, across wind and resultant response

Wind varies in both speed and direction so that the tree response also varies in magnitude and direction. The total instantaneous response of the tree is the sum of the response data from each instrument. By plotting a graph with one instrument output along the X axis and the other along the Y axis the total tree response can be represented graphically. For convenience, the X axis is chosen as the East/West axis and the Y axis is chosen as the North/South Axis. This configuration reflects the orientation of the sensors on the tree and places the north direction at the top of the page. The total response of the tree in all directions can be plotted (Figure 5.5) which shows the complex looping response of the tree due to a wind event coming from a northerly direction. Figure 5.5 represents a 30 minute time series plot of data from both instruments (in units of microns) for tree #3, Hoop pine on 3 March 2009. Instrument #1 is located on the south side of the tree to record movement in the North/South direction which is plotted on the Y axis. Instrument #2 is located on the east side of the tree and records East/West response that is plotted on the X axis. The zero point where the axes cross represents the point where the tree is at rest and no wind is blowing. The magnitude indicates the direction with north +ve and south -ve. For this wind event the wind blew from a Northerly direction (9° east of north).

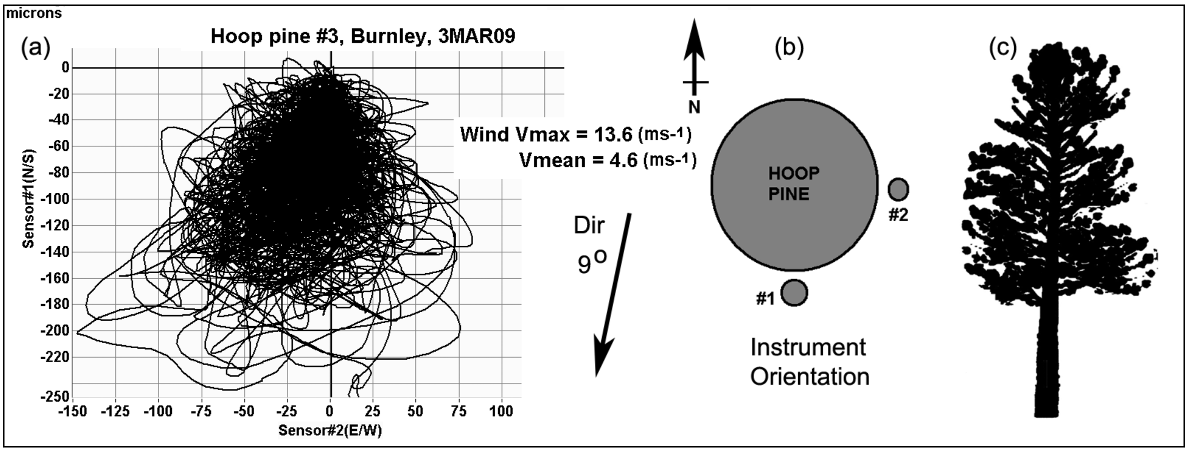

Figure 5.5. Example of a time series graph of strain data from two instruments plotted together for tree #3, a Hoop pine (*Araucaria cunninghamii*). (a) 30 minute period showing sway motion in two directions and wind details, (b)orientation of instruments on tree trunk, and (c) image of Hoop pine.

The tree response viewed this way has been reported previously by Gardiner (1995) who described it as a “Bird’s eye view” which can be interpreted as looking down the tree and observing the movement of the topmost point of the tree in space. This is a useful way to visualize the significance of the graph and would be true for a tree with a central trunk or a palm with no side branches, but would not be true for a multi-limbed tree. This style of plot is used for all trees, and represents forces in the trunk of the tree which pass from the canopy down through the trunk to the roots so can be taken as a force diagram on the root plate of a tree.

Wind in general does not blow from any one direction so there is a need to standardize the tree response data relative to the wind direction. This is done by resolving the instrument output into along wind and across wind components as in the wind code AS1170 part 2 (2002). The strain data are converted to engineering units of bending moment (kNm) by multiplying the strain data and the moment factor found during the static tree pull test (Refer Table 5.1). The along wind and across wind components of base bending moments (kNm) are plotted in Figure 5.6 with the X axis representing the along wind direction and the Y axis representing the across wind direction. The along wind direction is established by taking the average of the across wind component as zero.

Two different time series plots of 30 minutes data is shown (Figure 5.6) for the Hoop pine (*Araucaria cunninghamii* - Tree #3 in this study) for similar wind conditions when V_{mean} = 4.8 m s^{-1}, V_{max} = 13.6 m s^{-1}. During the first period (Figure 5.6a) the maximum bending moment response in the along wind direction was 252 kNm and in the second period (Figure 5.6b) the maximum bending moment response in the along wind direction was 197 kNm.

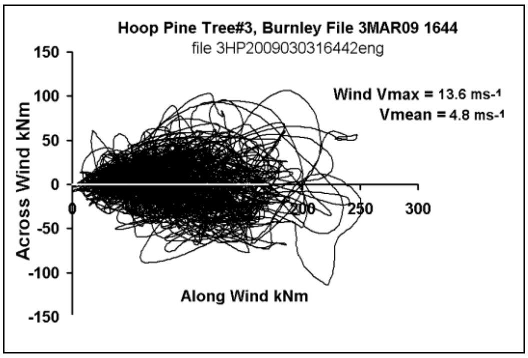

(a)

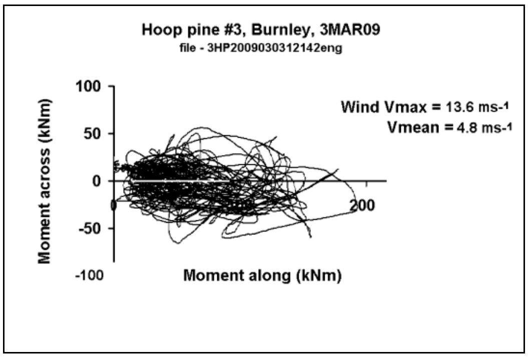

(b)

Figure 5.6. Time series plot of 30 minutes data on Hoop pine (*Araucaria cunninghamii* Tree #2) resolved into along wind and across wind components of bending moments (kNm). (a) Data as for Figure 5.5, maximum bending moment along wind is 252 kNm and (b) data from similar wind event showing different response.

This represents a 20% reduction during a period in which the wind has similar values of velocity and illustrates that similar wind events, as measured by average values of velocity over 30 minutes and maximum values for peak gusts do not produce the same tree response. The graph of 30 minutes of data crosses over itself many times and the individual responses are difficult to see. To illustrate the tree motion more clearly, data from another wind event on 19 December 2004 for the hoop pine is plotted (Figure 5.7) and shows two different responses to wind gusts. During a 150 second period (3000 data points at 20 Hz) several significant gusts of wind blew on the tree. In the first gust the tree response shows a circular looping motion with significant across wind bending moments. During this response the along wind bending moment reached 100 kNm and the across wind component varied from 60 on one side to 37 kNm on the other side. Shortly after another gust blew on the tree but the response was very different. Sway motion is seen to be almost completely in the along wind direction with little across wind components. The maximum along wind moment is 167 kNm. Wind data was not recorded for this event due to equipment malfunction.

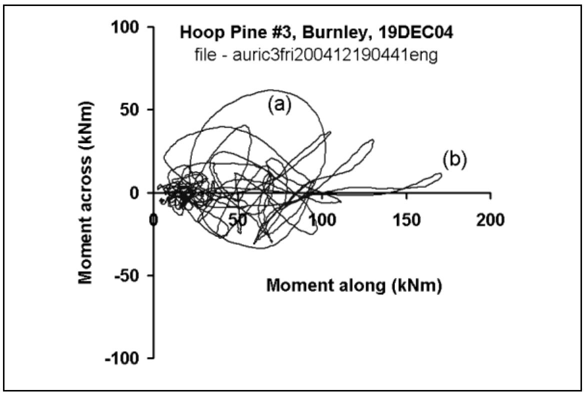

Figure5.7. Hoop pine (*Araucaria cunninghamii*) bending response to two different wind gusts on 19 December 2004, (time 0441 hrs) showing (a) a circular looping response with significant across wind component of bending, and (b) an along wind bending response with almost no across wind component.

The response of each tree in this study, to wind excitation over a 30 minute period is shown in Figure 5.8. A representative file is chosen for each of the trees and resolved into along and across wind components of base bending moment. It is apparent that all the trees except for the palm tree, sway in a downwind direction from the rest position and at no point do they sway back towards the wind. In light winds there may be some small sway back towards the direction of the wind but during periods of high wind, the tree sways only in a downwind direction.

The sway motion of the palm is different from all the other trees and it is evident that there is considerable sway response motion along and across the direction of the wind and also back towards the wind (Figure 5.8, vi). This occurs due to the sway motion of the palm which is a circular looping pattern rather than a simple backwards and forwards motion. The palm has no branches and the single flexible trunk with the attached leaves sway in an almost circular pattern in response to wind gusts.

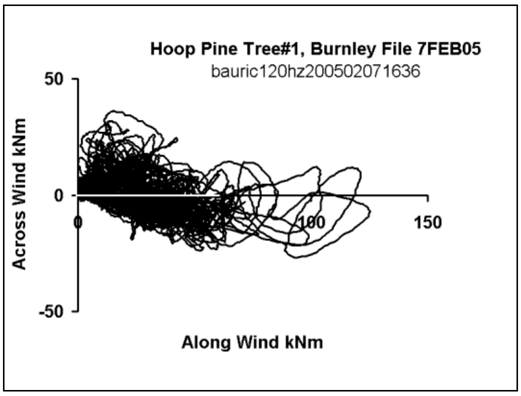

(i) *Tree #1 Hoop pine (Araucaria cunninghamii).*

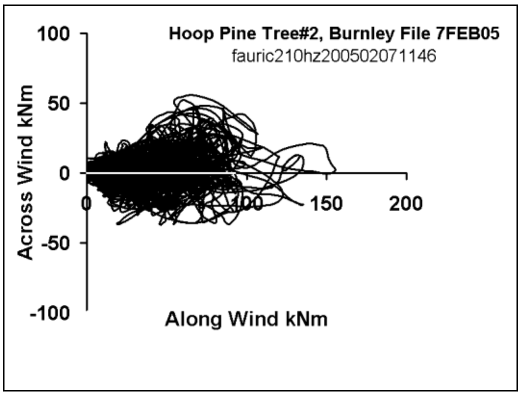

(ii) *Tree #2 Hoop pine (Araucaria cunninghamii).*

Figure 5.8. Graphs of 30 minutes data for selected trees in this study resolved into along and across wind components of bending moment.

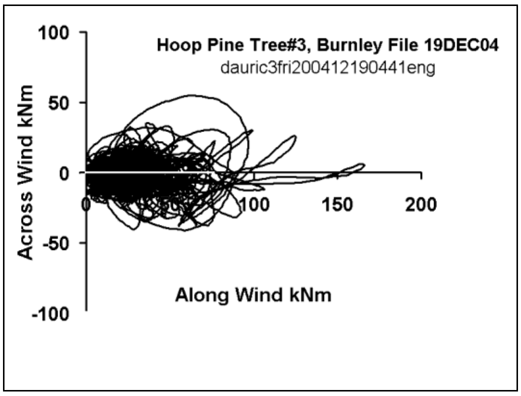

(iii) *Tree #3, Hoop pine (Araucaria cunninghamii).*

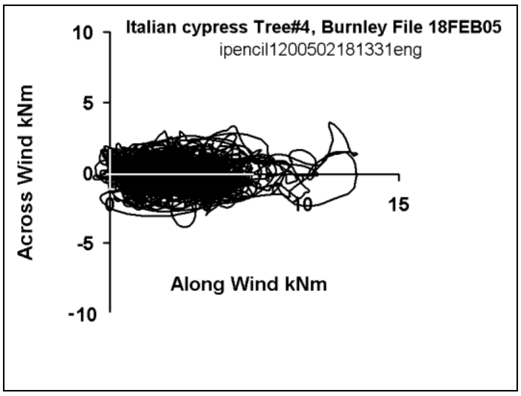

(iv) Tree #4, Italian cypress (Cupressus sempervirens).

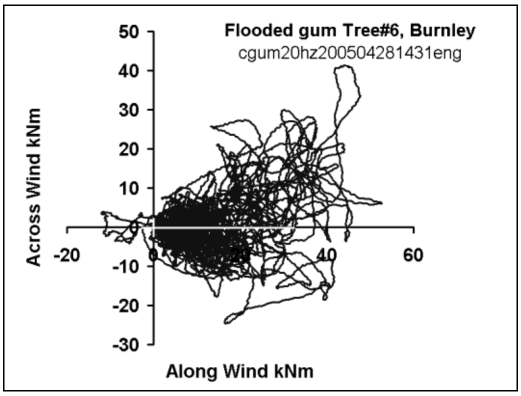

(v) Tree#6, E grandis (E. grandis).

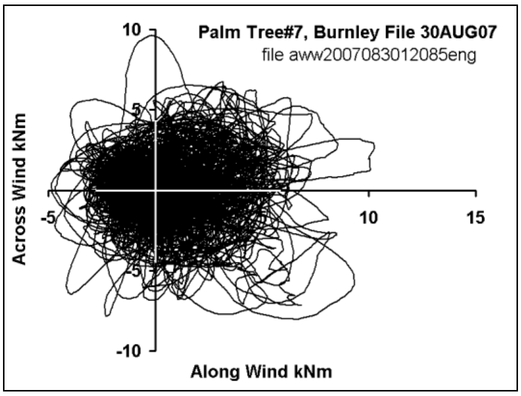

(vi) Tree # 7, Palm tree (Washingtonia robusta).

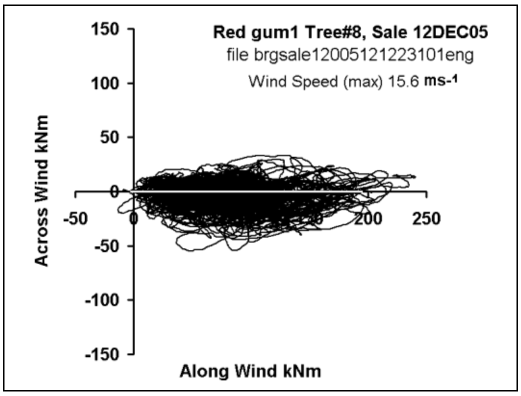

(vii) Tree #8, Red gum 1 (E. tereticornis).

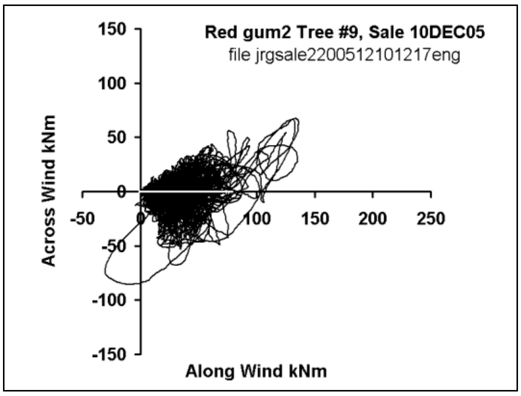

(viii) Tree #9, Red Gum 2 (E. tereticornis).

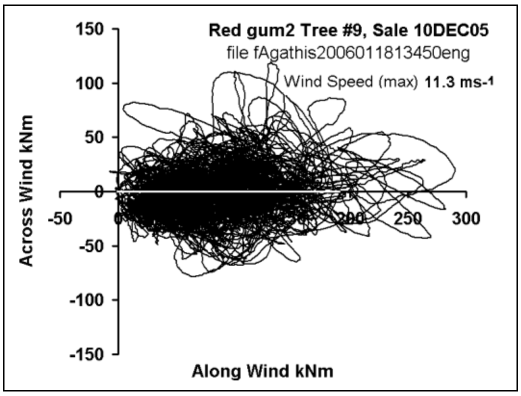

(ix) Tree #10, NZ Kauri (Agathis australis)

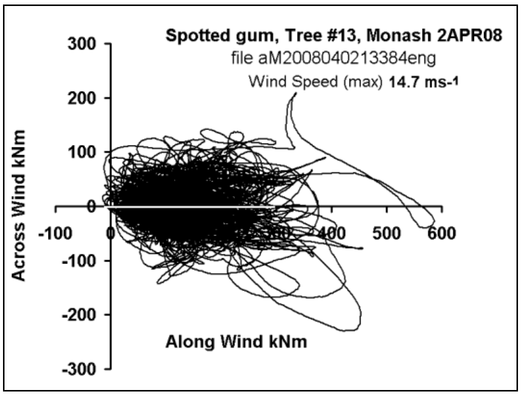

(x) Tree#13, Spotted gum (Corymbia maculata).

Figure 5.8(cont.). Graphs of 30 minutes data for selected trees in this study resolved into along and across wind components of bending moment. Wind data not available for all trees.

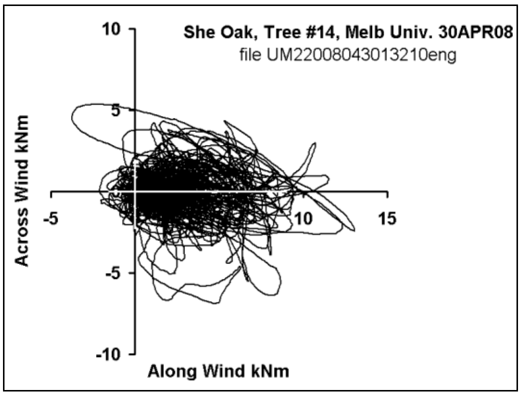

(xi) Tree#14, She Oak (Allocasuarina fraseriana).

Figure 5.8(cont.). Graphs of 30 minutes data for selected trees in this study resolved into along and across wind components of bending moment. Wind data not available for all trees.

The palm looping sway response is further illustrated over a shorter period (300 seconds) to show the sway motion more clearly (Figure 5.9).

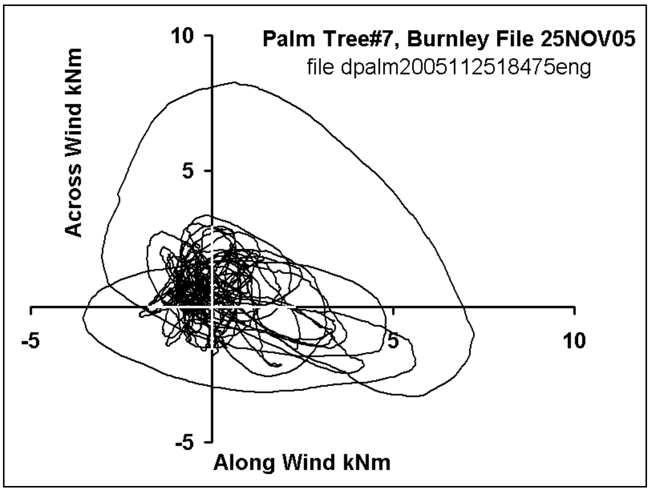

Figure 5.9. Palm (*Washingtonia robusta*) response to wind gusts over a 300 second period to show looping sway motion around the zero position.

The bending moment values are resolved into along wind (X axis) and across wind (Y axis) components. The central sway region in low winds can be seen at the intersection of the axes and the circular response of the palm to several gusts of wind is shown by the large looping path

5.2.3 Branch results

One of the first field tests of the instruments was on a branch of a Sydney Blue gum (*Eucalyptus saligna)*, located at Burnley. This was chosen for convenience as it was close to an office where power and computing facilities were available, and the instruments could be supervised closely during the initial operation. The branch was 2.4

m above the ground and 4.8 m long. The cross section at the point of attachment of the instruments was 290 mm in width and 290 mm in height.

A rope was attached to the outer part of the branch and weights added under controlled conditions to apply a known bending moment. The strain instruments recorded strain and so were calibrated to bending moment as described for the static pull test (Chapter 4). The resulting calibration factor (termed the moment factor) was 11.338 which can be interpreted as 1 micron of strain measured by the instruments is equivalent to 11.338 Nm of bending moment at the base of the branch. The Young's Modulus of the branch (Table 5.3) was calculated using results obtained during the static pull test. A wind event was recorded on 7 October 2004, and a plot of the instrument output is shown in Figure 5.10.

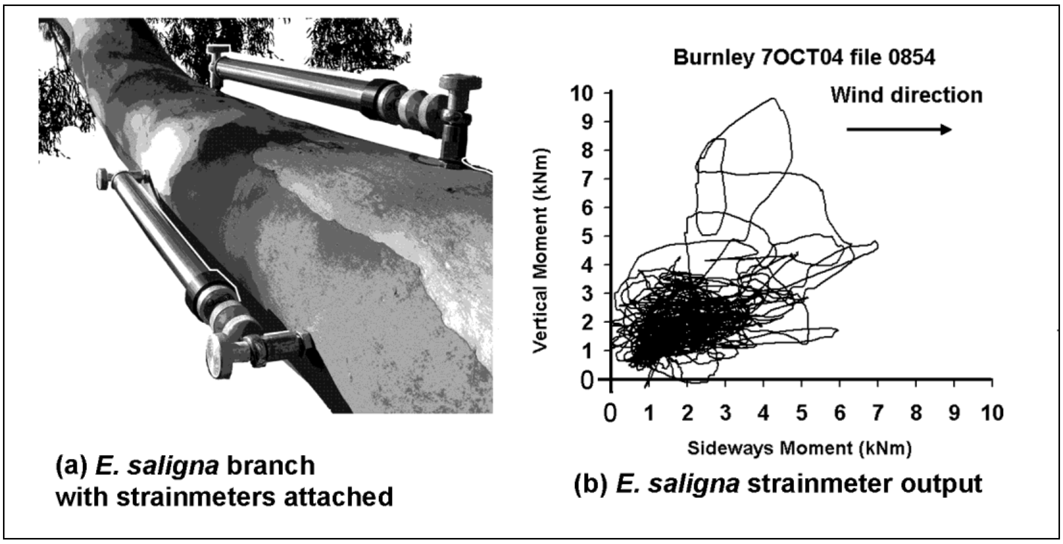

Figure 5.10. (a) instruments attached to a branch of a Sydney blue gum (*Eucalyptus saligna*) and (b) instrument output during wind storm showing side ways and upwards forces on the branch.

The plot of bending moment shows that the wind loads on this branch were sideways and upwards. There were no downward loads during the wind storm event which continued over many hours. The wind approached the branch from the side and the branch was oriented in an upwards direction of approximately 20 degrees.

The lack of any downward load was unexpected so further monitoring was undertaken to confirm that wind from the same direction loaded this branch in a sideways and upwards direction only. While this is not the main focus of the study it is an interesting result which confirmed the operation of the instruments and gave a new insight into branch movement under wind loading. It is also interesting to note that Shigo (1991) suggested that upwards forces on branches are a major contributing factor to many branch failures (Figure 5.11).

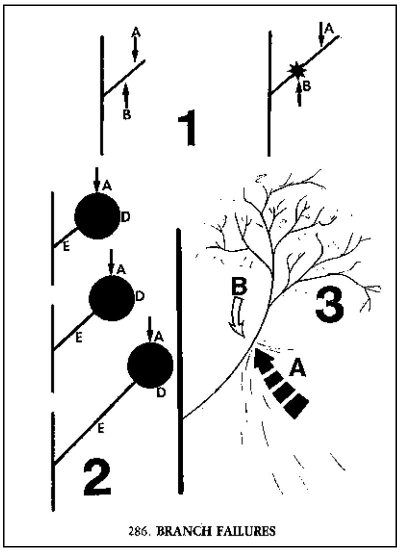

Figure 5.11. Diagram indicating upwards failure on tree branches (Shigo 1991)

Shigo's conclusion was based on careful study of the splinters on the branch portion still on the tree. "If they point upward, the branch fractured from upward loading" (Shigo 1991, p324). The wind loads produced a resulting bending moment at the base of the branch which was measured using the strain instrument data. The data averaged over 3 second intervals are graphed in Figure 5.12.

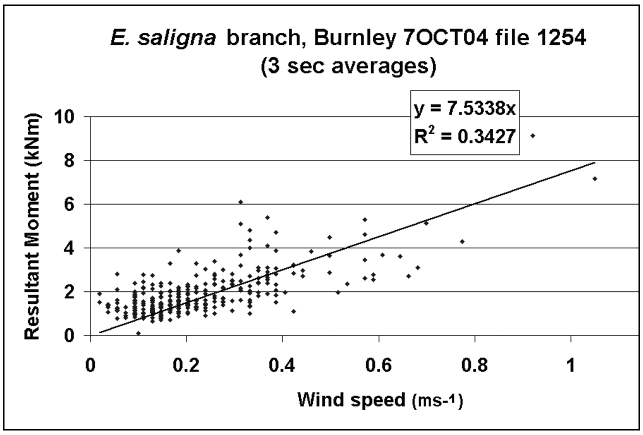

Figure 5.12. Graph of wind speed versus bending moment on a tree branch (*E. saligna*).

There is a spread of data but a clear relationship is evident between wind speed and resultant moment. More data at higher wind speeds are needed to determine how the curve continues and no extrapolation is done here. A straight line fit is made as a first approximation, to give an estimate of the spread of the data.

5.2.4 Wind loads and maximum values

The maximum values of wind load expressed in base bending moments, is of interest in order to compare values to those reported in the literature and to investigate the forces that occur at or near failure. Over the several years of monitoring trees the wind speeds were generally below 20 m s^{-1} and there were few extreme wind events that exceeded this figure. None of the trees in this study failed though on one occasion described below, surrounding trees did fail which indicates that the wind speed did get to critical values.

The maximum recorded bending moment value was 588 kNm on the spotted gum (*Corymbia maculata*) at Monash University during a wind storm in which the maximum gust measurement was recorded at 20 m s^{-1}. The spotted gum had a height of 25 m and DBH of 0.716 m and was located next to a 15 m high building so all the canopy was above the building and exposed to the wind. This value is the highest bending moment recorded on any of the trees studied and is considered to be a very high value. The maximum gust event is presented in Figure 5.13 which shows that the peak bending moment is a transient value corresponding to a wind gust measured at 20 m s^{-1}. The looping motion of the tree during this period is also shown and indicates that the motion is in the along-wind direction, though there is a considerable across wind bending moment of approximately 220 kNm.

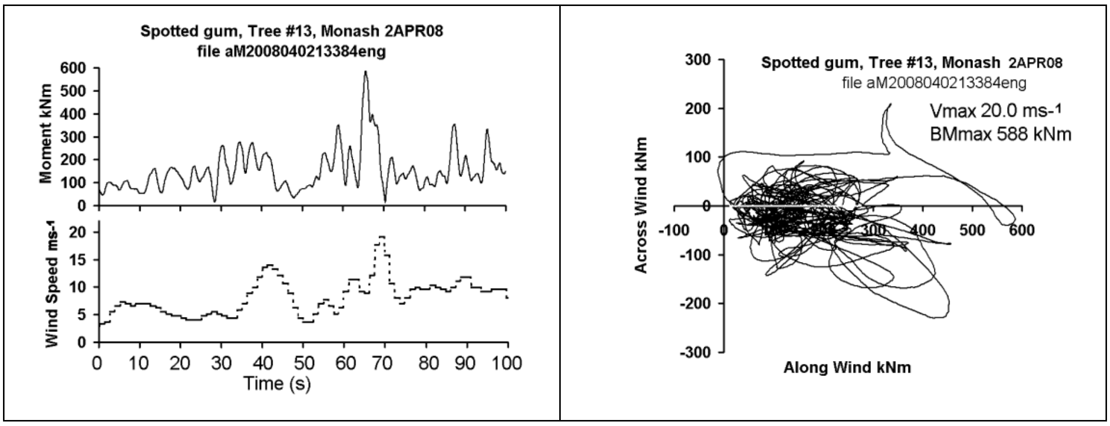

Figure 5.13. Maximum bending moment measurement of 588 kNm during a wind gust of 20 m s^{-1}, on Tree#13 Spotted gum (*Corymbia maculata*), Monash University.

The measured maximum bending moment of 588 kNm for the Spotted gum is useful to compare with values of maximum overturning moments quoted in the scientific literature and to determine the stress in the outer fibres of the tree in order to assess how close they may be to failure stresses. The bending moment values will depend on the wind speed and the tree's physical properties including height, canopy area, trunk size and material properties. Therefore, the maximum bending moment values and any comparisons with other trees need to be treated cautiously.

The bending moment of 588 kNm measured from the spotted gum in winds of 20 ms^{-1}, compares with a calculated bending moment of 1219 kNm (Mattheck and Bethge 2000) who derived their estimate from calculations based on the failure properties of wood for a theoretical tree with a triangular canopy and height of 25 m. The analysis was an estimate aimed at determining the wind load at failure (127 kN) acting at a height (9.6 m) on a theoretical tree with DBH = 0.7m. Although the values of wind force and height were given, the resulting bending moment value of 1219 kNm was not presented in the paper by Mattheck and Bethge (2000). This the highest value for bending moment that could be found in the literature and was a theoretical value with no supporting information to link the wind load to the wind speed. Lundstrom et al. (2007) quote values of 880 kNm for tree failure from pull tests conducted on 39m high spruce trees and Brudi (2002) estimated values of 505 kNm for a 25 m high computer generated tree based on static tree pulling analysis.

The spotted gum located at Monash University did not fail at 588 kNm bending moment so this figure is simply a maximum wind load value that was measured during the monitoring period. It should not be interpreted as a value for tree failure, although during this wind storm several mature trees of similar size in the near vicinity did fail by overturning or breaking which indicates that this was an extreme wind event. The bending moment values measured in this project are useful for comparisons and are amongst the largest measured values for trees under wind conditions that are reported in the literature.

How close to failure was the wood in the trunk of the spotted gum during this wind event when the bending moment was at its maximum? By calculating the stress in the outer fibres of the trunk, the value can be compared with other studies. During the wind event that produced the maximum bending moment (588 kNm), the stress in the outer fibres of the trunk at the point where the instruments were attached was calculated as 16 to 22 MPa. The range is due to taking different cross sections of the tree. A circular cross section is used in one calculation and a non-circular one used for the higher value. The failure stress values from previous studies are 14 MPa Horse chestnut (Brudi 2002), 22.5 MPa Beech (Brudi 2002) and a maximum theoretical value of 39 MPa (Mattheck and Bethge 2000). Depending on the failure value chosen, the spotted gum was loaded to approximately 60-90% of the trunk failure stress. This figure must be treated cautiously as there is no allowance for imperfections in the trunk which would reduce the failure stress, nor any analysis of the root plate and soil load bearing capacity. Table 5.4 gives values of the maximum bending moments and corresponding stresses that were recorded during this project.

Tree No.	Common Name	Botanical Name	Location	Height (m)	Dates	Maximum Bending Moment (kNm)	Max stress (N/mm^2) (MPa)	Wind Speed at max B.M. (ms^{-1})
3	Hoop pine #3	*Araucaria cunninghamii*	Burnley	23.5	14MAR09 File 1854	285	6.9	11.05
4	Italian Cypress	*Cupressus sempervirens*	Burnley With wind data	17	22DEC08, File 1320	19	15.5	16
7	Palm	*Washingtonia robusta*	Burnley	18	31AUG08 File 0807	27	3.3	16
8	Red gum1	*E. tereticornis*	Sale, Vic. Aust. Unpruned	14	21DEC05 File 1451	300	5.1	27
			Pruned 22/12/2005		1JAN06 File 1319	228	3.9	27
9	Red gum2	*E. tereticornis*	Sale	14	12DEC05	134	2.0	22
10	NZ Kauri pine	*Agathis australis*	Sale	23.2	9FEB06	300	7.2	15
13	Spotted Gum	*Corymbia maculata*	Monash Uni	25	24FEB08	588	16-22	20.0

Table 5.4. Base bending moment maxima for trees monitored during this study.

The stress values calculated represent the values experienced by each tree subject to the wind loads during the monitoring period. In general the wind speeds were not high enough to cause large stresses that approached failure. It is interesting to note that other than the spotted gum, the only tree to develop high stress levels was the Italian cypress with values of 15.5 MPa. Further work to collect more data at high wind speeds would be needed to assess the failure stresses in trees but is beyond the scope of this study.

5.2.5 Wind loads and wind speeds (averaging method)

The wind loads on the tree are a function of wind velocity and results from each tree are presented below. Because dynamic data are measured, the relationship between instantaneous bending moment and wind velocity is not as immediately apparent as might be expected. An example of 30 minutes of data from one wind event on a Hoop pine (Tree #3) is shown in Figure 5.14a. The data are spread and do not fit closely to a linear line of best fit (r^2 value = 0.0887). This is due to several factors which include (a) the dynamic nature of the wind and the tree response, (b) a phase relationship in which the wind gust and the tree response may be sometimes in phase and sometime out of phase, and (c) the quality of the data since wind is measured at 1 Hz and tree response is measured at 20 Hz.

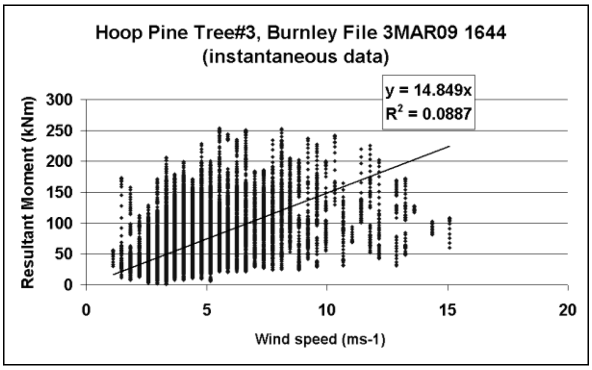

(a) instantaneous data

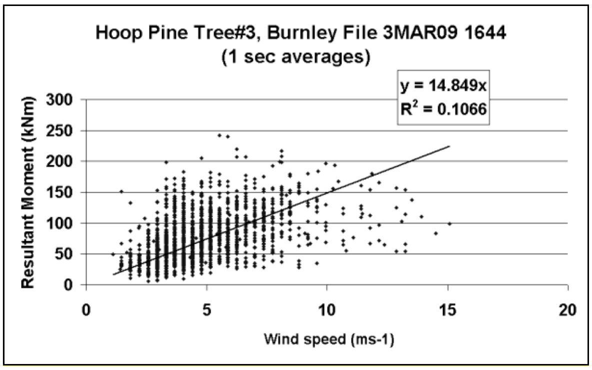

(b) 1 second averages

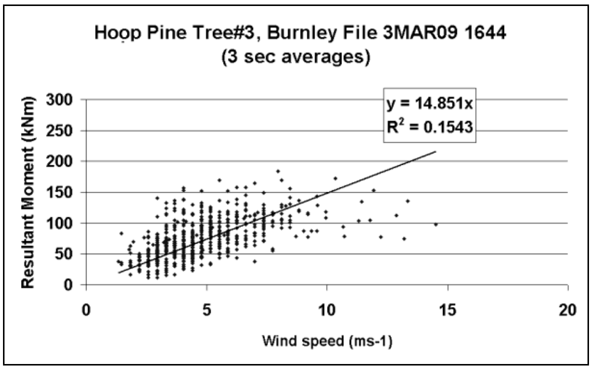

(c) 3 second averages

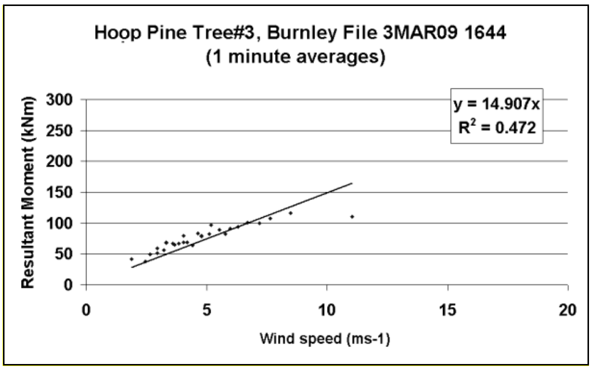

(d) 1 minute averages

Figure 5.14. Wind speed versus wind load data for tree#3, Hoop pine (*Araucaria cunninghamii*), using different averaging periods. 30 minute data presented as, (a) instantaneous data, (b) 1 second averages, (c) 3 second averages, (d) 1 minute averages. Average wind speed 4.8 (m s^{-1}), average resultant moment 76.0 (kNm).

The location of the wind anemometer was always as close as possible to the tree but because the wind direction varied, it was sometimes on the windward side and sometimes on the leeward side. This caused a delay between the wind and the tree response data so the peak wind speed may not match the peak tree response.

The wind speed varies as gusts push on the tree canopy with a range of frequencies. The tree has a natural frequency, as do the individual branches which may be different from the wind frequency of any particular gust. The phase relationship between individual branches, the tree and the wind gusts is important. There are times when a wind gust impacts on the tree canopy in phase with the sway motion so that a large response occurs. At other times the sway motion will be out of phase and coming back towards the wind as the gust impacts, so that the dynamic response will be less at the same wind speed. Because the tree canopy is a collection of branches, there will always be some branches in phase and some out of phase with the impacting wind gusts. The resultant response of the tree, when plotted as instantaneous values of wind speed and bending moment (Figure 5.14a) is not linear but is spread and the maximum wind speed does not correspond to the maximum bending moment. All plots of instantaneous data exhibit this pattern.

The different data rates may be averaged over selected time periods to reduce the spread of data and attempt to represent the relationship more clearly. To examine the effect of different averaging periods, the same 30 minute data from tree#3 is plotted using different averaging periods in Figure 5.14(b), (c) and (d). Using an average period of 1 second, the plot of wind speed versus moment in Figure 5.14(b), shows less spread of data. An average period of 3 seconds is a better approximation of the dynamic response time for the wind anemometer and the plot of wind speed versus moment in Figure 5.14(c) is considered the most realistic plot for the time domain response. A final comparison using 1 minute (60 seconds) averaging period is shown in Figure 5.14(d) and the resulting plot begins to show less spread in the data. The 30 minute averages for these data are wind speed 4.8 (m s^{-1}) and resultant moment 76.0 (kNm).

The time period of 20 seconds for averaging dynamic tree data was considered adequate (Peltola et al. 1993) when studying wind and tree response. If shorter averaging periods were used, such as five or ten second periods, the tree dynamic response became significant which for their quasi-steady state analysis was not considered useful.

Another example of different periods for averaging data is shown for Red gum 2 (*E. tereticornis* tree#9) in Figure 5.15. As the period increases the data have less spread and appears to fit the trend line more closely and at the limit, a 30 minute average gives only one point from 36000 data values. Figure 5.15d was created from 10 periods of 30 minutes or 5 hours of data so has 10 data points. This graph has a linear relationship whose equation approximates those from the shorter averaging periods and suggests that the quasi-static approach gives a good approximation for the tree bending moment response to winds.

The mean values above give a good representation of the relationship between wind speed and the resultant moment at the tree base, but the method restricts the range of wind speeds that can be plotted and does not indicate the magnitude of the maximum values that occurred during the 30 minute period of monitoring.

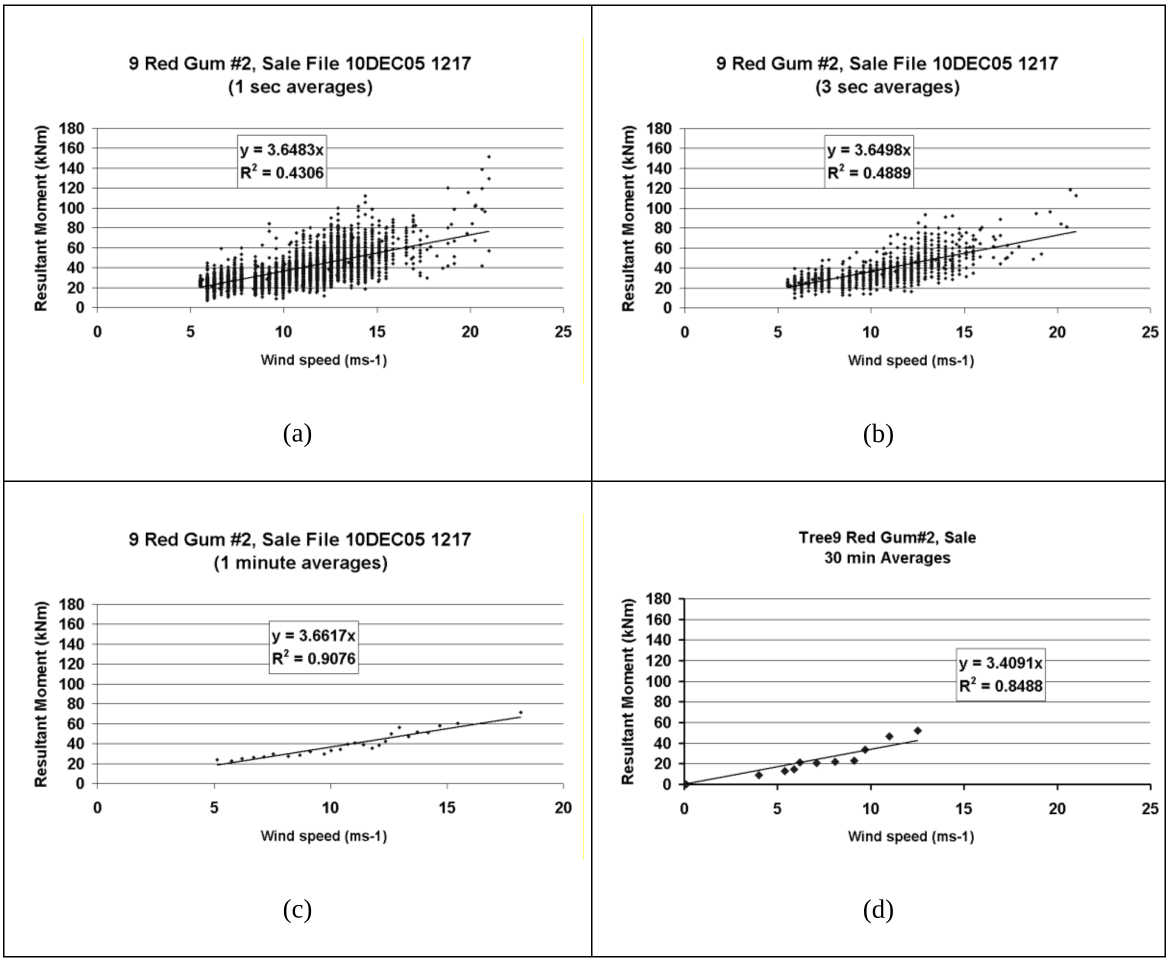

Figure 5.15. Wind speed versus wind load data for Red gum (*E. tereticornis* tree#9), using different averaging periods. 30 minute data presented as, (a) 1 second averages, (b) 3 second averages, (c) 1 minute averages and (d) 10 periods of 30 minute average values showing tree response over a 5 hour period.

The mean values with the line of best fit can be plotted with the maximum values so that the largest range of wind speeds can be presented (Figure 5.16). Bending moments as a function of wind speed are plotted and represent a summary of all the data collected for each tree. The equation to the line of best fit is useful to summarize the data and could be used for design purposes to calculate wind loads on trees. For some trees, wind speed data was not collected so no graph appears for them in Figure 5.16.

Mean and maxima data are identified to observe differences which in some cases are negligible, e.g. tree#3 (Hoop pine), tree#4 (Italian cypress) and tree#13 (Spotted gum). The exponential line of best fit shows the exponent varying from 1.07 for the Italian cypress to 1.8065 for the Spotted gum. This indicates that the wind load is not proportional to $\boldsymbol{V}^2$ for these open grown trees within the range of wind speeds tested. More data at higher wind speeds would be useful to confirm this.

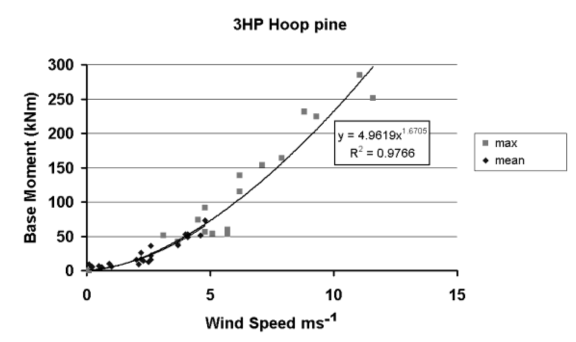

(a) Hoop pine (*Araucaria cunninghamii*)

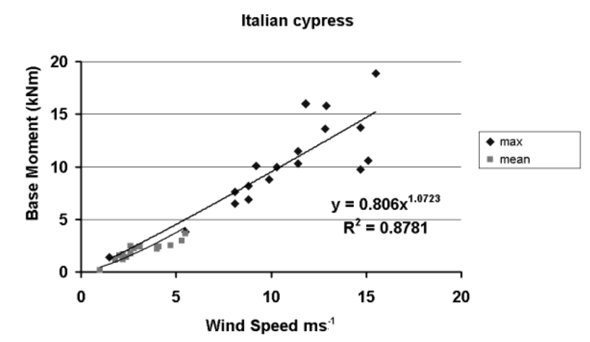

(b) Italian cypress (*Cupressus sempervirens*)

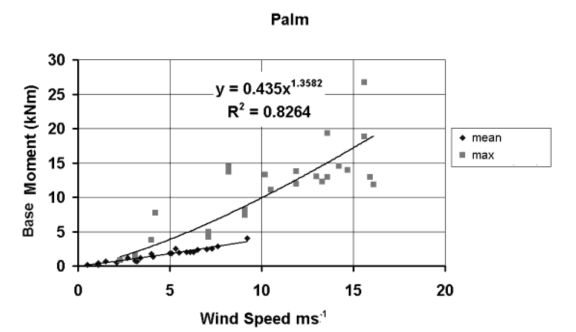

(c) palm (*Washingtonia robusta*)

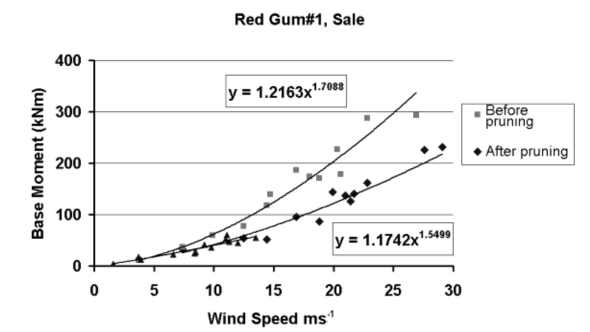

(d) Red gum 1 (*E. tereticornis*)

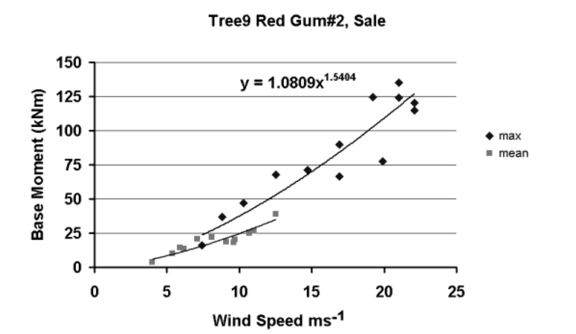

(e) Red gum 2 (*E. tereticornis*)

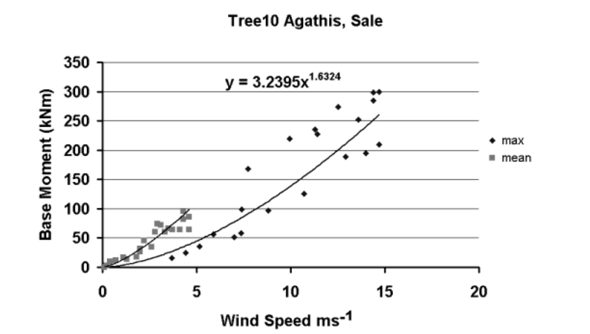

(f) Agathis (*Agathis australis*)

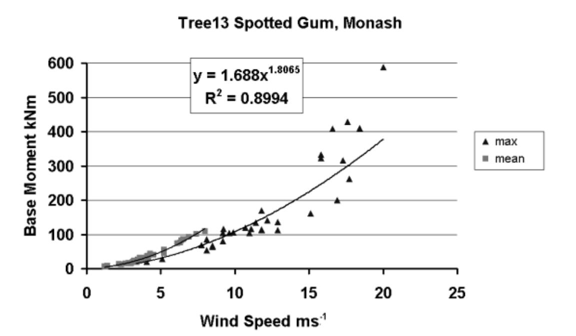

(g) Spotted gum (*Corymbia maculata*)

Figure 5.16. Wind speed versus wind load data for (a) Hoop pine *(Araucaria cunninghamii)*, (b) Italian cypress *(Cupressus sempervirens)*, (c) Palm *(Washingtonia robusta)*, (d) Red gum1 *(E. tereticornis)*, (e) Red gum2 *(E. tereticornis)*, (f) Agathis *(Agathis australis)*, (g) Spotted gum *(Corymbia maculata)*.

A comparative plot for all trees of wind loads versus wind speed (Figure 5.17) is based on the equations from each graph in Figure 5.16.

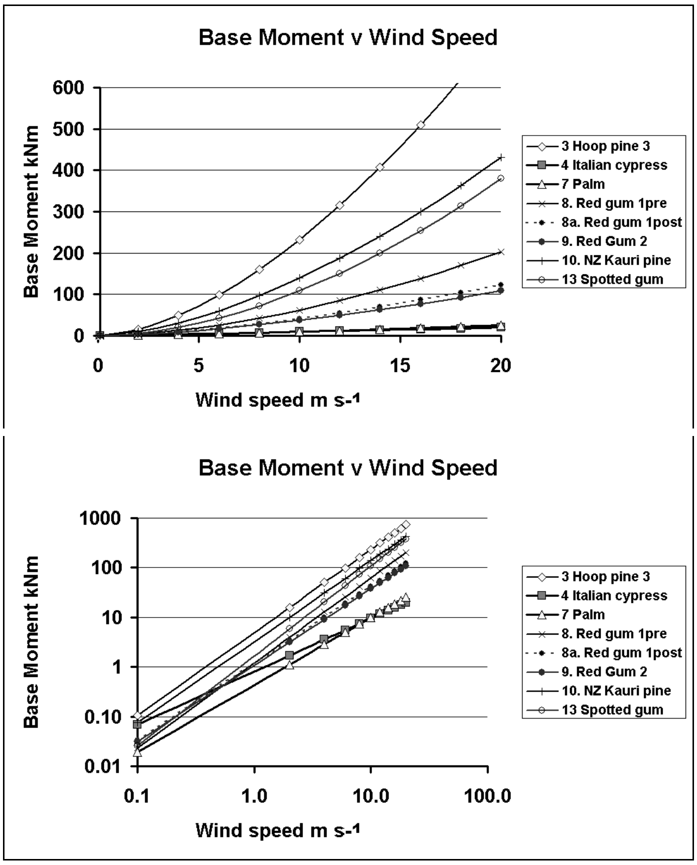

Figure 5.17. Wind speed (ms^{-1}) versus wind load (kNm) for all trees in this study, using linear and logarithmic scales.

Wind loads range from 20 to 600 kNm and the values for the smaller trees are difficult to see in the linear plot (Figure 5.17a). The palm and the Italian cypress have the lowest wind loading as expected due to the small canopy area of the palm and the thin slender canopy of the Italian cypress

Logarithmic scales are used to plot the same data in Figure 5.17b. The exponential curves appear linear in this plot and all trees show a similar gradient except the Italian cypress which has a lower gradient due to the exponent of 1.0723 which indicates that wind load is nearly proportional to velocity for this tree. The Italian cypress is very flexible and bends significantly in the wind which reduces its exposed area. It also has a second mode of sway which is apparent in the spectral analysis described in the next section. No other trees have this second mode of sway which seems to be an adaptation to increase the flexible response of the tree. The manner in which the Italian cypress responds to wind loading, by combining flexibility and the second mode sway, gives an almost linear relationship to wind speed as indicated by the exponent approaching unity. This is not evident in the other trees.

5.3 Dynamic Analysis of Tree Response

5.3.1 Free vibration and the pull/release test

The pull and release test was conducted on several trees in still air conditions in order to establish the dynamic characteristics of the tree, in particular the natural frequency and the damping. In this test, the tree is pulled sideways with a rope, and then suddenly released. Potential energy is stored in the deflected tree as it is pulled sideways and when the rope is released the potential energy transfers to kinetic energy as the tree starts to sway in a back and forth motion. A typical response curve of a tree (Figure 5.18) starts at the point of maximum deflection and upon release the sway cycles begin and repeat in a regular pattern. The amplitude gradually decreases as energy is lost from the system and the sway eventually stops as the damping absorbs all the energy and the curve reduces to zero amplitude.

The pull and release test was conducted using two different instruments to compare the measurements of the dynamic response. Triaxial accelerometers were attached to the upper part of the tree and strain meters were attached at the base of the tree. It is suggested that the accelerometers recording sway in the upper part of the tree during this test will be different to strain meters on the base of the trunk because there the energy in the lower branches contributes to the total tree response but not to the upper tree response. The base moment includes the integrated effects of the trunk and all branches above it, whereas the upper crown portion of the tree, where the accelerometers were located, would not necessarily include all these effects.

A 23m high She oak (*Allocasuarina fraseriana*) at Melbourne University was tested on 30 April 2008 by pulling and releasing then recording the subsequent sway response which is plotted in Figure 5.18a (strain meter) and Figure 5.18b (accelerometer). A theoretical curve (Equation 4.21) was fitted to each response curve to find the values of natural frequency (ω_n) and damping ratio (ζ). The curve fit is good for the strain meter response data in the first oscillation period up to 30 seconds, but after this the tree response departs significantly from the theoretical curve. This is because (a) the theoretical curve is for a SDOF system and the tree is a complex MDOF system due to the dynamic interaction of branches and (b) the response curve represents sway in one direction only and there is a proportion of the energy in the oscillations transferred to the across component of sway which is detected in the second instrument, oriented orthogonally to the one from which data is plotted. Further examples of the transfer of energy to the across direction are shown later in this section.

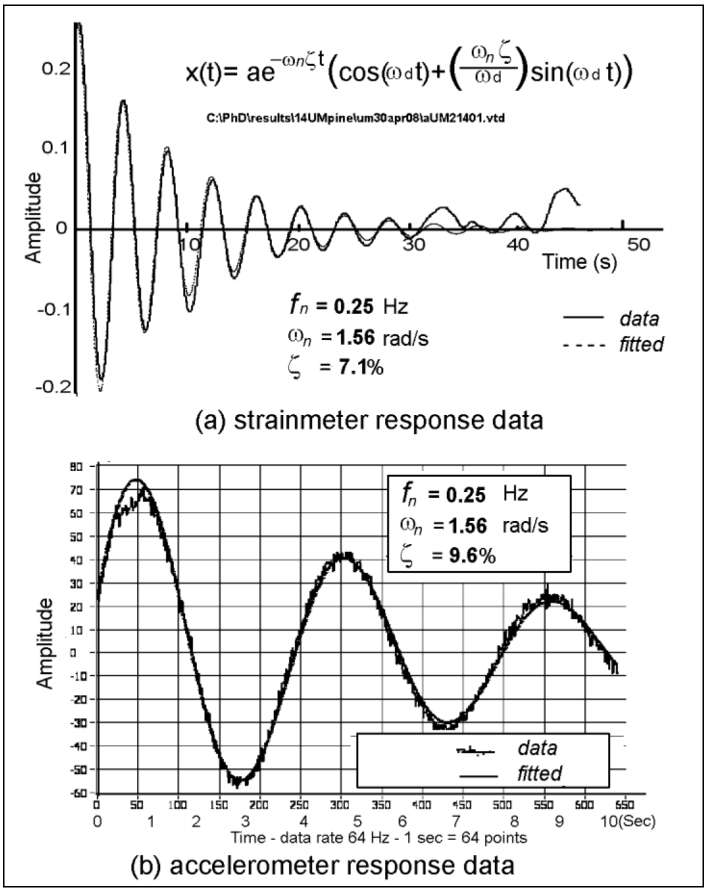

Figure 5.18. Pull and release test for a She oak (*Allocasuarina fraseriana*) (a) strain meter response and (b) accelerometer response.

The recordings from both instruments give the same results for natural frequency (ω_n=1.56 rad/s) but a slightly higher value of damping ratio is seen for the accelerometer (ζ=9.6%) compared to the strain meter at the base of the trunk (ζ=7.1%). The accelerometer data was recorded at 64 Hz, so the time scale on the x axis is divided by 64 to convert to seconds and shows ten seconds of data. During the first three cycles the response data follow the theoretical curve for the upper part of the tree trunk. This response may reflect only part of the overall tree response because branches which sway in the lower part of the trunk may not affect the sway response in the upper part of the canopy.

The strain meter records the sway motion at the base of the trunk and captures all the dynamic sway components of the tree, including all of trunk, main branches, and sub-branches. The difference in the damping ratio of 7.1% (strainmeter) to 9.6% (accelerometer) shows that the sway ceases in the upper regions before all of the sway of the lower branches stops. The higher damping value from the accelerometer may be the local effect in the upper part of the tree and the lower damping value from the strain meter may be a more accurate measure for the whole tree. A summary of the results from this test are presented in Table 5.5.

Variable	Strain meter data	Accelerometer data
Initial displacement (a) m	0.25	
Natural circular frequency (ω_n) rad/s	1.56	1.56
Natural frequency (f_n) Hz	0.248	0.25
Period (T) s	4.03	4.03
Damping ratio (ζ) %	7.1	9.6

Table 5.5. Pull and release test results for two instruments on a She oak (*Allocasuarina fraseriana*).

Branch pull and release

The pull and release test was applied to an individual branch of an elm tree (*Ulmus procera*) in full leaf, to test if the method was appropriate to a branch of a tree. The resulting sway motion is shown in Figure 5.19.

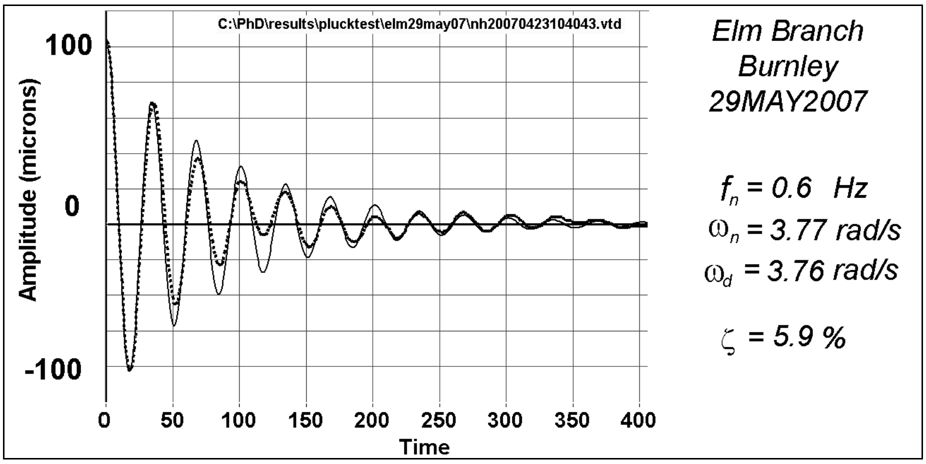

Figure 5.19 Pull and release test on a branch in leaf, elm tree (*Ulmus procera*) Burnley 29MAY2007.

The branch motion was mainly in a vertical, up and down direction and the branch response was close to a single degree of freedom system as shown by the close fit of the curve. The individual branch damping ratio was 5.9% in full leaf. This result is representative of other branches which also act as dynamic oscillators with their own natural frequency and damping. Since the tree is a collection of branches, each with their own dynamic characteristics, this test supports the concept of the multi-degree of freedom model put forward in this thesis.

Differences in along and across pull directions.

It was observed that different results were obtained when analyzing the data in the along pull direction and the across pull direction. This effect is discussed by Jonsson et al. (2007) and previously investigated by Milne (1991) who found no difference between fall-line and cross-slope natural frequencies for Sitka spruce in a Scottish plantation.

To test this effect a Mountain ash (*Eucalyptus regnans*) was pulled and released with two strain meters attached in orthogonal orientations to the trunk. The resulting sway motion was plotted in both the along (Figure 5.20a) and across sway directions (Figure 5.20b).

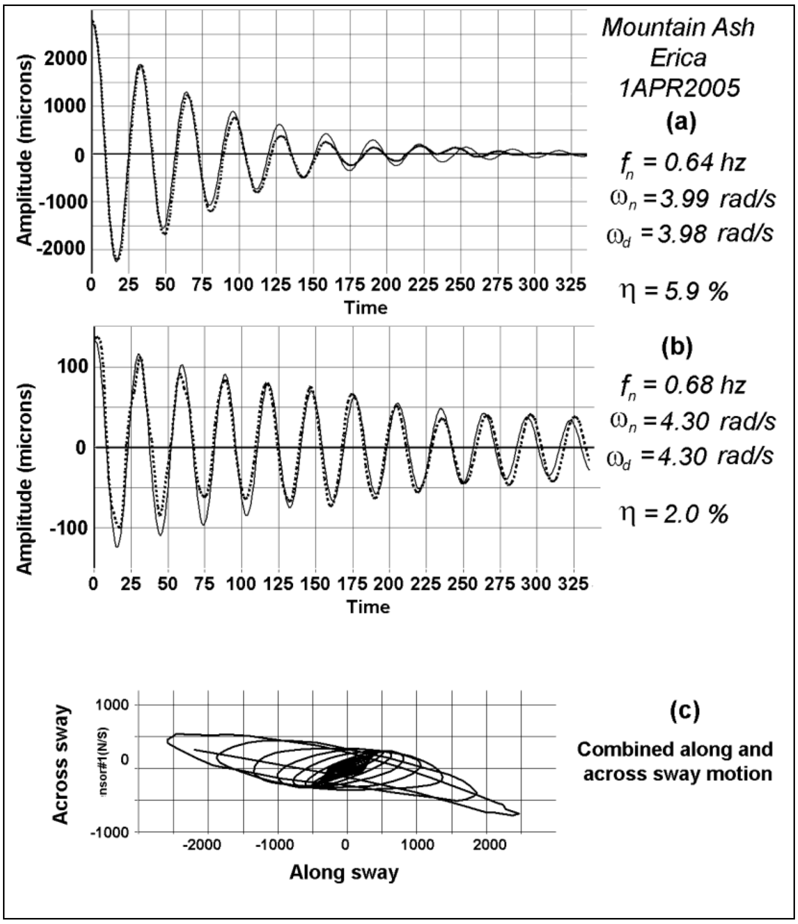

Figure 5.20. Mountain ash *(E. grandis)*, pluck test, Erica, 1 April 2005. (a) sway motion in along direction, (b) sway motion across direction, (c) combined data from along and across sway directions, showing looping motion of tree.

The natural frequency of sway is 3.99 rad/s in the along direction and 4.30 rad/s in the across direction. The two sway motions are plotted together in an XY plot in Figure 5.20c which shows that as the tree is released, a significant looping motion develops as the tree sways in a cyclical pattern with energy transferring from the along to the across direction. This motion is in part due to the non-circular cross-section of the trunk. The trunk had a significant difference in the section shape from the ground to about 7 meters, with a gradual spiral thickening occurring up the trunk. The normal diameter at breast height measurement did not accurately reflect the irregularities in the trunk but it is thought that this shape variation plays a significant role in developing complexity in the sway and is part of the explanation of the different values of natural frequency in each direction. The curve fitting was done some days after the tree test and no detailed trunk measurements were taken at the time of the test.

The sway response of trees is complex and generally develops a looping motion which is recorded when two instruments are used (Figure 5.21). The looping motion occurs in all trees tested and shows that energy is transferred from the along pull direction to the across pull direction and back again. This transfer of energy into the across pull direction, accounts for the experimental curve deviating from the theoretical curve. There was no significant difference found in the along and across directions for frequency for the hoop pine and the palm both of which had circular trunk sections, similar to the results of Jonsson et al. (2007).

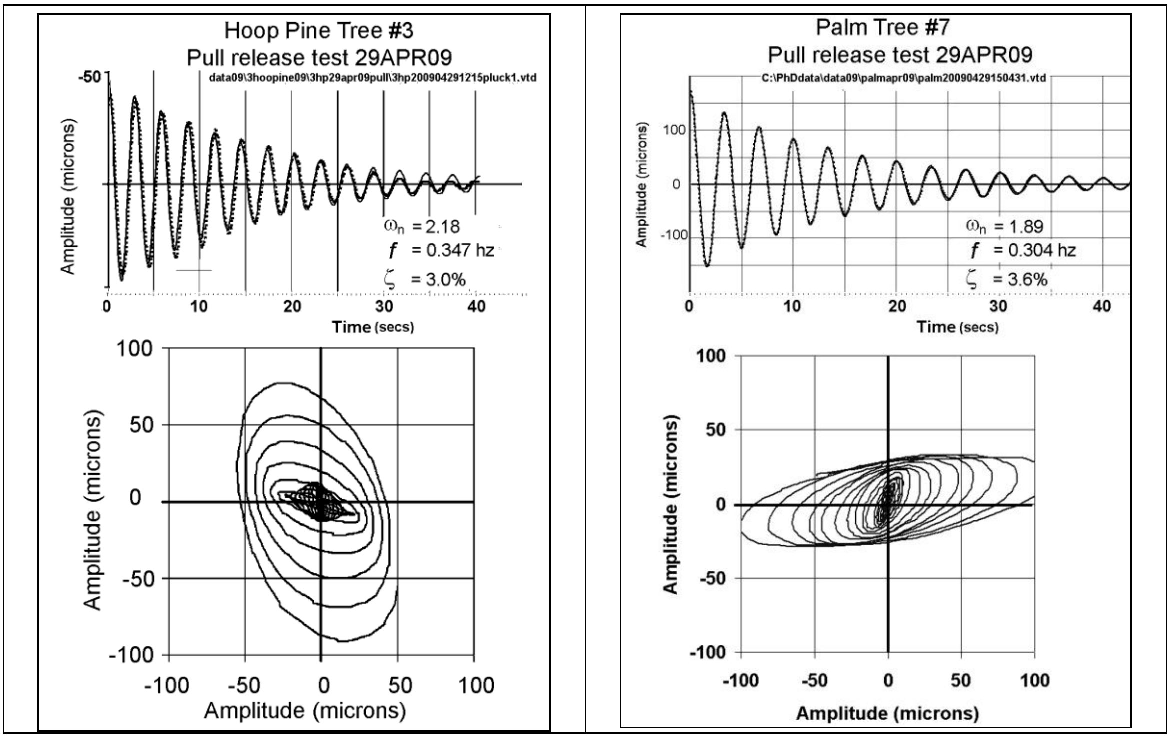

Figure 5.21. Pull release test for Hoop pine *(Araucaria cunninghamii)* and palm *(Washingtonia robusta)* showing response curve for one direction (upper) and looping motion when both instrument data is considered.

Some variation in damping was observed which was thought to be due to amplitude effects, as previously reported by Clough and Penzien (1993), and Moore and Maguire (2004), so for these tests the amplitude was always towards a maximum value where possible. The damping value is therefore an estimate of the damping in still air conditions, when wind velocity is zero.

Pull and release test on an Italian cypress

A pull and release test was conducted on a tree of significantly different form to examine the usefulness of this method on all trees. An Italian Cypress (*Cupressus sempervirens*), 17m high was tested on 6 January 2009 and the response curve is close to the theoretical curve with a natural frequency of 1.84 rad/s and a damping ratio of 4.2% (Figure 5.22). This tree is very slender with a slenderness ratio of 73.

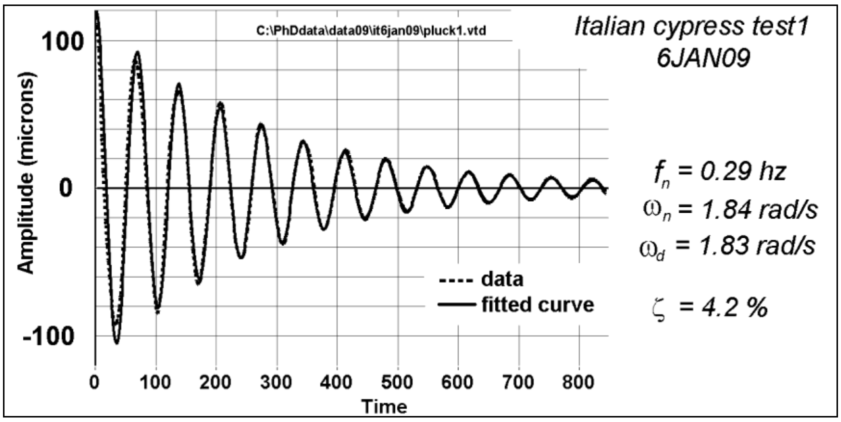

Figure 5.22. Pull and release test, Italian cypress (*Cupressus sempervirens*) 17 m high, first mode response.

This tree also exhibited a second mode of sway which could be induced by pulling the rope at the second mode frequency. The resulting response curve (Figure 5.23) shows that the second mode sway is not approximated by the theoretical mode response curve.

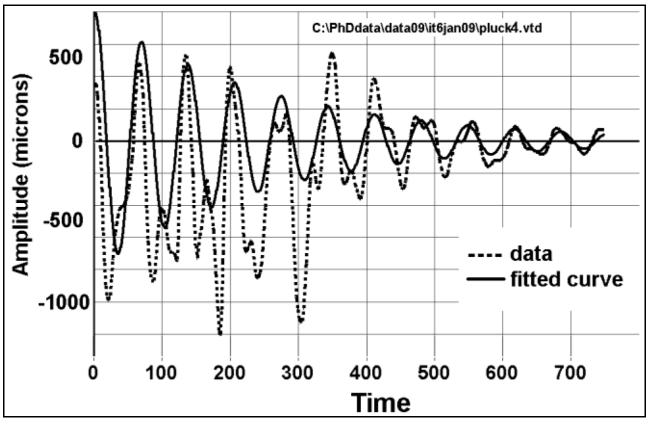

Figure 5.23. Pull release test, Italian cypress (*Cupressus sempervirens)*, with second mode sway different from first mode curve.

It appears that the pull and release test is useful on this tree to ascertain dynamic data of frequency and damping provided that the first mode is induced during the sway. If the second mode is induced and is significant, the curve fitting equation would need to be modified if the test is to provide valid information.

5.3.2 Spectra

Spectral analysis of the dynamic tree response examines the coupling between the wind and the tree in the frequency domain, and can be used to determine dynamic properties including the transfer function, natural frequencies and damping characteristics of a tree. Data from input wind velocity and the tree base bending moment response are used to determine the spectra and transfer functions.

In order to find the response spectrum of a tree the data files from the strain meters are converted from strain readings to along wind and across wind components of bending moments. The data sampling rate is 20 Hz and file length set to 30 minutes for convenience. Each file is "pre-conditioned" by subtracting the mean from the data series prior to determining the spectral response. The results were analyzed using Fast Fourier Transformations (FFT) to obtain the power spectra of the wind velocity $S_v(f)$, and of the tree bending moment response $S_M(f)$. Computer programs using a software package, Labview (8.1) were written to find the spectra and plot the results. An example of the base moment spectrum $S_M(f)$ for tree #3 (Hoop pine) is shown in Figure 5.24. The data from a 30 minute file (36000 points) were divided into 16 x 2048 smaller data sets (total 32768 points) and ensemble averaging was used to smooth the output spectral curves.

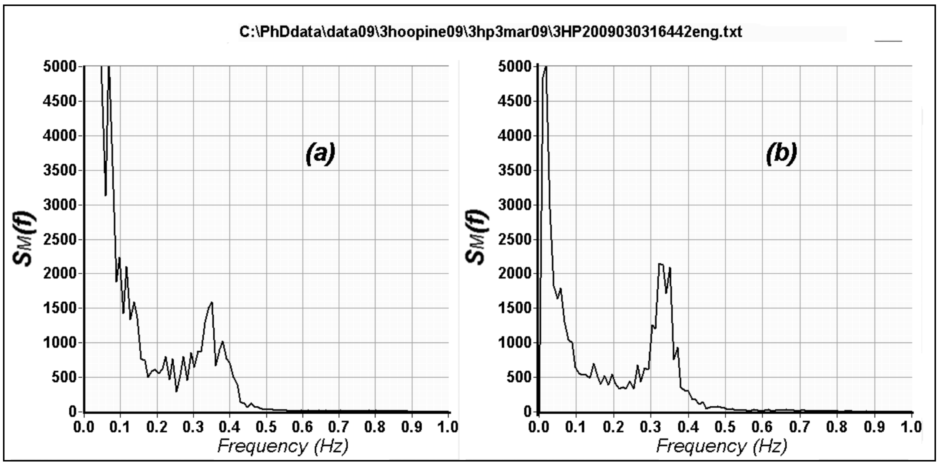

Figure 5.24. Spectra for Hoop pine (*Araucaria cunninghamii* tree#3) for base bending moment response to wind excitation, for 3 March 2009, file 1644. (a) along wind and (b) across wind response.

Figure 5.24(a) shows the along wind spectrum for tree #3 (Hoop Pine) for a 30 minute period. This is considered typical for all tree spectra and shows the background component of wind excitation in the frequency range below 0.15 Hz and the tree response component which peaks at approximately 0.34 Hz. The vertical scale is shortened which masks the wind peak and is used to show the tree response component more clearly. The tree response peak at 0.34 Hz indicates the fundamental natural frequency which corresponds to a period of 2.94 s. This spectrum represents the tree response under moderate wind conditions over a 30 minute period where the average wind speed was 4.8 ms^{-1} and the peak wind speed was 11.6 ms^{-1}. The average bending moment response at the base of the tree was 73 kNm and the maximum base bending moment was 251 kNm. These data represents the largest response measured during the monitoring period for the Hoop pine.

The across wind spectrum shows a peak at approximately 0.34 Hz (Figure 5.24b) which is approximately the same as for the along wind component but there is a larger amplitude. There are no peaks above 0.5 Hz which shows that no higher order harmonic modes of vibration occur. The tree response under wind loading only shows a first or fundamental frequency, and no higher modes of vibration are evident.

The area under the graph is the variance for the data and represents the amount of energy that is transferred from the wind into the tree. Higher wind speeds result in larger amplitudes of the peak in the spectral plot, but the peak occurs at the same frequency of 0.34Hz.

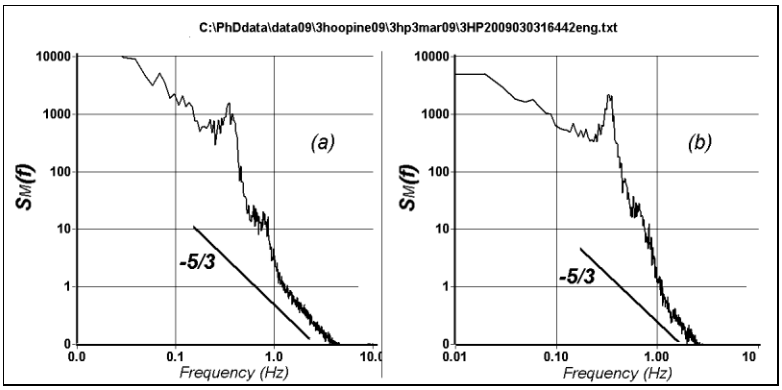

Figure 5.25. Logarithmic plot of spectra for Hoop pine (*Araucaria cunninghamii* tree#3). (a) along wind and (b) across wind response.

The spectra of the same data are plotted on a logarithmic scale in Figure 5.25. The peak in both graphs at approximately 0.34 Hz represents the tree's natural frequency in both the along and across wind spectra. The slope of the wind spectra is -5/3 in the inertial sub-range which is as expected for base bending moment data. This compares with a slope of -2/3 for the spectral wind plot from accelerometers as reported by Gardiner (1995).

5.3.3 Transfer functions

The dynamic coupling relationship between the wind excitation and the tree response is found by determining the transfer function $T^2(f)$ for each tree. The transfer function is obtained from dividing the tree response spectrum $S_M(f)$ by the wind spectrum $S_v(f)$.

$$T^2(f) = \frac{S_M(f)}{S_v(f)} \tag{5.1}$$

Data from a 30 minute file (total 36000 points) were divided into 16 sets of 2048 data points (total 32768 points). This produces 16 individual spectra which are difficult to interpret because of noise and variability in the resulting graphs. These 16 spectra are smoothed using ensemble averaging and the resulting curves are presented below. The same data for tree #3, Hoop pine, reported in the previous section is used to calculate the transfer function in Figures 5.26 and 5.27.

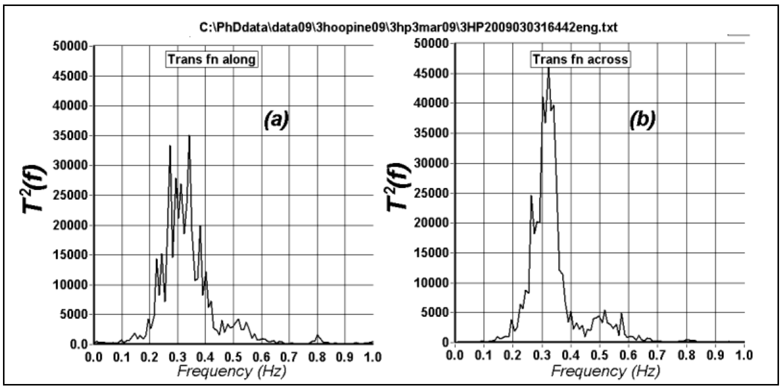

Figure 5.26. Plot of transfer function spectra for Hoop pine (*Araucaria cunninghamii* tree#3). (a) along wind and (b) across wind response.

The along wind transfer function for the Hoop pine (Figure 5.26a) shows a broad range of peaks between 0.28 to 0.34 Hz. The across wind transfer function (Figure 5.26b) has a similar broad range of peaks between 0.26 to 0.34 Hz and a maximum value greater than the along wind component. The energy in the across wind transfer function is 32% greater than the along wind component as measured by the area under the curve (the variance). Wind conditions for this period were maximum wind speed, V_{max} = 15.1 ms^{-1} and mean wind speed $\overline{V}$ = 4.8 ms^{-1}, over the 30 minute period. There were consistently higher values of energy in the across wind component of the transfer function for wind speeds ranging from 5 to 15 ms^{-1} in the data from other files of wind speed and bending moment during this wind event.

The same transfer functions are plotted using logarithmic scales (Figure 5.27) which shows a greater range of data than on plots with a linear scale. The peak values are clearly shown for the along and across wind components and there is an interesting small second peak at 0.5 Hz which is thought to be due to the dynamic contribution of some large branches with a natural frequency of 0.5 Hz. Data above 1 Hz show a series of peaks which are caused by errors in the wind spectrum due to the cup anemometer. This is considered to be noise so data above 1 Hz are not useful for detailed analysis and are ignored in further discussions.

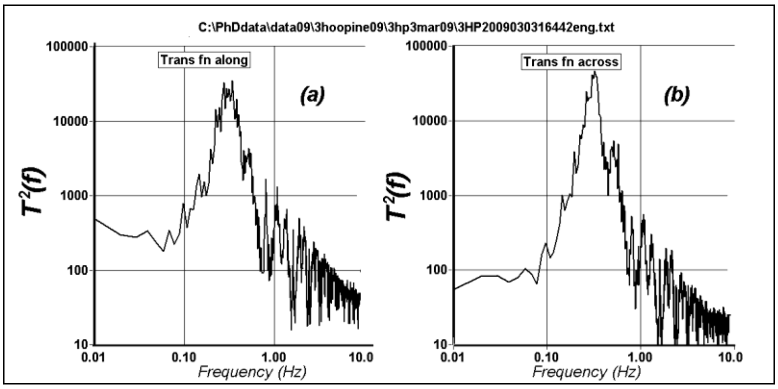

Figure 5.27. Logarithmic plot of transfer function spectra for Hoop pine (*Araucaria cunninghamii* tree#3). (a) along wind and (b) across wind response.

Another example of along wind and across wind components of a transfer function is shown in Figure 5.28 for a palm tree during a single wind event (31AUG2007) at two different wind speeds. The response of the palm to wind excitation changes from mainly along wind response (Figure 5.28a) to mainly across wind response (Figure 5.28b). This example illustrates that the response is not constant but changes considerably and shows that in a strong wind (Figure 5.28a) with V_{max} = 15.6 ms^{-1} the palm has a predominately along wind response and in light winds (Figure 5.28b) with V_{max} = 4.2 ms^{-1} the main response is in the across wind direction. This indicates that the palm has a looping response in light winds which is different to the response in high winds. The palm is a special case for a tree due to its single trunk, lack of branches and flexible response, so the different responses shown here apply to the palm only. Results from other trees in the study are not so marked but do occur and show that sway response of trees change considerably from one wind event to another.

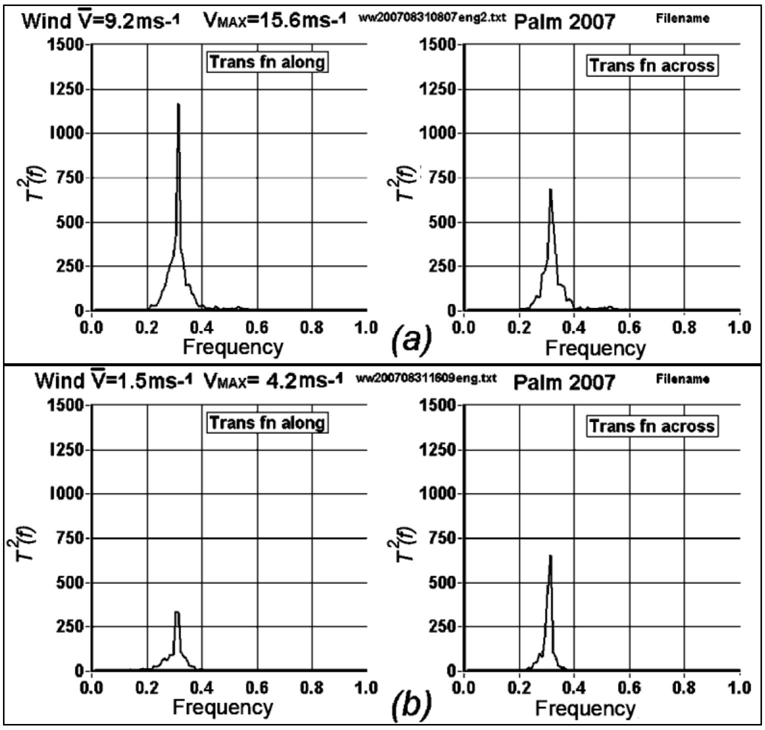

Figure 5.28. Transfer function for Palm *(Washingtonia robusta)*, 31 August 2007, showing different responses for two wind speeds. Response in (a) shows greater along wind response and (b) shows greater across wind response as palm develops a circular looping motion.

To further interpret the transfer function, a theoretical curve of the structural magnification factor $\chi_m^2(f)$ for a single degree of freedom (SDOF) model was plotted against the transfer function on a linear and a logarithmic graph (Figure 5.29). The linear scale is useful to show the amplitude of peak or resonant dynamic response and to identify small variations between the data and the theoretical SDOF model. The logarithmic plot is useful to show the low frequency (static) range below the peak, and the upper frequency (inertial) range above the peak of the curve.

The fit of the theoretical structural magnification factor $\chi_m^2(f)$ for a SDOF model to the transfer function of a tree $T^2(f)$ is not exact, particularly in the frequency range below 1 Hz where the aerodynamic admittance function has little influence. This suggests that the SDOF model does not fully describe the dynamic response of a tree which is a multi-degree of freedom system. However, the SDOF curve can be useful for interpreting the data and if the curve fitting is biased to different frequency ranges (static, dynamic and inertial) some conclusions may be made regarding the dynamic response characteristics for a tree. If the SDOF curve is aligned with the data so that the peak amplitude is the same on the linear and logarithmic plots (Figure 5.29a) the curve is much narrower and does not account for the spread of frequencies that appear in the data. This results in a smaller area under the SDOF curve and hence implies that less energy is transferred from the wind to the tree than is indicated in the data. The logarithmic plot shows that the fit in the static range below 0.1 Hz is good, but there is considerable deviation above the peak at 0.34 Hz, in the inertial sub-range of the data.

In order to fit the $\chi_m^2(f)$ curve, different criteria can be used, based on the method described by Haritos (1993) i.e.

- Fitting the curve to the low frequency or the static range of the curve
- Fitting the curve to the upper frequencies or the inertial range of the curve, and
- Fitting the curve so that the areas under the fitted curve and the transfer function are equal within the dynamic range of the tree response. For the Spotted gum shown, the dynamic range is taken to be between 0.2 and 0.4 Hz.

Fitting the curve in the static range.

The “static” range of frequencies, below approximately 0.1 Hz, represents the very low frequency range where dynamic response is low and the system behaves in a static or quasi-static manner. This range corresponds to data using mean values (averaging periods greater than 10 seconds) indicative of long term averages. Fitting the SDOF curve to the low frequency range and adjusting the damping value so the peak is the same as the data is shown in Figure 5.29a. Using this criterion, the curve is aligned in order to determine a coefficient (A_s) which in this case gives a value A_s =420 and is best seen on a logarithmic plot. The coefficient (A_s) is used to determine drag coefficients. Using this criterion for curve fitting, the upper frequency or inertial range of the tree response, is not appropriate as the two curves do not match so another criterion needs to be used for higher frequencies.

Fitting the curve in the dynamic range.

The part of the transfer function spectra where the amplitude is the greatest and a peak occurs is the dynamic response range where damping has the greatest influence. The greater the damping, the smaller the peak value of amplitude and conversely the smaller the damping the greater the peak amplitude in the spectrum. The curve is fitted so that both the amplitude peak and the width matches the data curve over the range of approximately 0.2 to 0.4 Hz. The area under the curve is a measure of the variance or spread in the data and also a measure of the energy in the transfer function, so matching the areas under the curve is useful for estimating the damping ratio (ζ). An example of this method is shown in Figure 5.29(c).

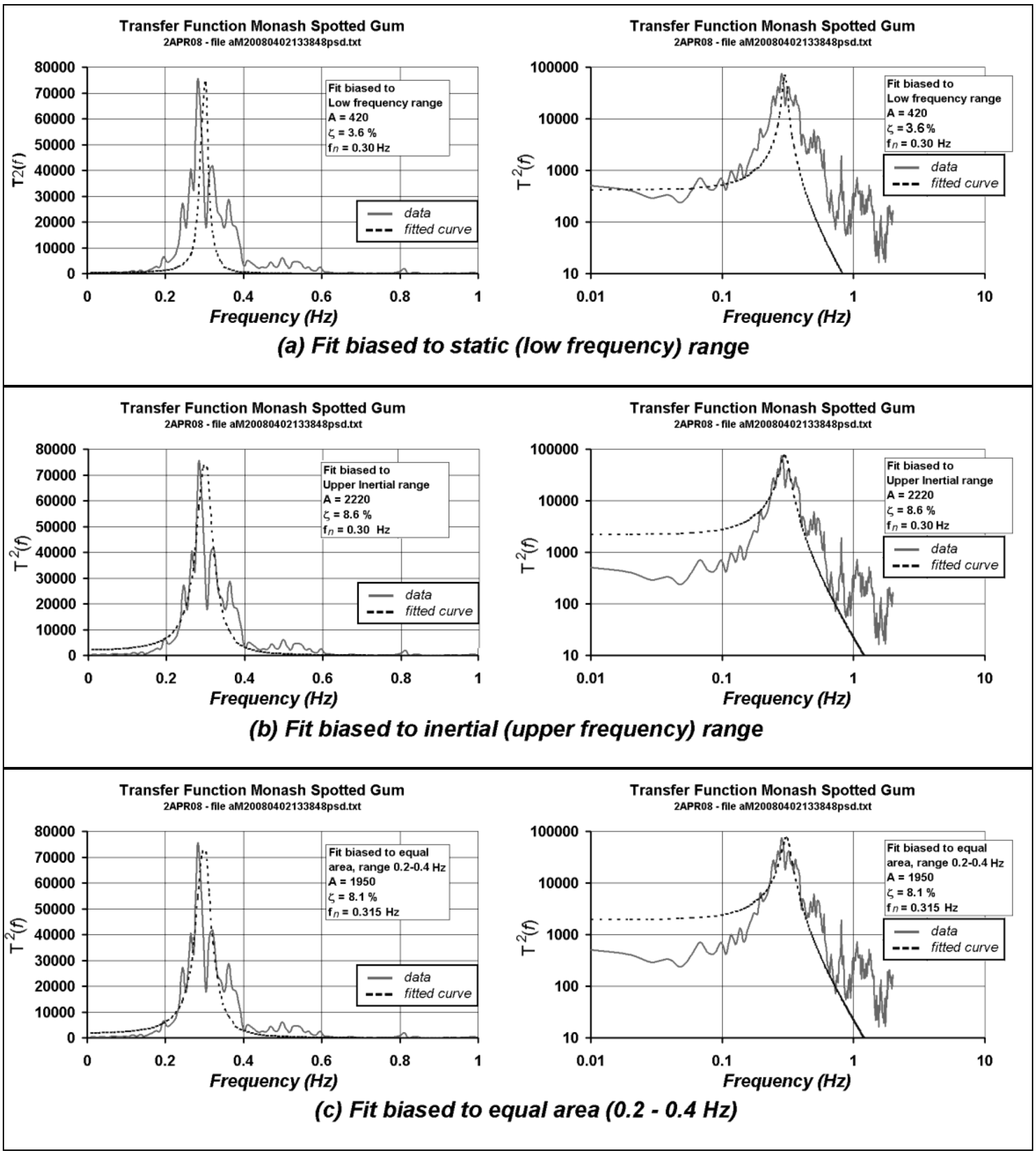

Figure 5.29. Transfer function and fitted curves for Spotted Gum *(Corymbia maculata)*, 2 April 2008, showing different criteria for of fitting (a) biased to static range, (b) biased to inertial range and (c) biased to equal area (0.2-0.4 Hz) range.

The transfer function data for the spotted gum has several peaks, spread over a range of frequencies from 0.2 Hz to 0.6 Hz, with most of the energy between 0.2 and 0.4 Hz. The value of ***As*** is higher than the static range, but the value for the damping ratio is more representative of the energy dissipation in this range. The frequency of the peak does not change. As a comparison, the criteria used for the static fit shown in the linear plot (a1) produces a curve that is narrow and does not have the spread over the frequency range of 0.2 to 0.4 Hz. This indicates that the fitted curve is not representing all the energy in the data signal.

Fitting the curve in the inertial range.

At frequencies above 1 Hz, mass dominates the dynamic response so this is known as the inertial region or the inertial sub-range. This is where high frequency wind gusts or vortices push on large masses of the canopy. The linear plot of these data (Figure 5.29(b)) does not show any significant peaks in this range, indicating that there is little energy transfer from the wind to the tree so the graph is terminated at 1 Hz. In a logarithmic plot of the same data, the fitted curve in the inertial range progressively moves away from the data curve indicating that the SDOF curve is not a good fit to the data.

The transfer functions for selected trees are shown in Figure 5.30 in both linear and logarithmic scales of the same data. The peak amplitude occurs at the fundamental natural frequency and a second peak is present only in tree#4 (Italian cypress).

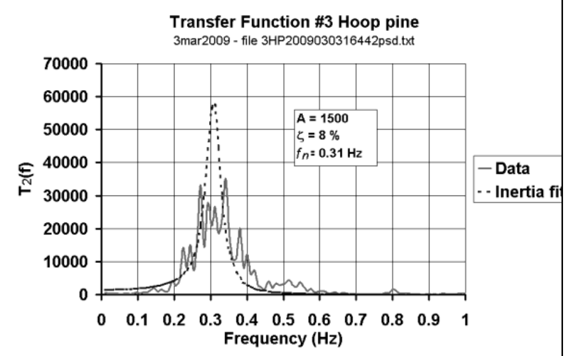

(a1) Tree #3, Hoop pine *(Araucaria cunninghamii)*

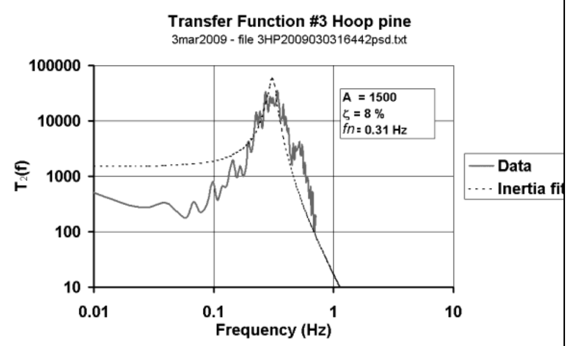

(a2) Tree #3, Hoop pine *(Araucaria cunninghamii)*

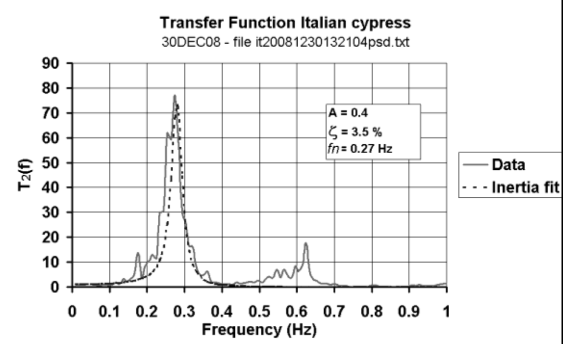

(b1) Tree #4, It. cypress *(Cupressus sempervirens)*

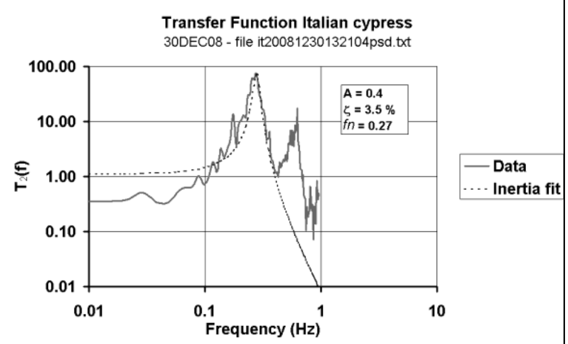

(b2) Tree #4, It. cypress *(Cupressus sempervirens)*

Figure 5.30. Transfer functions with curves fitted for a SDOF system.

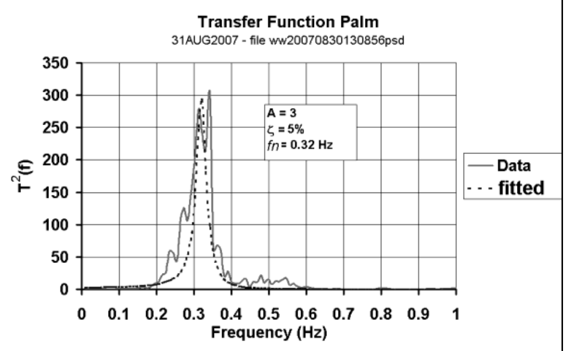

(c1) Tree #7, palm *(Washingtonia robusta)*

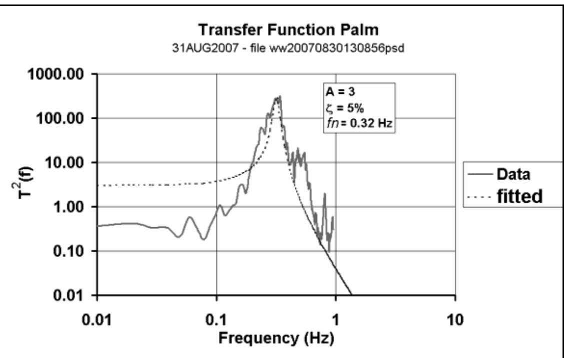

(c2) Tree #7, palm *(Washingtonia robusta)*

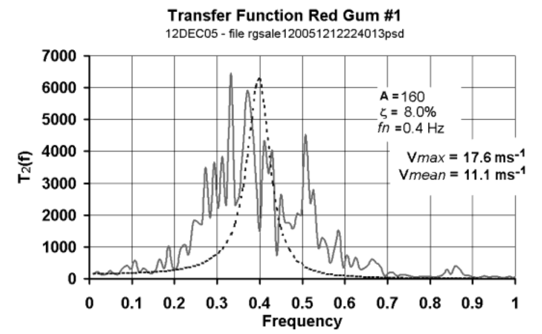

(d1) Tree #8, Red gum1 (E. tereticornis)
(before pruning)

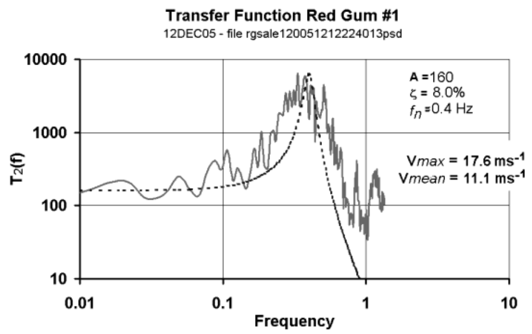

(d2) Tree #8, Red gum1 (E. tereticornis)
(before pruning)

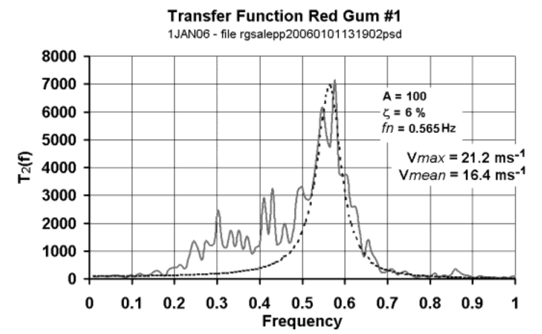

(e1) Tree #8, Red gum1 (E. tereticornis)
(after pruning)

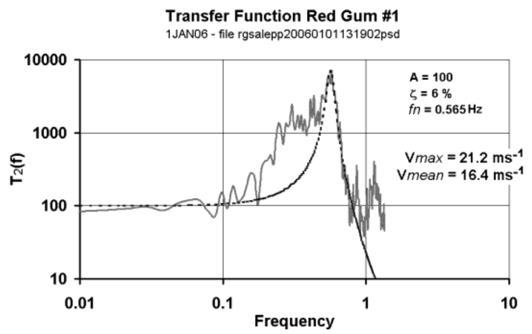

(e1) Tree #8, Red gum1 (E. tereticornis)
(after pruning)

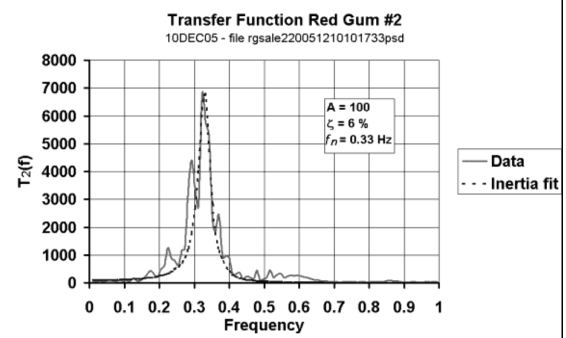

(f1) Tree #9, Red Gum 2 *(E. tereticornis)*

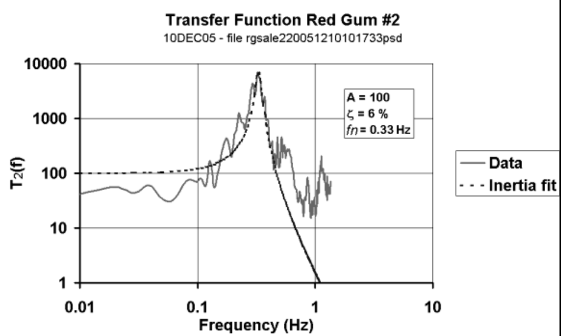

(f2) Tree #9, Red Gum 2 *(E. tereticornis)*

Figure 5.30 (cont.). Transfer functions with curves fitted for a SDOF system.

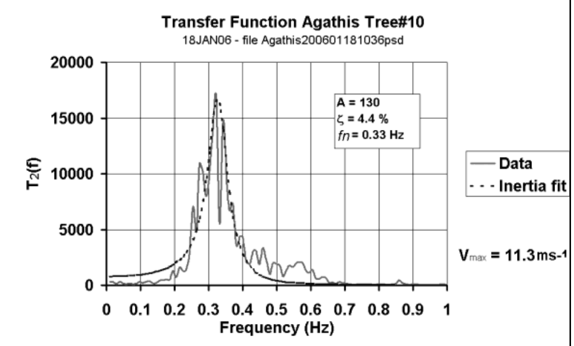

(g1) Tree #10, Agathis *(Agathis australis)*

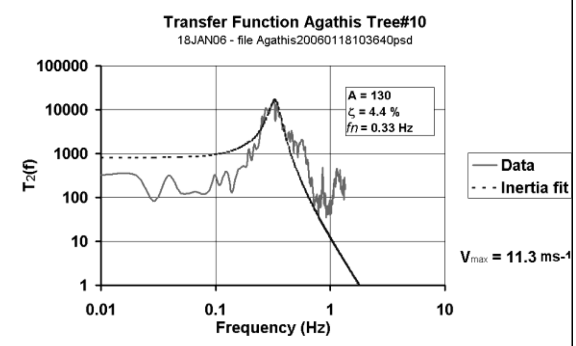

(g2) Tree #10, Agathis *(Agathis australis)*

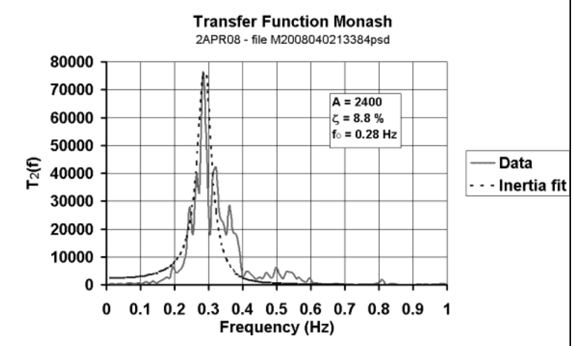

(h1) Tree #13, Spotted gum *(Corymbia maculata)*

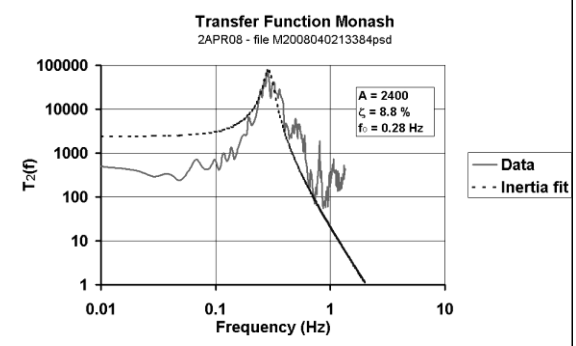

(h2) Tree #13, Spotted gum *(Corymbia maculata)*

Figure 5.30 (cont.). Transfer functions with curves fitted for a SDOF system.

The amplitude in the linear graph indicates the energy in the transfer function at each frequency and there is little energy evident in the plots above 1 Hz. The logarithmic scale is used to show the data over a greater range of frequency and amplitude and to clearly show the data in the low (static) range and the high (inertial) range of frequencies. In the higher frequency range of the spectrum peaks are very small and the data are affected by a dynamic response in the anemometer due to vibrations which cause small peaks that are considered to be "noise". This makes it difficult to interpret so data above 1 Hz is of limited value and is not presented. The numerical value of the transfer function on the Y axis is calculated from the bending moment data recorded in kilonewton meters for each tree. The transfer functions in Figure (5.30) are considered typical for each tree and represent a 30 minute period. Not shown are hundreds of hours of other data which are used later when calculating the drag and damping ratio.

A general observation on the transfer functions in Figure 5.30 is that all trees exhibit only one peak except tree #4 (Italian cypress) which has a main peak at 0.32 Hz and a second, smaller peak at 0.62 Hz. Trees with only one peak therefore sway with only one fundamental frequency under wind excitation and harmonics of this fundamental frequency, e.g. 2nd and 3rd modes of sway do not occur. The exception is the Italian cypress which is a tall, thin, slender tree which sways with a flexible response including the primary and secondary modes. The transfer functions for the open grown trees do not have a single defined peak as does the SDOF fitted curve. These trees have complex structures of many large branches whose dynamic response contribute significantly to the overall transfer function and are seen as many peaks over a broad range of frequencies. Trees with a structure that have little or no mass in the branches e.g. Tree#7 (palm), have a more pronounced peak and a narrow band of frequencies in the transfer function.

Tree#3 (Hoop pine) does not have any clearly defined peak (Figure 5.30 (a1)) and the data are clearly different from the fitted SDOF curve. Other transfer functions for this tree (Figure 5.26) show a series of peaks centred at 0.31 Hz and there is always a broad spread from 0.2-0.6 Hz with distinct peaks within this frequency range. These multiple peaks are interpreted as being caused by the dynamic sway of the branches which interact to cause modes of sway, each with a slightly different natural frequency.

Tree#8 (Red gum1) has two transfer functions to illustrate the before pruning and after pruning responses (Figure 5.30(d), (e)). In the before pruning case the transfer function shows many peaks between 0.2-0.7 Hz, with the peak amplitude centred around 0.4 Hz which is the natural frequency. After pruning there are also many peaks between 0.2-0.7 Hz but the peak amplitude occurs at a different frequency of 0.565 Hz. The increase in natural frequency is due to mass removal of approximately 20% of the canopy by thinning. The graphs of before and after pruning are for similar wind speeds. Tree#9 (Red gum2) has a peak at 0.33 Hz over the range 0.2-0.65 Hz. The two red gums were of a similar height and located together on the site. Tree #10 (Agathis) showed a peak at 0.33 Hz with a spread of data from 0.2-0.7 Hz and similarly for tree #13 (Spotted gum) there was a peak at 0.28 Hz and data spread from 0.2-0.6 Hz.

All these trees had multiple branches and were mature open grown trees with significant branch mass compared to trunk mass. If the branches are considered as dynamic masses attached to other branches or the trunk, as in the new model proposed in Chapter 3 of this thesis, the graphs of transfer function with several peaks indicate that the individual branches contribute to the transfer function with significant energy spread over a broad range of frequencies. The branches sway in a complex manner such that some move forwards and some move backwards, sometimes in phase and sometimes out of phase with the main trunk. The overall effect is to spread the energy over a range of frequencies which prevents a clear peak in the transfer function from appearing. This prevents the tree from swaying at its natural frequency and provides an energy dissipation mechanism which means damaging harmonic motion do not occur. Higher harmonic oscillations would show up as a second or third peak in the transfer function but this did not occur over hundreds of hours of monitoring. The complex dynamic motion demonstrates the effect of mass damping of the branches and the dissipation of energy over a range of frequencies close to the fundamental or natural frequency of the tree.

Tree#4 (Italian cypress) is noteworthy as the only tree to have two peaks in the transfer function (Figure 5.30 b) which indicate a second harmonic mode of sway is present for this tree. This tree has a tall, thin shape with the branches closely aligned to the main stem so that the whole tree sways together as one unit. The tree has a slenderness ratio of 73 which according to Mattheck et al. (2003) is over the limits for stability, yet is stable. This tree sways in a very flexible manner so that both first and second harmonic modes of sway are apparent. This may be an adaptation to wind loading that does not occur in other trees. Jonsson et al. (2007) report a second mode of sway in Norway spruce (*Picea abies*) but their results were from pull and release tests and not from wind excitation. This suggests that the pull and release test has limitations and that it is important to measure tree response in real wind conditions so as not to create data that may not exist naturally.

Aerodynamic admittance function

The aerodynamic admittance function accounts for size/frequency dependent features of how gusts of wind impact on parts of a structure and impart less energy than if the wind force was constant over the entire surface. It has been applied to large buildings (Holmes 2001) and has been found to be an important factor in determining the wind loads on large structures. The influence of the aerodynamic admittance function on trees was investigated by including the term into the spectral fit using the -5/3 power law to the wind data. The aerodynamic admittance function $\chi_a(f)$ was previously assumed to be unity so did not appear in previous equations. To include the aerodynamic admittance function Equation 5.1 can be re-written as;

$$T^2(f) = [\chi_m(f)\chi_a(f)]^2 = \frac{S_m(f)}{S_v(f)} \qquad (5.2)$$

Using Equation 2.9 for $\chi_a^2(f)$, the structural magnification factor $\chi_m^2(f)$can be determined using;

$$\chi_m{}^2(f) = T^2(f) \Big/ \chi_a^2(f) \tag{5.3}$$

An example using data from the Palm, fitting the wind spectrum assuming the -5/3 power law, and including the aerodynamic admittance function is shown in Figure 5.31.

The data follows the theoretical wind curve up to approximately 1 Hz and within this range the aerodynamic admittance function has little affect as would be expected. At frequencies above 1 Hz, the wind data are not reliable as errors were introduced due to harmonic effects from the anemometer and supporting arm. Adding the aerodynamic admittance factor brings the fitted curve closer to the measured data, but only at frequencies above 1 Hz which is not significant for the palm whose transfer function exhibits very little energy (very low magnitudes) above 1 Hz.

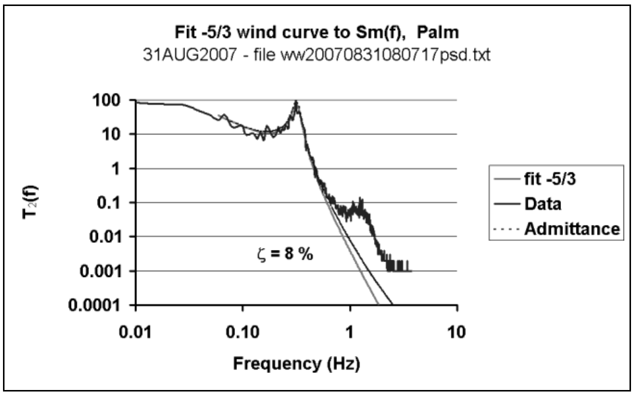

Figure 5.31. Palm *(Washingtonia robusta)* spectra, with -5/3 curve and aerodynamic admittance function fitted.

Even if the aerodynamic admittance function is included, the result for natural frequency (0.32 Hz) and the calculated damping ratio (8%) do not change. For this reason the addition of the aerodynamic function does not seem warranted for the palm.

The aerodynamic admittance function has little effect on the small canopy of the palm but may be significant on a larger tree with a bigger canopy. In order to investigate a large canopy tree, the aerodynamic admittance function was applied to data from tree#10 (Agathis). This tree was 23.2 m high with a spreading canopy of approximately 150 m^2. Fitting the SDOF structural magnification function curve to the spectral data for the Agathis (Figure 5.32) gives a natural frequency of 0.33 Hz and a damping ratio of 16%

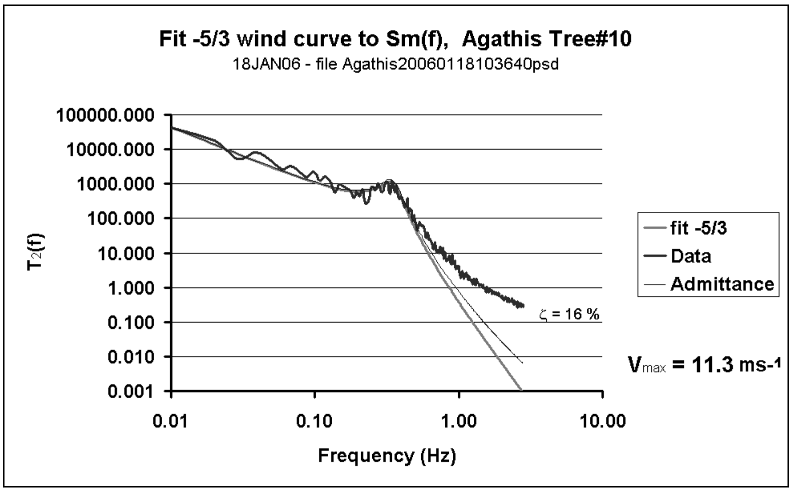

Figure 5.32. Tree #10, Agathis *(Agathis australis)*, showing -5/3 curve fitted to the bending moment spectra and modified using the aerodynamic admittance function.

The addition of the aerodynamic function does bring the fitted curve closer to the data curve at frequencies above the peak, but not enough to match the data and values of frequency and damping do not change. It appears that including the aerodynamic admittance function does not greatly contribute to the analysis of tree dynamic response in winds. This could be due to the fitted curve representing a SDOF system which does not fully describe the complex MDOF system of a tree, and also due to the wind effectively engulfing the whole canopy, even when it is gusty and constantly changing.

It appears that trees of the size studied in this project are not large enough for this gust effect to occur and it can be taken that the wind force impacts on the entire tree canopy at one time, rather than on one part then another. Taking the aerodynamic admittance factor as unity seems appropriate for calculations of frequency and damping.

5.3.4 Drag and damping ratio

The drag coefficient (C_D) for a tree can be estimated from the base bending moment and wind speed data using two methods, i.e.

1. the mean moment response method and solving Equation 4.37 or
2. a spectral modeling method which fits a theoretical structural magnification curve to the transfer function data of a wind event.

Mean moment method for calculating drag

An example of calculating the drag coefficient using the mean moment response method is shown below and applied to the Spotted gum at Monash University.

Repeating Equation 4.37 for convenience, the mean moment is;

$$\overline{M} = h_m \alpha_0 \left(1 + I^2\right) \overline{V}^n$$

Where $\alpha_o = ½\, \rho\, C_D\, A_o$,

For this tree the following values were measured;

Height of application of wind force (estimated at centre of canopy) h_m = 19 m,

Air density ρ = *1.2 kg m*$^{-3}$,

Turbulent Intensity (***I***) in range 03 to 04 (say 0.35), (I^2 = 0.123).

Substituting these values into Equation (4.37) gives an expression for mean moment as;

$$\overline{M} = 12.8 C_D A_o \overline{V}^n \tag{5.4}$$

In order to solve this equation, some estimate of the velocity exponent "*n*" must be made. The exponent can be estimated by plotting average values of velocity and bending moment. Using the data collected during wind events that occurred over many hours, and on different days, the mean values of base bending moment for a range of wind speed values can be determined. The results of this analysis are plotted to obtain a characteristic curve of wind speed versus moment at the base of the tree, using 30 min. averages (Figure 5.33). The theoretical relationship between wind speed and base bending moment depends on the term $\overline{V}^n$ where expected values of *n* lie between 1 and 2. Experimental values of mean wind speed up to 8 ms^{-1} have been measured and the average data follows a relationship close to values of *n*=2. Instantaneous values of wind speed up to 22 ms^{-1} have been measured and the line of best fit gives a value of *n* = 1.8065.

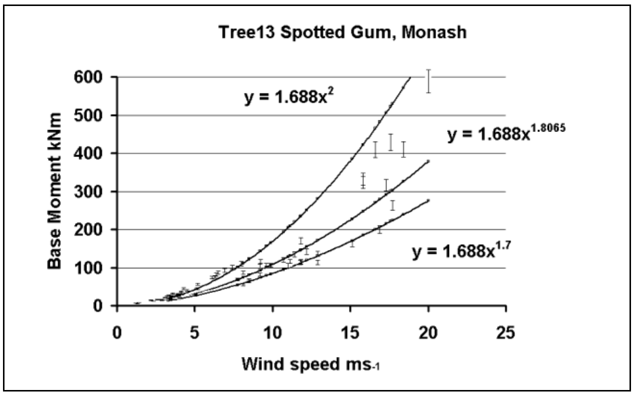

Figure 5.33. Wind load envelope for Spotted gum (*Corymbia maculata*) using 5% error estimate.

Using an estimate of 5% error due to the wind anemometer, error bars were included in the plot to show the limits in the data. When considering the minimum values it was possible to fit a curve with a exponent value of n = 1.7. The data indicate that the velocity exponent for the spotted gum has a maximum value of 2 and a minimum value of 1.7. A value of n=1.8065 was selected to complete the drag calculations as it represents a middle value for this data set.

Errors in the wind speed were apparent due to the limitations of the instrument and shielding effects from surrounding buildings. The wind speed was measured using a Davis cup anemometer (Model 7911) at a 1 Hz sampling rate, and a height of 10m, on the roof of the nearby building. Allowance was made for height variation in wind according to ASA wind code AS1170 part 2(2002), using terrain category 3 values. However, wind data from official recording stations located several kilometres from the site recorded maximum gust wind speeds 30% higher than were recorded by these instruments.

An attempt to extrapolate the data beyond the measured range of 22 ms^{-1} is not valid because the velocity exponent n varies significantly and absolute values for predicted bending moment at higher wind speeds also vary greatly. More data are needed at higher wind speeds, above 22 ms^{-1}, to establish the relationship between mean moment values to accurately determine the value of n. Using the best fit equation from the data presented in Figure 5.33, and converting bending moments to Nm gives;

$$\overline{M} = 1688\overline{V}^{1.8065} \tag{5.5}$$

From Equation 5.4, this gives;

$$C_D A_o = {}^{1688}\!/_{12.8} = 131$$

The parameters C_D and A_o are coupled and are difficult to separate, but estimates can be made for canopy area. Allowance for streamlining and changes in canopy shape under high winds would affect the drag value. The canopy area in still air (A_0) was estimated from photographs to be 150 m^2. Substituting this value into the above equation gives a value for C_D.

$$C_D = {}^{131}\!/_{A_o} = {}^{131}\!/_{150} = 0.87$$

The method of using average data is useful to develop estimates of drag for trees but the range of values for both the velocity exponent n are too large to do further calculations. More data in the upper mean wind speed range are needed to refine these values.

Spectral modeling method for calculating drag

The spectral modeling method attempts to fit a theoretical structural magnification curve to the transfer function calculated from wind speed and bending moment response data. This method is described previously in Section 5.3.3 and transfer function plots for selected trees are shown in Figure 5.30. The structural magnification factor (Equation 4.19) is based on a SDOF model and may not fully describe a complex MDOF dynamic system like a tree so the theoretical curve may not fit the data over the entire range of frequencies of the transfer function spectrum. The method of fitting is to align the theoretical curve with the static range of the transfer function. This region approximates the tree response in a quasi-static or average manner rather than in the dynamic or inertial range where the curve deviates from the data. The curve from structural magnification factor $\chi_m^2(f)$ is fitted to the static range of the transfer function $T^2(f)$ and adjusted by changing a multiplication constant (***A_s***) and the damping ratio (**ζ**) so that the peak amplitude of the two curves match.

This method is useful for determining the value of a constant ***As*** , which is used to match the structural magnification function to the transfer function;

$$T^2(f) = A_s \chi_m^2(f) \tag{5.6}$$

Substituting into Equation 4.35 and taking the aerodynamic admittance function $\chi_a^2(f)$ equal to 1 gives,

$$A_s \chi_m^2(f) = \left(2\beta\bar{V}\right)^2 \chi_m^2(f) \tag{5.7}$$

Since $\beta = h_m \alpha = h_m . \tfrac{1}{2}\rho C_D A$, this allows an estimate to be calculated for the drag C_D;

$$A_s \chi_m^2(f) = \left(2h_m . \tfrac{1}{2}\rho C_D A\bar{V}\right)^2 \chi_m^2(f)$$

$$C_D = \sqrt{A_s} \Big/ h_m \rho A \bar{V} \tag{5.8}$$

For each 30 minute file of wind and tree bending moment response, the theoretical structural magnification factor was fitted to the transfer function determined from the measured data, so that the constant A_s was determined. This allowed the drag for that 30 minute period to be calculated based upon the average wind speed. This method was used for each tree, using a range of average wind speed values, to calculate values of drag. The drag values as a function of wind speed could then be plotted and are shown in Figure 5.34 for selected trees. Each point represents 30 minutes of data.

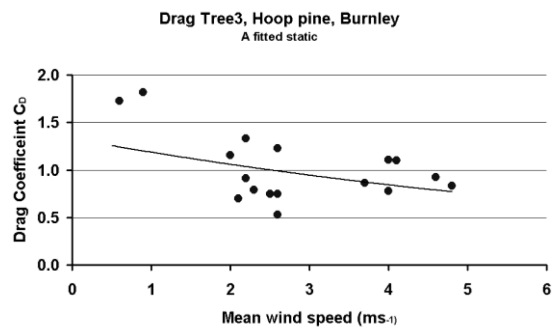

(i) Tree #3, Hoop pine (Araucaria cunninghamii)

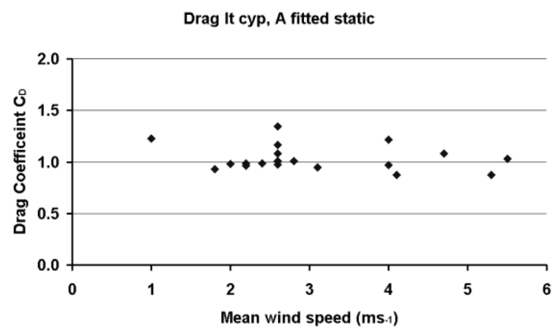

(ii) Tree #4, Italian cypress (Cupressus sempervirens)

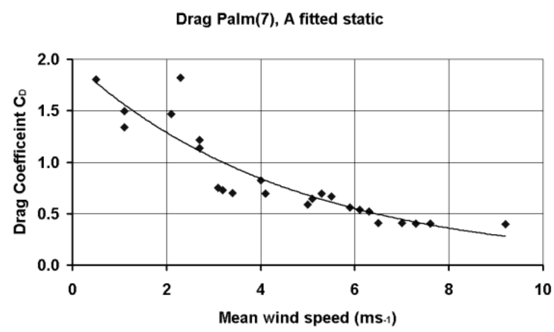

(iii) Tree #7, palm (Washingtonia robusta)

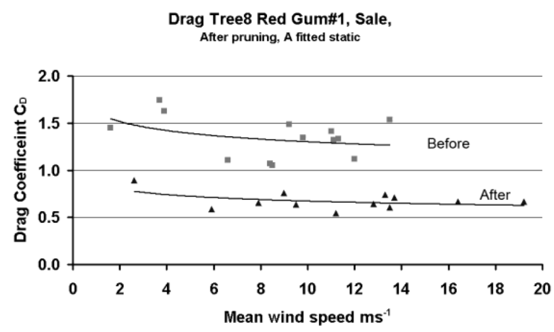

(iv) Tree #8, Red gum (E. tereticornis)

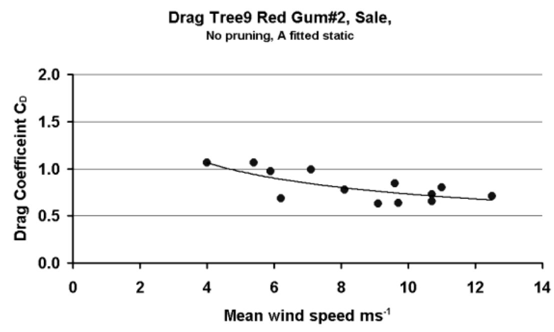

(v) Tree #9, Red Gum 2 (E. tereticornis)

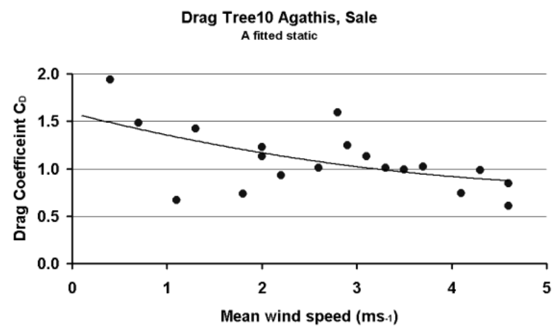

(vi) Tree #10, Agathis (Agathis australis)

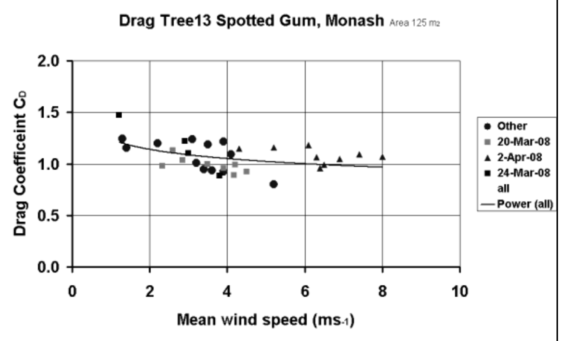

(vi) Tree #13, Spotted gum (Corymbia maculata)

Figure 5.34. Drag versus wind speed for several trees.

The drag values for each tree appear to be different for each species and the spread of data reflects the assumptions in the spectral modeling approach and the use of 30 minute average values. Because the data spread is large, lines of best fit are not quoted, but in some cases a line is drawn to indicate trends in the relationship between drag and mean wind speed.

Some general comments can be made as there appears to be a trend for the drag value of the trees studied to decrease with wind speed except in the case for Tree #4, the Italian cypress (*Cupressus sempervirens*) where the drag value appears constant in the wind speed range of 0 to 6 ms^{-1} (Figure 5.34(ii)). This is tall and slender tree and appears to have a very flexible response to wind loading including a second mode of oscillation which has been previously described. The drag characteristics may be influenced by the flexible response of the tree which is approximately constant with wind speed. Drag seems to decrease with wind speed for tree #7, the palm (Figure 5.34(iii)). This tree has no branches and its dynamic response appears to be a close approximation of the SDOF model that is the basis of the mathematical curve fitting. The drag values for the palm at low wind speed are higher than previously reported for other trees by Gardiner et al. (1997, 2005) and Rudnicki et al. (2004) but decrease rapidly to values which match these previous studies.

For all the other trees, which represent typical urban species the drag decreases with increasing wind speed. It is possible to draw linear or exponential lines of best fit and more data at higher mean wind speeds are needed before more definite conclusions can be made.

Drag values before and after pruning for tree #8, the Red gum, were investigated and there was a definite reduction in drag after pruning. The trend in both cases was approximately constant with wind speed and the post pruning drag reduction being attributable to a smaller cross sectional area of the tree canopy and a reduction in porosity.

Damping

The damping ratio for each tree is estimated by fitting the structural magnification factor $\chi_m^2(f)$ to the transfer function data $T^2(f)$ and biasing the curve so that the area under each curve is equal in the frequency range from 0.2-0.4 Hz (Figure 5.35). This is considered to be the best method for fitting the curve for damping as the area under the curve represents the energy in the data.

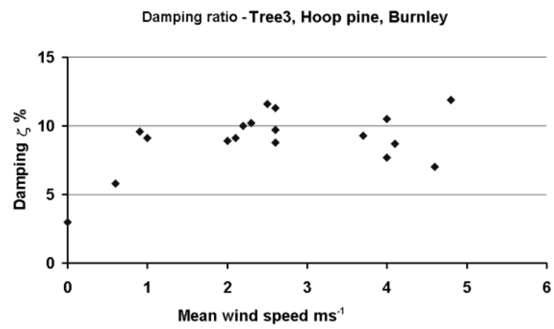

(i) Tree #3, Hoop pine (Araucaria cunninghamii)

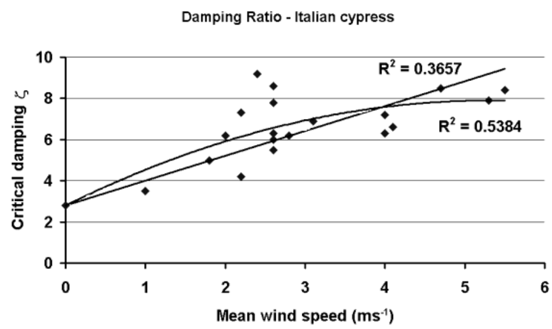

(ii) Tree #4, Italian cypress (Cupressus sempervirens)

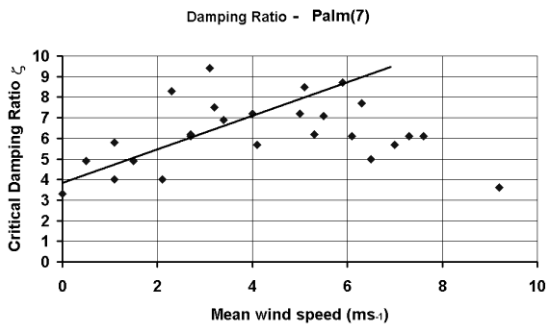

(iii) Tree # 7, Palm tree (Washingtonia robusta)

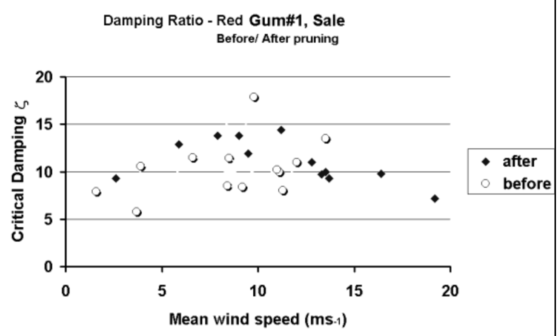

(iv) Tree #8, Red gum 1 (E. tereticornis)

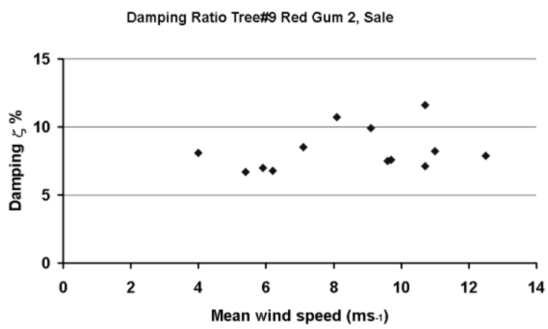

(v) Tree #9, Red Gum 2 (E. tereticornis)

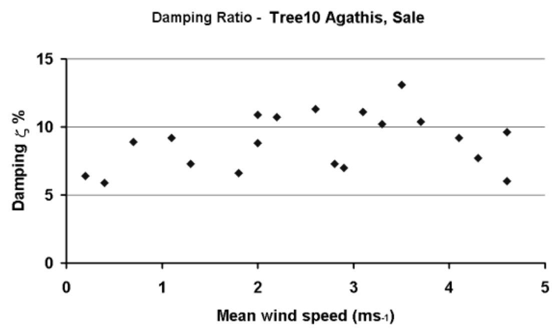

(vi) Tree #10, Agathis (Agathis australis)

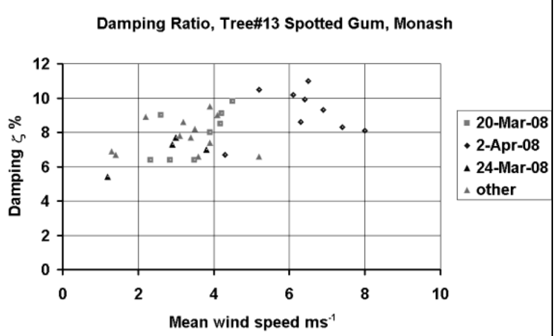

(vii) Tree #13, Spotted gum (Corymbia maculata)

Figure 5.35. Damping ratio of trees plotted against mean wind speed.

Since the damping is a measure of energy dissipation and significantly reduces the peak amplitude of the transfer function, matching the areas over this dynamic range would seem appropriate. The significance of changing damping values in this region is previously described in Chapter 4 and illustrated in Figure 4.16 after den Hartog (1956). The aerodynamic admittance function is taken as equal to 1. One data file (30 minutes or 36,000 data points) is used to calculate the spectra and transfer functions and by fitting the theoretical structural magnification function, using the equal area criteria, the damping ratio is determined. Many files were processed to generate the graph of damping versus mean wind speed (Figure 5.35) for each tree.

The plots for selected trees in Figure 5.35 do not indicate any clear relationship between damping and mean wind speed. This supports previous studies and the review of Moore and Maguire (2004) that found damping ratio varied from 1.2% to 15% in value, and also varied between individual trees and between species, with no clear relationship apparent. The damping ratio under still air conditions ($\overline{V} = 0$) is determined from a pull and release test which was performed on three trees, i.e. tree#3 (Hoop pine), tree#4 (Italian cypress) and tree#7 (palm). The damping values from each test are included in the respective graph and combined with the other points calculated from wind response data. The graph for tree #4 (Italian cypress, Figure 5.35 plot (ii)) is shown with both a linear and polynomial line of best fit. The data is more closely followed by the polynomial (r^2= 0.5834) than the linear (r^2 = 0.3657) best fit lines and flattens out at wind speeds above 5 m s^{-1}.

At $\overline{V} = 0$, the pull and release tests from previous studies indicate that damping is amplitude dependent (Gardiner 1992, Moore and Maguire 2004). An explanation could be that as the pull amplitude increases in still air conditions, so does the relative velocity between the tree and the air. This creates an aerodynamic component of damping which would be similar to the effect at low wind speeds and show up as a small increase in damping. The results from several trees (Figure 5.35) show an initial increase in the damping as wind speed increases from zero but after this the trend is not clear. Damping may reach a maximum value then stay constant (Figure 5.35 i) or may decrease after a maximum (Figure 5.35 iii). Further study with more data at higher wind speeds is needed to determine a definite relationship between damping and wind speed. For tree#7 (palm), the damping ratio from the pull and release test was 2.8%. As the wind velocity increases above zero, the damping ratio increases to a maximum value of approximately 9% at a mean wind speed of 3 ms^{-1} then remains constant until 6 ms^{-1}. Above this wind speed the damping appears to decrease though there are few data points to confirm this. One outlier data point occurred during the monitoring period at a mean wind speed of 9.2 ms^{-1} with a damping value of 3.6%. This suggests that damping decreases with wind speed and is complex in trees but there is insufficient data to draw conclusions. Energy loss mechanisms are seldom fully understood (Clough and Penzien 1993) and it is common practice to assume viscous damping in trees (Moore and Maguire 2004).

Damping for tree#8 (Red gum) follows a similar trend where damping increases from an initial value of 6% to 15% at $\overline{V} = 10$ ms^{-1} then remains constant or even decreases at higher wind speeds. The damping does not appear to change when the tree is pruned by removing 20% of the canopy by thinning. The damping for tree#11 (Spotted gum) also increases as $\overline{V}$ increases then stays approximately constant. The initial value of 5% increases to about 9-10% at wind speed of 4 ms^{-1} then remains constant. The graph in Figure 5.35 (vii) was generated with data from several wind events. If only data from 24 March 2008 is used there appears to be a linear relationship for damping and wind speed, indicated by the solid line. If all the data from several wind storms is added, the linear trend is not apparent and the damping appears to assume a constant value above about 4 ms^{-1}.

The damping did not correlate with any tree parameters such as DBH or tree height as found in previous studies (Moore and Maguire 2004, Jonsson et al. 2007). Damping was not constant (Wood 1996) and increases with increasing wind speed. Jonsson et al. (2007) suggests that this increase is due to stiffness and damping coefficients which are displacement dependent as found by Gardiner (1992). Their findings were based on values of damping determined using a pull and release test and the conclusions may not apply under high wind conditions. Damping may be more complex at higher wind speeds and not increase in a linear manner.

5.3.5 Dynamic Response Factor

When comparing data from each tree, it would be useful to quantify the dynamic response in some way. Previous studies have reported that tree failure occurs at wind speeds considerably lower than those predicted by static methods (Oliver and Mayhead 1994, Gardiner 1994) so if the dynamic response for a tree could be quantified, it may provide some insight into why there is such a difference between the static and the dynamic methods of analysis. Since the wind variation is quantified using a gust factor, it may be possible to develop a similar concept for the dynamic response and apply this to trees. The gust factor is defined as the ratio of the maximum wind speed divided by the mean wind speed. Gardiner et al (1997) used the term gust factor as the ratio of maximum to mean bending moments with values ranging between 9.1 to 12.7 for field measurements and 4.0 to 8.1 for wind tunnel tests.

The concept of quantifying the additional loads on buildings and engineering structures due to wind induced dynamic motion is used in the Australian Wind Code (AS/NZS 11702.:2002) and is termed the "Dynamic Response Factor" (DRF). A similar concept has been applied to trees (Sellier and Fourcaud 2009) and termed the "Dynamic Amplification Factor" (DAF).

The engineering definition of the DRF is complex and includes height of the structure, turbulence intensity of the wind, peak and background factors, resonance response, size reduction factors, turbulence spectrum and damping ratios. This definition may not be directly applicable to trees but there are some useful guidelines which could be considered including;

1. DRF=1 for frequencies above 1 Hz.
2. For tall buildings, frequencies less than 0.2 Hz are not considered.
3. DRF applies between frequencies of 0.2 to 1 Hz.

These guidelines could be useful for trees as it limits the application of a dynamic factor to trees which are neither too small, nor too big which seems appropriate for the open grown trees of this study.

The DAF applied to trees by Sellier and Fourcaud (2009) is defined as the ratio of the maximum displacement under turbulent wind to the displacement caused by the static, instantaneous wind force. DAF was calculated at breast height and at the base of the live crown, with values quoted between 0.98 and 1.19. These values seem low because the DAF is based on displacements, which at breast height would always be small.

The bending moments of trees at the base are large so if bending moment data rather than displacement data are used, the dynamic response ratio between maximum and mean values could provide a useful measurement. It is therefore proposed that a dynamic response factor (DRF) taken from engineering wind codes be applied to trees and be defined as the ratio of maximum base moment to mean base moment over some time period.

$$DRF = \frac{M_{Max}}{\overline{M}} \qquad (5.9)$$

The DRF from Equation 5.9 was calculated from 30 minute data files for each tree, using the same data files that were used to calculate the damping in the previous section. Each point represents a 30 minute period and graphs of DRF for each tree are plotted against mean wind speed in Figure 5.36.

For all trees tested, the dynamic response factor appears to be approximately constant with wind speed though there is considerable spread in the data. The value of DRF may be distorted at low mean wind speeds if a single gust or a wind change occurs during a 30 minute period. A single gust would give a high maximum yet the mean would be low over the thirty minute period and this would result in a high value for the DRF. Some of the data points exhibit this characteristic which occurs in intermittent or low winds. The highest DRF value occurs with tree#7 (palm) which has a DRF $\cong$7 and a maximum value of 9.3 over the wind speed range of 0-9 ms^{-1}. Tree #4 (Italian cypress) has a DRF $\cong$ 6 which appears to decease slightly at wind speeds above 5 ms^{-1}. For all other trees the DRF ranges in value from 3 to 5 with the largest and stiffest trees (trees #8,#9 red gum, tree #10, Agathis) having the lowest values.

The effect of removing 20% canopy by thinning on tree#8 (Red gum) does not significantly change the DRF (Figure 5.36(iv)). In an attempt to identify any difference in the data before and after pruning, a line of best fit was included for this graph. The trend line after pruning does indicate a slight reduction in the DRF value but there is not enough data to confirm any difference. Moore and Maguire (2004) suggest that up to 80% of branches need to be removed before any noticeable dynamic response changes so the lack of any difference in the DRF on tree#8 due to 20% removal of the canopy by pruning is not unexpected.

The DRF could be a useful measure to evaluate a tree's dynamic response in gusty wind conditions and to compare different species of trees. It may also be useful for estimating damping of the tree. Damping dissipates energy per oscillating cycle and the application of a DRF may be useful for evaluating the effect of removing branches which may increase dynamic sway because the damping effect of branches is removed from the tree.

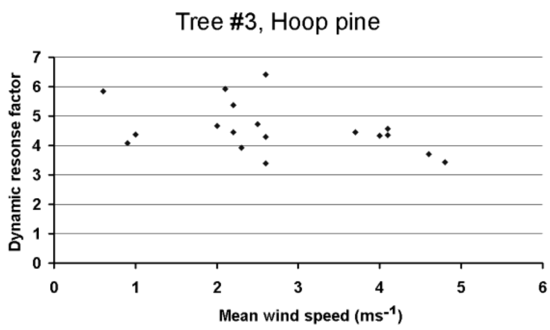

(i) Tree #3, Hoop pine (Araucaria cunninghamii)

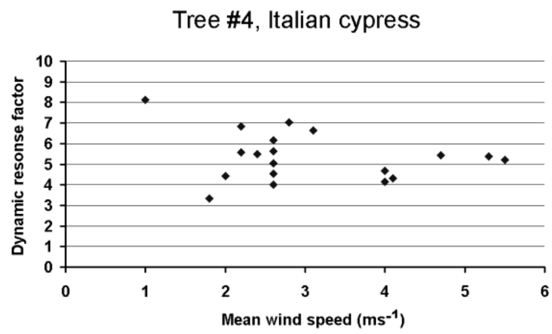

(ii) Tree #4, Italian cypress (Cupressus sempervirens)

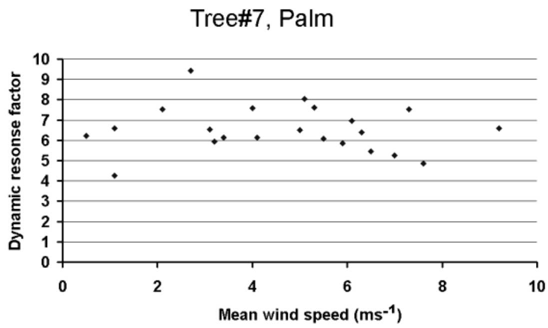

(iii) Tree # 7, Palm tree (Washingtonia robusta)

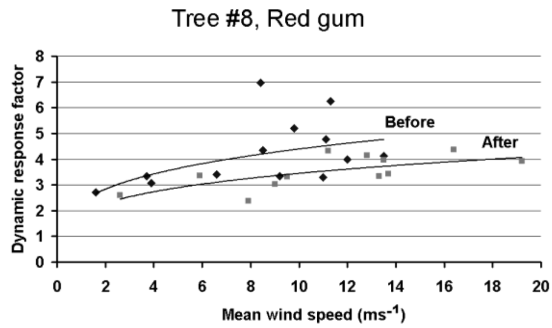

(iv) Tree #8, Red gum (E. tereticornis)

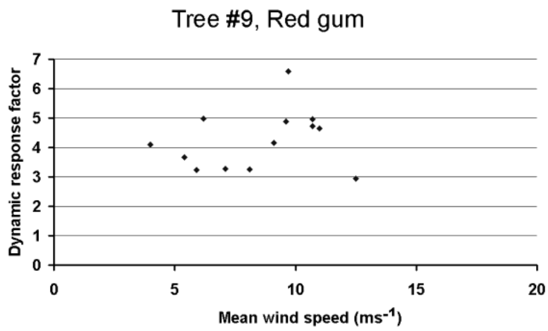

(v) Tree #9, Red Gum 2 (E. tereticornis)

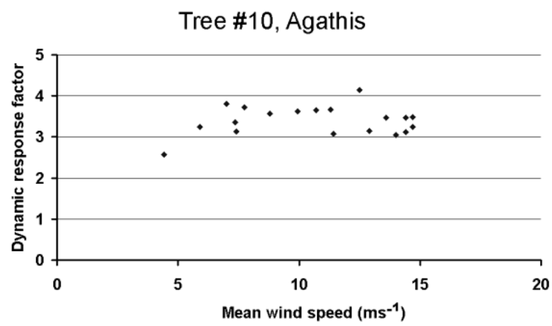

(vi) Tree #10, Agathis (Agathis australis)

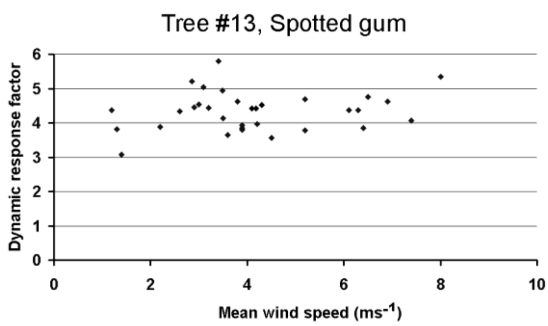

(vi) Tree #13, Spotted gum (Corymbia maculata)

Figure 5.36. Dynamic response factor for trees plotted against mean wind speed.

Chapter 6. DISCUSSION

6.1 Tree Dynamics and Mass Damping

The response of trees to wind loading presented in the previous chapter has been analysed using mathematics that describe a single degree of freedom (SDOF) system. The mature open grown trees used in this study have significant mass in their canopy which consists of dynamically swaying branches and leaves. Branch morphology of tree species is very diverse (Evans et al. 2008) and the dynamic contribution of branches will depend on the size, shape and orientation within the canopy to create a commensurately diverse and complex dynamic system. The open grown trees used in this study are essentially a collection of branches and how these branches dynamically interact with each other and the trunk to produce the overall tree response is the focus of this discussion. The wind loads on all the individual branches must travel down through the trunk and into the ground if the tree is to remain stable. By putting the strain meters on the trunk at the base, the complex force effects of all the branches collectively are measured and so the results give a measure of the total instantaneous wind load effect on the entire tree.

Previous studies reviewed in Chapter 3 have considered the tree as a pole or with a canopy with the masses rigidly attached to a central trunk (Guitard and Castera 1995). These models are either poles that may have different modes of sway or are SDOF systems which oversimplify the complex dynamic response of trees. The new model proposed in this thesis (Figure 3.10) treats the branches as dynamic masses attached to other dynamic masses so that a complex multi-degree of freedom (MDOF) system is described. It is suggested that his model is more appropriate for trees because the dynamic contribution of branches can be described.

A SDOF system will have only one mode of oscillation, usually called the fundamental or first mode which occurs at one specific frequency. The spectral plot of a SDOF system will show one peak, at the frequency known as the natural frequency for that system. More complex dynamic systems that are either poles with distributed mass, or several independently vibrating masses are known as MDOF systems which can have many modes of oscillation. The term mode can have two meanings in vibrating systems and may describe either;

(i) harmonics of a fundamental frequency in which a vibrating element like a beam may vibrate with different shapes at a primary, secondary, tertiary, and higher frequencies, or

(ii) modes of a MDOF system in which vibrating masses may sway in-phase or out-of-phase with each other. These two interpretations of modes are shown in Figure 6.1.

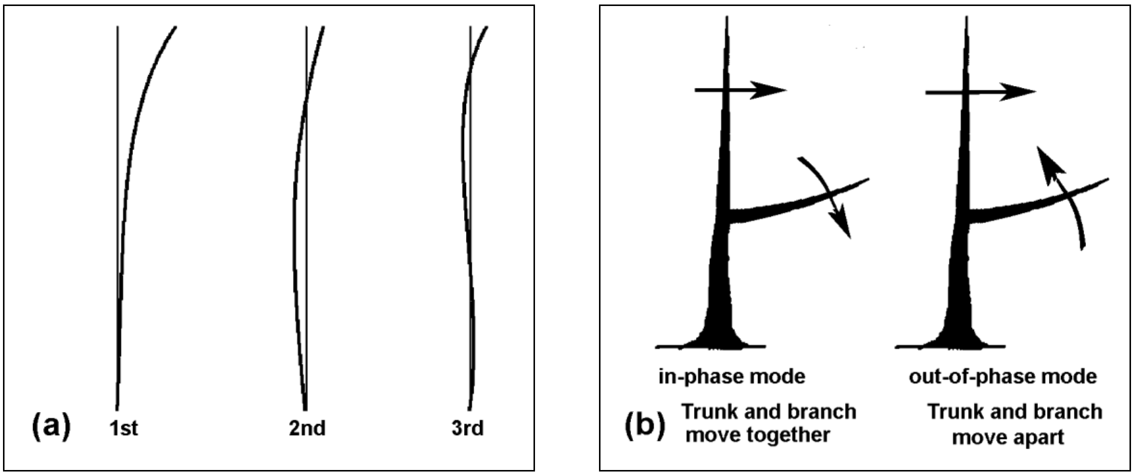

Figure 6.1. Two descriptions of modes in vibrating structures. (a) harmonic modes in a beam with 1st, 2nd and 3rd order harmonics and (b) modes in a 2DOF structure like a simple tree with two oscillating branches showing in-phase mode and out-of-phase mode.

The dynamic response of these two different systems is dramatic. For a pole or beam, the vibration may occur at the first mode or the second or third (or more) modes, each at different frequencies. The higher modes are known as harmonics of the first mode and appear as peaks on a spectral plot (Figure 6.2a). The amplitude and area under the curve represents the energy in the oscillations, and in Figure 6.2a, the greatest energy occurs at the fundamental or first mode, with progressively less energy in the higher order modes.

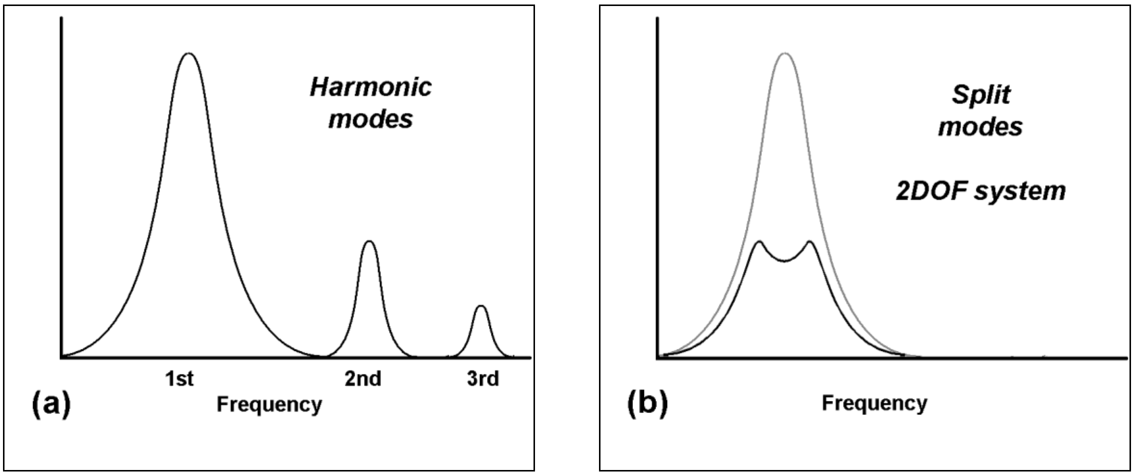

Figure 6.2. Spectral response of different modes. (a) harmonic modes showing 1st, 2nd and 3rd order modes at different frequencies, and (b) split modes of a 2DOF system showing two peaks at frequencies near the 1st mode and a reduction of amplitude and area under the curve.

The second system of two vibrating masses (a 2DOF system) could represent a simple tree model with two branches. The two masses can oscillate with two possible modes, either together from side to side in unison, or apart in opposition to each other (Figure 6.1b).

This 2DOF system has been described in Chapter 4 and introduces the concept of mass damping which only becomes apparent when two or more oscillating masses interact. The ratio of the two masses is important and when the masses are nearly of equal size, the effect on the dynamic response is dramatic and very different to the first case described. As the two masses oscillate, the effect is to reduce the amplitude of vibration and to develop two closely spaced frequencies (Figure 6.2b). The area under the curve representing the energy in the oscillations is also greatly reduced. There are no higher order harmonics present.

When dynamic masses are attached to other dynamic masses, as described in the model of trees (Figure 3.7), the resulting dynamic response depends on the mass ratio described above, and also on the other dynamic properties of the spring constants and the damping values of each element. The spring constants are related to the Young's modulus of a trunk or branch and cannot be considered constant for any one tree. Great caution should be exercised in treating the mechanical properties of botanical materials like wood as constants since they vary with the age and relative moisture content of the sample. (Niklas 2002). The Young's modulus value for new wood is different to older wood. As wood ages it changes its elastic properties and gradually becomes stiffer. Wood of Scots pine (*Pinus sylvestris L.)* that was one to five years old had Young's modulus values of 1.7 – 7.9 GN m^{-2} and this value gradually increased until a maximum of 7.9 GN m^{-2} was reached after 25 years then remained essentially constant (Mencunccini et al. 1997). The implications of this variation of Young's modulus on the response of a MDOF dynamic system will be to increase the complexity of the response and to further reduce any likelihood of a peak resonant oscillation occurring. This needs further examination but is beyond the scope of this study.

For open grown trees in this study, it has been found that only the first harmonic mode of sway occurs due to wind excitation, with one exception being the Italian cypress which exhibits a second harmonic mode and appears to be a special case. This is considered to be important because some studies of tree sway have reported a first and second harmonic mode (Jonsonn et al. 2007) but only from a pull and release test and not under wind loading. There is an implication that the second mode which occurs in the pull and release test also occurs in wind conditions but the data from the current study have found this not to be so.

It is also important to comment on the size and shape of a tree. As a tree shape becomes like a pole so the dynamic response approaches that of a pole and the second harmonic mode will appear. This occurs when most of the mass is located in the central trunk such as in a plantation tree, or when a tree has all its branches removed as in the case when it is being felled. Plantation trees have most of their mass in the central trunk, have a small canopy and have a slenderness ratio often greater than 80. These trees have a dynamic response similar to a slender cantilever beam and may develop a second harmonic mode of sway. Moore and Maguire (2005) found that up to 80% of the branches need to be removed from conifers before there is a significant change in the dynamic response of trees. Moore and Maguire emphasised the importance of branches and their contribution to damping and minimising dangerous sway motions and suggested that treating branches as lumped masses rather than individual cantilevers attached to the main stem may not be appropriate.

Sellier and Fourcaud (2009) studied the mechanical response of a 35 year old maritime pine (*Pinus pinaster*) subject to static and dynamic wind loads and found that small morphological variations in the tree can produce extreme behaviours such as either very little or nearly critical dissipation of stem oscillations. Spatz et al. (2007) offer an explanation for the interaction of branches and the effect on damping which they termed multiple resonance damping. They proposed that trees constitute systems of coupled oscillators tuned to allow optimal energy dissipation. This occurs because the tree trunk spectrum has a frequency range which overlaps that of the primary branch which in turns overlaps that of a secondary branch (Figure 6.3).

The explanation of Spatz et al. (2007) does not account for the observed multiple peaks in the tree spectral response which are centred on the natural frequency of the tree. Since the natural frequency depends on stiffness and mass ($\varpi = \sqrt{k/m}$), the trunk and branch natural frequencies will overlap and interact when the natural frequency of the branch is nearly coincident with that of the trunk which in turn splits the modes in the manner illustrated in Figure 6.2b. This dynamic interaction is dependent on the natural frequencies which are determined by the mass and stiffness of each oscillating element.

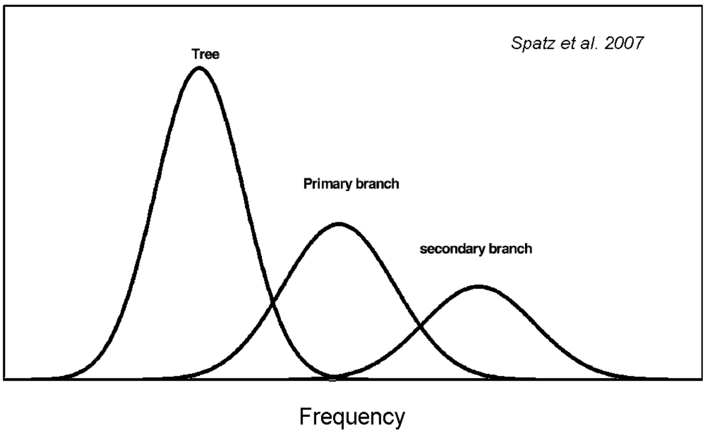

Figure 6.3. Suggested overlap of resonance spectra for trunk and branches, being a prerequisite for transfer of mechanical energy (Spatz et al. 2007).

This is further illustrated in Figure 6.4 and supported with an explanation by Connor (2002) who discusses the case of a 2DOF system consisting of an un-damped mass and a damped mass damper. The magnification factor (termed amplification factor H_2, Connor 2002) is shown for specific values of mass ratio ($\overline{m}$) and frequency ratio *(ρ)* and changes depending on the value of the damping ratio (ζ_d).

For the mass ratio ($\overline{m}$ =0.01) and when $\zeta_d = 0$, there are two peaks with infinite amplitude located on each side of ρ =1. As ζ_d increases, the peaks approach each other and then merge into a single peak located at $\rho \approx 1$. When $0 < \zeta_d < 1$, there are two peaks, one for the main structure and the other for the damped mass. The amplitude is greatly reduced and the behaviour suggests that there is an optimal value of ζ_d. A key observation is that all curves pass through two common points, P and Q. Since these curves correspond to different values of ζ_d, the location of P and Q (common points) must depend only on mass ratio ($\overline{m}$) and frequency ratio *(f)*.

This illustrates the operation of a mass damper and shows that for a small mass which is only 1% of the primary mass, the amplitude and energy of oscillation can be dramatically reduced, depending on the damping of the second mass. Other similar examples for a 2DOF system are presented by Den Hartog (1956). The equations to the curves in Figure 6.4 are for a 2DOF system and are even more complex for a MDOF system with many masses.

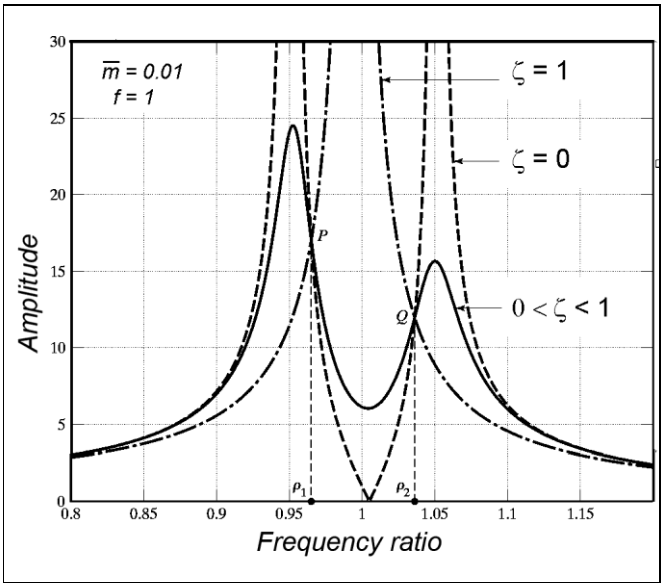

Figure 6.4. Variation in amplitude of the structural magnification function (H_2) for two masses of a TMD and the change of damping ratio ζ_d (Adapted from Connor 2002).

It is proposed that mass damping occurs in trees due to the branches acting as oscillating masses. By extending the 2DOF mass damping system described in Figure 6.4 to a more complicated MDOF system as described by Abe and Fujino (1993), a dynamic model for a tree may be developed that includes the trunk and the many branches. The effect of mass damping is to create a complex spectral plot of a transfer function which in trees would appear as a series of peaks, each with amplitudes much less than the amplitude of a single isolated trunk, and a spread in the range of frequencies depending on the modes created, but centered about the primary frequency of the trunk. Such a spectrum for an urban tree is shown in Figure 6.5 which shows the response for tree#9, Red gum under wind loading over a thirty minute period. This is a mature tree with a central trunk and several main branches that support a canopy of smaller branches attached to the main branches. The collection of oscillating branches creates a MDOF system in which mass damping effects show up as a range of peaks in Figure 6.5. These peaks have a spread in frequency from 0.2 to 0.7 Hz and are centered on the trunk primary frequency of 0.35 Hz. The spectral plot is generated from the bending moment response under wind excitation and is representative of all data from this tree. A theoretical curve based on a SDOF equation for the structural magnification function is fitted to the data and biased so that the area under the curve is equal over the frequency range of 0.2-0.4 Hz. This gives an estimate for the natural frequency of the structure (f =

0.345 Hz) and the damping ratio (ζ = 7.5 %) at the wind speed of V_{max} = 14.4 ms^{-1}, and V_{mean} = 8.4 ms^{-1}.

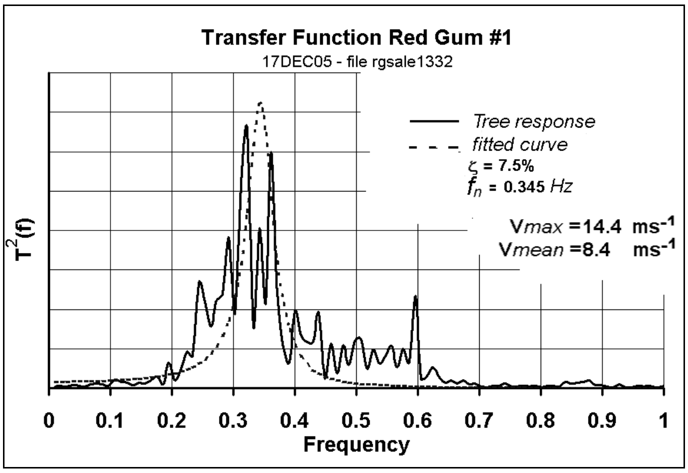

Figure 6.5. Spectral response for tree#9, Red gum (*E. tereticornis)*, showing a range of peaks centered on the fundamental frequency of 0.345 Hz.

The SDOF curve does not fit the tree response which has two peaks between 0.3-0.4 Hz and several other peaks between 0.2-0.7 Hz. The peaks at different frequencies indicate a MDOF system with modes developed by the branches acting as mass dampers. The explanation of overlapping frequencies by Spatz et al. (2007) would not explain the low frequency peaks between 0.2-0.3 Hz and the curve above 0.3 Hz would be smoother if a simple overlapping of branch natural frequencies occurred.

At the other extreme, a palm having no branches does not show the range of peaks in the spectral response to wind loading and a SDOF curve is a good approximation (Figure 6.6).

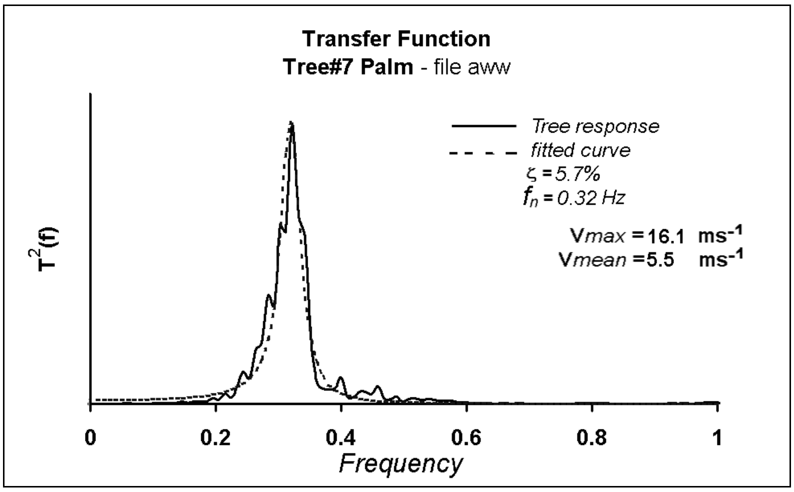

Figure 6.6. Spectral response for tree#7, Palm (*Washingtonia robusta*), showing single peak at the fundamental frequency (0.32 Hz).

Although the palm has no branches, the mass in the fronds may contribute some element of mass damping effect and it is interesting to note the small peaks in the response curve in Figure 6.6 at 0.4-0.5 Hz but these are probably due to “noise” in the data.

The Italian cypress, tree#4, is a tree with a very different response to the other trees in this study because there are two peaks appear in the curve the transfer function (Figure 6.7). The first and largest peak occurs at 0.27 Hz and the second smaller peak occurs at 0.62 Hz. The large peak at 0.27 Hz is the first or primary mode of sway and the second smaller peak at 0.62 Hz is a second mode of sway. The smaller amplitude of the second peak indicates that much less energy occurs at this frequency than for the first peak. This second peak is not caused by a mass damping effect but is due to a 2nd harmonic mode as shown in Figure 6.1a. The Italian cypress is a tall slender tree with a canopy of branches which are tightly aligned with the trunk in an almost vertical arrangement. They tend to sway in unison with the tree rather than as separate branches, though there is some independent movement which develops a small mass damping effect as shown by the small peaks on the two curves in Figure 6.7. This is a good illustration of the difference between harmonic modes and split modes of sway as previously described.

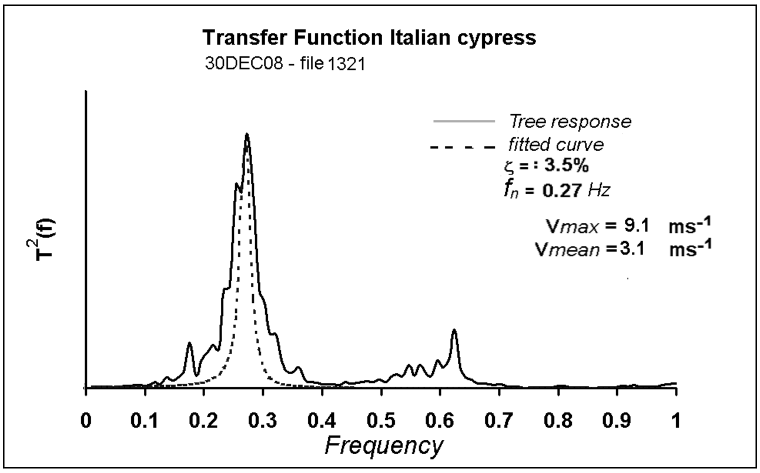

Figure 6.7. Spectral response for tree#4,Italian cypress (*Cupressus sempervirens)*, showing two peaks indicating a 1st and 2nd mode of sway.

For the trees studied, the sway response to wind occurred at the first natural frequency and there were no resonant dynamic effects at higher frequencies, except for the Italian cypress. The peak amplitude at the first natural frequency was not a tall defined peak as would be expected with a SDOF system and resonance did not occur. This is significant because Bell et al. (1991) suggested that tree failure at lower wind speeds than expected is due to a resonant dynamic effect that occurs when the wind gust frequency coincides with the natural sway period of trees. This is not supported by Baker (1997) who observed that there was a general lack of higher frequency harmonics in measured tree sway response to wind loading which indicates this resonant effect is of little significance in the occurrence of wind throw.

Results from the current study also show that trees do not resonate at a natural frequency but rather have a series of peaks spread over a range of natural frequencies and do not develop harmonic sways. Further, there are no higher mode harmonic sways except for tree #4, the Italian cypress which appears to be an exception. The wind peak is not at the same frequency as the tree peak so the energy transfer occurs over the spectral range associated with the "tail" in the wind spectrum.

6.2 Wind and Trees

A consistent observation from monitoring wind speed and wind loads on trees is that there is no direct temporal relationship between the two as would be expected. It seems intuitive that a large wind gust should result in a large response in the tree but this is not always the case. An example of a wind gust that does not result in a large sway response of a tree is shown in Figure 6.8.

In the time series shown, a large gust of wind is recorded at 70 seconds but the response of the tree occurs approximately 10 seconds later, and even then there is no single extreme bending moment response detected by the strain meters on the trunk. This is due to the dynamic nature of the wind and the tree response and a phase difference that can occur when the wind impacts at the moment the tree is swaying back into the wind.

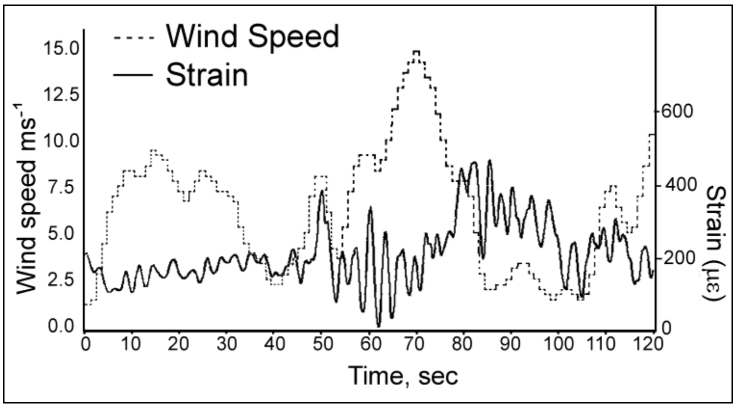

Figure 6.8. Time series graphs of one strain meter (με) on trunk at height of 1.3 m and wind speed (ms^{-1}) measured at height of 5 m above the ground. Experimental tree#8 (*E. tereticornis*), Sale, Victoria, 3 December, 2005. Strain measured at 20 Hz, wind speed 1 s average values (James and Kane 2008).

This effect was observed by Sellier et al. (2008) who compared the response of a finite element tree model to measured values from Maritime pine trees (*Pinus pinaster*) under wind excitation. The modeled trees exhibited strong similarities to the temporal behaviour of wind velocity but on the contrary the measured trees did not always respond to the recorded gust events. This lack of response to recorded gusts illustrates the difficulty in identifying drag forces based on wind velocity recordings that are not in the immediate vicinity of the tree. Sellier et al. (2008) did not offer an explanation but it seems that the wind gusts and tree sway may not always be in phase. Some gusts in phase with the tree sway would increase the displacement response, and at other times may be out of phase in which case the displacement response would be much less than expected.

The tree response is complex with no clear relationship to wind speed. Even in slender plantation trees, Gardiner (1995) found tree movement correlated with wind gusts but not very well, in a stand of Sitka spruce with a slenderness ratio or 116. The lack of a clear relationship between wind speed and tree response was reported by Blackburn et al. (1988) who used accelerometers to measure the response of a Sitka spruce tree. Figure 6.9 shows dynamic displacement response which is calculated from accelerometer measurements in the upper part of the tree.

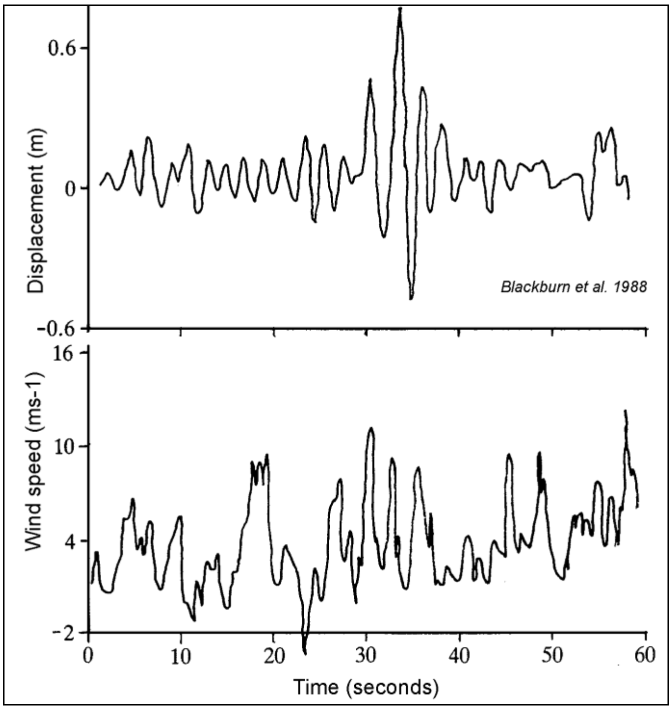

Figure 6.9. Time domain data of wind speed and tree response from along wind displacement of a Sitka spruce (*Picea sitchensis*) at height 12.7 m high, slenderness ratio 88. Wind speed measured at height of 11.4 m (Blackburn et al. 1988).

The wind load over a 60 second period. Similar wind gusts at 20 s and 30 s do not produce the same tree response.

Although there is no clear relationship between instantaneous wind speed and bending moment, it would be useful to be able to estimate the wind loads for a tree at different wind speeds so that the loads can be evaluated with stability tests such as the static tree pull. This is not to say that it is possible to predict failure because although the wind load may be estimated, the strength of the tree may be more difficult to evaluate because of imperfections caused by decay, rot, or hollows which would all contribute to a reduction of tree strength.

It is probably not possible with current methods to predict failure in living trees but estimating wind loads would be a useful step in assessing tree stability.

There is very little published data available on wind load effects on trees as measured in base bending moments. Gardiner et al. (1997) measured base bending moments on Sitka spruce in Cumbria, UK and presented a ratio of the maximum to mean bending moments measured in the field and wind tunnel tests. Gardiner termed this a gust factor but it is probably better termed as a bending moment factor or a dynamic response factor.

Measurements were made with a similar technique to this study by using linear variable differential transformers (LVDTs) mounted on the stem at right angles to each other, at 0.5m above the ground. Eleven experimental trees, Sitka spruce (*Picea sitchensis*), ranging in height from 14.3 to 21.8 m and slenderness ratio of 54 to 89 were monitored from a stand in Cumbria, UK. Results indicated that the bending moments vary approximately as the square of mean wind speed, measured at the top of the canopy (Figure 6.10), though the bending moments are low compared to values measured in large trees.

Using the results from the Spotted gum, and taking the bending moment values calculated from Equation 5.6 (velocity exponent taken as 1.8065) the wind load for similar trees of different height can be calculated. This is a little speculative as it is based on the Spotted gum tree height of 23 m and assumes constant canopy area proportions and the same tree responses at different tree heights. The curve for wind speed at 30 m s^{-1} is also extrapolated from the 20 ms^{-1} data and is not based on measured data. More data are needed to confirm the curves in Figure 6.11 because trees of the same species, and even apparently identical adjacent trees, may not respond the same to wind loading (Baker 1997).

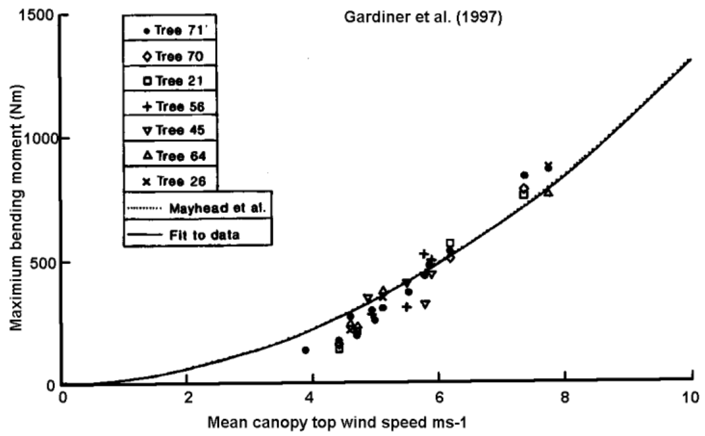

Figure 6.10. Field measurements of base bending moments (Nm) versus mean canopy top wind speed (ms^{-1}) of Sitka spruce (*Picea sitchensis*), UK, of height 14 to 21 m and slenderness ratio 54 to 89 (Gardiner et al. 1997).

To describe this difference, Baker used three categories of shape (Type I, II and III) based on their spectral response and noted that at any one tree size there is a fairly wide spread of values in natural frequency. This could result in significant variation in failure wind speed since the turbulent energy of the incoming wind decreases rapidly over the range from 0.1 to 1 Hz. Trees with a low natural frequency would thus react more strongly to fluctuations within the winds, with increasing displacements and base bending moments.

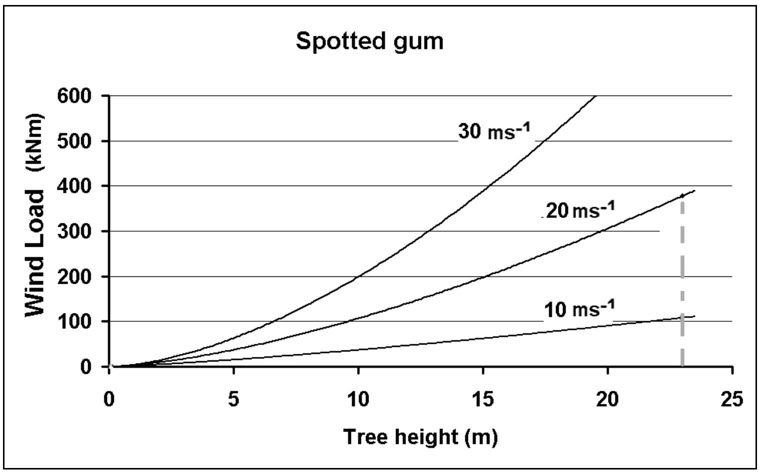

Figure 6.11. Wind load in base bending moments (kNm) versus tree height at different wind speeds. Calculations based on a 23 m high spotted gum (*Corymbia maculata*) (grey dotted line).

The peaks of the spectral response were not well defined in several trees which were of special interest because such trees had no preferred natural frequency when responding to turbulence fluctuations in the wind.

The importance of this lack of a direct relationship between wind gusts and tree response is that it minimises the energy transferred from the wind to the tree and so minimises the energy that may cause failure. The energy transfer is not only a function of frequency and damping but also of the phase relationship between wind and the tree. Under certain conditions the excitation of two or more branches can cancel each other out (Spatz et al. 2007). This is where the mass damping effect and the interaction of the branch dynamic masses with the main trunk mass becomes a critical factor. Further work is required to investigate other methods of measuring a tree's vulnerability to winds and to account for different species, different tree shapes and different tree environments. One such measure could be the dynamic response factor which quantifies how a tree will respond to wind gusts in storm conditions.

6.3 Spectral Analysis and Trees

Spectral analysis is used to identify frequency components in the turbulence mainly responsible for tree movement (Gardiner 1995) and to examine the energy transfer from the wind to the tree. The spectra of tree response at different wind speeds give a view of their energy at different frequencies and shifts in the spectra indicate changes in the energy transfer process. A comparison of the transfer function for Tree#8, Red gum 1 for two wind speeds indicates that there is a shift in the frequency response as the wind speed increases (Figure 6.12). The response at the lower wind speed (V_{max} = 9.6 ms^{-1}, V_{mean} = 6.6 ms^{-1}) has several small peaks between 0.2-0.4 Hz which are centered on a frequency of 0.31 Hz. At a higher wind speed (V_{max} = 17.6 ms^{-1}, V_{mean} = 11.1 ms^{-1}) the response shows peaks with a greater amplitude due to the higher energy transfer from the wind, and also an apparent shift in the frequency range of these peaks (0.2-0.7 Hz).

The fitted curve indicates a natural frequency of 0.34 Hz and it is apparent that there is more energy in the tree response with peak amplitudes at 0.5 Hz. It is suggested that the peaks at these closely spaced frequencies are due to the branches interacting with the main trunk and each other in a complex manner as described in the previous section, and illustrates the mass damping effect.

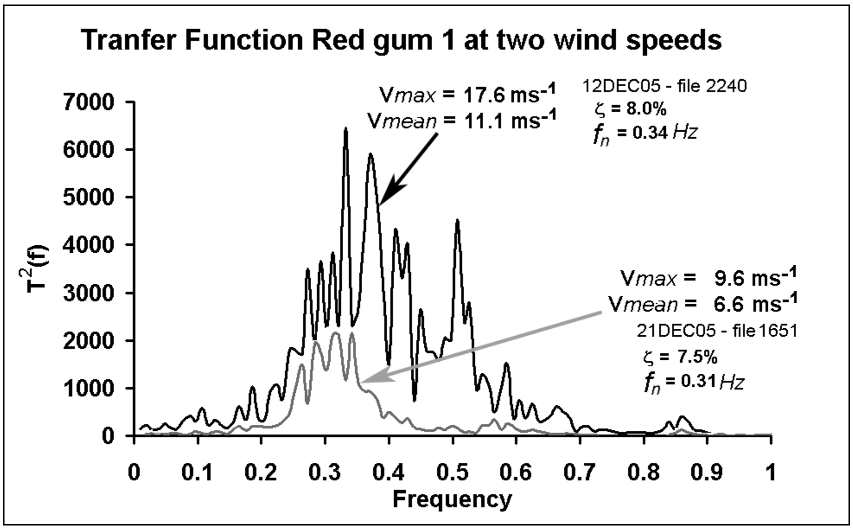

Figure 6.12. Transfer function of Tree#8, Red gum1 (*E. tereticornis)* for two wind speeds.

This is not a harmonic mode which would show up as a separate and distinct peak. There is a suggestion of a second peak at 0.85 Hz in Figure 6.12 but this is very small and is thought to be due to the anemometer noise which begins at around this frequency. A second harmonic mode as shown in Figure 6.6 for the Italian cypress has a distinct peak so for the red gum the second peak does not seem to be that of a second harmonic. This tree was 14 m high with a DBH=0.843 m giving a slenderness ratio of 16, so it is a very stable tree with a stiff rigid trunk, not a thin flexible tree like the Italian cypress, so it is unlikely to have a second harmonic mode of sway.

Rudnicki et al. (2008) examined the sway periods of lodge pole pine, (*Pinus contorta* var. *latifolia*) at two sites in Alberta, Canada. The trees were in closed forest canopies where the tree sway is thought to be mostly dampened by collisions with neighbours. Results from the Two Creeks site (Fig. 6.13a) indicates a change in the natural frequency of sway with wind speed. As the wind speed increases from 1.9-5.4 ms^{-1} there is a decrease in the frequency of the peak response from approximately 0.34 to 0.24 Hz. It was suggested that during the intense collisions experienced by these trees, kinetic energy was dissipated which resulted in the decrease in natural frequency. This change in natural frequency was not observed on the same species of trees in a closed forest environment at another site, Chickadee Creek, Canada (Fig. 6.13b) where the trees experienced more frequent but less intense collisions.

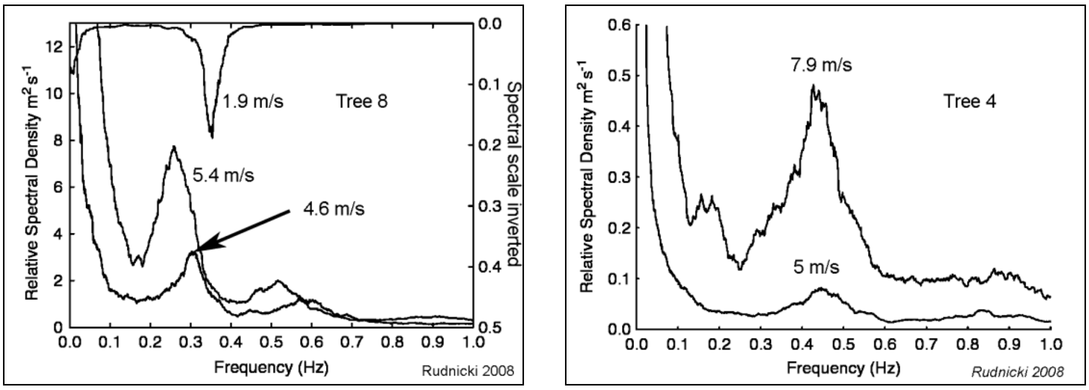

(a) *(b)*

Figure 6.13. Relative spectral density outputs for lodge pole pine, (*Pinus contorta* var. latifolia, tree#8), at (a) Two Creeks and (b) at Chickadee Creek, Alberta, Canada, for different wind speeds (Rudnicki et al. 2008).

The results of Rudnicki et al. (2008) indicate that the frequency response of a tree decreases with wind speed which is the opposite to the observed response of tree#8 (Red gum) in Figure 6.3.1. To check this effect on other trees, the transfer function at different wind speeds was found for a palm and a spotted gum (Figure 6.14).

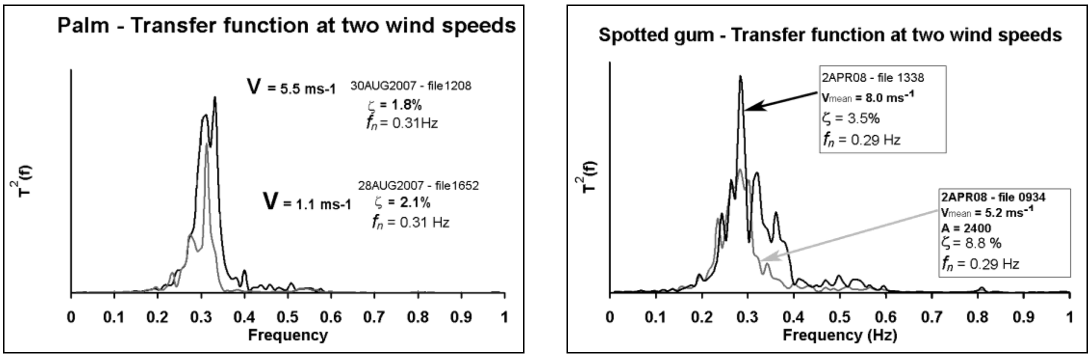

(a) *(b)*

Figure 6.14. Transfer function at two wind speeds for (a) palm tree (*Washingtonia robusta*) and (b) Spotted gum (*Corymbia maculata*).

There is an increase in the response for both the Palm and the Spotted gum at frequencies above the natural frequency which stays constant over the wind speed range that was measured. This is opposite to the response reported by Rudnicki et al. (2008) and appears to be due to more energy in the oscillating canopy which for the palm is composed of fronds and in the Spotted gum is composed of branches. Under wind excitation this effect is consistent among all the trees monitored.

6.4 Drag Force and Drag Coefficient

The drag forces due to the wind *(F(t))* on a tree are a function of the drag coefficient (C_D), the exposed area of the object (A) and velocity of the wind to the power n (taken as $n = 2$ for a bluff body, Equation 2.4). Trees are flexible structures that change their exposed area to the wind and also streamline their shape so that the effect of flexibility on drag is far from self evident (Vogel 1988). Mayhead (1973b) found that drag forces varied linearly with wind speed and not as the square, and that the drag coefficient also varied, but for simplicity, constant drag coefficients were developed for the tree species tested.

The results in this study of drag forces on trees, measured in base bending moments (Figure 5.17), indicates that different trees react differently under wind loading and that drag force was not proportional to the square of velocity (i.e. the velocity exponent $n \neq 2$). Speck (2003), suggests that drag force of trees is proportional to the square of wind speed (V^2) for wind velocities of 0 to 1 ms^{-1}, but as leaves realign themselves and the canopy shape streamlines to reduce the cross sectional area, the relationship reduces and drag is linearly proportional to velocity for wind speed values of 1.5 to 10 ms^{-1}.

The largest value was for the spotted gum where drag varied as $V^{1.8}$ (Figure 5.17g). This compares to values reported by Wood (1995) from wind tunnel tests on a scale model of forest trees who found that drag force does not follow the usual formula for a bluff body and is proportional to $V^{1.8}$ rather than V^2 at wind speeds between 0 and 27 ms^{-1}. For the other open grown trees in this study, the drag varied with $V^{1.5}$ for the red gum#2 and $V^{1.7}$ for the hoop pine, Agathis and red gum#1.

For the palm and the Italian cypress, the relationship between drag forces and wind speed was not the same as for the open grown trees. For the palm, the drag force varied as $V^{1.3}$ and for the Italian cypress drag force varied as $V^{1.07}$ for the wind speeds ranging from 0 to 15 ms^{-1}. These two trees are behaving quite differently under wind loading. The palm has a very flexible response in both the trunk and the alignment of its leaves. The looping nature of the sway response (Figure 5.8(iv)) shows that the palm sways around a central point and dissipates energy in both along and across wind directions. Not shown in these results is the large bending of the palm trunk which would significantly reduce the height of the top of the tree and move the canopy to a wind layer of lower speed. The palm leaves or fronds also realign themselves to a great extent and reduce the canopy area exposed to the wind and also streamline to reduce their drag. More work is required to gather data in high winds, but the results from this study indicate that for palms, drag is proportional to $V^{1.3}$, mainly due to their flexible response in winds.

The Italian cypress shows an almost linear relationship to wind speed which is the lowest exponent value of all the trees in this study. This tree has a dynamic response to winds that is different from all the other trees because it sways in a very flexible manner and exhibits a first and second harmonic mode of swaying which produces two distinct peaks in the spectral plots, as shown in Figure 5.30b. This flexible sway reduces the wind force on the tree so that it would experience lower wind loading than other trees at the same wind speed. Anecdotal reports indicate that this tree is not prone to failure in winds which may indicate that flexibility is a beneficial response for this tree.

Drag Coefficient

The discussion on drag force *(F(t))* and the determination of the velocity exponent (n) has so far assumed that the drag coefficient (C_D) and the area exposed to the wind (A) are constants. The canopy of a tree is flexible and will change its area and shape in high winds (Speck 2003, Rudnicki et al. 2004, and Vollsinger et al. 2005). Streamlining reduced frontal area by 54% for red cedar, 39% for hemlock and 36% for lodgepole pine in wind tunnel tests (Rudnicki et al. 2004) and also results in variable drag coefficients. During these tests on small trees, the frontal area of the crown was observed to increase from 0-4 ms^{-1} (Rudnicki et al. 2004). Detailed measurements were not made but it was observed that windward facing branches bent upwards and flattened perpendicular to the wind flow. Branches initially perpendicular to the wind lifted on the windward edge and rotated. In each case, the frontal area was greater at 4 ms^{-1} than in still air. As wind speed increased bending also increased and foliage began to realign with the wind so that frontal area decreased. This indicates that frontal area is not constant for trees and further work is needed to determine how this affects the calculations on drag forces in winds.

Mayhead (1973) found values of drag coefficient for lodgepole pine (0.20) and for western hemlock (0.14) at wind speeds of 30 $m\ s^{-1}$ and using full frontal area. Mayhead et al. (1975) obtained values of 0.35 at 26 ms^{-1} for lodgepole pine and recommended using this value for calculating windthrow.

Rudnicki et al. (2004) obtained values from wind tunnel tests of 0.22, 0.47 and 0.47 for redcedar, hemlock and lodgepole pine respectively at 20 m s^{-1}, using full frontal area. However the drag coefficient values increased to 0.6, 0.9 and 0.8 respectively when the wind-speed-specific frontal area was used for the calculations.

Volsinger et al. (2005) used wind tunnel tests to establish drag coefficients using similar methods to Rudnicki et al. (2004) and found values similar for hardwood trees (0.22) at 20 m/s. The hardwood drag coefficients are less than half the values typically reported for needled conifers (0.4 to 0.5). It was not clear why some trees like bigleaf maple have higher drag coefficients than other species and further study was suggested due to the complex relationship between crown-level drag and stem, branch axis, and leaf components.

The drag coefficients determined for the trees in this study were constant for the Italian cypress but for all other trees tended to decrease with increasing wind speed (Figure 5.34). The values are generally higher than found in wind tunnel tests (Rudnicki et al. 2004, Vollsinger et al. 2005) which may be due to the methodology used or a difference in scale between full grown trees and small test trees. Vollsinger et al. (2005) states that the uncertainties associated with scaling wind tunnel tests on small trees to large or old trees, means the values of drag from wind tunnel tests are best suited for windthrow risk evaluation in young or plantation trees. Further study is clearly needed to refine the methods and determine more accurate values of drag coefficients for trees.

The method of spectral modeling used to calculate the drag coefficient uses averages of data so the fluctuations in wind speed and wind loads are not evident. This is essentially a quasi-static approach and requires some assumptions regarding the height of the wind force (h_m) and how the theoretical magnification curve is fitted. For drag calculations the curve was fitted to the static range of the spectral data because this is where the average or quasi-static response of the tree is apparent. If the curve was fitted to the inertial range, the assumptions are no longer valid and the averaging method does not match the tree response so the values for drag are overestimated (Figure 6.15).

These assumptions mean that the drag coefficient calculations are not precise but since each point on the graph represents 30 minutes of data, there is a general trend that can be seen for each tree. The palm has the most change in the drag coefficient with the initial value of 1.5 at 1 ms^{-1} falling to 0.4 at 9 ms^{-1}. The other trees represent open grown trees with many branches and the drag coefficient was essentially constant but with a trend to decrease with increasing wind speed, but not definitively.

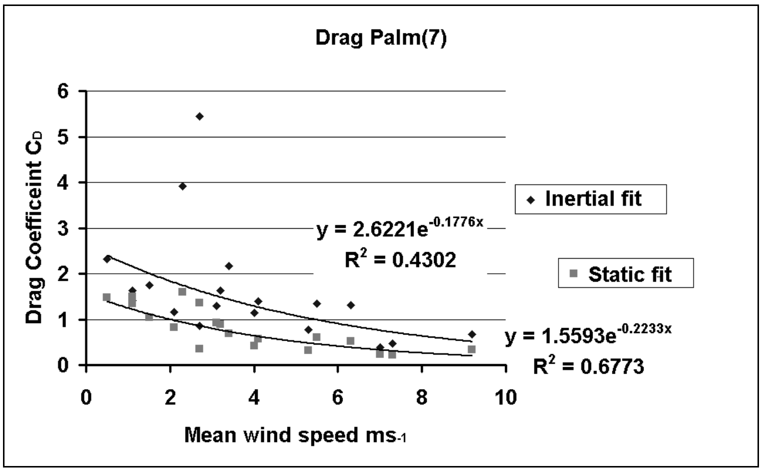

Figure 6.15. Drag values for palm (*Washingtonia robusta)* using different curve fitting criteria.

The effect of removing 20% of the canopy on tree#8, red gum, reduced the drag coefficient from 1.4 before pruning to 0.6 after pruning. Little work has been published on the effect of removing leaves but some supporting information was presented by Roodbaraky et al. (1994) in an investigation of the behaviour of open grown trees in high winds. It was found that for a tree in leaf the natural frequency was lower and the damping higher than when not in leaf. Drag coefficients were substantially greater when the tree was in leaf, than when it was not in leaf. However, these experiments did not lend support to the hypothesis that tree drag is proportional to velocity, rather than V^2, as has been previously suggested.

6.5 Energy Transfer and Damping

The energy in the wind transfers to the tree which responds by swaying, but because wind energy is difficult to measure and it is common to use wind speed as the indicator of wind energy. As wind speeds increase to critical values, the energy transfer to the branches and trunk may exceed their load bearing capacity and cause failure. The different wind speed ranges and their effect on trees are detailed in Table 6.1, with velocity expressed in several different units that are commonly used.

Understanding how energy is transferred to the tree and is absorbed or dissipated is necessary in order to understand the complex damping that occurs in trees. Wind energy is absorbed by trees at all its natural frequencies but most is absorbed at the first natural frequency (Holbo et al. 1980, Mayer 1989, Peltola 1996).

Tree Effect	Wind speed			
	mph	knot	kph	$m\ s^{-1}$
Leaves rustle	4-7	3-6	6-11	2-3
Whole trees in motion	32-38	28-33	51-61	14-17
Twigs break	39-46	34-40	63-74	17-21
Branches break	47-54	41-47	76-87	21-24
Trees break, or uproot	55-63	48-55	89-100	25-28
Hurricane	73<	63<	117<	33<

Table 6.1. The effect on trees of wind at different speeds (Cullen 2002a, 2002b).

It is therefore important to establish the tree's dynamic response and find the natural frequency and damping. Energy dissipation is caused by damping characteristics which for trees has been grouped into internal and external damping (Hoag et al. 1971). Internal damping is due to energy dissipation in the wood material of the trunk and branches, and in the roots and soil below ground level (Wood 1996, Moore and Maguire 2004). External damping is due to aerodynamic drag of the leaves and collision with neighbours in plantation trees (Milne 1991). The ratio of damping between contact, aerodynamic and stem/roots was reported as ~ 50/40/10 % (Milne 1991). The assumption that the trees in this study were rigidly anchored to the ground was not tested but there was no observed movement of the root plate for any trees during the testing period and the ratio of 10% for root related damping (Milne 1991) suggests that only any small movement would not greatly change the values of overall damping that were calculated.

Energy dissipation mechanisms in trees are not completely understood (Jonsson et al. 2007) but are known to be complex. It is common to combine all the damping components and assume viscous damping (Moore and Maguire 2004, Jonsson et al. 2007) which implies that damping is proportional to velocity. However damping is found to be non-linear (Moore and Maguire 2004) and amplitude dependent (Gardiner 1989) and the aerodynamic damping increases with wind speed (Wood 1996).

The results presented in Figure 5.35 confirm that damping for the trees is non-linear with respect to wind speed. Damping increases from $\mathbf{V}_{wind} = 0$ to some maximum value and then remains approximately constant or may even decrease in some cases. The value of damping at zero wind speed is determined from the pull and release test which does not capture all the components of damping that occur in winds. The damping at zero wind for trees studied varies from 3 to 5 % then increases to a maximum value which was 16% for tree #8, Red gum at 10 ms^{-1}. After this point, damping decreased at higher wind speeds to approximately 10%. This decrease at higher wind speeds was most evident for the Palm where the maximum value of 9% at $\mathbf{V}_{wind} = 6$ ms^{-1} decreased to 4% at $\mathbf{V}_{wind} = 9$ ms^{-1}. These values are determined from mean wind speeds over 30 minute periods and more data at the higher wind speeds are needed, but the trends in damping appear in all trees monitored. However, no clear relationship between damping and wind speed is apparent and this was also reported by Jonsson et al. (2007), who suggested that more complex models are needed to explain the non-linear relationship.

Damping is dependent upon amplitude of the oscillation (Clough and Penzien 1993, Moore and Maguire 2004) and Gardiner (1992) suggests that damping increases because both stiffness and damping are displacement dependent, but this may be true only for the pull and release test in still air conditions. The effect of branch removal and pruning is also likely to change the dynamic response of trees. In a study of plantation Douglas fir trees, Moore and Maguire (2005) found that up to 80% of the canopy needed to be removed before significant changes in the dynamic response of the trees was observed. This indicates that only one or two branches are needed to create significant damping and trees with a full canopy may have significant redundancy in damping due to their many branches as a result.

Energy dissipation due to branch oscillation has been reported previously and termed mechanical or structural damping (Scannell 1984, Niklas 1992, p183, Bruchert et al. 2003, Spatz et al. 2006). The term mass damping is taken from engineering texts (Connor 2002) and has been applied to trees (James 2003, James et al. 2006) and specifically relates to dynamic interaction of masses in a MDOF system (Den Hartog 1956, Connor 2002). The 2DOF system has been extended to a MDOF system with multiple tuned mass dampers (Abe and Fujino 1994) which is the basis for the model presented in this thesis.

Moore and Maguire (2008a, p82) suggest that trees transfer energy from the main axis to the primary branches and then to higher order branches and this requires the overlap of frequency bands of each element. This is similar to the concept described by Spatz et al. (2007).

It seems more logical to argue that the energy transfer is in the reverse direction and since the wind is the source of the energy, the transfer is from the wind (E_{wind}) to the leaves and branches ($E_{branches}$) of the canopy resulting in the complex sway response (Figure 6.16).

The energy in the canopy ($E_{branches}$) transfers either down via the trunk (E_{trunk}) then into the ground (E_{ground}) or via the leaves back into the wind stream as a series of small eddies (E_{eddy}). If trees have evolved to optimize themselves in order to survive, it is preferable to minimize the energy transfer from the canopy via the trunk to the ground. Logically, this requires that a maximum amount of energy should be returned to the air stream. Gardiner (1995) suggest that trees modify the turbulence spectra and short circuit the normal energy cascade process which may be a design feature that allows energy absorbed by the tree to be efficiently re-emitted as high frequency wake turbulence from needle and branch tips and which provides a method for reducing the growth of destructive resonance.

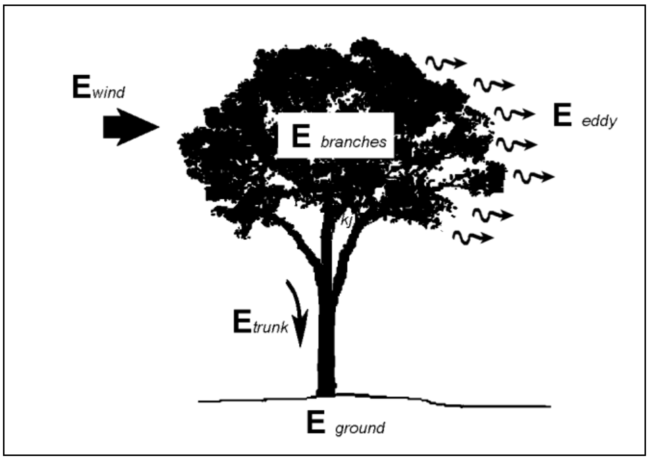

Figure 6.16. Energy transfer from the wind (E_{wind}) to the canopy ($E_{branches}$), and then either through the trunk (E_{trunk}) to the ground (E_{ground}), or via leaves and eddies (E_{eddy}) back to the wind.

This concept is supported by Scannell (1984) who found that the resonant frequency of the branches of spruce trees corresponds to a harmonic of the whole-tree frequency and the sub-branch resonance is a harmonic of the branch frequency, and so on down to the smallest scales on the tree. In this way energy absorbed by the whole tree can be transferred efficiently through the branches and sub-branches to the needles and re-emitted as wake turbulence at much higher frequencies. This is suggested as an extremely effective method for rapidly dissipating energy absorbed from the wind at a leaf sized scale where viscosity forces can act.

Vogel (1996) discusses storm resisting features of trees and suggests that it is the flexible nature of trees, including the leaves, branches, trunks and roots that allows trees to absorb and either store or dissipate energy. In a study of individual leaves in a wind tunnel, Vogel found that the drag and aerodynamic properties of leaves at high wind speeds indicate that the viscous forces at the leaf level are significant and collectively could account for the energy transfer. The small physical size of leaves and the rapid movement of leaf flutter is sufficient to make viscosity a significant factor at high wind speeds. This was indicated by the drag of white oak leaves which was quoted as being proportional to the cube rather than the square of wind speed (Vogel 1989, p945). It is possible that these viscous forces occur over the many leaves of a tree and collectively provide a mechanism to transfer energy back into the wind.

Baker and Bell (1995) discussed the energy transfer from wind to trees in a study on open grown trees at Nottingham University and suggested that the effect of varying natural frequency and damping changes the position of the resonant peak of oscillation relative to the wind spectrum. A low natural frequency means the resonant peak lies within the range of substantial wind energy, and a high natural frequency lies within the range of progressively decreasing wind energy. This effect can be represented on a spectral plot (Figure 6.17) in which the different energy components in Figure 6.16 can be shown at their respective frequency ranges. The high energy wind peak (E_{wind}) occurs at the low frequency range, the tree energy (E_{trunk}) occurs in the medium frequency range (about 0.3 Hz). The energy in the branches ($E_{branches}$) occurs at a slightly higher frequency range to the trunk and energy in the eddies (E_{eddy}) are smaller peaks occurring at higher frequencies. Baker (1995) makes an interesting point that for a tree to be fully loaded it must be enveloped by a gust of about three seconds duration or 0.33 Hz. He suggests that any energy from wind gusts above this frequency will play no part in the tree failure.

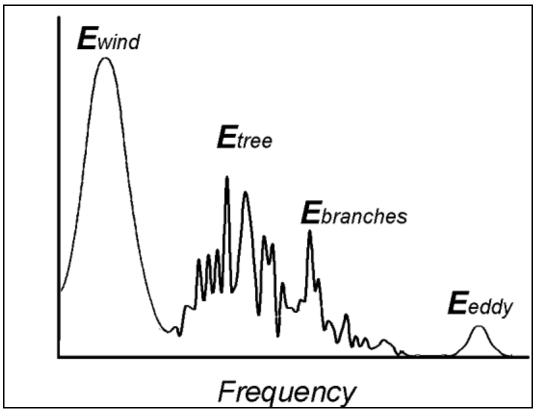

Figure 6.17. Spectra of wind, tree, branches and eddies showing different frequency ranges.

This focuses attention on the spectral energy below 1 Hz and suggests making use of an aerodynamic admittance function becomes unnecessary. The natural frequency peaks measured on trees in this study are in a similar range to 0.33 Hz so Baker's point of the importance of low frequency response, below about 1 Hz seems appropriate.

Recent studies of tree dynamic response have found that small morphological variations in a tree structure can produce extreme behaviors such as either very little or nearly critical dissipation of stem oscillations (Sellier and Fourcaud 2009). In contrast, material properties play only a limited role. Since branch morphologies of trees are very diverse, both between species and within species at different locations (Evans et al. 2008) trees may need to be treated as individuals. This seems appropriate for the Palm and the Italian cypress whose morphology and dynamic response differ significantly from the more typically structured trees.

The significance of morphological variations on tree dynamic response suggests that branches contribute to the damping and perhaps dominate the tree response to wind loading so that a more complex explanation of damping is needed. Introducing the concept of mass damping may assist in providing this more complex explanation.

Chapter 7. CONCLUSION

The wind loads on a range of open grown trees have been recorded over a 5 year period using new instruments to measure the dynamic response of trees during wind storms. The tree response was measured as bending moments at the trunk base. This method differs from most previous studies that have measured tree response in the upper canopy. The advantages of measuring the base bending moment are that (a) the total tree response is measured because the resultant of all forces from the individual branches pass via the trunk to the ground, (b) the resulting values in units of kilonewton meters can be used to compare wind loads on all trees, (c) the method is suited to all types of trees and is not restricted to any one species or structural shape of tree and (d) by using two orthogonally oriented instruments, the tree response to wind from any direction can be readily monitored.

Open grown trees have large branches and are used for shade and their amenity value. Their structural form differs from plantation grown forest trees because they have significantly more mass in their branches, compared to plantation trees that grow with a tall slender stem and small canopies. The slenderness ratio (height divided by diameter) is an important aspect of the dynamic response as tall slender trees respond to wind loading like single degree of freedom cantilever-like oscillators that have a well defined natural frequency. Open grown trees usually have a low slenderness ratio and large branches and consequently their dynamic response is like a multi-degree of freedom system that has greater damping and is better able to withstand wind forces.

New instruments

New instruments, termed strain meters have been constructed to measure the dynamic response of trees under wind loading. The strain meter instruments attach to the base of the tree trunk and can be calibrated with a static pull test so that strain readings can be converted to base bending moments which is used as the measure of wind load. By recording at 20 Hz the dynamic response of the tree can be measured during wind storms. Two instruments were mounted in orthogonal directions on the trunk, one to measure response in the North/South direction and the other to measure response in the Eat/West direction. This configuration allowed monitoring of the tree response for wind coming from any direction. The data were used to evaluate wind loads, wind spectra and to determine the dynamic properties of a tree.

A range of trees that are commonly used in urban areas were monitored under wind conditions in the field over a period of several years to capture storm events and high wind speeds. All trees were as large as possible in order to represent typical trees found in urban situations. Different structural shapes of trees have been studied to investigate the influence of branches on the dynamic response of the tree. The structural shapes of trees included:

- trees with no branches – Palm (*Washingtonia robusta)*
- trees with a tall, slender form – Italian cypress (*Cupressus sempervirens*),
- trees with a central trunk, and side branches – Hoop pine 1 (*Araucaria cunninghamii),* NZ Kauri pine (*Agathis australis),* She Oak (*Allocasuarina fraseriana)*
- trees with no central trunk, and a spreading form with considerable side branches – Flooded gum (*E. grandis),* Red gum1 (*E. tereticornis),* Spotted Gum (*Corymbia maculata*).

The results indicate that trees with significant branch mass sway in a complex looping pattern under wind loading, and sway occurs only at the first natural frequency and no higher order harmonic modes occur. This is true for all trees except the Italian cypress (*Cupressus sempervirens*) which does exhibit a first harmonic response at 0.27 Hz and a second harmonic sway at 0.62 Hz. Most of the energy occurs at the first harmonic frequency as indicated by the higher amplitude in the spectral plot of the transfer function. This tree appears to behave differently from the other trees with a more flexible response to wind loading and was stable at wind speeds up to 20 m s^{-1} even though the slenderness ratio of 73 is above published limits for open grown trees (Mattheck et al. 2003). The sway motion of open grown trees has both along-wind and across-wind components and they do not sway back towards the wind, past the point of zero displacement, which is the point at which the tree would be under no wind conditions. The palm shows a more circular or looping sway motion which is different from all the other trees.

Base bending moments and wind loads

The measurement of base bending moments is used as a method of evaluating the wind loads on trees. For the trees in the current study, the maximum base bending moment recorded was 588 kNm for the 25m high Spotted Gum (*Corymbia maculata*) which occurred at a wind speed of 20 ms^{-1}. During this wind event there was considerable across wind bending moment of approximately 220 kNm. This value compares with previously published values of 880 kNm for tree failure from pull tests (Lundstrom et al. 2007) and 505 kNm for a 25m high computer generated tree (Brudi 2002). Several trees failed in the vicinity of the spotted gum during the same wind event and it is estimated that the stress values in the trunk approached 60-90% of the failure stress. It is not suggested that this method predicts failure in trees because the variability in material properties of biological structures makes estimates of failure difficult, but the results are presented to illustrate that by quantifying the wind loads it is possible to evaluate the forces and stresses that occur in individual trunks and branches using this method. Further measurements of trees under extreme wind loading up to the failure point of trees are needed before predictions of failure can be made.

A branch of a Sydney blue gum (*E. saligna*) was monitored to verify that the instruments were able to detect dynamic motion of a branch. The results indicated that during a moderate wind event, the sway motion of the side branch was in an upwards and sideways direction, and no downwards sway occurred. The lack of any downwards sway motion was unexpected. Shigo (1991) discussed upwards failure of branches from his observations of wood fibres at the point of failure. It appears that the sway of individual branches may be different and more complex than previously thought, and is an interesting area for further work.

Palm

The response of the palm (*Washingtonia robusta)* is more like a SDOF system because there are no branches. This is seen in the transfer function which has a peak at 0.32. There are some other peaks present and a small amount of energy from 0.4 to 0.6 Hz and it is suggested that the sway masses of the palm leaves could provide a mass damping effect although they are not connected as branches. The maximum recorded bending moment for the palm was 27 kNm at a wind speed of 16 ms^{-1}. The palm exhibits a much greater looping motion under wind excitation than other trees and there is considerable movement back towards the wind, past the zero displacement point. This does not occur in a simple back and forth motion but is an elliptical close to circular pattern in which the along-wind and across wind components of bending moment may be nearly equal. The time domain plots of bending moments for each tree represent the along and across wind components of bending moment passing through the trunk to the ground. They may also be considered as representing the forces on the roots and show that there are considerable across wind components of force on trees during wind storms.

Red gum and pruning treatment

The red gum (*E. tereticornis*) response to winds shows most of the resultant bending moment occurs in the along wind direction and a small proportion in the across wind direction. The maximum recorded bending moment was 300 kNm at a wind speed of 27 ms^{-1}. This tree has a low slenderness ratio of 15 and was an old tree (age unknown). This response is due to a rigid trunk with a large mass, and is in contrast to the flexible response of the palm and the Italian cypress. This tree was pruned by thinning and 20% of the canopy was removed. After pruning the maximum recorded bending moment was 228 kNm at a wind speed of 26 ms^{-1}. The pruning treatment resulted in a reduction of the bending moment with respect to wind speed due to the thinner canopy.

Velocity Exponent

The relationship between wind speed and wind load is an exponential function (V^n) and for bluff bodies is a squared relationship with $n = 2$. This is not true for the trees monitored and the value of n changed with the tree species. The highest value ($n = 1.8065$) was found for the spotted gum (*Corymbia maculata*). For the other trees n varied from n=1.3582 (palm (*Washingtonia robusta*) to $n = 1.7088$ (red gum *E. tereticornis*). The lowest value ($n = 1.0723$) was found for the Italian cypress (*Cupressus sempervirens*) and indicates that at high wind speeds, the wind loads on this tree do not increase as quickly as for other trees which is presumably due to its flexible response as it bends over and greatly reduces its frontal area exposed to the wind.

Branch dynamics

The relationship between wind speed and base bending moments on the tree had a large spread when plotted as instantaneous data. This occurred in all trees and frequently the maximum bending moment did not correlate with the maximum wind speed. This indicates that sometimes the wind gust and the tree sway may be in phase so that the gust pushes as the tree is swaying in the direction of the wind and so produces a large response and at other times the gust may push on the tree as it is swaying back towards the wind and so produces little or no response. The timing of the wind gust and the tree sway depends on the phase relationship between them which is never constant. Since the tree consists of a collection of branches which all sway individually, some in phase and some out of phase with the wind, the total effect is to effectively cancel out each other and minimise the total sway response.

Each branch acts as a dynamic oscillator and the combination of individual branch responses minimises the overall sway response of a tree. Branch dynamics contribute to the overall dynamic characteristics of a tree to dissipate energy and provide a dynamic damping due to their mass. The importance of tree morphology and the mass distribution of branches in a canopy has also been identified by Sellier and Fourcaud (2009) who found that small morphological variations in the tree can produce extreme behaviours such as either very little or nearly critical dissipation of stem oscillations. The results indicate that under wind loading, branches sway like coupled oscillators in a complex manner and their collective motion contribute to the dynamic response of open grown trees that act like a multi-degree of freedom system.

New Model

A new dynamic structural model for a tree has been proposed which considers the trunk as an oscillating mass, and the branches as oscillating masses attached to the trunk mass. Smaller branches are also treated as smaller oscillating masses attached to their parent branch in a pattern that reiterates itself as a series of oscillating masses to represent the entire structure of the tree. This model is a complex multi-degree of freedom system and introduces a damping component termed mass damping.

The model differs from previous models which have represented the tree as a single degree of freedom system in which mass damping does not occur. The effect of the dynamic masses is to minimise the amplitude of sway by moving in a complex manner and so provide an energy dissipation mechanism or damping. Mass damping for two masses has been described and the effect on minimising dynamic response is strongest when the natural frequency of the two masses is close together. Since the natural frequency depends on stiffness and mass, these two quantities of each element in the model would determine the total response. A mass damper of only 1% of the primary mass has been shown to dramatically reduce the amplitude and energy of oscillation for a two degree of freedom system. In a tree with many masses the overall effect is to prevent any large sway amplitudes from developing under wind excitation.

The spectral curve of the trees studied show that only the first mode of sway occurs and there is a broad spread of peaks across a range of frequencies in contrast to a single peak that would be present in a single degree of freedom system. Typically, the spectral curve has many closely spaced peaks, spread over a range of frequencies which are grouped around the natural frequency of the tree which is consistent with considering the branches as dynamic masses which produce a mass damping effect. The tree may be considered as a complex, multi-degree-of-freedom system with many local modes near the natural frequency, primarily located on secondary branches as reported by Castro and Garcia (2008) in a study of olive trees (*Olea europaea*) under forced excitation by mechanical shaking.

Transfer function

A structural magnification function for a SDOF system $\chi_m^2(f)$ was plotted against the transfer function data $T^2(f)$ for each tree and the two curves did not correspond over the entire range of frequencies. This supports the concept that a tree is not a SDOF system and must be considered as a MDOF system. The transfer function curve of each tree was fitted to different regions of the structural magnification function by biasing the curve in the static, dynamic and inertial sub-ranges. Biasing the curve in the static or low frequency range was used to determine the coefficient (A_s) which was used in the calculation of drag using a quasi-static method of analysis. Biasing the curve in the dynamic range was used to determine the damping ratio (ζ) because in this region the energy dissipation or damping has the most influence. Biasing the curve in the inertial sub-range is the region where mass dominates the dynamic response and the high frequency gusts or vortices push on the tree canopy. This region was used to evaluate the aerodynamic admittance function. This method was considered appropriate as the mathematics for MDOF systems are complex and have not been developed for trees yet and the mathematics of the SODF system are sufficient for investigative purposes, if modified within the biased range. This method was applied to data for each tree in order to determine the dynamic parameters of natural frequency, damping characteristics and drag coefficients.

Natural frequency

The natural frequencies of trees were evaluated using spectral analysis and identifying peak amplitudes which occur at the resonant or natural frequency of an oscillating system. For the open grown trees monitored, the sway response occurred only at the fundamental or first natural frequency except for the Italian cypress (*Cupressus sempervirens*). For all other trees other there were no higher order frequency harmonics recorded over hundreds of hours of monitoring under high wind conditions and results are consistent with those previously reported by (Baker 1997). The Italian cypress (*Cupressus sempervirens*) has a second harmonic sway response which shows as a second well separated peak in the spectrum. This is a second harmonic mode and indicates that this tree responds in winds with a flexible response that is different to the other trees in the study. The natural frequencies ranged from f_o = 0.27 Hz for the Italian cypress (*Cupressus sempervirens*) and f_o = 0.32 Hz for the palm (*Washingtonia robusta*), and between f_o = 0.31 Hz for the hoop pine (*Araucaria cunninghamii*) and f_o = 0.565 Hz for the red gum#1(*E. tereticornis*).

Damping

The damping ratio for each tree was estimated by fitting the structural magnification factor $\chi_m^2(f)$ to the transfer function data $T^2(f)$ and biasing the curve so that the area under each is equal in the frequency range from 0.2-0.4 Hz. This method attempts to match the energy values over the dynamic response range of the tree. The damping in still air conditions (V_{mean} = 0 ms^{-1}) was determined using data from a pull and release test which was always the minimum value recorded. The damping of each tree increased with wind speed and reached a maximum value which then remained constant over the range of wind speeds measured. The highest damping was observed in the red gum#1 (*E. tereticornis*) with ζ=16% and the lowest value of damping was in the Italian cypress (*Cupressus sempervirens*) with ζ=8% and the palm (*Washingtonia robusta*) with ζ=9%. A slight decrease from the maximum damping was observed at high wind speeds for the palm and the red gum but data at high mean wind speeds are needed to confirm this trend.

Damping is a complex parameter and is a measure of how the mechanical energy dissipates in the structure. For mass damping to be effective, the frequencies of the oscillating masses need to be close to each other and since the natural frequency depends on both stiffness and mass, the ratios of both of these quantities will influence the overall effect. The main branch frequencies need to be close to the trunk frequency to produce a mass damping interaction. Secondary branches need to have frequencies close to their parent branches to also have a mass damping effect, if somewhat smaller than the main branches. This cascading sequence of dynamic branch masses may reiterate through the tree and produce a complex but effective damping system. This would reduce the energy absorbed by the tree and reduce the wind load effects that might otherwise be expected. A significant aspect of the branch interaction would be the phase relationship between branches. Further studies are needed to identify the components of damping that occur in trees under wind excitation.

The aerodynamic admittance function was applied to the dynamic analysis and did not significantly change the response curve at frequencies below 1 Hz. It is concluded that aerodynamic admittance is not significant in medium sized open grown trees because the major tree response occurs below a frequency of 1 Hz and the impact of an aerodynamic admittance function is not apparent in this region.

Drag

Drag values for trees have been calculated using a mean moment response method and a spectral modelling approach. The mean moment method uses a quasi-static approach and depends on the velocity exponent (n) which has been estimated to be between 1 and 2. For the spotted gum data the velocity exponent was found to be $n = 1.81$ and for the Italian cypress the n was close to unity. This indicates that different values for n apply to each tree.

The two parameters of drag and canopy area are coupled so the calculated value of drag depends on the measured value of canopy area which changes in high winds due to streamlining and realignment so the frontal area exposed to the wind decreases. For these calculations using averaged data, the canopy area was taken as constant so the actual drag values need to be treated with caution but the method is useful for examining the relationship of drag and wind speed and does show different responses for each tree species. Further work is recommended to collect data in the high wind velocity range to more closely define the velocity exponent n for each tree.

The spectral modelling approach was used to determine drag for several trees. For the palm (*Washingtonia robusta*) the drag coefficient was $C_D = 1.5$ at a mean wind speed of 1 ms^{-1}, which reduced to $C_D = 0.4$ at mean wind speed of 9 ms^{-1}. For all other trees the drag was approximately constant though there was a trend towards a slight decrease as the mean velocity increased. This is most likely due to a change in the canopy frontal area and a streamlining effect as wind speed increases. The effect of pruning on the Red gum (*E. tereticornis*) with a 20% thinning treatment reduced the apparent drag evaluated in this way from $C_D = 1.4$ to $C_D = 0.6$.

Dynamic response factor

A dynamic response factor (DRF) is proposed as a measure of the dynamic response of a tree and to indicate the difference between static and dynamic loads on a tree subject to winds. This concept is based on the gust factor methodology and is defined as the ratio between the maximum base bending moment and the mean base bending moment over a period of time which is taken as 30 minutes. A more complex version of the DRF is used in engineering wind codes (AS/NZS 1170.2:2000) and a similar concept termed the Dynamic Amplification Factor (DAF) based on displacement ratios as trees bend, has been proposed for trees (Sellier and Fourcaud (2009). The DRF could be used to evaluate a tree's dynamic response in gusty winds and the higher the value of DRF, the more flexible is the response (Table 7.1).

Tree	**Dynamic Response Factor (DRF)**	**Comment**
Palm (*Washingtonia robusta*)	≅ 7	Flexible tree
Italian cypress (*Cupressus sempervirens*)	≅ 6	Flexible tree, two modes
Spotted gum (*Corymbia maculata*)	≅ 4.5	Middle value
Hoop pine (*Araucaria cunninghamii*)	≅ 4.5	Middle value
Red gum (*E. tereticornis*)	≅ 4	Middle value
NZ Kauri pine (*Agathis australis*)	≅ 3.5	Stiffest tree, most rigid response

Table 7.1. Dynamic Response Factor of trees.

The trees with the least dynamic response (the most rigid tree) are the NZ Kauri pine (*Agathis australis*) with a DRF of 3.5 and the Red gum (*E. tereticornis*) with a DRF of

4. Both these trees were mature or over mature with well developed trunks which contained a high proportion of the total mass. The physical dimensions of both trees (height 23.2m, DBH 0.75m (*Agathis australis*) and height 14.0 m and DBH 0.886m (*E. tereticornis*)) indicate that these were well developed trees with slenderness ratios of 31 and 15 respectively. These large trees develop high bending moment values (~300 kNm) under wind loading conditions experienced during this project.

The Palm (*Washingtonia robusta*) and the Italian cypress (*Cupressus sempervirens*) were the most flexible trees with DRF values of 7 and 6. Both of these trees have a very flexible response and a tall slender habit with slenderness ratios of 41.5 and 73 respectively. The palm develops a pronounced circular looping response to wind loading, as well as bending sideways and reducing the exposed frontal area to withstand high winds. The Italian cypress also has a very flexible response and from observation, bends sideways much more than other trees, though this was not measured. This tree develops a second mode of oscillation and its high slenderness ratio suggests a tendency to instability but it appears from anecdotal reports that this is not so and the tree rarely fails in wind storms. Although both these trees appear to have a high DRF value, they do not develop high absolute values of bending moments (maximum recorded <30 kNm) due to their small canopy frontal area and flexible response.

No firm conclusions can be made from the DRF values so further development of this concept is recommended. This concept is put forward to demonstrate the differences in tree species and indicate that more understanding is needed of how different types of trees cope with the dynamic forces of wind so that they can be managed as individuals rather than by a standard which attempts to include all trees.

Energy transfer in trees

The dynamic analysis of the trees assists in the understanding of how energy is transferred from the wind and then becomes dissipated in the trees. Energy dissipation mechanisms in trees are not yet fully understood and the damping mechanisms have usually been combined and taken as viscous damping which implies that damping is proportional to velocity. Results indicate that this is not true and damping is non-linear.

It is concluded that the dynamic contribution of branches greatly influences the overall response of the tree because the branches act as individual dynamic masses to develop a mass damping effect which has the greatest effect when the frequencies of the branches are close to the frequency of the trunk. This allows optimal energy dissipation and prevents the tree from developing large and dangerous oscillations that may lead to failure. In effect the tree is an optimally de-tuned structure where the branches act to effectively cancel out individual sway so that the overall response is minimised. This view is supported from other recent studies which have found that tree morphology and how branch masses are distributed through the tree greatly influence the stability of the trees under wind loading (Sellier and Fourcaud 2009). This suggests that trees need to be treated as individuals, both within species and across species and branch removal when pruning may need to be different for each structural form of tree species. The effect of pruning was investigated on only one tree, the red gum#1 (*E. tereticornis*) so the results are only preliminary. A 20% thinning of the canopy resulted in a reduction of the mean bending moment response of this tree. There was a significant reduction in the drag after pruning but there was no difference in the damping ratio.

Future work

Further work is needed to collect more data in a range of trees at high wind speeds to extend the range of results and confirm how trees respond under extreme wind conditions. If data are collected at winds up to and including tree failure, it may be possible to get reliable data that can be used for design purposes. At present, dynamic and static methods are unlikely to predict failure of trees under wind loading due to the many variations in tree material properties and structural morphologies.

It is suggested that future work on modelling should investigate the coupling between bending and torsion in order to better predict and understand breaking mechanisms. Torsional forces will add to the total forces on a tree during a wind storm and may be significant. The proposed dynamic model assists to describe the observed dynamic response of trees in winds but is limited to bending response and does not consider torsional forces which are yet to be measured on trees in the field.

New methods may be developed, by adapting some of the dynamic theory to trees. The pull and release test or the pluck test could be developed into a non-destructive method to estimate the mass of the tree. At present, assuming a SDOF model, it is possible to estimate the spring (k), damping (c), of a tree. By fitting the curves of the pull and release test response to the structural magnification curve, it is possible to determine an equivalent mass for the tree. This method is based on modelling displacement so accurate displacement data high in the tree would be required. The difficulty would be to choose the correct position up the trunk to measure displacement so that the equivalent mass is close to real mass.

Concluding remarks

This project has presented a structural dynamic analysis of trees by applying engineering principles of dynamics. New research instruments have been developed to measure the bending moments at the base of trees which are taken as the measurement of wind loading. Wind loads of open grown trees have been measured under storm conditions and the results may be useful to guide managers and assess tree stability.

The results have led to a new theoretical model that considers trees as multi-degree of freedom systems and differs from it's predecessors by considering branches as dynamic masses attached to the trunk. A consequence from this model is the identification of mass damping which has not previously been described for trees. The principle of mass damping is well established in structural engineering and is used in tall building design to minimize sway response due to winds. The same principle applies to the sway branch masses which act to minimize the sway response of trees in winds.

The application of this model may lead to a better understanding of how trees dissipate energy and survive in high winds. Results indicate that trees of different species and structural form have varying dynamic response and need to be treated as individuals and not as collections or groups of trees. Further work may examine the critical roles of branches in damping the sway of tress and how branch removal and pruning methods may be improved to aid tree stability in high winds.

Chapter 8. BIBLIOGRAPHY

1. Abe, M. and Fujino, Y. 1994. Dynamic Characterization of Multiple Tuned Mass Dampers and Some Design Formulas. Earthquake Engineering and Structural Dynamics, 23(8): 813-836.
2. Achim, A., Nicoll, B., Mochan, S. and Gardiner, B. 2003. Wind stability of trees on slopes. In: B. Ruck (Editor), Proceedings of International Conference on Wind Effects on Trees, University of Karlsruhe, Germany.
3. Achim, A., Ruel, J.-C., Gardiner, B.A., Laflamme, G. and Meunier, S. 2005. Modelling the vulnerability of balsam fir forests to wind damage. Forest Ecology and Management, 204: 35-50.
4. AS/NZS 1170.2. 2006. Minimum design loads on structures. Part 2: Wind loads, Standards Association of Australia.
5. ASCE. 1975. Wood structures: A design guide and commentary. American Society of Civil Engineers, New York.
6. ASTM Standard D143 2009 Standard Test Methods for Small Clear Specimens of Timber. American Society for Testing and Materials.
7. Baker, C.J. 1995. The development of a theoretical model for the windthrow of plants. Journal of Theoretical Biology, 175: 355-372.
8. Baker, C.J. 1997. Measurements of the natural frequencies of trees. Journal of Experimental Botany, 48(310): 1125-1132.
9. Baker, C.J. and Bell, H.J. 1992. Aerodynamics of urban trees. Journal of Wind Engineering and Industrial Aerodynamics., 44: 2655-2666.
10. Balachandran, B. and Magrab, E.B. 2004. Vibrations. Thomson Pub.
11. Bell, H.J., Dawson, A.R., Baker, C.J. and Wright, C.J. 1991. Tree Stability. In: S.J. Hodge (Editor), Research for Practical Arboriculture. HMSO, London, University of York, pp. 94-101.
12. Bergeron, C., Ruel, J.-C., J.-G., É. and Mitchell, S.J. 2009. Root anchorage and stem strength of black spruce (*Picea mariana*) trees in regular and irregular stands. Forestry, 82(1): 29-41.
13. Blackburn, P., Petty, J.A. and Miller, K.F. 1988. An assessment of the static and dynamic factors involved in windthrow. Forestry, 61(1): 29-43.
14. Blackwell, P.G., Rennolls, K. and Coutts, M. 1990. A root anchorage model for shallowly rooted Sitka spruce. Forestry, 63: 73-91.
15. Brudi, E. 2002. Trees and Statics: An introduction. Arborist News: 28-33.
16. Brüchert, F., Becker, G. and Speck, T. 2000. The mechanics of Norway spruce [*Picea abies* (L.) Karst]: mechanical properties of standing trees from different thinning regimes. Forest Ecology and Management, 135: 45-62.
17. Brüchert, F. and Gardiner, B.A. 2000. Wind Exposure Effects on the Mechanical Properties of Sitka Spruce (Picea sitchensis), Proceedings of 3rd Plant Biomechanics Conference., Freiberg, pp. 403-412.
18. Brüchert, F., Speck, O. and Spatz, H.-C.H. 2003. Oscillations of plants' stems and their damping: theory and experimentation. Philosophical Transactions of the Royal Society of London Series B-Biological Sciences, 358(1437): 1487-1492.
19. Burgert, I., Okuyama, T. and Yamamoto, H. 2003. Generation of radial growth stresses in the big rays of konara oak trees. J Wood Sci., 49: 131-134.
20. Cannell, M.G.R. and Morgan, J. 1987. Young's modulus of sections of living branches and tree trunks. Tree Physiology, 3: 355-364.
21. Cannell, M.G.R., Morgan, J. and Murray, M.B. 1988. Diameters and dry weight

of tree shoots: effects of Young's modulus, taper, deflections and angle. Tree Physiology, 4: 219-231.

22. Castro-Garcia, S., Blanco-Roldan, G.L., Gil-Ribes, J.A. and Aguera-Vega, J. 2008. Dynamic analysis of olive trees in intensive orchards under forced vibration. Trees, 22(6): 795-802.
23. Chapra, S.C. and Canale, R.P. 2002. Numerical Methods for Engineers. 4th Ed. Mcgraw-Hill, 926 pp.
24. Chopra, A.K. 1995. Dynamics of structures. Prentice Hall.
25. Clough, R.W. and Penzien, J. 1993. Dynamics of structures. McGraw Hill, New York.
26. Coder, K.D. 2000. Sway Frequency in Tree Stems. University of Georgia.
27. Connor, J.J. 2002. Introduction to Structural Motion Control. Prentice Hall.
28. Coutts, M.P. and Grace, J. 1995. Wind and Trees. Wind and Trees. Cambridge University Press.
29. Coutts M. 1986. Components of tree stability in Sitka spruce on peaty grey soil. Forestry 59, 173-197.
30. Cucchi V, Stokes A, Meredieu C, Berthier S, Najar M & Bert D. 2003. Root anchorage of Maritime pine (*Pinus pinaster* Ait.) growing in different soil conditions. In Wind Effects on Trees, ed. Ruck B, pp. 307-314. IUFRO, University of Karlsruhe, Germany.
31. Cucchi V & Bert D. 2003. Wind-firmness in Pinus pinaster Ait. stands in Southwest France: influence of stand density, fertilisation and breeding in two experimental stands damaged during the 1999 storm. Annals of Forest Science 60, 209-226.
32. Cucchi V, Meredieu C, Stokes A, Berthier S, Bert D, Najar M, Denis A & Lastennet R. 2004. Root anchorage of inner edge trees in stands of Maritime pine *(Pinus pinaster* Ait.) growing in different podzolic soil conditions. Trees 18, 460-466.
33. Cucchi V, Meredieu C, Stokes A, deColigney F, Suarez J & Gardiner B. 2005. Modelling the windthrow risk for simulated forest stands of Maritime pine (*Pinus pinaster* Ait.). Forest Ecology and Management 213, 184-196.
34. Cullen, S. 2002a. Trees and Wind: A bibliography for tree care professionals. Journal of Arboriculture., 28(1): 41-51.
35. Cullen, S. 2002b. Trees and Wind; Wind Scales and Speeds. Journal of Arboriculture, 28(5): 237-242.
36. Davenport, A.G. 1960. Wind Loads on Structures. Technical Paper No. 88 of the Division of Building Research, Natural Resources Council, Canada, 100 pp.
37. Davenport, A.G. 1967. Gust loading factors. Journal of the Structural Division, ASCE, 93: pp.11-34.
38. Davenport, A.G. 1967. Gust loading factors. American Society of Civil Engineers Environmental Engineering Conference -- Preprint. American Society of Civil Engineers (ASCE), New York, NY, United States, pp. 20.
39. de Langre, E. 2007. Effects of wind on plants. Annual review of fluid mechanics, 40, 141-168.
40. Den Hartog, J.P. 1956. Mechanical Vibrations. Mechanical Vibrations. McGraw-Hill, N.Y.
41. Detter, A., Cowell, C., McKeown, L., and Howard, P. 2008. Evaluation of current rigging and dismantling practices used in arboriculture. Research Report RR668): Health and Safety Executive (HSE) and Forestry Commission (FC), UK, pp 370.

42. Edberg RJ, Berry AM & Costello LR. 1994. Patterns of structural failure in Monterey pine. Journal of Arboriculture 20, 297-304.
43. England, A.H., Baker, C.J. and Saunderson, S.E.T. 2000. A dynamic analysis of windthrow of trees. Forestry, 73(3): 225-237.
44. Ennos, A.R. 1999. The aerodynamics and hydrodynamics of plants. Journal of Experimental Biology. 202: 3281-3284.
45. Espinasse, M. 1956. Robert Hooke. London : Heinemann.
46. Farquar, T. and Zhao, Y. 2006. Fracture mechanics and its relevance to Botanical Structures. American Journal of Botany, 93(10): 1289-1294.
47. Finnegan, J.J. and Mulhearn, P.J. 1978. Modelling waving crops in a wind tunnel. Boundary-Layer Meterology. 14(253-277).
48. Flesch, T.K. and Wilson, J.D. 1999. Wind and remnant tree sway in forest cutblocks. I Measured winds in experimental cutblocks. Agricultural and Forest Meterology, 93: 229-242.
49. Flesch, T.K. and Wilson, J.D. 1999. Wind and remnant tree sway in forest cutblocks. II. Relating measured tree sway to wind statistics. Agricultural and Forest Meteorology, 93: 243-258.
50. Fleurant, C., Duchesne, J. and Raimbault, P. 2004. An allometric model for trees. Journal of Theoretical Biology, 227: 137-147.
51. Fourcaud, T., Ji, J., Zhang, Z. and Stokes, A. 2008. Understanding the impact of root morphology on overturning mechanisms: A modelling approach. Annals of Botany, 101: 1267-1280.
52. Fourcaud, T. and Lac, P. 2003. Numerical modelling of shape regulation and growth stresses in trees. 1. An incremental static finite element formulation. Trees, 17: 23-30.
53. Fraser, A.I. and Gardiner, J.B.H. 1967. Rooting and stability in Sitka spruce., Forestry Commission Bulletin. No. 40. HMSO, London.
54. Fridman, J. and Valinger, E. 1998. Modelling probability of snow and wind damage using tree, stand, and site characteristics from *Pinus sylvestris* sample plots. Scandinavian Journal of Forest Research, 13: 348-356.
55. Gaffrey, D. and Kniemeyer, O. 2002. The elasto-mechanical behaviour of Douglas fir, its sensitivity to tree-specific properties, wind and snow loads, and implications for stability - a simulation study. Journal of Forest Science, 48(2): 49-69.
56. Galilei, G., 1638. Dialogues concerning two new sciences. Translation by Henry Crew and Alfonso de Salvio. 1954. Book. Dover Publications, New York.
57. Gardiner, B., Marshall, B., Achim, A., Belcher, R. and Wood, C. 2005. The stability of different silvicultural systems: A wind-tunnel investigation. Forestry, 78: 471-483.
58. Gardiner, B.A. 1989. Mechanical characteristics of Sitka Spruce, Forest Commission Occasional Paper No. 24.
59. Gardiner, B.A. 1992. Mathematical Modelling of the static and dynamic characteristics of plantation trees. In: J. Franke and A.E. Roeder (Editors), Mathematical Modelling of Forest Ecosystems. Saunders Verlag, Frankfurt, pp. 40-61.
60. Gardiner, B.A. 1994. Wind and wind forces in a plantation spruce forest. Boundary-Layer Meterology, 67: 161-186.
61. Gardiner, B.A. 1995. The interactions of wind and tree movement in forest canopies. In: M.P. Coutts and J. Grace (Editors), Wind and Trees. Cambridge University Press., pp. 41-59.

62. Gardiner, B.A., Stacey, G.R., Belcher, R.E. and Wood, C.J. 1997. Field and wind tunnel assessments of the implications of respacing and thinning for tree stability. Forestry, 70(3): 234-252.
63. Gardiner, B.H. and Quine, C.P. 2000. The mechanical adaption of tree to environmental influences, Proceeding of 3rd Plant Biomechanics Conference, Freiberg, pp. 71-82.
64. Gardiner, B., Peltola, H., and Kellomaki, S. 2000. Comparison of two models for predicting the critical wind speeds required to damage coniferous trees. Ecological modelling, 129, pp. 1-23.
65. Gardiner, B., Marshall, B., Achim, A., Belcher, R., and Wood, C. 2005. The stability of different silvicultural systems: A wind-tunnel investigation. Forestry, 78, 471-483.
66. Gardiner, B., Byrne, K.E., Hale, S., Kamimura, K., Mitchell, S.J., Peltola, H., and Ruel, J.-C. 2008. A review of mechanistic modelling of wind damage risk to forests. Forestry, 81(3), 447-463.
67. Gilman, E.F., Grabosky, J.C., Jones, S., and Harchick, C. 2008a. Effects of Pruning Dose and Type on Trunk Movement in Tropical Storm Winds. Arboriculture and Urban Forestry, 34(1), 13-19.
68. Gilman, E.F., Masters, F. and Grabosky, J.C. 2008b. Pruning Affects Tree Movement in Hurricane Force Wind. Arboriculture and Urban Forestry, 34(1): 20-28.
69. Gordon, J.E. 1968. The New Science of Strong Materials. Penguin Books.
70. Grace, J. 2003. Mechancial stress and wind damage. In: B. Thomas (Editor), Encyclopedia of Applied Plant Sciences. Elsevier Academic Press.
71. Greenhill, G., 1881. Determination of the greatest height consistent with stability that a vertical pole or mast can be made and the greatest height to which a tree of given proportions can grow. Proc. Cambridge Phi. Soc., 4: 65-73.
72. Gromke, C., and Ruck, B. 2008. Aerodynamic modelling of trees for small-scale wind tunnel studies. Forestry, 81(3), 243-258.
73. Guitard, D.G.E. and Castera, P. 1995. Experimental analysis and mechanical modelling of wind-induced tree sways. In: M.P. Coutts and J. Grace (Editors), Wind and Trees. Cambridge University Press., pp. 182-194.
74. Haritos, N. 1993. The "Equivalent Area" Method for estimating damping levels., Proceedings of the 13th Australasian Conference on the Mechanics of Structures and Materials (ACMSM13), Woollongong, pp. 341-348.
75. Haritos, N. and James, K.R. 2008a. Dynamic Response Characteristics of Urban Trees, Australian Earthquake Engineering Society 2008 Conference, Ballarat, Victoria.
76. Haritos, N. and James, K.R. 2008b. Dynamic Response Characteristics of Trees from Excitation by Turbulent Wind, 20th Australasian Conf. on the Mechanics of Structures and Materials. CRC Press., Toowoomba, Qld., pp. 147-152.
77. Harris, R.W., Clark, J.R. and Matheny, N.P. 1999. Arboriculture. Integrated management of landscape trees, Shrubs and vines. Prentice Hall, N.J., 680 pp.
78. Hassinen, A., Lemettinen, M., Peltola, H., Kellomaki, D. and Gardiner, B.A. 1998. A prism-based system for monitoring the swaying of trees under wind loading. Agricultrual and Forest Meteorology, 90(1998): 187-194.
79. Hedden, R.L., Fredericksen, T.S. and Williams, S.A. 1995. Modeling the effect of crown shedding and streamlining on the survival of lobllolly pine exposed to acute wind. Canadian Journal of Forest Research, 25(5): 704-712.
80. Herajarvi, H. 2004. Static bending properties of Finnish birch wood. Wood

Science and Technology, 37: 523-530.
81. Hoag, D.L., Fridley, R.B. and Hutchinson, J.R. 1971. Experimental measurement of internal and external damping properties of tree limbs. Transactions of the ASAE, 16: 20-28.
82. Holbo, H.R., Colbett, T.C. and Horton, P.J. 1980. Aeromechanical behaviour of selected Douglas-fir. Agricultural. Meteorology, 21: 81-91.
83. Holmes, J.D. 2007. Wind Loading on Structures. 2nd Ed.: Taylor and Francis, NY. pp.380.
84. Ilic, J. 2001. Relationship among the dynamic and static elastic properties of air-dry Eucalyptus delegatensis R. Baker. Holz als Roh-und Werkstoff, 59(3): 169-175.
85. Jacobs, M.R. 1936. The effect of wind on trees. Australian Forestry, 1(2): 25-32.
86. James, K.R. 2003. Dynamic Loading of Trees. Journal of Arboriculture, 29(3): 165-171.
87. James, K.R. 2006a. Tree dynamics and wind storms. Western Arborist, International Society of Arboriculture, 32(1): 18-22.
88. James, K.R. 2006b. Tree stability and wind storms in urban parks. IFPRA World (International Federation of Parks and Recreation Administration), June: 8-10.
89. James, K.R. 2008. Trees, Wind, and Dynamic Loads, Arborist News, pp. 44-47.
90. James, K.R. and Haritos, N. 2008. Dynamic Wind Loading Effects on Trees - a structural perspective., Australasian Structural Engineering Conference, Melbourne.
91. James, K.R., Haritos, N. and Ades, P.K. 2006. Mechanical stability of trees under dynamic loads. American Journal of Botany, 93(10): 1361-1369.
92. James, K.R. and Kane, B. 2008. Precision digital instruments to measure dynamic wind loads on trees during storms. Journal of Agricultural and Forest Meteorology, 148(5): 1055-1061.
93. Jenkins, G.M. and Watts, D.G. 1968. Spectral analysis and its applications. Holden-Day.
94. Jonsonn MJ, Foetzki A, Kalberer M, Lundstrom T, Ammann W & Stockli V. 2006. Root-soil rotation stiffness of Norway spruce (*Picea abies* (L.) Karst) growing on subalpine forested slopes. Journal of Plant and Soil 285, 267-277.
95. Jonsson MJ, Foetzki A, Kalberer M, Lundstrom T, Ammann W & Stockli V. 2007. Natural frequencies and damping ratios of Norway spruce (*Picea abies* (L.) Karst) growing on subalpine forested slopes. Trees 21, 541-548.
96. Kerzenmacher, T. and Gardiner, B.A. 1998. A mathematical model to describe the dynamic response of a spruce tree to the wind. Trees, 12: 385-394.
97. Kubler, H. 1959. Studies on growth stresses in trees. 2. Longitudinal stresses. Holz als Roh- und Werkstoff, 17(2): 44-54.
98. Kubler, H. 1987. Growth stresses in trees and related wood properties. Forestry Abstracts, 48: 131-189.
99. Lilly, S. and Davis Sydnor, T. 1995. Comparison of branch failure during static loading of Silver and Norway maples. Journal of Arboriculture, 21(6): 302-305.
100. Lundstrom, T., Jonsson, M.J. and Kalberer, M. 2007. The root-soil system of Norway spruce subject to turning moment; resistance as a function of rotation. Plant Soil, 300: 35-49.
101. Mattheck, C. 1990. Why they grow, how they grow: The mechanics of trees. Arboriculture Journal, 14: 1-17.
102. Mattheck, C. and Bethge, K. 2000. Simple mathematical approaches to tree biomechanics. Arboricultural Journal, 24: 307-326.

103. Mattheck, C., Bethge, K., Kappel, R., Mueller, P. and Tesari, I. 2003. Failure modes for trees and related criteria., International Conference "Wind Effects on Trees", University of Karlsruhe, Germany.
104. Mattheck, C. and Breloer, H. 1994. The body language of trees. HMSO, Dept of Environment.
105. Mattheck, C. and Kubler, H. 1995. Wood, The internal optimisation of trees. Springer, 129 pp.
106. Mayer, H. 1987. Wind induced tree sways. Trees, 1: 195-206.
107. Mayhead, G.J. 1973a. Sway periods of forest trees. Scottish Forestry, 27: 19-23.
108. Mayhead, G.J. 1973b. Some drag coefficients for British trees derived from wind tunnel studies. Agric. Meteorology. 12: 123-130.
109. Mayhead, G.J., Gardiner, B.H. and Durrant, D.W. 1975. A report on the physical properties of conifers in relation to plantation stability., Forest Commission Research and Development Division, Roslin, Midlothian, UK.
110. Mencuccini, M., Grace, J. and Fioravanti, M. 1997. Biomechanical and hydraulic determinants of tree structure in Scots Pine: anatomical characteristics. Tree Physiology, 17: 105-113.
111. Milne, R. 1988. The dynamics of swaying trees. New Scientist, 21: 46.
112. Milne, R. and Blackburn, P. 1989. The elasticity and vertical distribution of stress within stems of Picea sitchensis. Tree Physiology, 5: 195-205.
113. Milne, R. 1991. Dynamics of swaying of Picea sitchensis. Tree-Physiology, 9(3): 383-399.
114. Milne, R. 1995. Modelling mechanical stresses in living Sitka spruce stems. In: M.P. Coutts and J. Grace (Editors), Wind and Trees. Cambridge University Press, pp. 165-181.
115. Moore, J.R. 2000. Differences in maximum resistive bending moments of *Pinus radiata* trees grown on a range of soil types. Forest Ecology and Management, 135: 63-71.
116. Moore, J.R. 2002. Mechanical Behaviour of Coniferous Trees Subjected to Wind Loading. Ph.D. Thesis, Oregon State University, 205 pp.
117. Moore, J.R. and Maguire, D.A. 2004. Natural sway frequencies and damping ratios of trees: concepts, review and synthesis of previous studies. Trees, 18(2): 195-203.
118. Moore, J.R., Gardiner, B.A., Blackburn, G.R.A., Brickman, A. and Maguire, D.A. 2005. An inexpensive instrument to measure the dynamic response of standing trees to wind loading. Agricultural and Forest Meteorology, 132: 78-83.
119. Moore, J.R. and Maguire, D.A. 2005. Natural sway frequencies and damping ratios of trees: influence of crown structure. Trees, 19: 363-373.
120. Moore, J.R. and Maguire, D.A. 2008. Simulating the dynamic behaviour of Douglas-fir trees under applied loads by the finite element method. Tree Physiology, 28: 75-83.
121. Moore, J.R., Tombleson, J.D., Turner, J.A. and Van der Colf, M. 2008. Wind effects on juvenile trees: a review with special reference to toppling of radiata pine growing in New Zealand. Forestry, 81(3): 377-387.
122. Morgan, J. and Cannell, M.G.R. 1987. Structural analysis of tree trunks and branches: tapered cantilever beams subject to large deflections under complex loading. Tree Physiology, 3: 365-374.
123. Morgan, J. and Cannell, M.G.R. 1987. Young's modulus of sections of living branches and tree trunks. Tree Physiology, 3: 355-364.
124. Morgan, J. and Cannell, M.G.R. 1988. Structural analysis of tree trunks and

branches: tapered cantilever beams subject to large deflections under complex loading. Tree Physiology, 3: 365-374.
125. Morgan, J. and Cannell, M.G.R. 1988. Support costs of different branch designs: effects of position, number, angle and deflection of laterals. Tree Physiology, 4: 303-313.
126. Mortimer, M.J. and Kane, B. 2004. Hazard tree liability in the United States: Uncertain risks for owners and professionals. Urban Forestry and Urban Greening, 2(3): 159-165.
127. Neild, S.A. and Wood, C.J. 1999. Estimating stem and root-anchorage flexibility in trees. Tree Physiology, 19: 141-151.
128. Newland, D.E. 1989. Mechanical vibration analysis and computation. Longman, Essex, UK.
129. Niklas, K.J. 1992. Plant Biomechanics. An engineering approach to plant form and function. University of Chicago Press. Uni. Chicago Press., 607 pp.
130. Niklas, K.J. 2002. Wind, Size, and Tree Safety. Journal of Arboriculture, 28(2): 84-93.
131. Niklas, K.J. and Spatz, H.-C.H. 2000. Wind-induced stresses in cherry trees: evidence against the hypothesis of constant stress levels. Trees, 14: 230-237.
132. Novak, M.D., Orchansky, A.L., Warland, J.S., and Ketler, R. 2001. Wind tunnel modelling of partial cuts and cutblock edges for windthrow. In: S.J. Mitchell (Editor), Windthrow assessment and management in British Columbia. Richmond, British Columbia., pp 176-192.
133. Oliver, H.R. and Mayhead, G.J. 1974. Wind measurements in a pine forest during a destructive gale. Forestry, 47: 185-195.
134. O'Sullivan, M.F. and Ritchie, R.M. 1992. An apparatus to apply dynamic loads to forest trees. Journal of Agricultural Engineering Research, 51: 153-156.
135. Papesch, A.J.G. 1974. A simplified theoretical analysis of the factors that influence the windthrow of trees. In: A.J. Sutherland, and D. Lindley (Editors), Fifth Australasion Conference on Hydraulics and Fluid Mechanics, University of Canterbury, Christchurch, NZ., pp. 235-242.
136. Papesch, A.J.G., Moore, J.R. and Hawke, A.E. 1997. Mechanical stability of Pinus radiata trees at Eyrewell Forest investigated using static tests. New Zealand Journal Forest Science, 27: 188-204.
137. Peltola, H. and Kellomaki, D. 1993. A mechanistic model for calculating windthrow and stem breakage of Scots pines at stand edge. Silva Fennica, 27(2): 99-111.
138. Peltola, H., Kellomaki, D., Hassinen, A., Lemettinen, M. and Aho, J. 1993. Swaying of trees as caused by wind: analysis of field measurements. Silva Fennica, 27(2): 113-126.
139. Peltola, H. 1995. Studies in the Mechanism of Wind Induced damage of Scots Pine., University of Joenssu, Finland.
140. Peltola, H. 1996a. Model computations on wind flow and turning moment by wind for Scots pines along the margins of clear-cut areas. Forest Ecology and Management, 83(3): 203-215.
141. Peltola, H. 1996b. Swaying of trees in response to wind and thinning in a stand of Scots pine. Boundary-Layer Meteorology. 77: 285-304.
142. Peltola, H. 1999. Model Computations of the impact of climatic change on the windthrow risk of trees. Climate Change, 41: 17-36.
143. Peltola, H., Kellomaki, S., Vaisanen, H. and Ikonen, V.P. 1999. A mechanistic model for assessing the risk of wind and snow damage to single trees and stands

of Scots pine, Norway spruce, and birch. Canadian Journal of Forest Research, 29: 647-661.
144. Peltola, H., Kellomaki, S., Hassinen, A. and Granander, M. 2000. Mechanical stability of Scots Pine, Norway spruce and birch: an analysis of tree-pulling experiments in Finland. Forest Ecology and Management, 135: 143-153.
145. Peltola, H.M. 2006. Mechanical stability of trees under static loads. American Journal of Botany, 93(10): 1341-1351.
146. Petty, J.A. and Swain, C. 1985. Factors influencing stress breakage of conifers in high winds. Forestry, 58: 75-84.
147. Quine, C.P., Coutts, M.P., Gardiner, B.A. and Pyatt, G. 1995. Forests and Wind: Management to Minimise Damage, Forest Authority, Northern Research Station. Roslin, Midlothian.
148. Rodgers, M., Casey, A., McMenamin, C. and Hendrick, E. 1995. An experimental investigation of the effects of dynamic loading on coniferous trees planted on wet mineral soils. In: M.P. Coutts and J. Grace (Editors), Wind and Trees. Cambridge University Press., pp. 204-219.
149. Rodriguez, M., deLangre, E., and Moulia, B. 2008. A scaling law for the effects of architecture and allometry on the vibration modes suggests a biological tuning to modal compartmentalization. American Journal of Botany, 95(12): 1523-1537.
150. Roodbaraky, H.J., Baker, C.J., Dawson, A.R. and Wright, C.J. 1994. Experimental Observations of the Aerodynamic Characteristics of Urban Trees. Journal of Wind Engineering and Industrial Aerodynamics, 52(1994): 171-184.
151. Rudnicki, M., Silins, U., Liefferd, V.J. and Josi, G. 2001. Measure of simultaneous tree sways and estimation of crown interactions among a group of trees. Trees, 15: 83-90.
152. Rudnicki, M.R., Mitchell, S.J. and Novak, M.D. 2004. Wind tunnel measurements of crown streamlining and drag relationships for three conifer species. Canadian Journal of Forest Research, 34: 666-676.
153. Rudnicki, M.R., Meyer, T.H., Lieffers, V.J., Silins, U. and Webb, V.A. 2008. The periodic motion of lodgepole pine tree as affected by collisions with neighbors. Trees, 22: 475-482.
154. Sagar, R.M., and Jull, M.J. 2001. Wind climatology and high wind events in Northeast British Columbia 1995-2000. In Windthrow assessment and management in British Columbia. (Mitchell S.J., Ed., Richmond, British Columbia., pp 81-90.
155. Saunderson, S.E.T., England, A.H. and Baker, C.J. 1999a. A Dynamic Model of the Behaviour of Sitka Spruce in High Winds. Journal of Theoretical Biology, 200: 249-259.
156. Saunderson, S.E.T., England, A.H. and Baker, C.J. 1999b. Modelling the failure of trees in high winds. 10th International Wind Conference on Wind Engineering.
157. Schelhaas, M.J. 2008. The wind stability of different silvicultural systems for Douglas-fir in the Netherlands: a model-based approach. Forestry, 81(3): 399-414.
158. Schonborn, J., Schindler, D., and Mayer, H. 2009. Measuring vibrations of a single, solitary broadleaf tree. In Proceedings of the 2nd International Conference. Wind Effects on Trees (Mayer, H. and Schindler, D., ed, Albert-Ludwigs-University of Freiburg, Germany.
159. Schindler, D. 2008. Responses of Scots pine trees to dynamic wind loading.

Agricultural and Forest Meteorology, 148, 1733-1742.
160. Seeger, R.J. 1966. Galileo Galilei, his life and works. Pergamon Press.
161. Sellier, D., Soulier, D., Fourcaud, T., and Brunet, Y. 2003. The Venfor Project: Influence of the aerial architecture on tree swaying - An experimental approach. In Wind effects in trees. (B. Ruck, ed, University of Karlsruhe, Germany.
162. Sellier, D. and Fourcaud, T. 2005. A mechanical analysis of the relationship between free oscillations of Pinus pinaster Ait. saplings and their aerial architecture. Journal of Experimental Botany, 56(416): 1563-1573.
163. Sellier, D., Fourcaud, T., and Lac, P. 2006. A finite element model for investigating effects of aerial architecture on tree oscillations. Tree Physiology, 26, 799-806.
164. Sellier, D., Fourcaud, T. and Lac, P. 2008. A finite element model for investigating effects of aerial architecture on tree oscillations. Tree Physiology, 26: 799-806.
165. Sellier, D. and Fourcaud, T. 2009. Crown structure and wood properties: Influence on tree sway and response to high winds. American Journal of Botany, 96(5): 885-896.
166. Shigo, A. 1985. How tree branches are attached to trunks. Canadian Journal of Botany, 63, 1391-1401.
167. Shigo, A. 1991. A New Tree Biology. Shigo and Tree Associates, Durham, NH., USA.
168. Silins, U., Lieffers, V.J. and Bach, L. 2000. The effect of temperature on mechanical properties of standing lodgepole pine trees. Trees, 14(8): 424-428.
169. Sinn, G. 2003. Baumstatik. Stand- und Bruchsicherheit von Baumen an StraBen, in Parks und der freien Landschaft: biologische Aspekte und eine Einfuhrung in die Baumstatik unter besondere Berucksichtigung der Neigungs- und Dehnungsmessverfahren, Braunschweig. In Detter et al. 2008. Evaluation of current rigging and dismantling practices used in arboriculture: Health and Safety Executive (HSE) and Forestry Commission (FC), UK.
170. Skatter, S. and Kucera, B. 2000. Tree breakage from torsional wind loading due to crown asymmetry. Forest Ecology and Management, 135: 97-103.
171. Slodicak, M. and Novak, J. 2006. Silvicultural measures to increase the mechanical stability of pure secondary Norway spruce stands before conversion. Forest Ecology and Management, 224: 252-257.
172. Smith, V.G., Watts, M. and James, D.F. 1987. Mechanical stability of black spruce in the clay belt region of northern Ontario. Canadian Journal of Forest Research, 17: 1081-1091.
173. Soong, T.T., and Dargush, G.F. 1997. Passive Energy Dissipation Systems in Structural Engineering. John Wiley and Sons, N.Y., 356 pp.
174. Spatz, H.-C.H. 2000. Greenhill's Formula for the Critical Euler Buckling Length revisited. In: H.-C.H. Spatz and T. Speck (Editors), 3rd Plant Biomechanics Conf. Plant Biomechanics 2000. Georg Thieme Verlag, Freiburg, pp. 30-37.
175. Spatz, H.-C.H. and Bruechert, F. 2000. Basic biomechanics of self-supporting plants: wind loads and gravitational loads on a Norway spruce tree. Forest Ecology and Management, 135(2000): 33-44.
176. Spatz, H.-C.H. and Speck, O. 2002. Oscillation frequencies of tapered plant stems. American Journal of Botany, 89: 1-11.
177. Spatz, H.-C.H. and Zebrowski, J. 2001. Oscillation frequencies of plant stems with apical loads. Planta, 214(2): 215-219.
178. Spatz, H.-C., Bruchert, F., and Pfisterer, J. 2007. Multiple resonance damping or

how trees escape dangerously large oscillations. American Journal of Botany, 94(10), 1603-1611.
179. Speck, O. 2003. Field Measurements of wind speed and reconfiguration in Arundo donax (Poaceae) with estimates of drag forces. American Journal of Botany, 90(8): 1253-1256.
180. Speck, O. and Spatz, H.-C.H. 2004. Damped Oscillations of the Giant Reed *Arundo donax* (Poaceae). American Journal of Botany, 91(6): 789-796.
181. Stokes, A. 1999. Strain distribution during anchorage failure of Pinus pinaster Ait. at different ages and tree growth response to wind-induced root movement. Plant Soil, 217: 17-27.
182. Sugden, M.J. 1962. Tree sway period - a possible new parameter for crown classification and stand competition. Forestry Chronicle, 38: 336-344.
183. Telewski, F.W. 1995. Wind induced physiological and developmental responses in trees. In: M.P. Coutts and J. Grace (Editors), Wind and Trees. Cambridge University Press, pp. 237-263.
184. Tevar Sanz, G., Sanz-Andres, A., Fernandez Canadas, M., and Grande Ortiz, M.A. 2003. Wind effects on Populus sp. In Wind Effects on Trees, University of Karlsruhe, Germany.
185. Timoshenko, S. 1955. Strength of Materials, 3rd Ed. Van Nostrand, N.Y.
186. Vickery, B.J. 1971. On the reliability of Gust Loading Factors. Civil Engineering Transaction, I.E. Aust., 13: 1-9.
187. Vidal, M.H., Sanchez, C.I. and Hurtado, L.A. 2003. Mechanical Parameters during static bending of Pinus radiate growing in a silvopastoral system 1: elasticity and strength. J. Wood Science, 49: 125-130.
188. Vogel, S. 1989. Drag and Reconfiguration of Broad Leaves in High Winds. Journal of Experimental Biology, 40(217): 941-948.
189. Vogel, S. 1996. Blowing in the Wind: Storm-resisting features of the design of trees. Journal of Arboriculture, 22(2): 92-98.
190. Vogel, S. 2007. Living in a physical world. XI. To twist or bend when stresses. Journal of Bioscience, 32(4): 643-655.
191. Vollsinger, S., Mitchell, S.J., Byrne, K.E., Novak, M.D. and Rudnicki, M. 2005. Wind tunnel measurements of crown streamlining and drag relationships for several hardwood species. Canadian Journal of Forest Research, 35: 1238-1249.
192. Wessolly, L. 1995. Fracture diagnosis of trees, Part 1: Statics-Integrated Methods, measurement with tension test. Stadt und Grun, 6: 416-422.
193. White, M.E. 1986. The greening of Gondwana. Reed Books Pty Ltd.
194. Wood, C.J. 1995. Understanding wind forces on trees. In: M.P. Coutts and J. Grace (Editors), Wind and Trees. Cambridge University Press., pp. 133-164.
195. Wood, M.J., Scott, R., Volker, P.W. and Mannes, D.J. 2008. Windthrow in Tasmania, Australia: Monitoring, prediction and management. Forestry, 81(3): 415-427.
196. Zeng, H., Pukkala, T. and Peltola, H. 2007. The use of heuristic optimization in risk management of wind damage in forest planning. Forest Ecology and Management, 241: 189-199.
197. Zhou, Y. and Kareem, A. 2001. Gust Loading Factor: New Model. Journal of Structural Engineering: 168-175.
198. Zhu, J., Matsuzaki, T. and Sakioka, K. 2000. Wind speed within a single crown of Japanese black pine (*Pinus thunbergii* Parl.). Forest Ecology and Management, 135: 19-31.